ABSTRACT

Progress Toward the Total Synthesis of Actinophyllic Acid

Joshua James Day

Yale University, 2010

The search for natural products with biological activity related to cardiovascular disorders resulted in the isolation and structure elucidation of the indole alkaloid actinophyllic acid in 2005. Following isolation from the leaves of *Alstonia actinophylla* it was found to inhibit carboxypeptidase U (CPU) with an IC_{50} of 0.84 μM using a CPU/hippuricase coupled enzyme assay.

Efforts toward the total synthesis of actinophyllic acid are described, which includes two strategies. The first relied upon a sequential Michael addition/alkylation sequence to install the polycyclic carbon framework found in the natural product. The second strategy relied upon a more convergent route to the polycyclic core of actinophyllic acid. Both routes accessed intermediates possessing all carbon atoms requisite for the natural product. Highlights from these routes include a *net* amine conjugate addition through the intermediacy of a phosphonium salt and formation of a quaternary carbon by trapping a putative aza-isobenzofulvene intermediate with an enamine nucleophile, respectively.

Progress Toward the Total Synthesis of Actinophyllic Acid

A Dissertation
Presented to the Faculty of the Graduate School
of
Yale University
in Candidacy for the Degree of
Doctor of Philosophy

by
Joshua James Day

Dissertation Director: John L. Wood

May 2010

© 2010 by Joshua James Day
All rights reserved.

To My Family and Friends

Acknowledgments

First and foremost I would like to thank my advisor John L. Wood, who gave me the opportunity to work in W6. Over the years I learned a great deal from John and always appreciated his advice. The support that John provides to his students is something that I will always remember. My favorite thing about John is that he is both smart and creative without having to tell the world. I have found this to be unique in our field and it is something that I strive to emulate.

During the last two years of my graduate career I was fortunate to work on actinophyllic acid with Rishi Vaswani, a talented postdoctoral scholar. Rishi's willingness to talk chemistry was always appreciated. His knowledge of organic chemistry was truly impressive and I learned a lot from him.

The Wood group has been a fantastic place to spend the past five years of my life. I enjoyed my first two years at Yale with senior graduate students Dave Spiegel, Andy Nickel, Ivar McDonald, Che-Wah Lee, Gregg Keaney, Sarah Reisman, Amélie Bérubé, and postdocs Tatsuya Shirhata, Akio Kakefuda, Hideyuki Kitamura, and Atsushi Hasuoka. I thank all of you for creating an environment in which I was able to ask a lot of questions and learn from your experience and good nature. In particular, Sarah Reisman and Amélie Bérubé dealt with the majority of my questions and where always patient and helpful. I must thank Elnaz Menhaji, Barry Twenter, and Matt Medeiros for helping to make the trek to Colorado State University enjoyable. I always enjoyed our interactions

in and out of lab. Matt, you have become a great friend to me and my family. Your selfless support and help over the years meant a lot. You are also an excellent cook. Thank you for being you. I wish you the best with your future plans. I have also had the pleasure to spend a significant amount of time with graduate students at Colorado State University. I would like to thank Ping Dong, Brett Prigaro, Sarah Stevens, Jennifer Howell, Adam Stout, Genessa Smith, Sam Levine, and Travis McMahon for being easy to talk to and spend time in lab. I wish all of you the best of luck with your time remaining in lab and beyond. I was lucky to overlap with two postdocs at Colorado State. Graham Murphy and Ke Kong are both excellent chemists who positively influenced my experience in lab. I must thank Graham for proofreading this dissertation and making it significantly better. I briefly overlapped with Nancy Tao and Noah Dieterich, two undergraduates who have a promising future in chemistry. Last, but not least, I must thank Dave Freeman whose humor and friendship was just what I needed. I consider myself lucky to have worked next to you. You are sure to succeed and I wish you good luck as you finish your graduate work. I already miss our lunches.

I would like to briefly thank all former Wood group members for their hard work and the legacy that they left behind. I am proud to have been a part of W6 and thank you for helping to make it what it is.

My time at Yale and Colorado State University would have been much more difficult if not for help with instruments from Eric Paulson, Dr. Chris Rithner,

Don Heyse, Don Dick, and solved crystal structures from Susie. I appreciate your time and patience.

My family and friends have played an important role over the past five years. Your support helped me get past difficult times and your visits were always uplifting. Specifically, I would like to thank my mom and dad for unwavering support and my brothers Ryan and Cam for providing encouragement to the “dumbest smart kid I know”.

To my beautiful wife Melissa I owe you more than I can repay. Your love, encouragement, and positive attitude made the last five years possible and I am forever grateful. To my wonderful boys Caiden and Landon, I cannot tell you how much your smiling faces meant to me everyday when I would get home from lab. My life is wonderful right now because I share it with the three of you.

Table of Contents

Dedication iii

Acknowledgments iv

Table of Contents vii

List of Figures x

List of Schemes xiii

List of Tables xv

List of Abbreviations xvi

Chapter 1: Actinophyllic Acid: A Bridged Polycyclic Indole Alkaloid Natural Product from *Alstonia actinophylla* 1

1.1 Introduction and Background 1

1.1.1 Isolation and Biological Activity 1

1.1.2 The Role of CPU in Fibrinolysis 2

1.1.3 CPU/Hippuricase Coupled Enzyme Assay Irregularity 3

1.1.4 Related Natural Products 4

1.2 Proposed Biosynthesis 5

1.2.1 Derived from Precondylocarpine 5

1.3 Previous Synthetic Studies 7

1.3.1 Martin's Effort toward Actinophyllic Acid 7

1.3.2 Overman's Total Synthesis of Actinophyllic Acid 9

1.3.3 Determination of Absolute Stereochemistry 10

1.4 Summary 11

1.5 Notes and References 12

Chapter 2: Synthesis of an Advanced Cycloheptenone Intermediate 15

2.1 Sequential Michael Addition/Alkylation Strategy. 15

2.1.1 Initial Considerations and Retrosynthetic Analysis 15

2.1.2 Initial Forward Synthesis 17

2.1.3 An Unstable Ring-Closing Metathesis Product 22

2.1.4 Construction of an Advanced Michael Acceptor 24

2.1.5 Insight into the Oxidative Transposition Mechanism 26

2.2 Summary 28

2.3 Experimental 28
2.3.1 Materials and Methods 28
2.3.2 Preparative Procedures 30

2.4 References and Notes 46

Appendix 1: Characterization Spectra Relevant to Chapter Two 50

Chapter 3: Synthesis of an Advanced Intermediate Possessing All Requisite Carbon Atoms 81

3.1 Preventing Lactone Formation 81
3.1.1 Use of Di-*tert*-butyl Malonate to Increase Steric Bulk 81
3.1.2 Finding a Balance between Steric Bulk and Reactivity 84
3.1.3 Elaboration of an Advanced Michael Acceptor 86

3.2 Conclusion 90

3.3 Experimental 91
3.3.1 Materials and Methods 91
3.3.2 Preparative Procedures 92

3.4 Notes and References 111

Appendix 2: Characterization Spectra Relevant to Chapter Three 113

Appendix 3: X-Ray Crystallography Report Relevant to Chapter Three 150
A.3.1 X-Ray Crystallography Report for Silyl enol ether **71** 151

Chapter 4: Alternative Approaches to the Complex Framework of Actinophyllic Acid 164

4.1 Aldehyde Alkylation Strategy 164
4.1.1 Synthetic Planning 164
4.1.2 Retrosynthetic Analysis 165
4.1.3 Dibutyrolactone as a Masked Dichloro Ketone 166
4.1.4 Elaboration of Lactone Malonate **87** 169

4.2 Late Stage Amine Incorporation Strategy 174
4.2.1 Initial Considerations and Revised Retrosynthesis 174
4.2.2 Precedent for Bis-Alkylation Strategy 176
4.2.3 Trapping an Aza-isobenzofulvene Intermediate 178

4.3 Conclusions 182
4.3.1 Summary of Actinophyllic Acid Progress 182

4.4 Experimental 183
4.4.1 Materials and Methods 183
4.4.2 Preparative Procedures 184

4.5 Notes and References 194

Appendix 4: Characterization Spectra Relevant to Chapter Four 198

Appendix 5: X-Ray Crystallography Report Relevant to Chapter Four 215
A.5.1 X-Ray Crystallography Report for Pentacycle **106** 216

Appendix 6: Notebook Cross-Reference 225

Bibliography 228
Index 239
About the Author 240

List of Figures

CHAPTER 1

Figure 1.1.1.1 Actinophyllic Acid 2

CHAPTER 2

Figure 2.1.2.1 Vinyl Grignard Addition Side Products 20

APPENDIX 1

Figure A.1.1 ^{1}H NMR spectrum (400 MHz, DMSO-d_6) of compound **31** 51
Figure A.1.2 FTIR spectrum (NaCl/thin film) of compound **31** 52
Figure A.1.3 ^{13}C NMR spectrum (100 MHz, DMSO-d_6) of compound **31** 52
Figure A.1.4 ^{1}H NMR spectrum (400 MHz, $CDCl_3$) of compound **32** 53
Figure A.1.5 FTIR spectrum (NaCl/thin film) of compound **32** 54
Figure A.1.6 ^{13}C NMR spectrum (100 MHz, $CDCl_3$) of compound **32** 54
Figure A.1.7 ^{1}H NMR spectrum (400 MHz, $CDCl_3$) of compound **33** 55
Figure A.1.8 FTIR spectrum (NaCl/thin film) of compound **33** 56
Figure A.1.9 ^{13}C NMR spectrum (100 MHz, $CDCl_3$) of compound **33** 56
Figure A.1.10 ^{1}H NMR spectrum (400 MHz, $CDCl_3$) of compound **34** 57
Figure A.1.11 FTIR spectrum (NaCl/thin film) of compound **34** 58
Figure A.1.12 ^{13}C NMR spectrum (100 MHz, $CDCl_3$) of compound **34** 58
Figure A.1.13 ^{1}H NMR spectrum (400 MHz,$CDCl_3$) of compound **40** 59
Figure A.1.14 FTIR spectrum (NaCl/thin film) of compound **40** 60
Figure A.1.15 ^{13}C NMR spectrum (100 MHz, $CDCl_3$) of compound **40** 60
Figure A.1.16 ^{1}H NMR spectrum (400 MHz, $CDCl_3$) of compound **42** 61
Figure A.1.17 FTIR spectrum (NaCl/thin film) of compound **42** 62
Figure A.1.18 ^{13}C NMR spectrum (100 MHz, $CDCl_3$) of compound **42** 62
Figure A.1.19 ^{1}H NMR spectrum (400 MHz, $CDCl_3$) of compound **43** 63
Figure A.1.20 FTIR spectrum (NaCl/thin film) of compound **43** 64
Figure A.1.21 ^{13}C NMR spectrum (100 MHz, $CDCl_3$) of compound **43** 64
Figure A.1.22 ^{1}H NMR spectrum (400 MHz, $CDCl_3$) of compound **41** 65
Figure A.1.23 FTIR spectrum (NaCl/thin film) of compound **41** 66
Figure A.1.24 ^{13}C NMR (100 MHz, $CDCl_3$) spectrum of compound **41** 66
Figure A.1.25 ^{1}H NMR (400 MHz, Benzene-d_6) spectrum of compound **46** 67
Figure A.1.26 FTIR spectrum (NaCl/thin film) of compound **46** 68
Figure A.1.27 ^{13}C NMR (100 MHz, Benzene-d_6) spectrum of compound **46** 68
Figure A.1.28 ^{1}H NMR spectrum (400 MHz, $CDCl_3$) of compound **44** 69
Figure A.1.29 FTIR spectrum (NaCl/thin film) of compound **44** 70
Figure A.1.30 ^{13}C NMR spectrum (100 MHz, $CDCl_3$) of compound **44** 70
Figure A.1.31 ^{1}H NMR spectrum (400 MHz, $CDCl_3$) of compound **39** 71
Figure A.1.32 FTIR spectrum (NaCl/thin film) of compound **39** 72
Figure A.1.33 ^{13}C NMR spectrum (100 MHz, $CDCl_3$) of compound **39** 72
Figure A.1.34 ^{1}H NMR spectrum (400 MHz, $CDCl_3$) of compound **37** 73
Figure A.1.35 FTIR spectrum (NaCl/thin film) of compound **37** 74
Figure A.1.36 ^{13}C NMR spectrum (100 MHz, $CDCl_3$) of compound **37** 74
Figure A.1.37 ^{1}H NMR spectrum (400 MHz, $CDCl_3$) of compound **49** 75
Figure A.1.38 FTIR spectrum (NaCl/thin film) of compound **49** 76
Figure A.1.39 ^{13}C NMR spectrum (100 MHz, $CDCl_3$) of compound **49** 76

Figure A.1.40 ^{1}H NMR spectrum (400 MHz, $CDCl_3$) of compound **50** 77
Figure A.1.41 FTIR spectrum (NaCl/thin film) of compound **50** 78
Figure A.1.42 ^{13}C NMR spectrum (100 MHz, $CDCl_3$) of compound **50** 78
Figure A.1.43 ^{1}H NMR spectrum (400 MHz, $CDCl_3$) of compound **51** 79
Figure A.1.44 FTIR spectrum (NaCl/thin film) of compound **51** 80
Figure A.1.45 ^{13}C NMR spectrum (126 MHz, $CDCl_3$) of compound **51** 80

APPENDIX 2

Figure A.2.1 ^{1}H NMR spectrum (400 MHz, $CDCl_3$) of compound **52**. 114
Figure A.2.2 FTIR spectrum (NaCl/thin film) of compound **52**. 115
Figure A.2.3 ^{13}C NMR spectrum (100 MHz, $CDCl_3$) of compound **52**. 115
Figure A.2.4 ^{1}H NMR spectrum (400 MHz, $CDCl_3$) of compound **53**. 116
Figure A.2.5 FTIR spectrum (NaCl/thin film) of compound **53**. 117
Figure A.2.6 ^{13}C NMR spectrum (100 MHz, $CDCl_3$) of compound **53**. 117
Figure A.2.7 ^{1}H NMR spectrum (400 MHz, $CDCl_3$) of compound **54**. 118
Figure A.2.8 FTIR spectrum (NaCl/thin film) of compound **54**. 119
Figure A.2.9 ^{13}C NMR spectrum (100 MHz, $CDCl_3$) of compound **54**. 119
Figure A.2.10 ^{1}H NMR spectrum (400 MHz, $CDCl_3$) of compound **55**. 120
Figure A.2.11 FTIR spectrum (NaCl/thin film) of compound **55**. 121
Figure A.2.12 ^{13}C NMR spectrum (100 MHz, $CDCl_3$) of compound **55**. 121
Figure A.2.13 ^{1}H NMR spectrum (400 MHZ, $CDCl_3$) of compound **58**. 122
Figure A.2.14 FTIR spectrum (NaCl/thin film) of compound **58**. 123
Figure A.2.15 ^{13}C NMR spectrum (100 MHz, $CDCl_3$) of compound **58**. 123
Figure A.2.16 ^{1}H NMR spectrum (400 MHz, $CDCl_3$) of compound **57**. 124
Figure A.2.17 FTIR spectrum (NaCl/thin film) of compound **57**. 125
Figure A.2.18 ^{13}C NMR spectrum (100 MHz, $CDCl_3$) of compound **57**. 125
Figure A.2.19 ^{1}H NMR spectrum (400 MHz, $CDCl_3$) of compound **56**. 126
Figure A.2.20 FTIR spectrum (NaCl/thin film) of compound **56**. 127
Figure A.2.21 ^{13}C NMR spectrum (100 MHz, $CDCl_3$) of compound **56**. 127
Figure A.2.22 ^{1}H NMR spectrum (400 MHz, $CDCl_3$) of compound **59**. 128
Figure A.2.23 FTIR spectrum (NaCl/thin film) of compound **59**. 129
Figure A.2.24 ^{13}C NMR spectrum (100 MHz, $CDCl_3$) of compound **59**. 129
Figure A.2.25 ^{1}H NMR spectrum (400 MHz, $CDCl_3$) of compound **60**. 130
Figure A.2.26 FTIR spectrum (NaCl/thin film) of compound **60**. 131
Figure A.2.27 ^{13}C NMR spectrum (100 MHz, $CDCl_3$) of compound **60**. 131
Figure A.2.28 ^{1}H NMR spectrum (400 MHz, $CDCl_3$) of compound **61** 132
Figure A.2.29 FTIR spectrum (NaCl/thin film) of compound **61** 133
Figure A.2.30 ^{13}C NMR spectrum (100 MHz, $CDCl_3$) of compound **61** 133
Figure A.2.31 ^{1}H NMR spectrum (400 MHz, $CDCl_3$) of **63** 134
Figure A.2.32 FTIR spectrum (NaCl/thin film) of **63** 135
Figure A.2.33 ^{13}C NMR spectrum (100 MHz, $CDCl_3$) of **63**. 135
Figure A.2.34 ^{1}H NMR spectrum (400 MHz, $CDCl_3$) of compound **64**. 136
Figure A.2.35 FTIR spectrum (NaCl/thin film) of compound **64**. 137
Figure A.2.36 ^{13}C NMR spectrum (100 MHz, $CDCl_3$) of compound **64** 137
Figure A.2.37 ^{1}H NMR spectrum (400MHz, $CDCl_3$) of compound **62**. 138
Figure A.2.38 FTIR spectrum (NaCl/thin film) of compound **62** 139
Figure A.2.39 ^{13}C NMR spectrum (100MHz, $CDCl_3$) of compound **62**. 139
Figure A.2.40 ^{1}H NMR spectrum (400MHz, $CDCl_3$) of compound **65**. 140
Figure A.2.41 FTIR spectrum (NaCl/thin film) of compound **65** 141

Figure A.2.42 ^{13}C NMR spectrum (100 MHz,, $CDCl_3$) of compound **65**. 141
Figure A.2.43 ^{1}H NMR spectrum (400 MHz, $CDCl_3$) of compound **66**. 142
Figure A.2.44 FTIR spectrum (NaCl/thin film) of compound **66** 143
Figure A.2.45 ^{13}C NMR spectrum (100 MHz, $CDCl_3$) of compound **66**. 143
Figure A.2.46 ^{1}H NMR spectrum (400 MHz, $CDCl_3$) of compound **70**. 144
Figure A.2.47 FTIR spectrum (NaCl/thin film) of compound **70**. 145
Figure A.2.48 ^{13}C NMR spectrum (100 MHz, $CDCl_3$) of compound **70**. 145
Figure A.2.49 ^{1}H NMR spectrum (400 MHz, $CDCl_3$) of compound **69**. 146
Figure A.2.50 FTIR spectrum (NaCl/thin film) of compound **69**. 147
Figure A.2.51 ^{13}C NMR (100 MHz, $CDCl_3$) spectrum of compound **69**. 147
Figure A.2.52 ^{1}H NMR spectrum (400 MHz, Benzene-d_6) of compound **71**. 148
Figure A.2.53 FTIR spectrum (NaCl/thin film) of compound **71**. 149
Figure A.2.54 ^{13}C NMR spectrum (100 MHz, Benzene-d_6) of compound **71**. 149

CHAPTER 4

Figure 4.2.1.1 Bis-Alkylation Strategy. 175
Figure 4.2.3.1 Aminal Stability. 180

APPENDIX 4

Figure A.4.1 ^{1}H NMR spectrum (400 MHz, $CDCl_3$) of compound **87**. 199
Figure A.4.2 FTIR spectrum (NaCl/thin film) of compound **87**. 200
Figure A.4.3 ^{13}C NMR spectrum (100 MHz, $CDCl_3$) of compound **87**. 200
Figure A.4.4 ^{1}H NMR (400 MHz, Benzene-d_6) spectrum of **89**. 201
Figure A.4.5 FTIR spectrum (NaCl/thin film) of compound **89**. 202
Figure A.4.6 ^{13}C NMR spectrum (100 MHz, Benzene-d_6) of compound **89**. 202
Figure A.4.7 ^{1}H NMR spectrum (400 MHz, $CDCl_3$) of compound **92**. 203
Figure A.4.8 FTIR spectrum (NaCl/thin film) of compound **92**. 204
Figure A.4.9 ^{13}C NMR spectrum (100 MHz, $CDCl_3$) of compound **92**. 204
Figure A.4.10 ^{1}H NMR spectrum (400 MHz, $CDCl_3$) of compound **93**. 205
Figure A.4.11 FTIR spectrum (NaCl/thin film) of compound **93**. 206
Figure A.4.12 ^{13}C NMR spectrum (100 MHz, $CDCl_3$) of compound **93**. 206
Figure A.4.13 ^{1}H NMR spectrum (400 MHz, $CDCl_3$) of compound **103**. 207
Figure A.4.14 FTIR spectrum (NaCl/thin film) of compound **103**. 208
Figure A.4.15 ^{13}C NMR spectrum (100 MHz, $CDCl_3$) of compound **103**. 208
Figure A.4.16 ^{1}H NMR spectrum (400 MHz, DMSO-d_6) of compound **104**. 209
Figure A.4.17 FTIR spectrum (KBr pellet) of compound **104**. 210
Figure A.4.18 ^{13}C NMR spectrum (100 MHz, DMSO-d_6) of compound **104**. 210
Figure A.4.19 ^{1}H NMR spectrum (400 MHz, $CDCl_3$) of compound **106**. 211
Figure A.4.20 FTIR spectrum (NaCl/thin film) of compound **106**. 212
Figure A.4.21 ^{13}C NMR spectrum (100 MHz, $CDCl_3$) of compound **106**. 212
Figure A.4.22 ^{1}H NMR spectrum (400 MHz, $CDCl_3$) of compound **109**. 213
Figure A.4.23 FTIR spectrum (NaCl/thin film) of compound **109**. 214
Figure A.4.24 ^{13}C NMR spectrum (100 MHz, $CDCl_3$) of compound **109**. 214

List of Schemes

CHAPTER 1

Scheme 1.1.2.1 Regulation of Fibrin 4
Scheme 1.1.3.1 CPU/Hippuricase Coupled Enzyme Assay 10
Scheme 1.1.4.1 Related Natural Products 10
Scheme 1.2.1.1 Proposed Biosynthesis 11
Scheme 1.3.1.1 Martin's Synthetic Efforts 13
Scheme 1.3.2.1 Overman's Total Synthesis 14
Scheme 1.3.3.1 Elucidation of Absolute Stereochemistry 15

CHAPTER 2

Scheme 2.1.1.1 Polycyclic Framework and Initial Disconnections 16
Scheme 2.1.1.2 Retrosynthetic Analysis 17
Scheme 2.1.2.1 Preparation of Allyl Indolemalonate **34** 18
Scheme 2.1.2.2 a) Elaboration of **34** *via* Aldol Strategy 19
Scheme 2.1.2.2 b) Elaboration of **34** *via* Ring-Closing Metathesis Strategy 19
Scheme 2.1.2.3 Vinyl Grignard Addition to **34** 20
Scheme 2.1.2.4 Side Product Formation 21
Scheme 2.1.2.5 Preparation of Metathesis Precursor 21
Scheme 2.1.3.1 Unexpected Cyclopropane Formation 23
Scheme 2.1.3.2 Plausible Mechanism to Yield **46** 24
Scheme 2.1.4.1 Preparation of Enone **37** and **49** 25
Scheme 2.1.4.2 Challenges Associated with Route 26
Scheme 2.1.5.1 Oxidative Transposition Pathways 26
Scheme 2.1.5.2 Acid Mediated Isomerization of **39** 27

CHAPTER 3

Scheme 3.1.1.1 Preparation of Allyl Indolemalonate **53** 82
Scheme 3.1.1.2 Preparation of Allylic Alcohol **55** 82
Scheme 3.1.1.3 Oxidative Transposition of **55** 83
Scheme 3.1.1.4 Formation of Bridged Bicycle **56** 83
Scheme 3.1.2.1 Synthesis of Allylic Alcohol **62** 84
Scheme 3.1.2.2 Instability of Diene **61** 85
Scheme 3.1.2.3 Preparation of Enone **65** 86
Scheme 3.1.3.1 Aromatization of Enone **65** 86
Scheme 3.1.3.2 Plausible Mechanism for Aromatization of Enone **65** 87
Scheme 3.1.3.3 Aza-Michael Reaction to Install Tertiary Amine 88
Scheme 3.1.3.4 Strategy to Elaborate Silyl Enol Ether **71** 89
Scheme 3.1.3.5 Attempts to Oxidize Silyl Enol Ether **71** 90

CHAPTER 4

Scheme 4.1.1.1 Proposed Radical Cyclization of a Functionalized Intermediate 165
Scheme 4.1.2.1 Updated Retrosynthetic Analysis 166
Scheme 4.1.3.1 Cleavage of Acetal and β-Keto Ester Functionalities 167
Scheme 4.1.3.2 Unexpected Preparation of Lactone **87** 168
Scheme 4.1.4.1 Proposed Radical Cyclization of Lactone **87** 170
Scheme 4.1.4.2 Oxidation of Lactone **87** with Ceric Ammonium Nitrate 171

Scheme 4.1.4.3 Proposed Cyclization of **87** under Ionic Conditions..... 172
Scheme 4.1.4.4 Preparation of Bromo Malonate **92**..... 172
Scheme 4.1.4.5 Isolation of Bromo Acetal **93** as a Minor Product..... 173
Scheme 4.1.4.6 Attempted Elaboration of Bromo Acetal **93** 174
Scheme 4.2.1.1 Final Retrosynthetic Analysis 175
Scheme 4.2.2.1 Literature Precedent for Enamine Trapping of Reactive Intermediates176
Scheme 4.2.2.2 Proposed Enamine Bis-Alkylation Strategy..... 177
Scheme 4.2.2.3 Proposed Equilibration of Two Reactive Enamine Intermediates 177
Scheme 4.2.3.1 Preparation of Chloro Indolemalonate **104**..... 178
Scheme 4.2.3.2 Key Step and Preparation of Pentacycle **106** 179
Scheme 4.2.3.3 Proposed Mechanism for Formation of **106** 179
Scheme 4.2.3.4 Elaboration of Pentacycle **106** to Carbamate **109**..... 181

List of Tables

APPENDIX 3

Table A.3.1.1 Crystal Data and Structure Refinement for Compound **71** 151
Table A.3.1.2 Atomic Coordinates for Compound **71** 153
Table A.3.1.3 Bond Lengths and Angles for Compound **71** 155
Table A.3.1.4 Anisotropic Displacement Parameters for Compound **71** 159
Table A.3.1.5 Hydrogen Coordinates for Compound **71** 161

APPENDIX 5

Table A.5.1.1 Crystal Data and Structure Refinement for Compound **106** 216
Table A.5.1.2 Atomic Coordinates for Compound **106** 218
Table A.5.1.3 Bond Lengths and Angles for Compound **106** 219
Table A.5.1.4 Anisotropic Displacement Parameters for Compound **106** 222
Table A.5.1.5 Hydrogen Coordinates for Compound **106** 223

LIST OF ABBREVIATIONS

Ac	acetyl, acetate
aq.	aqueous
Bn	benzyl
BOC	*tert*-butoxycarbonyl
br	broad
t-Bu	*tert*-butyl
BuLi	butyl lithium
calc'd	calculated
CAN	ammonium cerium(IV) nitrate
ca.	circa
cat.	catalytic
CI	chemical ionization
δ	chemical shift downfield from $(CH_3)_4Si$
d	doublet
dd	doublet of doublets
ddd	doublet of doublet of doublets
DCM	dichloromethane
DCE	dichloroethane
DMAP	*N*,*N*-dimethylaminopyridine
DMF	*N*,*N*-dimethylformamide
DMSO	dimethylsulfoxide
DMS	dimethylsulfide
dt	doublet of triplets
ESI+	electrospray, positive ionization mode
equiv	equivalent
Et_3N	triethylamine
Et_2O	diethyl ether

EtOAc	ethyl acetate
FTIR	Fourier transform infrared
h	hour
[H]	reductant
HRMS	high-resolution mass spectrometry
hrs	hours
$h\nu$	light
Hz	hertz
IPA	*iso*-propyl alcohol
IR	infrared
J	coupling constant
LDA	lithium diisopropylamide
LHMDS	lithium bis(trimethylsilyl)amide
m	multiplet or medium
MHz	megahertz
min.	minute(s)
mmol	millimole
MeCN	acetonitrile
NBS	*N*-bromosuccinimide
nfom	non-first order multiplet
NMR	nuclear magnetic resonance
Nu	nucleophile
[O]	oxidant
OAc	acetate
OMs	mesylate
OTf	triflate
PCC	pyridinium chlorochromate
PhH	benzene
PhMe	toluene
PPh_3	triphenylphosphine

ppm	part per million
PPTS	pyridinium *p*-toluenesulfonic acid
i-Pr	*iso*-propyl
pyr	pyridine
q	quartet
s	singlet or strong
t	triplet
TBS	*tert*-butyldimethylsilyl
THF	tetrahydrofuran
TIPS	triisopropylsilyl
TLC	thin layer chromatography
TMS	trimethylsilyl
p-TsOH	*p*-toluenesulfonic acid
UV	ultraviolet
w	weak
Δ	heat at reflux

CHAPTER ONE

Actinophyllic Acid: A Bridged Polycyclic Indole Alkaloid Natural Product from *Alstonia actinophylla*

1.1 Introduction and Background

1.1.1 Isolation and Biological Activity

Polycyclic natural products containing the indole nucleus are abundant and often possess biological activity.[1] Actinophyllic acid **1** (Figure 1.1.1.1), isolated from the leaves of *Alstonia actinophylla* in 2005, displays a novel bridged polycyclic framework including indole, cycloheptane, pyrrolidine, azacyclooctane, and γ-butyrolactol rings.[2] Prior to characterization, actinophyllic acid was recognized to inhibit carboxypeptidase U (CPU) with an IC_{50} of 0.84 μM using a CPU/hippuricase coupled enzyme assay. Within the highly regulated hemostatic process CPU suppresses the removal of blood clots from blood vessels.[3] This enzyme has garnered considerable attention over the last 10 years as it provides an exploitable link between the mechanism of blood clot formation and clot removal.[4] Compounds that inhibit CPU are of interest for preventing or alleviating

cardiovascular disorders ranging from heart attack, stroke, pulmonary embolism, and deep vein thrombosis.[5]

Figure 1.1.1.1

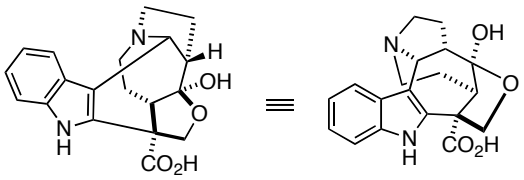

(–)-**1** Actinophyllic Acid

1.1.2 The Role of CPU in Fibrinolysis

CPU is an enzyme inhibitor of fibrinolysis, which is the natural process of blood clot removal from blood vessels.[4] One component of blood clots is fibrin, which exists in the form of fibrin polymers. The regulated formation and removal of fibrin is depicted in Scheme 1.1.2.1. Fibrin is generated by the action of thrombin on fibrinogen and conversely is degraded by the peptidase plasmin. The enzyme plasmin is derived from plasminogen through actions of tissue PLG activator (tPA) and urokinase (uPA). The initial degradation of fibrin by plasmin exposes lysine residues on the remaining fibrin scaffold. These exposed residues act to promote further plasmin production and thus enhance fibrin destruction through a positive feedback loop. To counter this, CPU suppresses plasmin activity. This occurs by CPU-mediated cleavage of the exposed lysine residues on fibrin, thus interrupting the positive feedback loop and limiting further plasmin production. CPU itself is derived from procarboxypeptidase U through activation

by thrombin and, therefore, connects the mechanisms of clot formation and clot removal.

Scheme 1.1.2.1

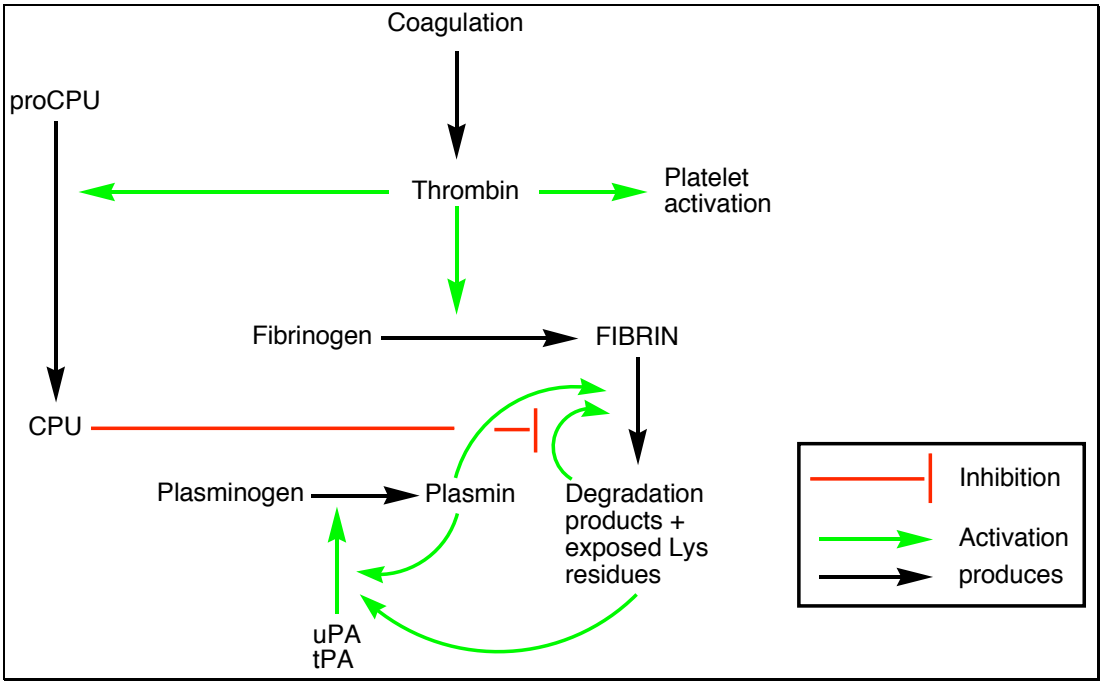

1.1.3 CPU/Hippuricase Coupled Enzyme Assay Irregularity

The inhibition of CPU by actinophyllic acid was determined indirectly through the use of a coupled CPU/Hippuricase assay.[2] This assay involved the initial hydrolysis of 4-hydroxyhippurylarginine by CPU to 4-hydroxyhippuric acid. This product, in turn, was hydrolyzed to 4-hydroxybenzoic acid by Hippuricase (Scheme 1.1.3.1). Enzyme activity was monitored by the observation of a red quinoneimine dye formed through the oxidative coupling of 4-hydroxybenzoic acid and 4-aminoantipyrine. Thus, 4-aminoantipyrine was necessary to observe

the results for the coupled CPU/Hippuricase assay. However, it was found that actinophyllic acid did not inhibit CPU when a different CPU assay was conducted which excluded 4-aminoantipyrine by isolating the substrate and products by HPLC. These conflicting results indicate that an actinophyllic acid:4-aminoantipyrine adduct may be responsible for CPU inhibition *in vitro*.

Scheme 1.1.3.1

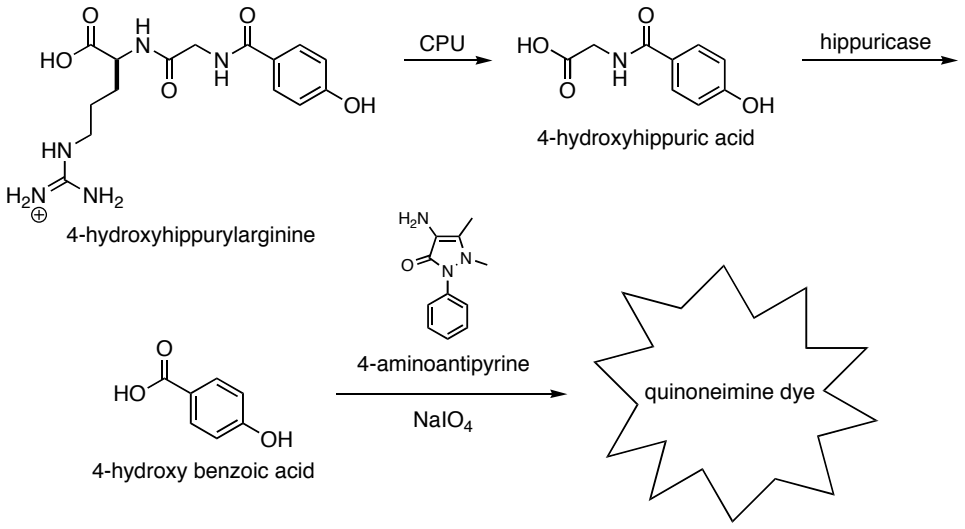

1.1.4 Related Natural Products

As noted in the isolation paper, actinophyllic acid possesses a unique architecture. Focusing on the tertiary amine functionality revealed similarity to other alkaloid natural products. Included in this group are uleine[6] and its derivatives,[7-9] dasycarpidone[9] and its derivatives,[7,9] ervitsine,[10] gilbertin,[11] undulifoline,[12] tronoharine,[13] pausperadine,[14] and alstilobanines B & C which possess moderate vasorelaxant activity (Scheme 1.1.4.1).[15]

Scheme 1.1.4.1

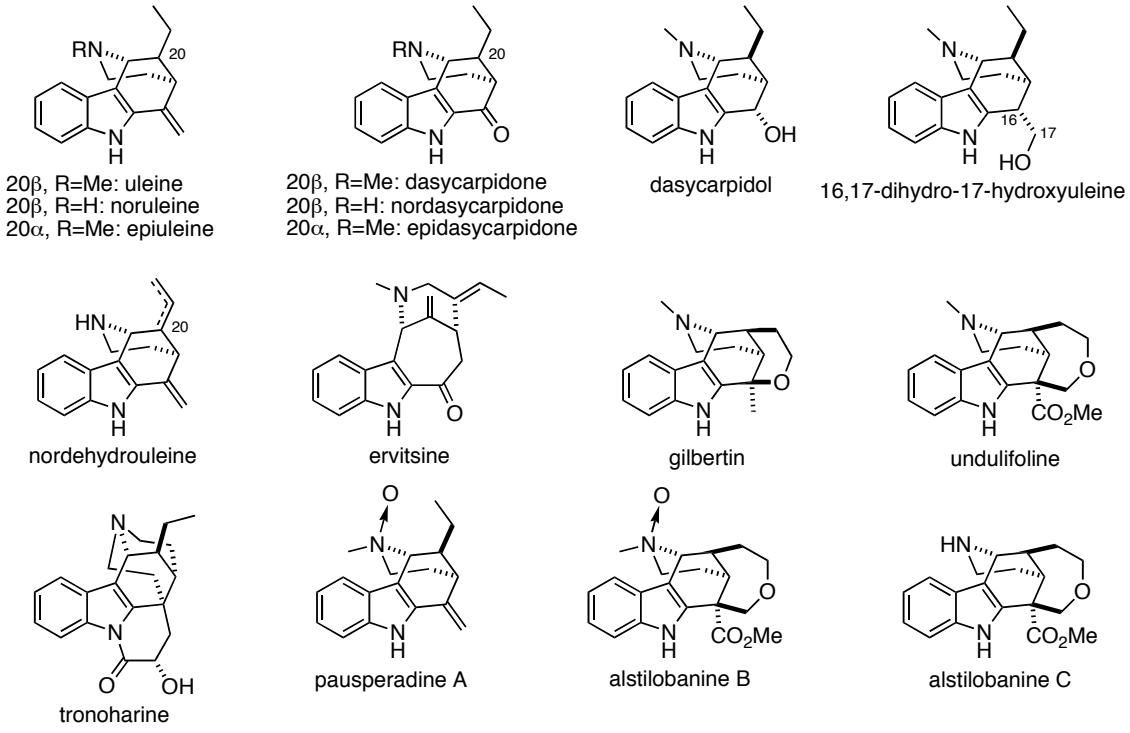

1.2 Proposed Biosynthesis

1.2.1 Derived from Precondylocarpine

A proposed biosynthesis for actinophyllic acid was included with the disclosed isolation and structure elucidation (Scheme 1.2.1.1).[2] The common precursors tryptamine and (–)-secologanin glucoside were used as a starting point based upon the monoterpene indole alkaloid's isolation from a tree of the family Apocynaceae.[2] An initial condensation is proposed to produce the known alkaloid geissoschizine, which could rearrange via a stemmadenine iminium

cation to the alkaloid precondylocarpine. Subsequent epoxidation to **2** and elimination would furnish tertiary allylic alcohol **3**. A second epoxidation event to form **4** would precede a Grob-type fragmentation producing an intermediate **5** poised for an ensuing intramolecular Mannich reaction. Following cyclization to yield **6**, an oxidation sequence is imagined to result in β-keto acid **7**, which could decarboxylate to enol intermediate **8**. Rearomatization of the indole nucleus could deliver a carbocation (**9**), which is trapped intramolecularly by the pendant enol to arrive at intermediate **10**. A final methyl ester hydrolysis and acetal formation completes the proposed biosynthesis.

Scheme 1.2.1.1

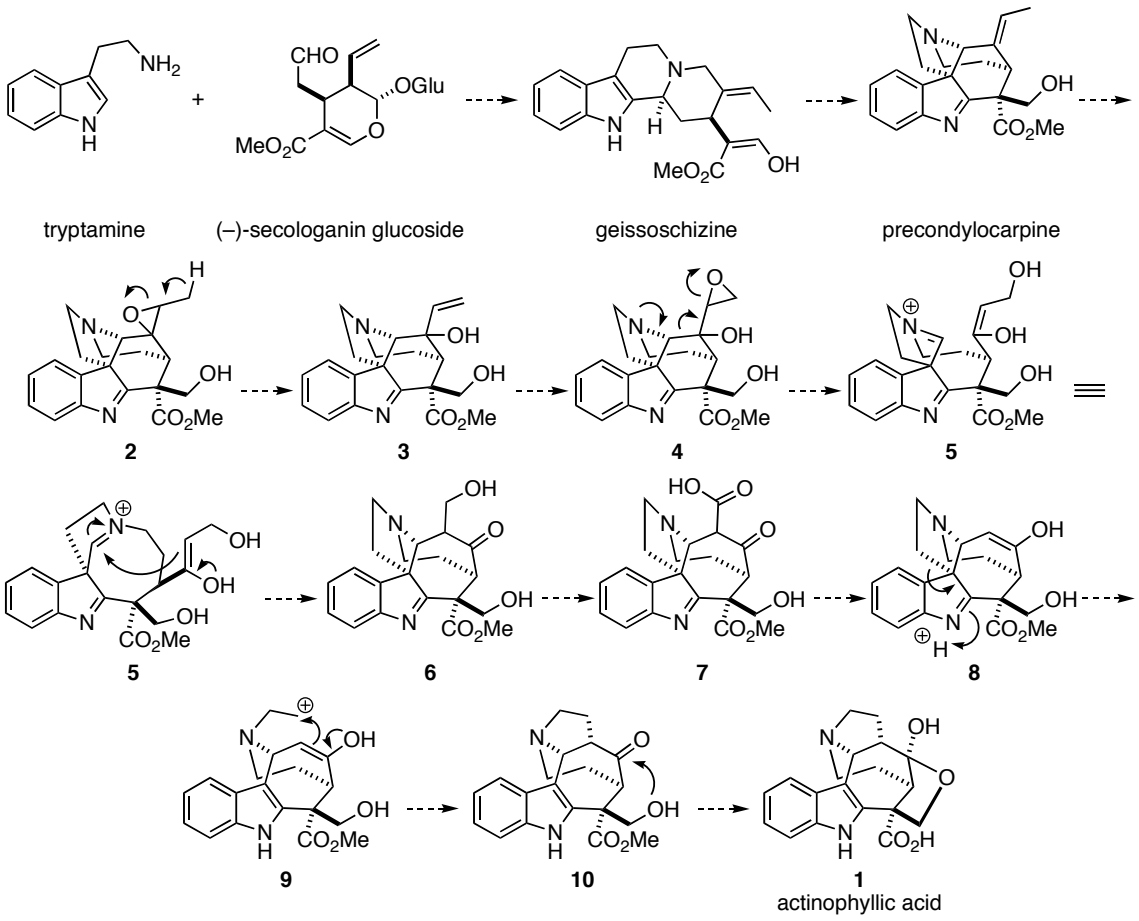

1.3 Previous Synthetic Studies

1.3.1 Martin's Effort toward Actinophyllic Acid

The laboratory of Professor Stephen Martin outlined a route toward actinophyllic acid in a dissertation by C.-L. Chen, which proposed to utilize an oxidative Mannich reaction to install the bridged polycyclic framework (Scheme 1.3.1.1).[16] Disclosure of preliminary results revealed that the synthesis began with a Knoevenagel condensation to provide malonate **11**. Conjugate addition

with an alkynylcuprate species in the presence of TMSCl allowed isolation of alkyne **12**. This intermediate was elaborated in two steps to alkynyl aniline **13**, which underwent dealkoxycarbonylation yielding aniline **14**. Lastly, a Au(III) catalyzed cycloisomerization produced indole intermediate **15** as the most advanced substrate toward actinophyllic acid. Proposed future work included a Mannich reaction sequence to install an azacycloheptane ring (**16**) and further elaboration to explore the key intramolecular oxidative Mannich reaction.

Scheme 1.3.1.1

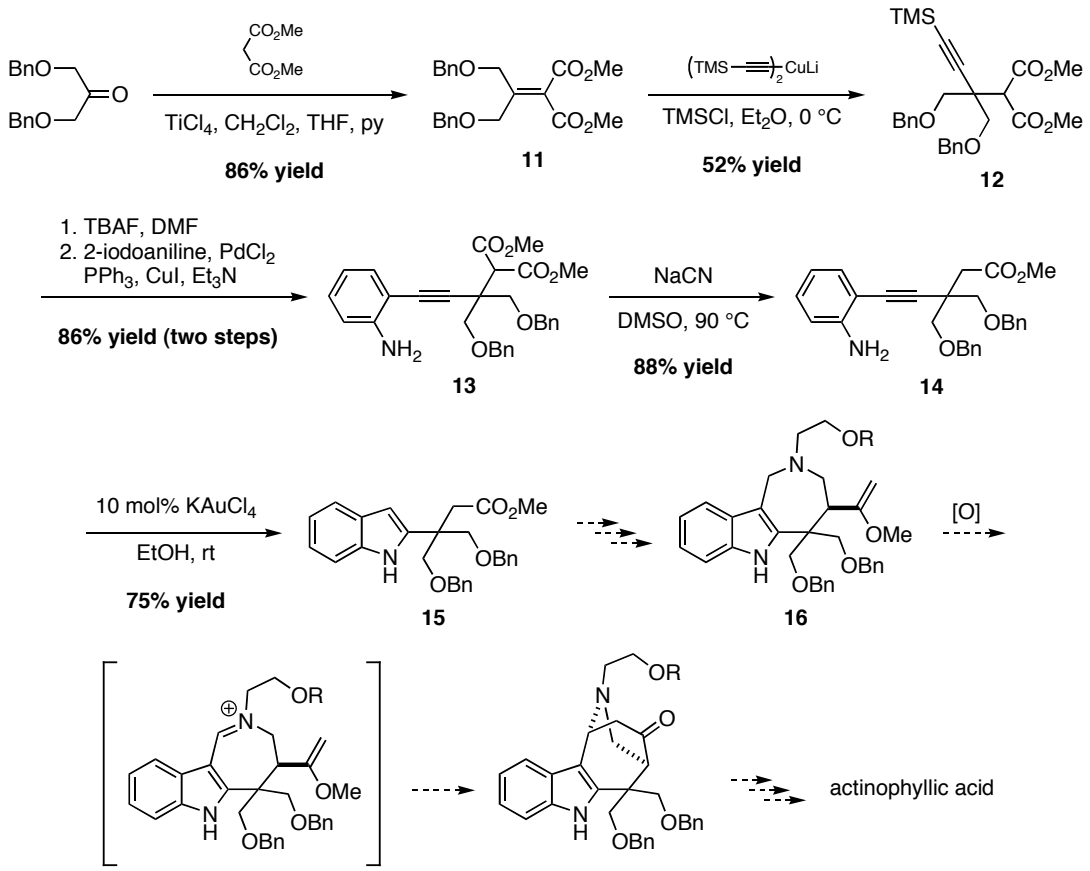

1.3.2 Overman's Total Synthesis of Actinophyllic Acid

During the course of our investigations the laboratory of Professor Larry Overman published an impressive first total synthesis of actinophyllic acid.[17] The route relied upon an oxidative coupling between malonate and ketone carbanions to establish an advanced intermediate, which was further elaborated for a key aza-Cope/Mannich sequence to construct the complex polycyclic carbon core (Scheme 1.3.2.1). In the forward sense, di-*tert*-butyl malonate was advanced in two steps to β-keto diester **17**. Reduction of the nitro functionality led to spontaneous indole formation (**18**) and subsequent reaction with *N*-Boc bromopiperidone **19** provided gram quantities of indole **20**. The Overman lab formed bridged polycyclic intermediate **21** *via* an intramolecular oxidative coupling of ketone and malonate carbanions. Elaboration of intermediate **21** occurred through stereoselective addition of vinylcerium to the bridged ketone furnishing tertiary allylic alcohol **22**. Treatment of this intermediate with TFA removed the Boc group and exposure to paraformaldehyde initiated an aza-Cope/Mannich sequence to construct a polycyclic compound. This intermediate was elaborated to indole **23** as a 1:1 mixture of methyl ester epimers in the same pot. The first total synthesis of actinophyllic acid was completed in two additional steps through ester enolate alkylation with monomeric formaldehyde and methyl ester hydrolysis.

Scheme 1.3.2.1

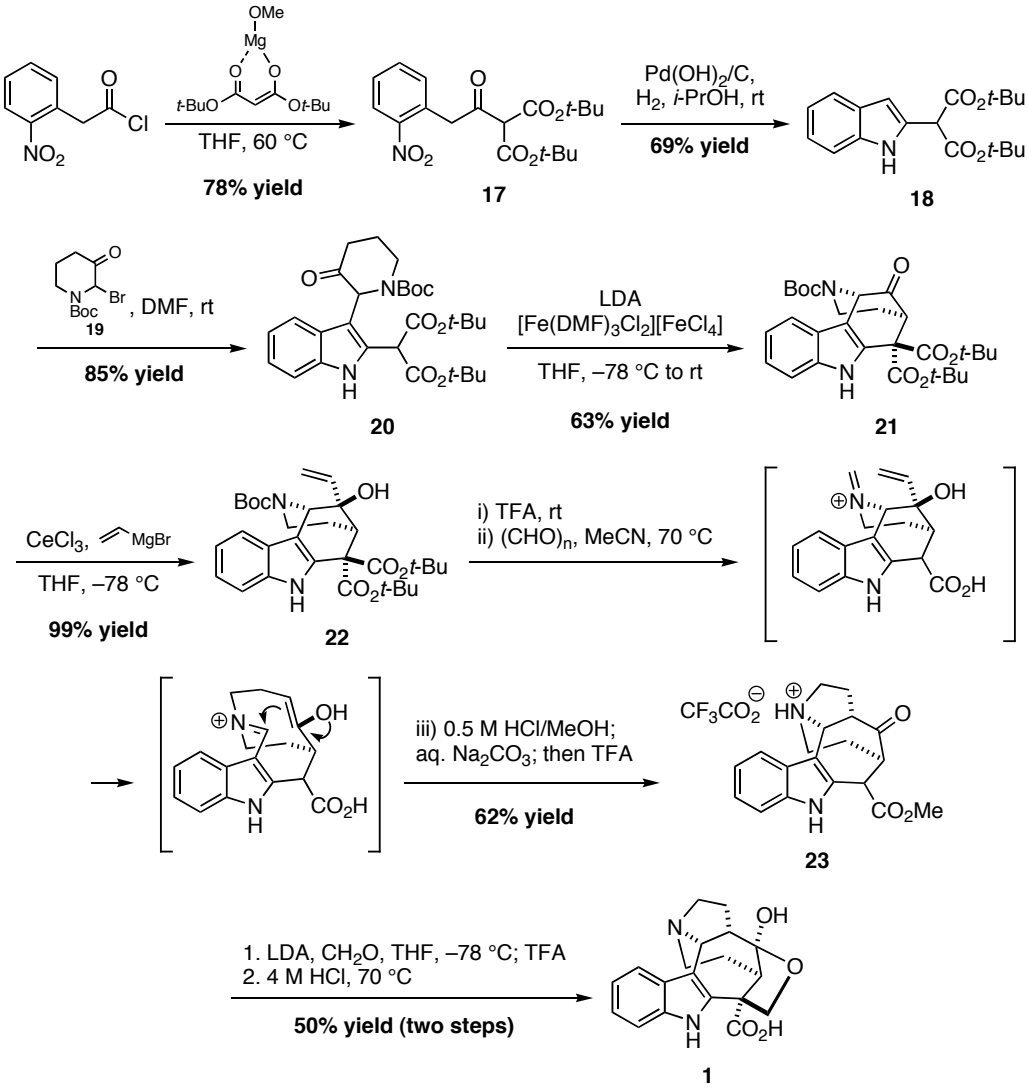

1.3.3 Determination of Absolute Stereochemistry

Following the first total synthesis of actinophyllic acid was a report of the absolute configuration based upon optical rotation and electronic circular dichroism of the separated methyl ester enantiomers (+)-**24** and (–)-**25** (Scheme 1.3.3.1).[18] Experiments were performed on the methyl ester substrates as

opposed to synthetic actinophyllic acid due to anticipation that intermolecular interactions provide data that could deviate from calculations for a single molecule. Based upon the spectroscopic data and chemical correlation between (–)-**25** and (–)-**1**, the absolute configuration of natural actinophyllic acid was assigned as 15*R*,16*S*,19*S*,20*S*,21*R*. This assignment supports Carroll's proposed biosynthesis starting from tryptamine and (–)-secologanin glucoside.

Scheme 1.3.3.1

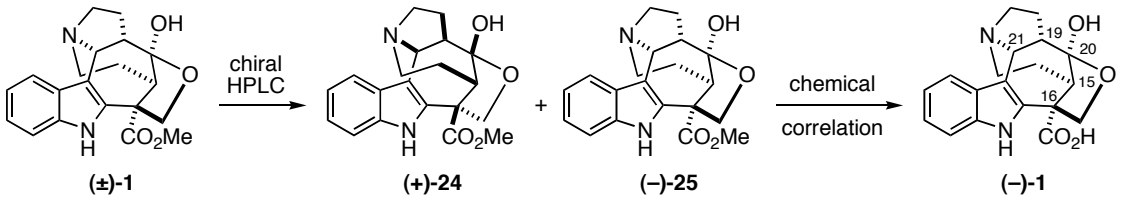

1.4 Summary

The indole alkaloid actinophyllic acid, isolated in 2005, has been shown to possess biological activity relevant to cardiovascular disorders through its action on CPU, an enzyme active in hemostasis. The unique structure of actinophyllic acid, in addition to its therapeutic potential, prompted the Wood group to pursue a total synthesis of this target. In addition to our own efforts two other groups have documented synthetic strategies toward actinophyllic acid, one of which led to the first total synthesis. This achievement, from the laboratory of Professor

Larry Overman, provided synthetic material used in experimentation that led to an assignment of actinophyllic acid's absolute stereochemistry.

1.5 Notes and References

1. (a) *"Indole Alkaloids in Medicine"*, Ban, Y.; Murakami, Y.; Iwasawa, Y.; Tsuchiya, M.; Takano, N. *Med. Res. Rev.* **1988**, *8*, 231–308; (b) *"Biologically-Active Indole-Derivatives"*, Joshi, K. C.; Chand, P. *Pharmazie* **1982**, *37*, 1–12.
2. *"Actinophyllic Acid, a Potent Indole Alkaloid Inhibitor of the Coupled Enzyme Assay Carboxypeptidase U/Hippuricase from the Leaves of Alstonia actinophylla (Apocynaceae)"*, Carroll, A. R.; Hyde, E.; Smith, J.; Quinn, R. J.; Guymer, G.; Forster, P. I. *J. Org. Chem.* **2005**, *70*, 1096–1099.
3. (a) *"Carboxypeptidase U (TAFIa) Prevents Lysis from Proceeding into the Propagation Phase through a Threshold-Dependent Mechanism"*, Leurs, J.; Nerme, V.; Sim, Y.; Hendriks, D. *J. Thromb. Haemostasis* **2004**, *2*, 416–423; (b) *"On the Mechanism of the Antifibrinolytic Activity of Plasma Carboxypeptidase B"*, Sakharov, D. V.; Plow, E. F.; Rijken, D. C. *J. Biol. Chem.* **1997**, *272*, 14477–14482; (c) *"A Study of the Mechanism of Inhibition of Fibrinolysis by Activated Thrombin-Activatable Fibrinolysis*

Inhibitor", Wang, W.; Boffa, M. B.; Bajzar, L.; Walker, J. B.; Nesheim, M. E. *J. Biol. Chem.* **1998**, *273*, 27176–27181.

4. *"Molecular Mechanisms of Fibrinolysis"*, Cesarman-Maus, G.; Hajjar, K. A. *Br. J. Haematol.* **2005**, *129*, 307–321.

5. (a) *"Diseases of the Veins"*, Beckman, J. A. *Circulation* **2002**, *106*, 2170–2172; (b) *"Treatment of Blood Clots"*, Goldhaber, S. Z.; Grasso-Correnti, N. *Circulation* **2002**, *106*, e138–e140.

6. *"The Structure Of Uleine"*, Buchi, G.; Warnhoff, E. W. *J. Am. Chem. Soc.* **1959**, *81*, 4433–4434.

7. *"Structure Of Uleine-Relative Stereochemistry"*, Gaskell, A. J.; Joule, J. A. *Chem. Ind. (London)* **1967**, 1089.

8. *"Alkaloid Studies-53 Structures Of Nine New Alkaloids From Aspidosperma Dasycarpon A DC"*, Joule, J. A.; Ohashi, M.; Gilbert, B.; Djerassi, C. *Tetrahedron* **1965**, *21*, 1717–1734.

9. *"Structures of Five New Aspidosperma Alkaloids Related to Uleine"*, Ohashi, M.; Gilbert, B.; Joule, J. A.; Djerassi, C. *Experientia* **1964**, *20*, 363–364.

10. *"Structure of Ervitsine, A New Type of Alpha Acyl Indolic Alkaloid"*, Andriantsiferana, M.; Besselievre, R.; Riche, C.; Husson, H. P. *Tetrahedron Lett.* **1977**, *30*, 2587–2590.

11. *"Gilbertin, A New Indole Alkaloid Type"*, Miranda, E. C.; Blechert, S. *Tetrahedron Lett.* **1982**, *23*, 5395–5398.

12. *"Alkaloids from Alstonia-undulifolia"*, Massiot, G.; Boumendjel, A.; Nuzillard, J. M.; Richard, B.; Lemenolivier, L.; David, B.; Hadi, H. A. *Phytochemistry* **1992**, *31*, 1078–1079.

13. *"Tronoharine, a Novel Hexacyclic Indole Alkaloid from a Malayan Tabernaemontana"*, Kam, T. S.; Sim, K. M.; Lim, T. M. *Tetrahedron Lett.* **1999**, *40*, 5409–5412.

14. *"Two New Indole Alkaloids from Aspidosperma subincanum and Geissospermum vellosii"*, Ishiyama, H.; Matsumoto, M.; Sekiguchi, M.; Shigemori, H.; Ohsaki, A.; Kobayashi, J. *Heterocycles* **2005**, *66*, 651–658.

15. *"Alstilobanines A-E, New Indole Alkaloids from Alstonia angustiloba"*, Koyama, K.; Hirasawa, Y.; Zaima, K.; Hoe, T. C.; Chan, K. L.; Morita, H. *Biorg. Med. Chem.* **2008**, *16*, 6483–6488.

16. Chen, C.-L. *Methodologies for the Synthesis of Functionalized Naphthols and Progress Toward the Total Synthesis of Vineomycinone B_2 Methyl Ester and Actinophyllic Acid*, Ph.D. Dissertation, University of Texas at Austin, 2007.

17. *"Total Synthesis of (+/–)-Actinophyllic Acid"*, Martin, C. L.; Overman, L. E.; Rohde, J. M. *J. Am. Chem. Soc.* **2008**, *130*, 7568–7569.

18. *"Absolute Configuration of Actinophyllic Acid as Determined through Chiroptical Data"*, Taniguchi, T.; Martin, C. L.; Monde, K.; Nakanishi, K.; Berova, N.; Overman, L. E. *J. Nat. Prod.* **2009**, *72*, 430–432.

CHAPTER TWO

Synthesis of an Advanced Cycloheptenone Intermediate

2.1 Sequential Michael Addition/Alkylation Strategy

2.1.1 Initial Considerations and Retrosynthetic Analysis

The structural feature present within actinophyllic acid that demanded immediate consideration was the bridged polycyclic framework. This impressive fusion of 5,7, and 8 membered nitrogen-containing rings was seen as the major hurdle toward a total synthesis. It was realized early on that the daunting polycyclic framework could be drastically simplified by disconnection of one carbon–nitrogen bond (*bond a*) and one carbon–carbon bond (*bond b*) (Scheme 2.1.1.1). Removing two of the six rings found within actinophyllic acid revealed compound **25** with an enone functional group and pendant 2-haloethylamino functionality. In the forward sense, an aza-Michael addition/alkylation sequence appeared aptly suited to construct the polycyclic architecture of actinophyllic acid in *one step*.[1] With this key step in mind a detailed synthesis strategy was developed.

Scheme 2.1.1.1

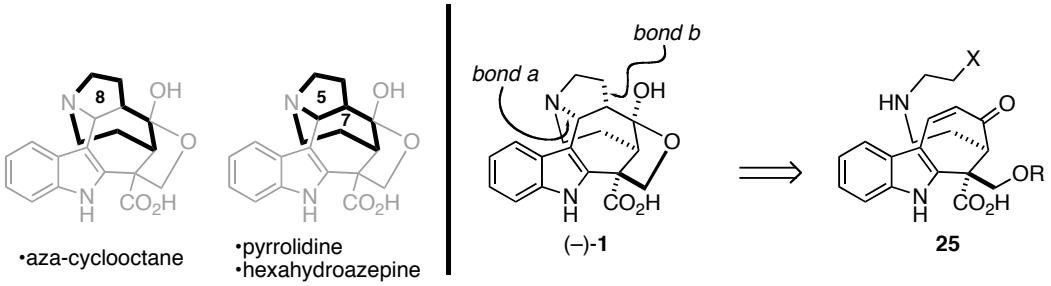

Retrosynthetic disconnections, as depicted in Scheme 2.1.1.2, began with opening of the hemiacetal and oxidation state adjustment at C17 providing penultimate intermediate **26**. Breaking two carbon–carbon bonds α to the ketone and a carbon–nitrogen bond adjacent to the indole moiety led to enone **27** and symmetric bifunctional amine **28**. These bonds were disconnected because traditional enolate chemistry was envisioned in the forward direction, in particular the previously mentioned sequential aza-Michael addition/alkylation. Lastly, disconnection of enone **27** provided indolecarboxaldehyde **29** as the initial synthetic target. Disconnection at the olefin permitted a synthetic strategy in the forward direction that could rely on the multitude of reactions known to form carbon–carbon double bonds. Initial considerations included aldol condensation, Wittig olefination, and ring-closing metathesis. The final disconnection of a carbon–carbon single bond was based upon the routine use of malonate functionality as carbon nucleophiles and α-halo ketones as activated electrophiles.

Scheme 2.1.1.2

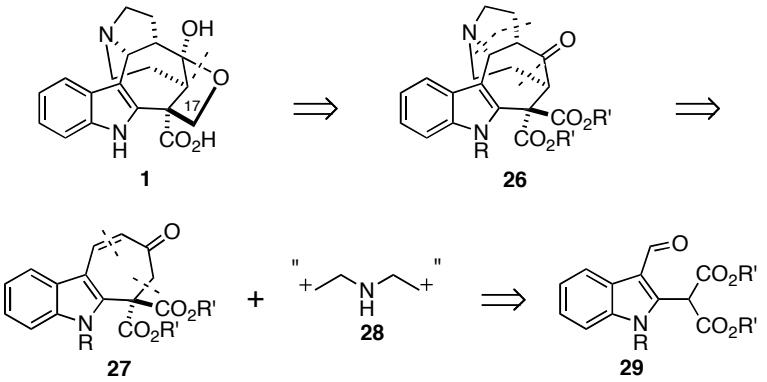

2.1.2 Initial Forward Synthesis

Our efforts commenced with commercially available oxindole **30**, which was elaborated to 2-chloroindole-3-carboxaldehyde **31** by treatment with phosphorus oxychloride, DMAP, and DMF.[2,3] Boc-carbamate protection of the indole nitrogen produced **32** (Scheme 2.1.2.1).[3] The malonate moiety was introduced *via* an addition-elimination sequence that proceeded in 93% yield furnishing indolemalonate **33**. Malonate carbanions traditionally undergo facile alkylation, however compound **33** proved difficult to modify when exposed to a variety of three-carbon electrophiles.[4] After considerable experimentation it was discovered that Tsuji-Trost Pd-catalyzed allylation proceeded smoothly and in 96% yield to afford allyl indolemalonate **34**.[5]

Scheme 2.1.2.1

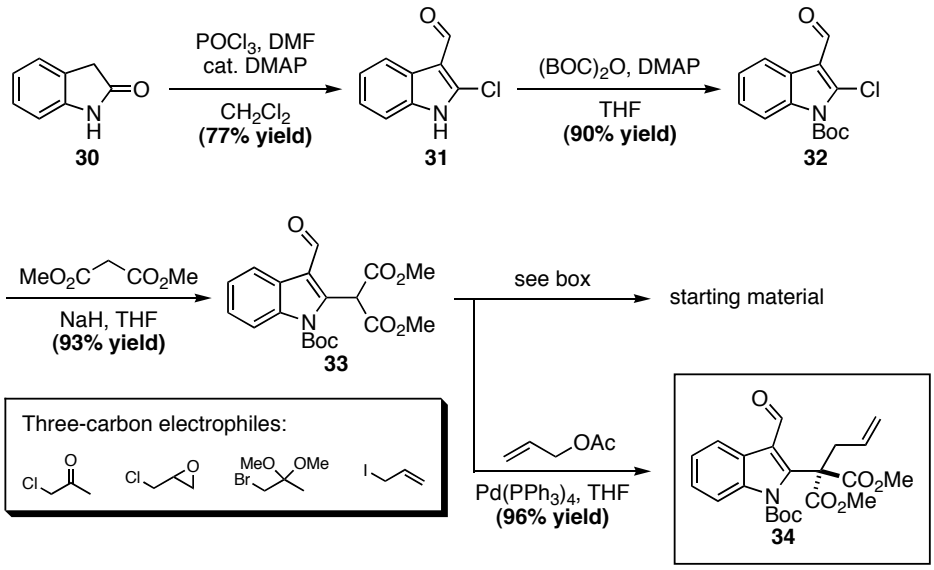

The success of allylation provided an intermediate with a terminal olefin that would be incorporated into a seven-membered ring. Manipulation of the terminal olefin (**34**) to the corresponding ketone (**35**) was seen as a potential substrate for aldol condensation onto the pendant aldehyde (Scheme 2.1.2.2a). However, concerns over five-membered ring formation (**36**) over seven-membered ring formation (**37**) prompted consideration of other strategies. Elaboration of the terminal olefin by ring-closing metathesis was attractive as a selective method for seven-membered ring formation (Scheme 2.1.2.2b). This strategy required installation of one additional olefin. It was realized that the electrophilic aldehyde could undergo addition of a vinyl nucleophile to yield a suitable intermediate (**38**) for seven-membered ring formation using ring-closing metathesis. The expected allylic alcohol product **39** was seen as a direct precursor to the key enone retrosynthetic intermediate **37**.

Scheme 2.1.2.2

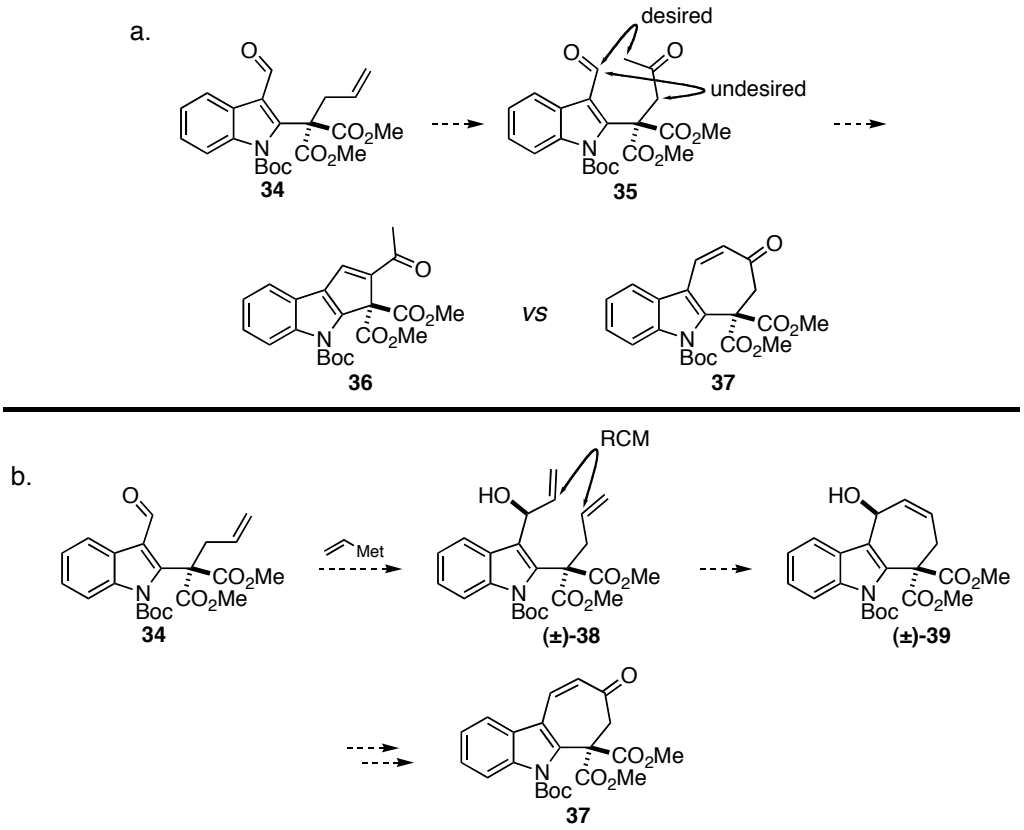

Implementation of this strategy began with elaboration of allyl indolemalonate **34** (Scheme 2.1.2.3) *via* addition of vinyl magnesium bromide at –78 °C. Warming to room temperature provided a 6:1 mixture of chromatographically inseparable diastereomers **40** and **41**, favoring the *trans* diene isomer **40**. Importantly, it was noted that an analytically pure sample of *trans* diene could be precipitated upon exposure of the crude reaction material to methanol. The *trans* assignment to the major diastereomers was made only after characterization of the corresponding *cis* diastereomer (*vide infra*).

Scheme 2.1.2.3

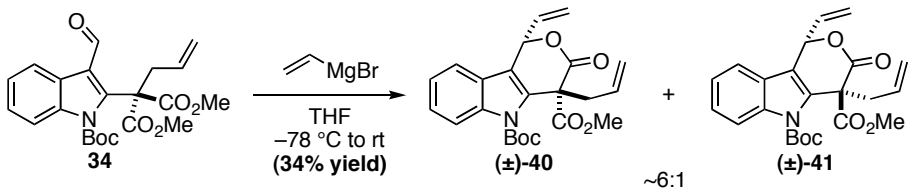

Two products were isolated in addition to the depicted lactone products (Figure 2.1.2.1). These two compounds, **42** and **43**, which were partially separable by flash chromatography, were believed to arise through the mechanisms depicted in Scheme 2.1.2.4.[6,7] Following lactone formation and upon warming, carbon dioxide was lost to generate a common reactive intermediate. This intermediate gave rise to cyclohexene **42** and polyene **43** characterized as the (*E*)-olefin isomer based on nOe experiments. Cyclohexene **42** is thought to form *via* a 6π electrocyclization reaction. On the other hand, the reactive azaquinone methide intermediate could undergo a [*1,5*]-sigmatropic rearrangement to furnish polyene **43**.

Figure 2.1.2.1

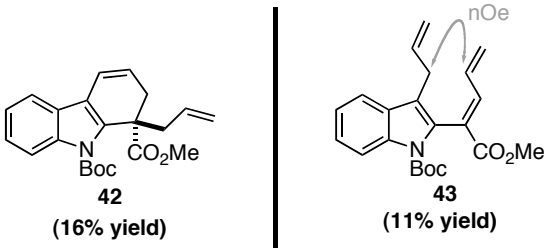

Scheme 2.1.2.4

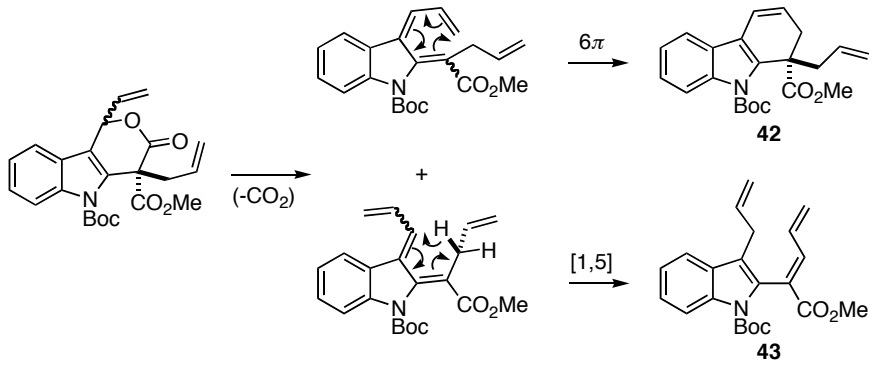

Further experimentation revealed that these two side products could be eliminated if the reaction was initiated and quenched at –78 °C (Scheme 2.1.2.5). Surprisingly, this modification also reversed the lactone isomeric product ratio. Thus, a 3:1 ratio of *cis*:*trans* diene products was observed by crude ^{1}H NMR. Even more fortunate was the observation that the desired *cis* diene isomer **41** could be precipitated in pure form upon exposure of the crude reaction material to methanol; analogous to the *trans* diene isomer (*vide supra*).

Scheme 2.1.2.5

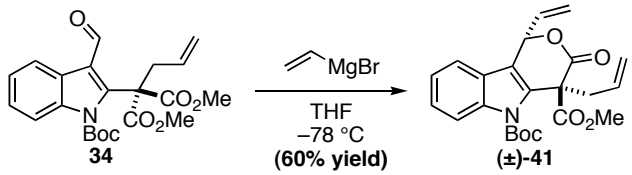

2.1.3 An Unstable Ring-Closing Metathesis Product

Pushing forward, the predominant *cis* diene isomer **41** was poised for conversion to the corresponding seven-membered ring *via* ring-closing metathesis.[8] Indeed, exposure of the diene mixture to the Grubbs 2nd generation catalyst provided bicyclic lactone **44** (Scheme 2.1.3.1). This compound required transposition of the allylic acetate functionality to access the desired enone intermediate **37**. This was envisioned to occur upon exposure to catalytic Pd, whereby π-allyl formation would access an intermediate that could cyclize to place the double bond in conjugation with the indole nucleus and form a desired carbon–oxygen bond (**45**). It was with this expectation that crude bicyclic lactone **44** was treated with $Pd(PPh_3)_4$. The product from this reaction was not the desired transposed lactone **45**, but an unexpected cyclopropane product **46** in 74% yield over the two steps.

Scheme 2.1.3.1

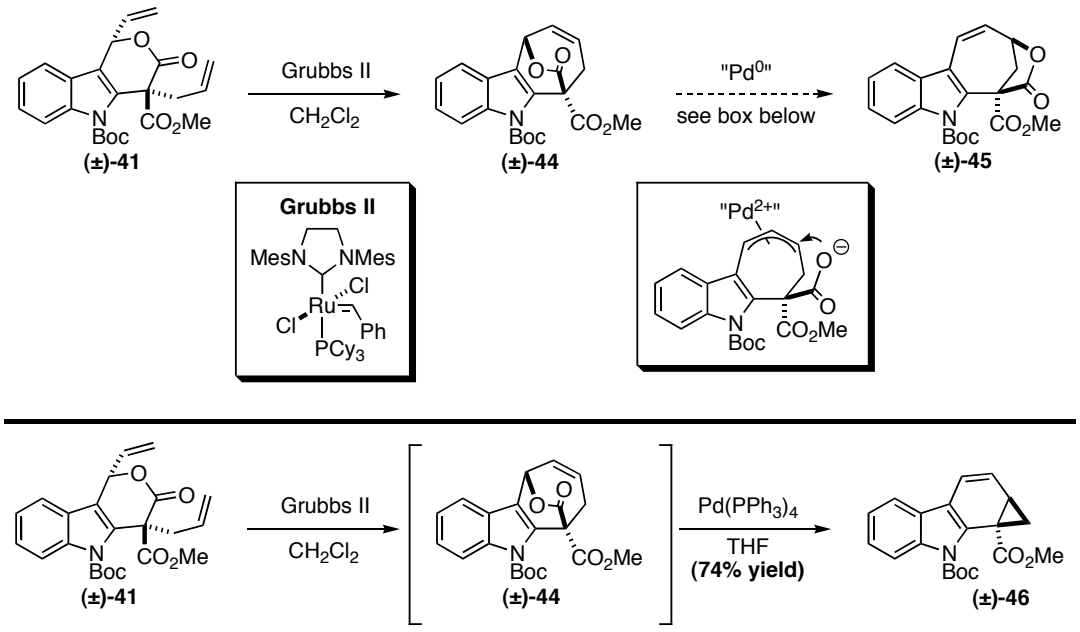

Further experimentation revealed that **46** was obtained upon gentle heating without Pd and was observed upon extended storage at room temperature. Formation of this product could occur by the mechanism depicted in Scheme 2.1.3.2. Loss of CO_2, facilitated by a Pd catalyst, in analogy to a Tsuji-allylation, would have generated a π-allyl Pd intermediate **47**, which could close transannularly to cyclopropane **46**.[9] Loss of CO_2 under thermal conditions *via* retro-[4+2] cycloaddition could not furnish a stabilized π-allyl intermediate and instead would generate cycloheptatriene **48**. Ring closure to cyclopropane **46** would occur following 6π electrocyclization. Due to these stability issues, bicyclic lactone **44** was typically advanced immediately as the crude material (*vide infra*).

Scheme 2.1.3.2

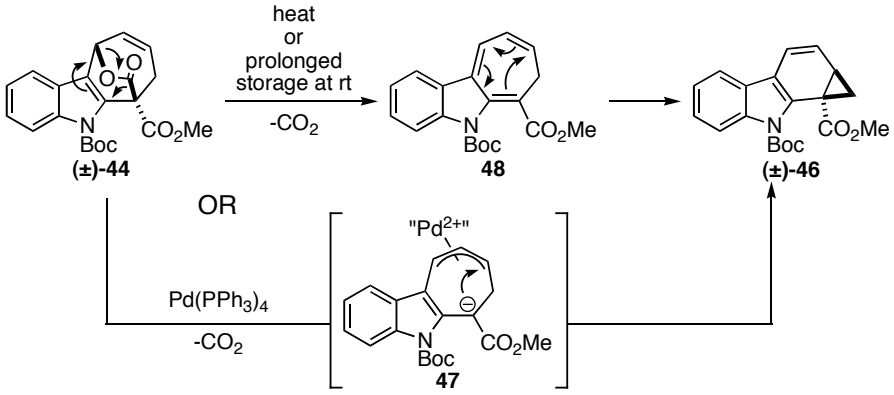

2.1.4 Construction of an Advanced Michael Acceptor

The instability of lactone **44**, due to facile loss of CO_2, necessitated transformation of the bridging lactone moiety into a robust functional group for subsequent chemistry. Methanolysis of this crude intermediate with sodium methoxide revealed allylic alcohol **39** with regeneration of the dimethyl malonate moiety in 57% yield over two steps (Scheme 2.1.4.1). It was postulated that an oxidative transposition of allylic alcohol **39** might proceed employing a chromium oxidant. Ample precedent exists for oxidative transpositions of tertiary allylic alcohols utilizing pyridinium chlorochromate (PCC).[10] The alcohol present in compound **39** is not tertiary, however, it is both allylic and benzylic, which led us to hypothesize that it may transpose and place the double bond in linear conjugation as opposed to the cross conjugated system resulting from oxidation without transposition.[11]

Scheme 2.1.4.1

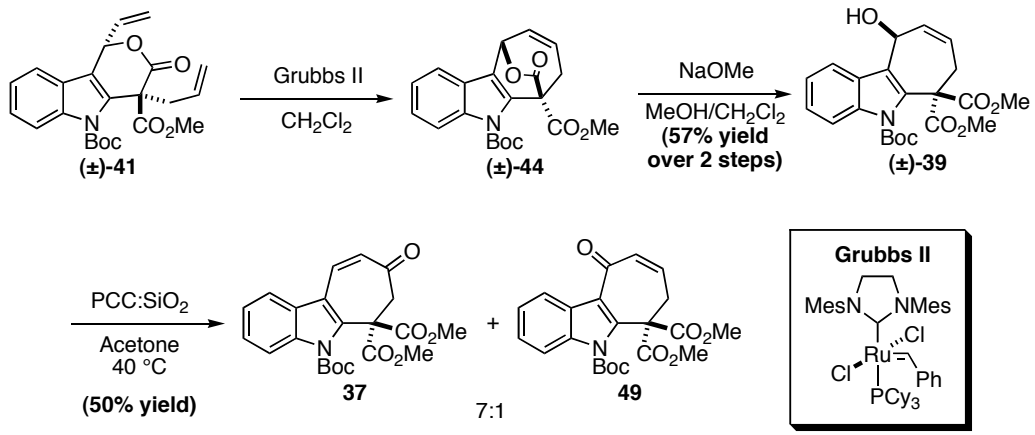

Gratifyingly, the desired ketone **37**, in addition to the non-transposed oxidation product **49**, was isolated after exposure of alcohol **39** to dilute $PCC:SiO_2$ in hot acetone. Despite this initial success it was apparent that the current route to allylic alcohol **39** was inefficient. At issue was the re-formation of both dimethyl malonate and allylic alcohol functionalities, which were transformed during the addition of vinyl magnesium bromide to indolecarboxaldehyde **34** (Scheme 2.1.4.2). Therefore, an alternative to **34** was necessary to prevent lactone formation. These efforts are discussed in the following chapter.

Scheme 2.1.4.2

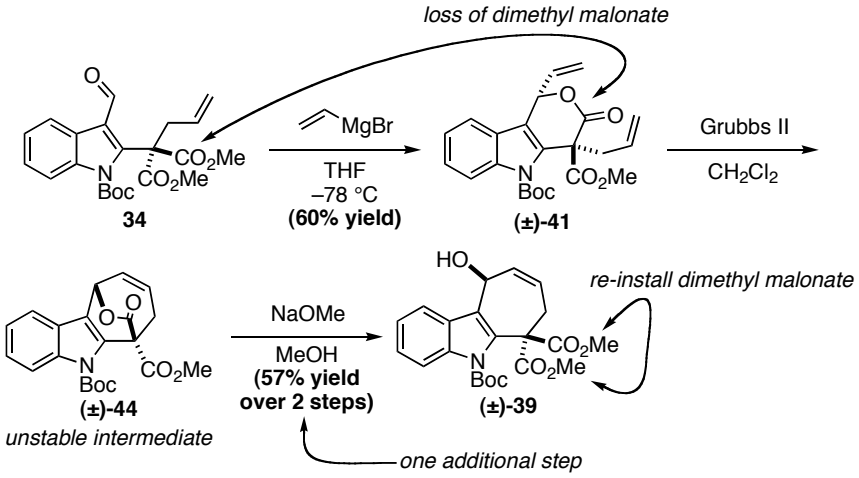

2.1.5 Insight into the Oxidative Transposition Mechanism

The oxidative rearrangement mediated by PCC deserves additional consideration. Due to the acidic nature of PCC there was a possibility that transposition of a chromate ester followed by oxidation was not operable, but that a sequence of steps including allylic alcohol isomerization, chromate ester formation, and oxidation was promoted by mild acid (Scheme 2.1.5.1).[12]

Scheme 2.1.5.1

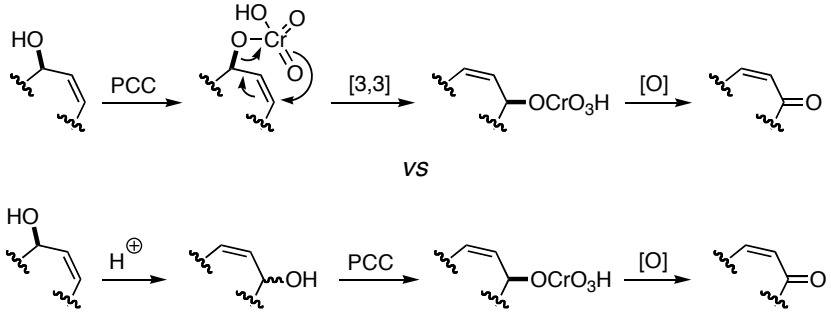

To explore this ambiguity allylic alcohol **39** was exposed to the oxidation reaction conditions, with the exception that PPTS was substituted for PCC (Scheme 2.1.5.2). The products isolated from this reaction were isomerized allylic alcohol **50** and cycloheptatriene **51**. Exposure of isomerized allylic alcohol **50** to the PCC reaction conditions and on a similar time scale provided a 1:1 mixture of enone product and recovered starting material. It was thus inferred that the allylic alcohol isomerization, chromate ester formation, and oxidation sequence is plausible, however the transposition of a chromate ester cannot be ruled out. Further investigation is warranted to elucidate the mechanism of this interesting reaction.

Scheme 2.1.5.2

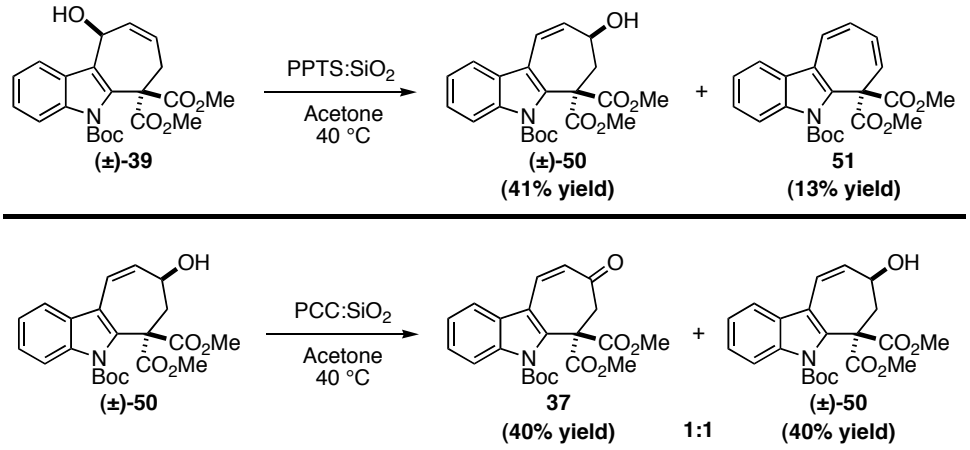

2.2 Summary

Key retrosynthetic intermediate **37** was synthesized in eight steps from commercially available oxindole. Key to this route was a PCC mediated oxidative transposition of an allylic and benzylic alcohol. The outlined synthetic route provided proof of concept for this transformation and furnished initial quantities of material for further elaboration. However, the sequence was determined to be inefficient due to the loss of one methyl ester—as a result of lactone formation during vinyl grignard addition to aldehyde **34**—which had to be reinstated later in a subsequent step. In addition, the bridged bicyclic product **44** resulting from ring-closing metathesis proved to be an unstable intermediate. At this point in time efforts were focused on finding a synthetically useful route to enone **37**, with particular emphasis on preventing lactone formation.

2.3 Experimental

2.3.1 Materials and Methods

Unless otherwise sated, reactions were performed under a nitrogen atmosphere using freshly dried solvents. Tetrahydrofuran (THF) was dried either by distillation from sodium/benzophenone or by passing through activated alumina columns. Methylene chloride (CH_2Cl_2), diethyl ether (Et_2O), benzene (PhH), and toluene (PhMe) were dried by passing through activated alumina

columns. Dimethylformamide (DMF) was dried over activated molecular sieves or purchased anhydrous from Sigma-Aldrich. MeOH was distilled over magnesium oxide. All other commercially obtained reagents were used as received. All reactions were monitored by thin-layer chromatography using EMD/Merck or Silicycle silica gel 60 F254 pre-coated plates (0.25 mm). Flash chromatography was performed with the indicated solvents using silica gel (particle size 0.040-0.063 mm) purchased from Silicycle. ^{1}H NMR spectra were recorded at 400 MHz using a Varian Inova 400 instrument. ^{13}C NMR spectra were recorded at 100 MHz using a Varian Inova 400 instrument. Chemical shift are reported relative to internal chloroform (^{1}H, δ = 7.26, ^{13}C, δ = 77.2), dimethyl sulfoxide (^{1}H, δ = 2.50, ^{13}C, δ = 39.5), benzene (^{1}H, δ = 7.16, ^{13}C, δ = 128.1) as indicated. Splitting patterns are reported as such, app = apparent, br = broad, s = singlet, d = doublet, dd = doublet of doublets, ddd = doublet of doublets of doublets, dddd = doublet of doublets of doublets of doublets, t = triplet, q = quartet, m = multiplet, nfom = non-first order multiplet. Infrared spectra were recorded on a Nicolet Avatar 320 FT-IR. Melting points were obtained on a Gallenkamp variable temperature melting point apparatus and are uncorrected. High-resolution mass spectra were acquired at the Colorado State University CIF using an Agilent 6210 TOF LCMS.

2.3.2 Preparative Procedures

Preparation of 2-chloro-indole-3-carboxaldehyde **31**

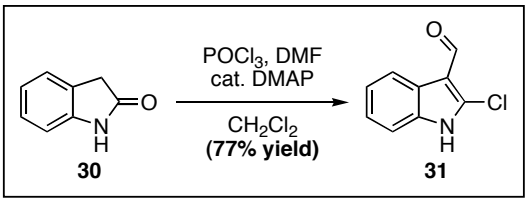

The following is a modification of the procedure of Showalter.[2] To a solution of DMF (240 mL, 3.1 mol) in CH_2Cl_2 (1 L) cooled to 0 °C in an ice-water cold bath was added $POCl_3$ (240 mL, 2.6 mmol) dropwise *via* addition funnel over 44 min. The cold bath was removed and the contents were stirred at room temperature for 2 hrs after which the reaction mixture was cooled again to 0 °C in an ice-water bath. Oxindole **30** (137.3 g, 1.0 mol) was added over 45 min. *via* solid addition funnel. The cold bath was removed following addition and the solution was stirred 11.5 hrs before it was quenched by slow transfer to a 6 L separatory funnel containing ice water (ca. 2 L, CAUTION: keep additional ice available to control any subsequent exotherm!). The aqueous layer was extracted with CH_2Cl_2 (ca. 200 mL) and additional ice was added if required. The organic layer was extracted with H_2O (3 x ca. 350 mL) and all of the aqueous layers were combined into a 4 L Erlenmeyer flask and stirred at room temperature overnight. Filtration of the precipitated solid and washing with copious amounts of H_2O was followed by air-drying for two days yielding **31** (142.5 g, 77% yield) as a light brown amorphous solid. This crude material was sufficiently pure for subsequent

steps. An analytically pure sample was obtained after silica gel chromatography (gradient elution, 25 → 50% Et_2O/Hexanes) as a white amorphous solid.

2-chloroindole-3-carboxaldehyde 31: m.p. = 201.0 °C (decomposed); FTIR (thin film/NaCl) 3144 (s), 3093 (s), 3037 (m), 2919 (w), 2847 (w), 1649 (s), 1582 (w), 1516 (w), 1490 (w), 1449 (m) cm^{-1}; ^1H NMR (400 MHz, DMSO-d_6) δ 13.06 (br s, 1H), 9.99 (s, 1H), 8.06–8.08 (nfom, 1H), 7.41–7.43 (nfom, 1H), 7.21–7.29 (nfom, 1H and nfom, 1H); ^{13}C NMR (100 MHz, DMSO-d_6) δ 183.3, 134.8, 134.6, 124.3, 123.8, 122.8, 120.0, 112.0, 111.7; HRMS (TOF LCMS) calc'd for C_9H_7ClNO $[M+H]^+$ 180.0211, found 180.0212.

Preparation of Boc-2-chloro-indole-3-carboxaldehyde **32**

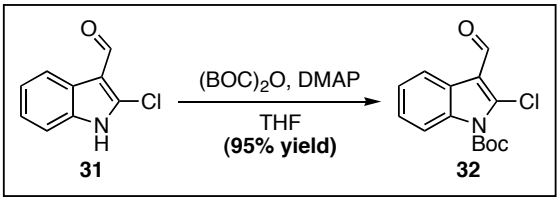

31 **32**

To 2-chloroindole-3-carboxaldehyde **31** (30.0 g, 167.0 mmol) in a flame dried 1 L flask was added DMAP (658 mg, 5.38 mmol) followed by anhydrous THF (325 mL, 0.5 M). The contents were stirred and cooled to 0 °C in an ice-water bath. At this time $(BOC)_2O$ (38.3 g, 175.4 mmol) was added as a solid. After addition the ice-water bath was removed and the contents allowed to warm to room temperature and aged for 1 h. The reaction mixture was quenched by addition of H_2O (475 mL) before transfer to a 4 L Erlenmeyer flask. An additional 1.15 L of water was added and the contents stirred for 1 hr. The precipitated solid

was filtered and dried under high vacuum providing crude **32** (44.4 g, 95% yield) as an orange-brown amorphous solid. This crude material was typically advanced without further purification. An analytical sample was obtained following recrystallization from hexanes.

Boc-2-chloroindole-3-carboxaldehye 32: m.p. = 93.1–93.6 °C; FTIR (thin film/NaCl) 3052 (w), 2980 (m), 2929 (w), 2847 (w), 2822 (w), 2750 (w), 1762 (s), 1669 (s), 1536 (m), 1475 (m), 1434 (m) cm^{-1}; ^{1}H NMR (400 MHz, $CDCl_3$) δ 10.24 (s, 1H), 8.25–8.27 (nfom, 1H), 8.01–8.03 (nfom, 1H), 7.32–7.39 (nfom, 1H and nfom, 1H), 1.72 (s, 9H); ^{13}C NMR (100 MHz, $CDCl_3$) δ 185.8, 148.1, 135.6, 135.3, 125.9, 125.0, 124.5, 121.1, 117.5, 114.8, 86.9, 28.2; HRMS (TOF LCMS) calc'd for $C_{14}H_{15}ClNO_3$ $[M+H]^+$ 280.0735, found 280.0740.

Preparation of Indolemalonate_Me **33**

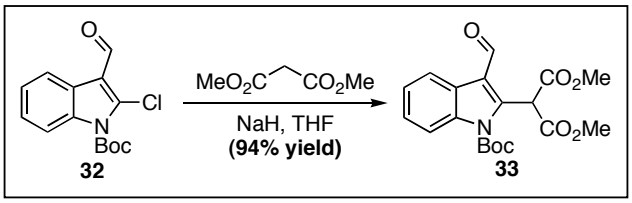

To two flame dried 1 L three-neck roundbottom flasks were added 60% NaH (9.45 g, 236.4 mmol; 9.46 g, 236.6 mmol) followed by THF (215 mL, 0.5 M). The contents were stirred and cooled to 0 °C with ice-water baths. At this time Boc-2-chloroindole-3-carboxaldehyde **31** (30.0 g, 107.3 mmol) was added to each flask as a solid without observation of bubbles. To these solutions were added dimethyl malonate (14.8 mL, 129.2 mmol) dropwise *via* addition funnel at

a rate allowing controlled gas evolution (ca. 55 min.). The reactions were stirred 1 h before they were quenched by addition of 1N HCl (ca. 360 mL) dropwise. The quenched reactions were diluted with H_2O (ca. 400 mL) and stirred for 1 h 30 min. The two mixtures were combined, the solids filtered, and the filter cake washed with of cold H_2O (1 L). Residual H_2O was azeotropically removed with PhMe (500 mL) under reduced pressure. The solid was transferred to an Erlenmeyer flask and rinsed with HPLC grade Hexanes (3 x 500 mL) followed by decanting. The obtained off-white amorphous solid **33** (75.4 g, 94% yield) was sufficiently pure for subsequent steps. An analytical sample was obtained after silica gel chromatography (25% EtOAc/Hexanes) provided pure **33** as a white amorphous solid.

Indolemalonate-Me 33: m.p. = 111.0 °C (decomposition); FTIR (thin film/NaCl) 2980 (w), 2945 (w), 1736 (s, br), 1669 (m), 1557 (w), 1454 (m), 1429 (m) cm^{-1}; ^1H NMR (400 MHz, $CDCl_3$) δ 10.37 (s, 1H), 8.20–8.22 (nfom, 1H), 8.02–8.04 (nfom, 1H), 7.36–7.43 (nfom, 1H and nfom, 1H), 6.25 (s, 1H), 3.76 (s, 6H), 1.69 (s, 9H); ^{13}C NMR (100 MHz, $CDCl_3$) δ 186.2, 165.9, 150.1, 139.3, 135.6, 126.5, 125.9, 124.6, 120.2, 119.2, 115.7, 86.9, 53.2, 49.2, 28.1; HRMS (TOF LCMS) calc'd for $C_{19}H_{21}NNaO_7$ $[M+Na]^+$ 398.1210, found 398.1214.

Preparation of Allylindolemalonate-Me **34**

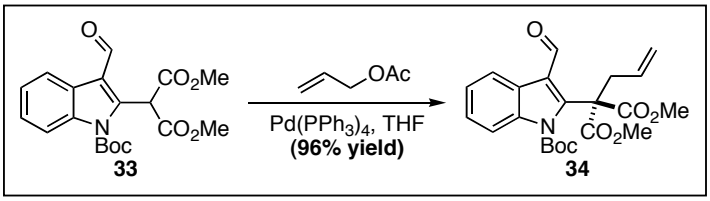

To a solution of indolemalonate-Me **33** (1.0016 g, 2.66 mmol) in THF (20 mL) was added allyl acetate (300 μL, 2.8 mmol) followed by $Pd(PPh_3)_4$ (154.9 mg, 0.134 mmol, 5 mol%) at room temperature under N_2. The reaction was stirred 2 hrs before it was concentrated under reduced pressure and purified by silica gel chromatography (gradient elution, 10 → 20% EtOAc/Hexanes) providing pure **34** (1.0681 g, 96% yield) as a white amorphous solid.

Allylindolemalonate-Me 34: m.p. = 103.1 °C (decomposition); FTIR (thin film/NaCl) 3052 (w), 2986 (m), 2955 (m), 2968 (w), 2770 (w), 1757 (s, br), 1675 (s), 1531 (m), 1475 (m), 1449 (s) cm^{-1}; ^1H NMR (400 MHz, $CDCl_3$) δ 9.97 (s, 1H), 8.33–8.36 (nfom, 1H), 7.89–7.92 (nfom, 1H), 7.32–7.41 (nfom, 1H and nfom, 1H), 5.84 (dddd, *J* = 16.5, 10.6, 7.4, 7.4 Hz, 1H), 5.03 (d, *J* = 16.4 Hz, 1H), 5.02 (d, *J* = 10.8 Hz, 1H), 3.77 (s, 6H), 3.44 (d, *J* = 7.4 Hz, 2H), 1.71 (s, 9H); ^{13}C NMR (100 MHz, $CDCl_3$) δ 186.8, 168.9, 150.7, 142.5, 135.3, 132.9, 126.1, 125.8, 124.6, 121.8, 120.6, 120.2, 114.7, 86.8, 62.0, 53.7, 39.2, 28.2; HRMS (TOF LCMS) calc'd for $C_{22}H_{25}NNaO_7$ $[M+Na]^+$ 438.1523, found 438.1522.

Preparation of trans/cis-Lactone-Me **40/41**, *Cyclohexene* **42**, *and Triene* **43**

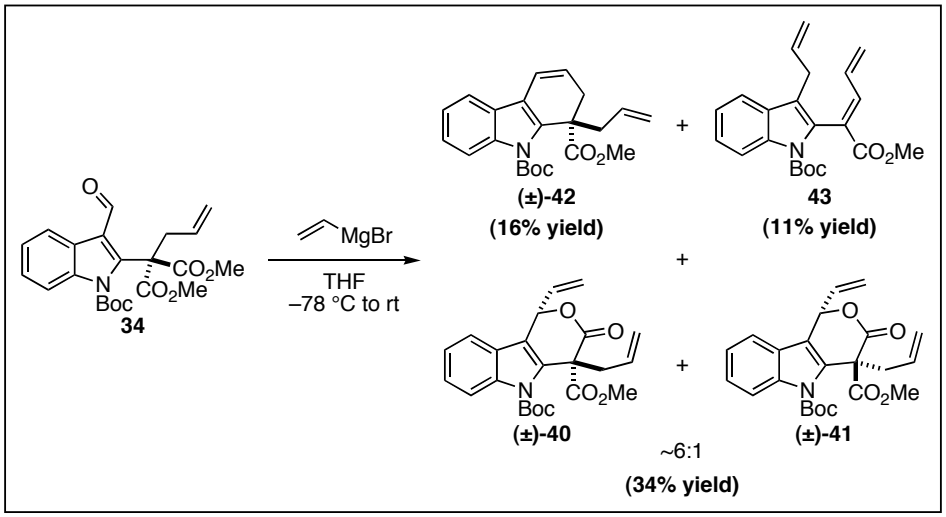

To a solution of allylindolemalonate-Me **34** (450 mg, 1.08 mmol) in THF (10 mL) cooled to –78 °C was added vinyl magnesium bromide (1.80 mL of a 0.94 M soln. in THF, 1.7 mmol) over 1 min. *via* addition funnel under N_2. Following addition the cold bath was removed and the mixture warmed to room temperature. The reaction was aged 8.5 hrs before it was quenched by addition of saturated aqueous NH_4Cl (ca. 10 mL) at 0 °C. The reaction was diluted with EtOAc and filtered through Celite to remove solids. The filtrate was transferred to a separatory funnel and the layers separated. The organic layer was washed with 1N HCl, brine, and dried over Na_2SO_4. Filtration followed by concentration under reduced pressure provided a substance that was dissolved in a minimal amount of CH_2Cl_2 and triturated with hexanes. Precipitated solids were filtered and the filtrate was concentrated under reduced pressure yielding an amorphous solid. Dissolving this material in MeOH and letting it stand at room temperature precipitated an analytical sample of *trans* lactone **40** (66 mg, 15% yield) as a

white amorphous solid. The mother liquor was concentrated under reduced pressure and the remaining material purified by silica gel chromatography (gradient elution, 5 → 10 → 25% EtOAc/Hexanes) yielding **43** (45 mg, 11% yield, contaminated with **42**) as a colorless oil, **42** (65 mg, 16% yield, contaminated with **43**) obtained as a colorless oil, and an inseparable 3:1 (*trans*:*cis*) mixture of lactone-Me **40/41** (88 mg, 19% yield; 34% combined yield corresponding to a 6:1 *trans*:*cis* lactone-Me ratio) as a white amorphous solid.

***trans*-Lactone-Me 40**: m.p. = 139.2 °C (decomposition); FTIR (thin film/NaCl) 3083 (w), 2975 (w), 2945 (w), 1767 (s), 1731 (s), 1480 (w), 1454 (m) cm^{-1}; ^1H NMR (400 MHz, $CDCl_3$) δ 8.02 (d, *J* = 8.5 Hz, 1H), 7.46 (d, *J* = 7.8 Hz, 1H), 7.35–7.39 (nfom, 1H), 7.24–7.28 (nfom, 1H), 5.99–6.09 (2H), 5.65 (d, *J* = 16.2 Hz, 1H), 5.50 (d, *J* = 9.6 Hz, 1H), 5.40 (m, 1H), 5.05 (app dd, *J* = 17.0, 1.3 Hz, 1H), 4.97 (app dd, *J* = 10.1, 1.6 Hz, 1H), 3.73 (s, 3H), 3.47 (dd, *J* = 14.1, 8.3 Hz, 1H), 3.22 (dd, *J* = 14.1, 10.9 Hz, 1H), 1.70 (s, 9H); ^{13}C NMR (100 MHz, $CDCl_3$) δ 167.9, 167.4, 150.2, 136.6, 135.4, 131.5, 129.8, 125.5, 125.1, 123.3, 121.1, 120.5, 119.5, 116.2, 114.7, 85.7, 78.6, 57.5, 53.2, 41.0, 28.2; HRMS (TOF LCMS) calc'd for $C_{23}H_{25}NNaO_6$ $[M+Na]^+$ 434.1574, found 434.1579.

Cyclohexene 42: FTIR (thin film/NaCl) 3067 (w), 3047 (w), 2980 (m), 2945 (m), 2868 (w), 2832 (w), 1731 (s, br), 1634 (w), 1567 (w), 1480 (m), 1454 (s), 1434 (m) cm^{-1}; ^1H NMR (400 MHz, $CDCl_3$) δ 7.99–8.01 (nfom, 1H), 7.55–7.57 (nfom, 1H), 7.24–7.32 (nfom, 1H and nfom, 1H), 6.61 (dd, *J* = 9.5, 3.4 Hz, 1H), 5.90 (dddd, *J* = 17.1, 9.8, 7.4, 7.4 Hz, 1H), 5.77 (ddd, *J* = 9.3, 6.1, 2.9 Hz, 1H),

4.97 (dd, *J* = 17.0, 1.6 Hz, 1H), 4.88 (dd, *J* = 10.0, 1.7 Hz, 1H), 3.68 (s, 3H), 2.93 (app dt, *J* = 17.4, 3.1 Hz, 1H), 2.88 (d, *J* = 7.6 Hz, 2H), 2.71 (app dd, *J* = 17.4, 5.9 Hz, 1H), 1.69 (s, 9H); ^{13}C NMR (100 MHz, $CDCl_3$) δ 176.2, 150.5, 135.9, 135.1, 134.2, 126.8, 124.3, 123.0, 121.8, 118.7, 118.2, 117.2, 117.2, 116.0, 84.6, 52.1, 48.9, 41.4, 37.1, 28.3; HRMS (TOF LCMS) calc'd for $C_{22}H_{25}NNaO_4$ $[M+Na]^+$ 390.1676, found 390.1677.

Triene 43: FTIR (thin film/NaCl) 3078 (w), 3052 (w), 3006 (w), 2980 (w), 2955 (w), 1726 (s), 1634 (w), 1588 (w), 1572 (w), 1480 (w), 1454 (m), 1434 (w) cm^{-1}; ^{1}H NMR (400 MHz, $CDCl_3$) δ 8.21–8.23 (nfom, 1H), 7.56–7.59 (nfom, 1H), 7.54 (d, *J* = 11.3 Hz, 1H), 7.32–7.37 (nfom, 1H), 7.23–7.27 (nfom, 1H), 6.37 (ddd, *J* = 17.0, 11.3, 10.1 Hz, 1H), 5.86 (dddd, *J* = 16.9, 10.3, 6.3, 6.3 Hz, 1H), 5.72 (ddd, *J* = 17.0, 1.6, 0.7 Hz, 1H), 5.47 (ddd, *J* = 10.1, 1.6, 0.7 Hz, 1H), 4.99–5.08 (m, 2H), 3.71 (s, 3H), 3.28 (nfom, 2H), 1.56 (s, 9H); ^{13}C NMR (100 MHz, $CDCl_3$) δ 167.3, 150.1, 141.6, 136.5, 135.4, 133.4, 129.5, 129.0, 126.3, 126.0, 124.8, 122.6, 119.8, 119.7, 116.0, 115.7, 84.1, 52.1, 29.0, 28.1; HRMS (TOF LCMS) calc'd for $C_{22}H_{25}NNaO_4$ $[M+Na]^+$ 390.1676, found 390.1673.

***cis*-Lactone-Me 41**: see below

Preparation of cis-Lactone-Me **41**

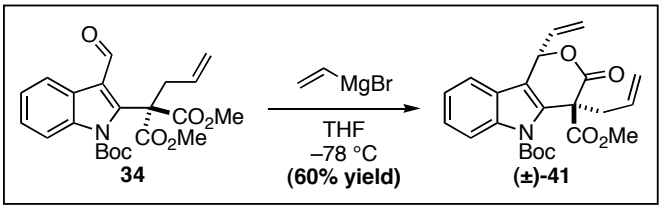

To a solution of allylindolemalonate-Me **34** (3.00 g, 7.24 mmol) in THF (70 mL) cooled to –78 °C was added vinyl magnesium bromide (10.8 mL of a 1.0 M solution in THF, 11 mmol) over 15 min. *via* addition funnel under N_2. The reaction was stirred 2 hrs before it was quenched by addition of saturated aqueous NH_4Cl (ca. 70 mL) at 0 °C. The solution was diluted with H_2O (50 mL) and the layers separated. The aqueous layer was extracted with EtOAc (3 x 10 mL) and the combined organic layers were washed once with saturated aqueous $NaHCO_3$, brine, and dried over $MgSO_4$. Filtration followed by concentration under reduced pressure and precipitation from MeOH provided pure **41** (1.78 g, 60% yield) as a white amorphous solid.

***cis*-Lactone-Me 41**: m.p. = 137.3 °C (decomposition); FTIR (thin film/NaCl) 3073 (w), 2980 (w), 2950 (w), 1767 (s), 1731 (s), 1449 (m) cm^{-1}; ^1H NMR (400 MHz, $CDCl_3$) δ 8.02 (d, J = 8.5 Hz, 1H), 7.35–7.41 (2H), 7.25–7.29 (nfom, 1H), 6.10 (d, J = 7.6 Hz, 1H), 5.99 (ddd, J = 17.0, 9.8, 7.4 Hz, 1H), 5.58 (d, J = 16.8 Hz, 1H), 5.42–5.52 (2H), 5.04 (app dd, J = 17.0, 1.3 Hz, 1H), 4.98 (d, J = 10.0 Hz, 1H), 3.71 (s, 3H), 3.49 (dd, J = 14.1, 8.2 Hz, 1H), 3.26 (dd, J = 14.1, 7.3 Hz, 1H) 1.69 (s, 9H); ^{13}C NMR (100 MHz, $CDCl_3$) δ 167.9, 167.3, 150.2, 136.4, 135.8, 132.6, 129.6, 125.5, 125.2, 123.4, 120.7, 120.4, 119.2, 116.4,

114.4, 85.7, 78.7, 57.5, 53.2, 40.9, 28.2; HRMS (TOF LCMS) calc'd for $C_{23}H_{25}NNaO_6$ $[M+Na]^+$ 434.1574, found 434.1584.

Preparation of Cyclopropane **46**

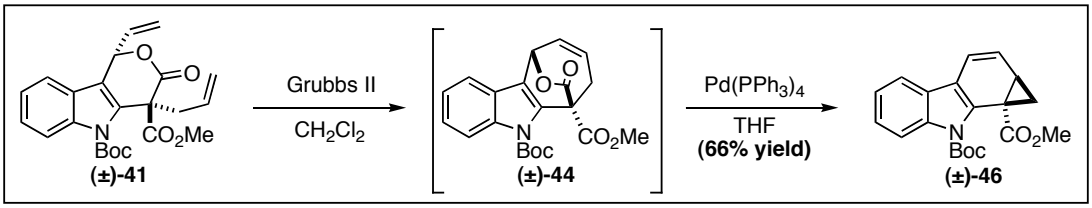

To a solution of *cis*-lactone-Me **41** (307.8 mg, 0.748 mmol) in CH_2Cl_2 (7 mL) was added the Grubbs 2nd generation catalyst (31.9 mg, 0.0375 mmol) at room temperature under N_2. The reaction was heated to reflux and stirred 5.3 hrs before it was cooled to room temperature. Addition of $Pd(PPh_3)_4$ (39.7 mg, 0.0343 mmol) was followed by stirring at room temperature under N_2 until the reaction was complete as judged by TLC. Concentration under reduced pressure and silica gel chromatography (10% EtOAc/Hexanes) yielded cyclopropane **46** (187.9 mg, 74% yield) as a colorless oil.

Cyclopropane 46: FTIR (thin film/NaCl) 3047 (w), 2980 (w), 2945 (w), 1731 (s), 1475 (w), 1460 (m), 1434 (m) cm^{-1}; ^1H NMR (400 MHz, Benzene-d_6) δ 8.46 (d, J = 8.2 Hz, 1H), 7.42–7.45 (nfom, 1H), 7.24–7.28 (nfom, 1H), 7.15–7.19 (nfom, 1H), 6.46 (d, J = 9.7 Hz, 1H), 5.77 (dd, J = 9.7, 5.2 Hz, 1H), 3.34 (s, 3H), 2.32 (ddd, J = 8.5, 8.5, 5.2 Hz, 1H), 1.41 (s, 9H and m, 2H); ^{13}C NMR (100 MHz, Benzene-d_6) δ 171.0, 150.9, 137.3, 132.5, 127.1, 124.7, 123.3, 122.5, 118.4,

117.4, 115.7, 113.6, 83.8, 51.8, 32.5, 29.1, 27.9, 9.0; HRMS (TOF LCMS) calc'd for $C_{20}H_{22}NO_4$ $[M+H]^+$ 340.1543, found 340.1540.

Preparation of Allylic alcohol-Me **39**

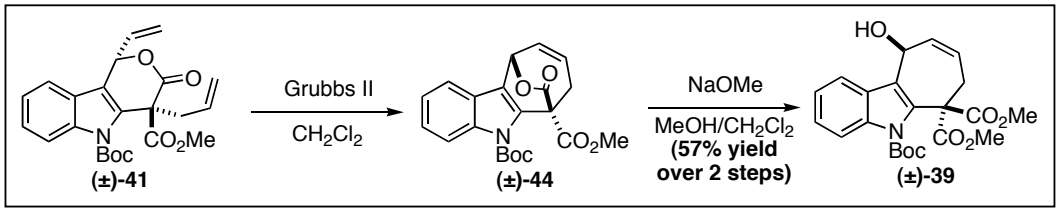

To a flame dried flask equipped with a stir bar was added *cis*-lactone-Me **41** (231.8 mg, 0.564 mmol) followed by the Grubbs 2nd generation catalyst (23.2 mg, 0.0273 mmol). A flame-dried condenser was added and the apparatus was placed under vacuum and subsequently back-filled with N_2. This process was repeated 4x. At this time anhydrous CH_2Cl_2 (6 mL) was added and the contents heated to reflux while N_2 was bubbled through the solution. After TLC showed consumption of starting material (1.3 h) the reaction was cooled to room temperature and 2-mercaptonicotinic acid (48.8 mg, 0.314 mmol) was added—to quench the ruthenium catalyst activity[13]—and the contents of the flask stirred open to the atmosphere for 1 h. The solution was diluted with saturated aqueous $NaHCO_3$ (10 mL) and stirred for 10 min. The contents of the flask were transferred to a separatory funnel and additional saturated aqueous $NaHCO_3$ (10 mL) was added. The layers were separated and the aqueous layer was extracted with CH_2Cl_2 (3 x 3 mL) and the combined organic layers were washed once with brine and dried over Na_2SO_4. Filtration followed by concentration under reduced

pressure provided crude bicycle **44** (233.5 mg, 108% yield) which was typically advanced to the next step due to instability. An analytical sample was obtained by precipitation from MeOH providing a white foam.

Bicycle-Me 44: FTIR (thin film/NaCl) 3047 (w), 2980 (m), 2950 (m), 1767 (s, br), 1726 (s, br), 1454 (s), 1413 (s) cm^{-1}; ^1H NMR (400 MHz, $CDCl_3$) δ 7.98 (d, J = 8.1 Hz, 1H), 7.49–7.51 (nfom, 1H), 7.28–7.37 (nfom, 1H and nfom, 1H), 6.43 (dddd, J = 11.1, 6.7, 2.3, 2.3 Hz, 1H), 5.78 (dt, J = 10.9, 3.7 Hz, 1H), 5.73 (d, J = 6.7 Hz, 1H), 3.82 (s, 3H), 3.33 (ddd, J = 19.7, 3.6 2.3 Hz, 1H), 2.88 (d, J = 19.7 Hz, 1H), 1.69 (s, 9H); ^{13}C NMR (100 MHz, $CDCl_3$) δ 170.2, 167.4, 150.3, 136.1, 131.4, 130.8, 128.5, 125.1, 124.1, 123.6, 123.5, 118.0, 115.7, 85.8, 68.7, 57.4, 53.0, 31.1, 28.2; HRMS (TOF LCMS) calc'd for $C_{21}H_{21}NNaO_6$ $[M+Na]^+$ 406.1261, found 406.1260.

To a solution of crude bicycle-Me **44** (233.5 mg, assume 0.564 mmol) in a mixed MeOH/CH_2Cl_2 (5.5/4 mL) solvent system—due to low solubility of the starting material in MeOH—was added NaOMe (137.6 mg of a 25 wt% soln. in MeOH, 0.620 mmol) at 0 °C and stirred at this temperature for 3.3 h. The reaction temperature was warmed to room temperature and stirred for 1.7 hrs after which it was quenched with saturated aqueous NH_4Cl (five drops). The reaction mixture was filtered through Celite and the fritted funnel washed with CH_2Cl_2 (45 mL). Concentration under reduced pressure and silica gel chromatography (50%

EtOAc/Hexanes) provided pure **39** (134.6 mg, 57% yield over two steps) as a white amorphous solid.

Allylic alcohol-Me 39: m.p. = 58.8 °C (decomposition); FTIR (thin film/NaCl) 3503 (w, br), 2980 (w), 2950 (w), 1762 (s, br), 1721 (s, br), 1454 (m) cm^{-1}; ^1H NMR (400 MHz, $CDCl_3$) δ 8.01 (d, *J* = 8.4 Hz, 1H), 7.73 (d, *J* = 7.7 Hz, 1H), 7.25–7.35 (2H), 6.28 (dd, *J* = 9.7, 6.7 Hz, 1H), 5.94 (ddd, *J* = 9.7, 7.5, 7.5 Hz, 1H), 5.56 (d, *J* = 6.3 Hz, 1H), 3.67 (s, 3H), 3.59–3.63 (s, 3H and m, 1H), 3.02 (dd, *J* = 13.4, 8.0 Hz, 1H), 2.51 (br s, 1H), 1.64 (s, 9H); ^{13}C NMR (100 MHz, $CDCl_3$) δ 170.0, 168.8, 151.3, 136.4, 135.1, 134.8, 129.3, 128.4, 124.9, 122.9, 120.7, 118.8, 116.0, 84.9, 62.3, 59.2, 52.9, 52.6, 35.0, 28.1; HRMS (TOF LCMS) calc'd for $C_{22}H_{25}NNaO_7$ $[M+Na]^+$ 438.1523, found 438.1523.

Preparation of Enone-Me **37** *and iso-Enone-Me* **49**

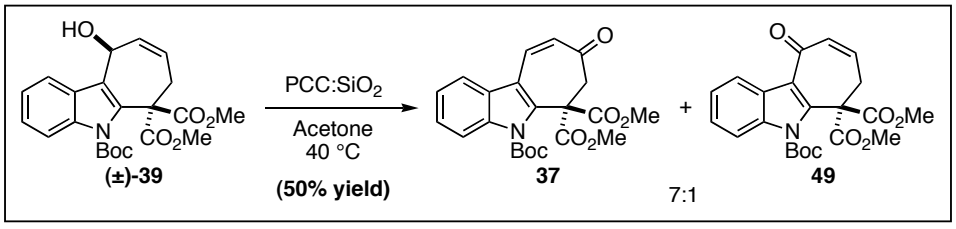

To a solution of SiO_2 (192 mg) in acetone (1.3 mL) was added PCC (18.6 mg, 0.0862 mmol) and the heterogeneous solution was pre-warmed to 40 °C before addition of allylic alcohol-Me **39** (24 mg, 0.057 mmol) as a solution in acetone (1 mL) *via* syringe pump at a rate of 0.085 mL/hr (ca. 12 hrs). The reaction was stirred for an additional 4.2 hrs before it was quenched by addition

of IPA (1 mL). Stirring for 1 h at room temperature was followed by filtration through Celite and concentration under reduced pressure. The isolated material was purified by silica gel chromatography (gradient elution, 25 → 50% EtOAc/Hexanes) to yield a 7:1 mixture of enone-Me **37**:*iso*-enone-Me **49** (12 mg, 50% yield) as a colorless oil. Analytical samples of **37** and **49** were obtained following preparative thin layer chromatography (10% Et_2O/CH_2Cl_2) as colorless oils.

Enone-Me 37: FTIR (thin film/NaCl) 2986 (w), 2950 (w), 1736 (s, br), 1664 (m), 1557 (w), 1454 (m), 1429 (m) cm^{-1}; ^1H NMR (400 MHz, $CDCl_3$) δ 7.99–8.01 (nfom, 1H), 7.68–7.70 (nfom, 1H), 7.48 (d, *J* = 12.1 Hz, 1H), 7.33–7.42 (nfom, 1H and nfom, 1H), 6.23 (d, *J* = 12.0 Hz, 1H), 3.75 (s, 6H), 3.45 (s, 2H), 1.68 (s, 9H); ^{13}C NMR (100 MHz, $CDCl_3$) δ 195.3, 168.2, 150.6, 139.2, 135.3, 133.1, 128.4, 127.2, 125.8, 123.8, 118.0, 117.9, 115.8, 86.2, 57.8, 53.4, 50.3, 28.2; HRMS (TOF LCMS) calc'd for $C_{22}H_{23}NNaO_7$ $[M+Na]^+$ 436.1367, found 436.1370.

***iso*-Enone-Me 49**: FTIR (thin film/NaCl) 2950 (m), 2919 (m), 2847 (w), 1772 (m), 1736 (s, br), 1649 (w), 1618 (w), 1449 (m) cm^{-1}; ^1H NMR (400 MHz, $CDCl_3$) δ 8.63–8.66 (nfom, 1H), 7.99–8.01 (nfom, 1H), 7.34–7.41 (nfom, 1H and nfom, 1H), 6.44 (dt, *J* = 11.4, 6.8 Hz, 1H), 6.34 (d, *J* = 11.4 Hz, 1H), 3.72 (s, 6H), 3.25 (d, *J* = 6.8 Hz, 2H), 1.67 (s, 9H); ^{13}C NMR (100 MHz, $CDCl_3$) δ 188.5, 168.3, 150.9, 143.4, 137.0, 135.3, 132.8, 127.6, 125.9, 124.7, 123.4, 122.1, 115.3, 86.6,

61.1, 53.2, 36.4, 28.2; HRMS (TOF LCMS) calc'd for $C_{22}H_{24}NO_7$ $[M+H]^+$ 414.1547, found 414.1545.

Preparation of iso-allylic alcohol-Me **50** *and Cycloheptatriene* **51**

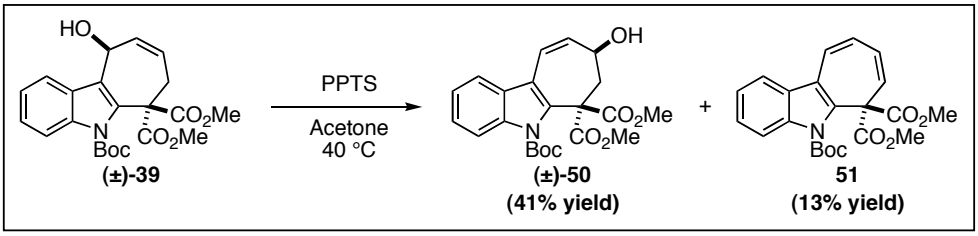

To a solution of SiO_2 (213 mg) in acetone (1.3 mL) was added PPTS (22.5 mg, 0.00895 mmol) and the heterogeneous solution was pre-warmed to 40 °C before addition of allylic alcohol-Me **39** (24 mg, 0.057 mmol) dropwise as a solution in acetone (1 mL). The reaction was stirred 14 hrs before it was filtered through Celite, concentrated under reduced pressure, and subjected to silica gel chromatography (gradient elution, 25 → 50% EtOAc/Hexanes) to provide two pure compounds. The first to elute was cycloheptatriene **51** (3 mg, 13% yield) as a colorless oil. The last compound to elute was *iso*-allylic alcohol-Me **50** (10 mg, 41% yield) as a colorless oil.

Cycloheptatriene 51: FTIR (thin film/NaCl) 2975 (w), 2950 (w), 1746 (s, br), 1726 (s, br), 1454 (m) cm^{-1}; ^1H NMR (400 MHz, $CDCl_3$) δ 7.95 (d, J = 8.4 Hz, 1H), 7.67 (d, J = 7.3 Hz, 1H), 7.25–7.36 (3H), 6.60–6.64 (m, 1H), 6.42–6.43 (2H), 3.68 (s, 6H), 1.65 (s, 9H); ^{13}C NMR (100 MHz, $CDCl_3$) δ 168.1, 151.3, 136.5, 127.6, 126.9, 126.8, 126.4, 125.2, 123.8, 123.2, 123.2, 121.6, 118.9, 115.4, 85.2,

60.6, 53.5, 28.4; HRMS (TOF LCMS) calc'd for $C_{22}H_{23}NNaO_6$ $[M+Na]^+$ 420.1418, found 420.1411.

***iso*-Allylic alcohol-Me 50**: FTIR (thin film/NaCl) 3493 (m, br), 2980 (w), 2950 (w), 2924 (w), 2852 (w), 1767 (s, br), 1726 (s, br), 1480 (w), 1460 (m), 1429 (w) cm^{-1}; ^1H NMR (400 MHz, $CDCl_3$) δ 8.00 (d, J = 8.2 Hz, 1H), 7.65 (d, J = 7.2 Hz, 1H), 7.33–7.37 (nfom, 1H), 7.28–7.31 (nfom, 1H), 6.65 (dd, J = 11.6, 2.3 Hz, 1H), 6.10 (ddd, J = 11.5, 2.6, 1.7 Hz, 1H), 4.47 (m, 1H), 3.69 (s, 3H), 3.67 (s, 3H), 2.92 (m, 1H), 2.66 (dd, J = 13.3, 10.1 Hz, 1H), 2.07 (d, J = 4.9 Hz, 1H), 1.65 (s, 9H); ^{13}C NMR (100 MHz, $CDCl_3$) δ 170.2, 169.8, 151.5, 136.1, 135.1, 134.1, 129.0, 125.2, 123.0, 118.5, 118.1, 117.5, 116.1, 85.1, 68.0, 59.4, 53.1, 52.9, 44.9, 28.2; HRMS (TOF LCMS) calc'd for $C_{22}H_{25}NNaO_7$ $[M+Na]^+$ 438.1523, found 438.1520.

Oxidation of iso-Allylic alcohol-Me **50**

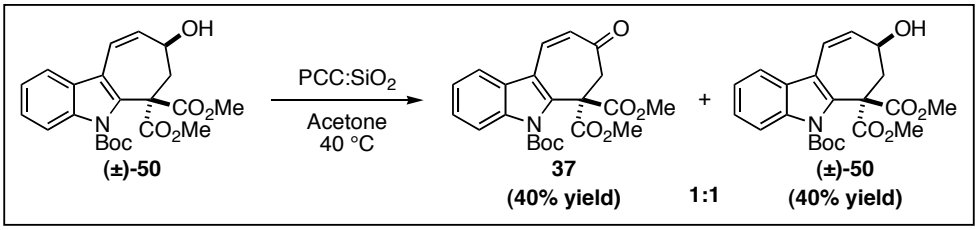

To a solution of SiO_2 (45 mg) in acetone (0.5 mL) was added PCC (4.8 mg, 0.0190 mmol) and the heterogeneous solution was pre-warmed to 40 °C before addition of *iso*-allylic alcohol-Me **50** (5.0 mg, 0.0120 mmol) as a solution in acetone (1 mL) *via* syringe pump at a rate of 0.12 mL/hr (ca. 8.3 hrs). The

reaction was stirred for an additional 4.5 hrs before it was quenched by addition of IPA (1 mL). Stirring for 1 h at 40 °C was followed by filtration through Celite and concentration under reduced pressure. The isolated material was purified by preparative thin layer chromatography (50% EtOAc/Hexanes) to yield enone-Me **37** (2 mg, 40% yield) as a colorless oil and *iso*-allylic alcohol-Me **50** (2 mg, 40% yield) as a colorless oil.

Enone-Me 37: identical to a characterized sample (^{1}H NMR, TLC).

***Iso*-Allylic alcohol-Me 50**: identical to a characterized sample (^{1}H NMR, TLC).

2.4 Notes and References

1. (a) *"The Michael-Alkylation Ring Synthesis: Piperidine and Pyrrolidine Construction"*, Dolfini, J. E.; Dolfini, D. M. *Tetrahedron Lett.* **1964**, *5*, 2103–2107; (b) *"Total Synthesis of (+)-Aspidospermidine: A New Strategy for the Enantiospecific Synthesis of Aspidosperma Alkaloids"*, Marino, J. P.; Rubio, M. B.; Cao, G. F.; de Dios, A. *J. Am. Chem. Soc.* **2002**, *124*, 13398–13399.
2. *"Tyrosine Kinase Inhibitors. 6. Structure-Activity Relationships Among N- and 3-Substituted 2,2'-Diselenobis(1H-indoles) for Inhibition of Protein Tyrosine Kinases and Comparative in vitro and in vivo Studies Against Selected Sulfur Congeners"*, Showalter, H. D. H.; Sercel, A. D.; Leja, B. M.; Wolfangel, C. D.; Ambroso, L. A.; Elliott, W. L.; Fry, D. W.; Kraker, A.

J.; Howard, C. T.; Lu, G. H.; Moore, C. W.; Nelson, J. M.; Roberts, B. J.; Vincent, P. W.; Denny, W. A.; Thompson, A. M. *J. Med. Chem.* **1997**, *40*, 413–426.

3. *"Synthetic Studies on Diazonamide A. Benzofuranone-Tyrosine and Indole-Oxazole Fragment Support Studies"*, Konopelski, J. P.; Hottenroth, J. M.; Oltra, H. M.; Veliz, E. A.; Yang, Z. C. *Synlett* **1996**, 609–611.

4. Standard conditions include:

Electrophile	Base	Solvent
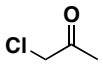	K_2CO_3 NaH K_2CO_3	neat THF THF: DMF
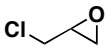	NaO*t*Bu NaO*t*Bu	THF DMF
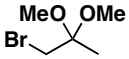	NaO*t*Bu NaH	THF THF
	NaH	THF

5. (a) *"Organopalladium Intermediates in Organic Synthesis"*, Trost, B. M. *Tetrahedron* **1977**, *33*, 2615–2649; (b) *"New Synthetic Reactions of Allyl Alkyl Carbonates, Allyl Beta-Keto Carboxylates, and Allyl Vinylic Carbonates Catalyzed by Palladium Complexes"*, Tsuji, J.; Minami, I. *Acc. Chem. Res.* **1987**, *20*, 140–145.

6. *"Regioselective Suprafacial 1,5-Hydrogen Shifts in o-Quinodimethanes-A Route to 4-Deoxypodophyllotoxin"*, Jones, D. W.; Thompson, A. M. *J. Chem. Soc. Chem. Commun.* **1988**, 1095–1096.

7. (a) *"General Synthetic Entry to Highly-Oxygenated, Angularly-Fused Polycyclic Aromatic-Compounds"*, Koo, S. H.; Liebeskind, L. S. *J. Am.*

Chem. Soc. **1995**, *117*, 3389–3404; (b) *"Mechanistic Aspects of the Annelation Reactions of Benzocyclobutenedione Monoketals with Vinyllithium Reagents"*, Spangler, L. A.; Swenton, J. S. *J. Org. Chem.* **1984**, *49*, 1800–1806; (c) *"An Efficient Access to Alpha-Tetralones and their Derivatives via o-Quinodimethanes Generated by Isochromene Ring Cleavage"*, Verin, S. V.; Tosunyan, D. E.; Kuznetsov, E. V. *Mendeleev Commun.* **1992**, 20–21.

8. (a) *"Ring-Closing Metathesis and Related Processes in Organic Synthesis"*, Grubbs, R. H.; Miller, S. J.; Fu, G. C. *Acc. Chem. Res.* **1995**, *28*, 446–452; (b) *"The Development of $L_2X_2Ru=CHR$ Olefin Metathesis Catalysts: An Organometallic Success Story"*, Trnka, T. M.; Grubbs, R. H. *Acc. Chem. Res.* **2001**, *34*, 18–29.

9. *"BF_3•Et_2O-Mediated Intramolecular Allylstannane-Ketone Cyclizations: Formation of Bicyclo[4.1.0]hept-4-en-1-ols from 5-(Tributylstannyl)-3-cycloheptenones"*, Takeda, K.; Nakajima, A.; Yoshii, E. *Synlett* **1996**, 753–754.

10. *"Pyridinium Chlorochromate: A Versatile Oxidant in Organic Synthesis"*, Piancatelli, G.; Scettri, A.; D'Auria, M. *Synthesis* **1982**, 245–258.

11. (a) *"Structure Determination and Synthesis of a New Trihydroxy Gibberellin from Brassica campestris cotyledons and a Related Tetrahydroxy Derivative from Immature Seeds of Prunus persica"*, Bhaskar, K. V.; Chu, W. L. A.; Gaskin, P. A.; Mander, L. N.; Murofushi, N.;

Pearce, D. W.; Pharis, R. P.; Takahashi, N.; Yamaguchi, I. *Tetrahedron Lett.* **1991**, *32*, 6203–6206; (b) *"1,3-Oxidative Rearrangements of Dienols"*, Majetich, G.; Condon, S.; Hull, K.; Ahmad, S. *Tetrahedron Lett.* **1989**, *30*, 1033–1036.

12. *"Pyridinium Chlorochromate-Efficient Reagent for Oxidation of Primary and Secondary Alcohols to Carbonyl Compounds"*, Corey, E. J.; Suggs, J. W. *Tetrahedron Lett.* **1975**, 2647–2650.

13. *"Efficient Large-Scale Synthesis of BILN 2061, a Potent HCV Protease Inhibitor, by a Convergent Approach Based on Ring-Closing Metathesis"*, Yee, N. K.; Farina, V.; Houpis, I. N.; Haddad, N.; Frutos, R. P.; Gallou, F.; Wang, X.; Wei, X.; Simpson, R. D.; Feng, X.; Fuchs, V.; Xu, Y.; Tan, J.; Zhang, L.; Xu, J.; Smith-Keenan, L. L.; Vitous, J.; Ridges, M. D.; Spinelli, E. M.; Johnson, M.; Donsbach, K.; Nicola, T.; Brener, M.; Winter, E.; Kreye, P.; Samstag, W. *J. Org. Chem.* **2006**, *71*, 7133–7145.

Appendix 1: Characterization Spectra Relevant to Chapter Two

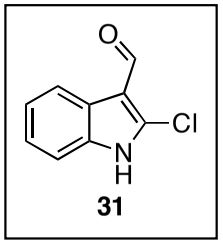

31

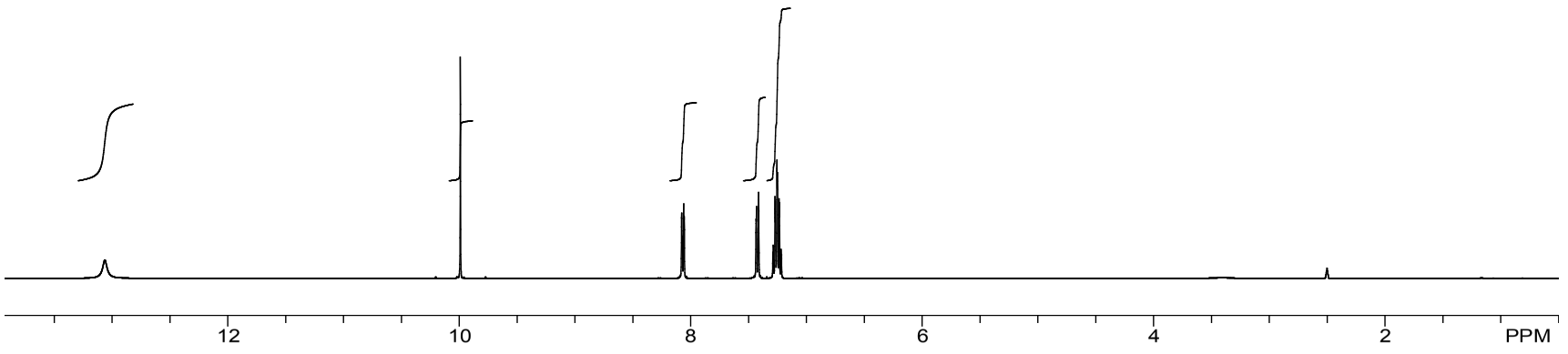

Figure A.1.1 ^{1}H NMR spectrum (400 MHz, DMSO-d_6) of compound **31**

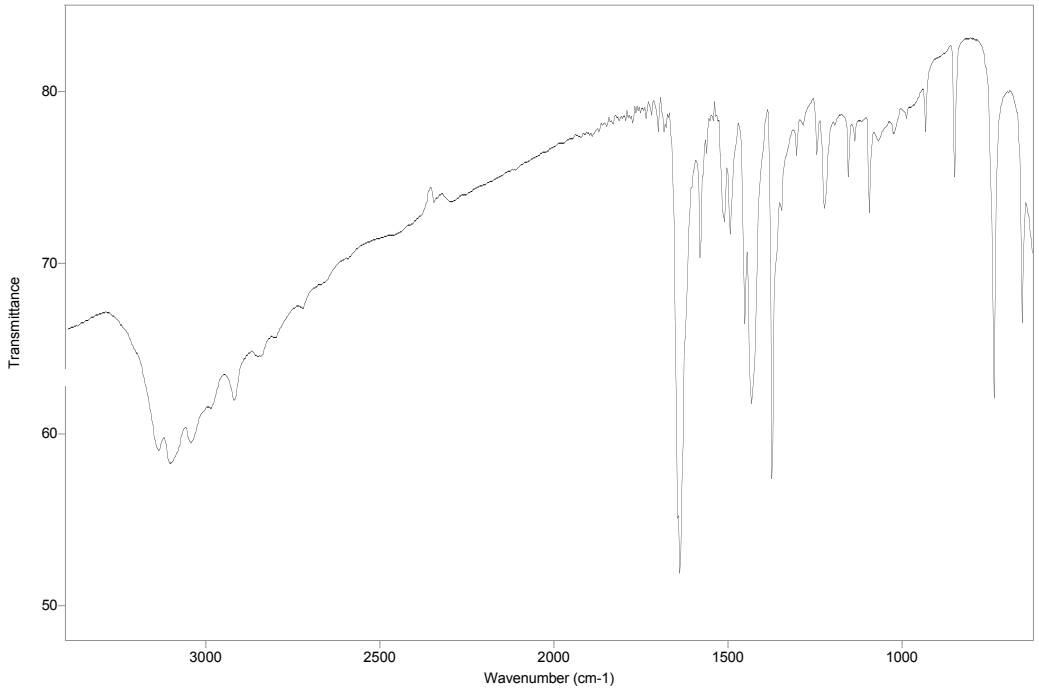

Figure A.1.2 FTIR spectrum (NaCl/thin film) of compound **31**

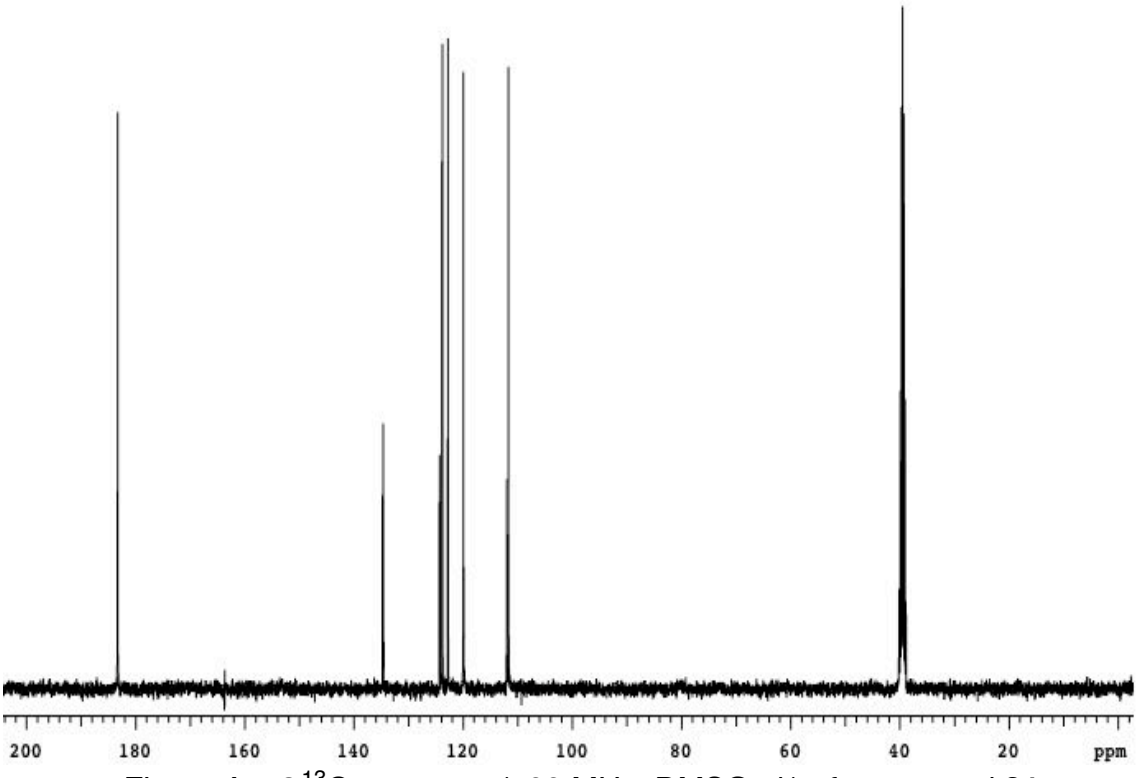

Figure A.1.3 ^{13}C spectrum (100 MHz, DMSO-d_6) of compound **31**

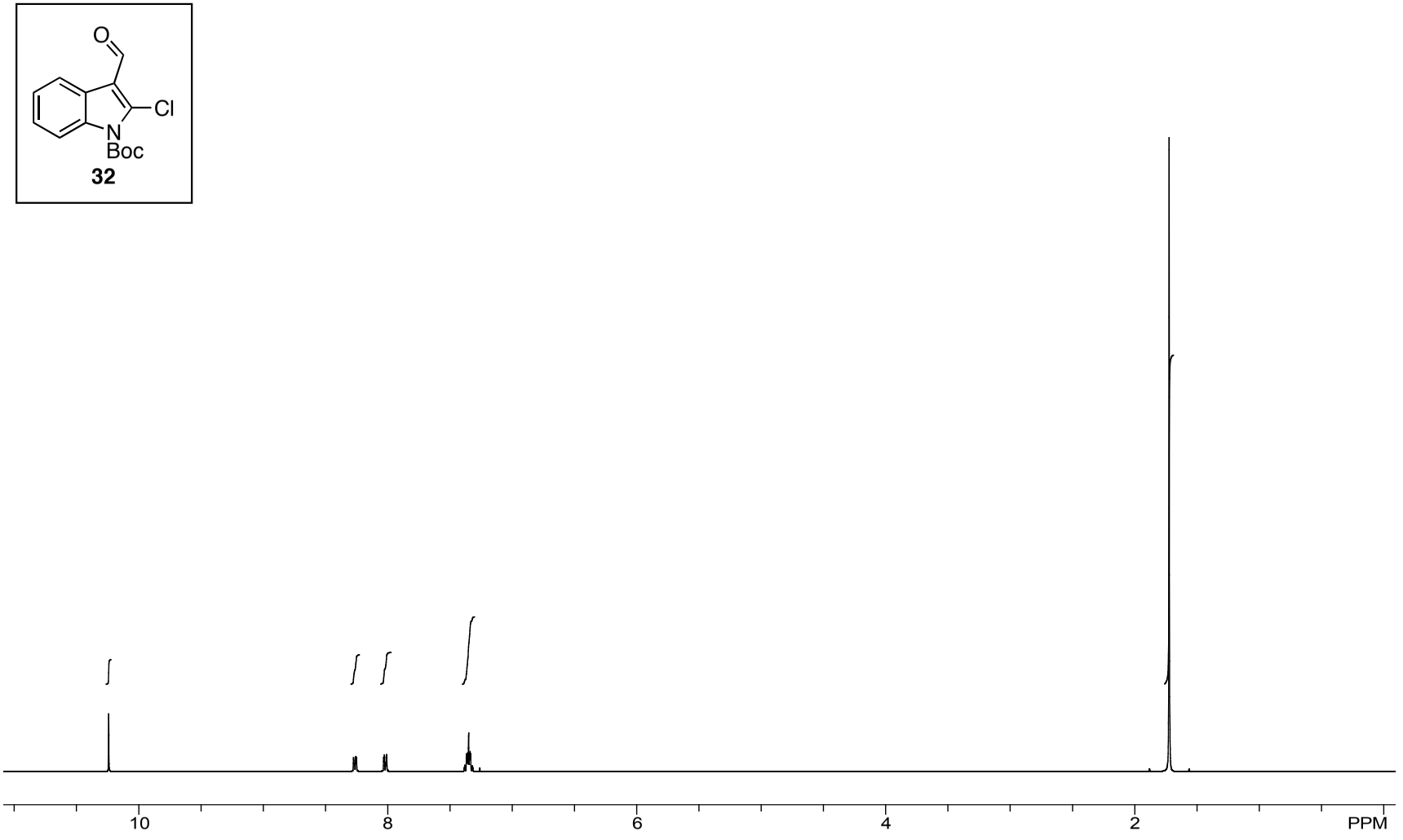

Figure A.1.4 ^{1}H NMR spectrum (400 MHz, $CDCl_3$) of compound **32**

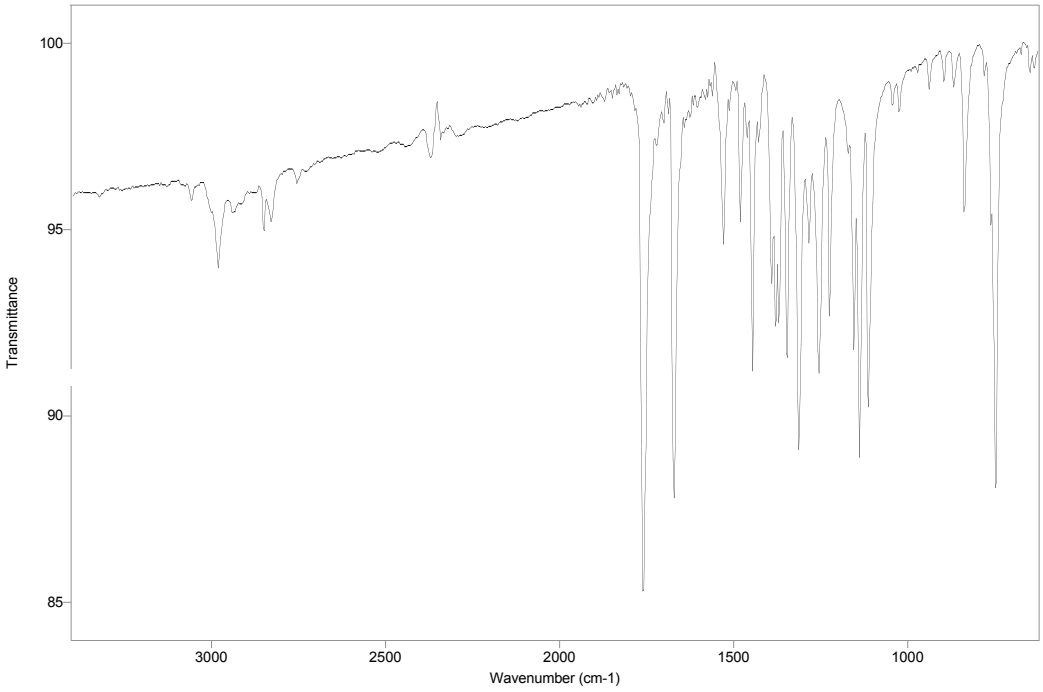

Figure A.1.5 FTIR spectrum (NaCl/thin film) of compound **32**

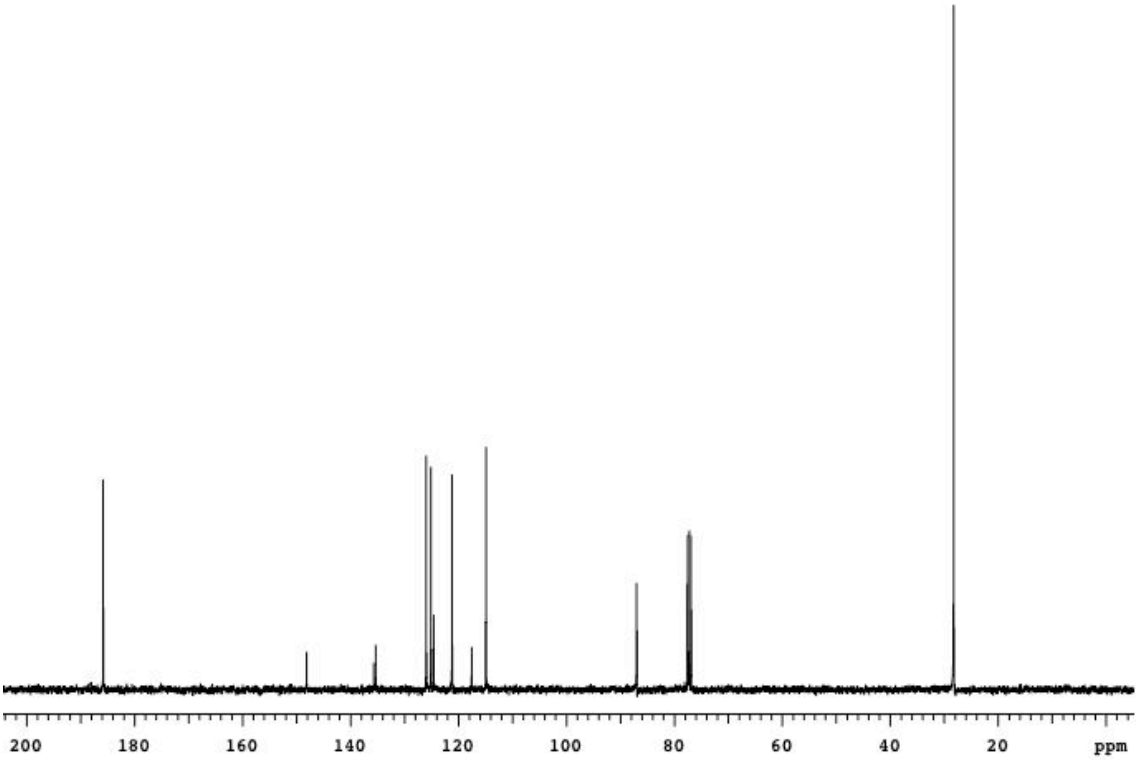

Figure A.1.6 ^{13}C spectrum (100 MHz, $CDCl_3$) of compound **32**

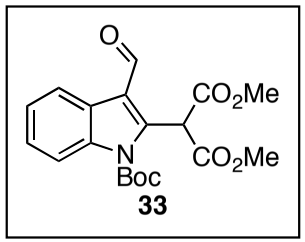

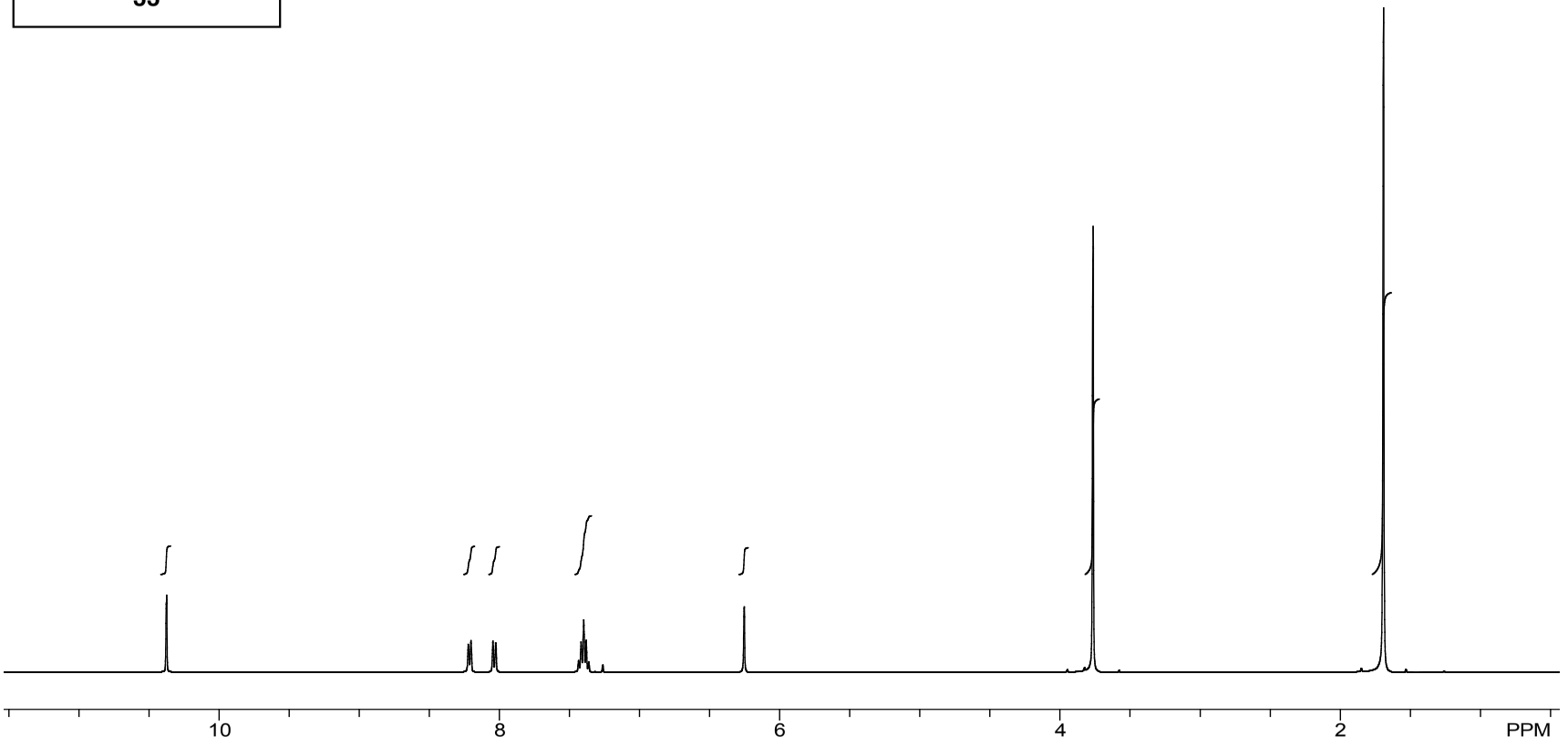

Figure A.1.7 ^{1}H NMR spectrum (400 MHz, $CDCl_3$) of compound **33**

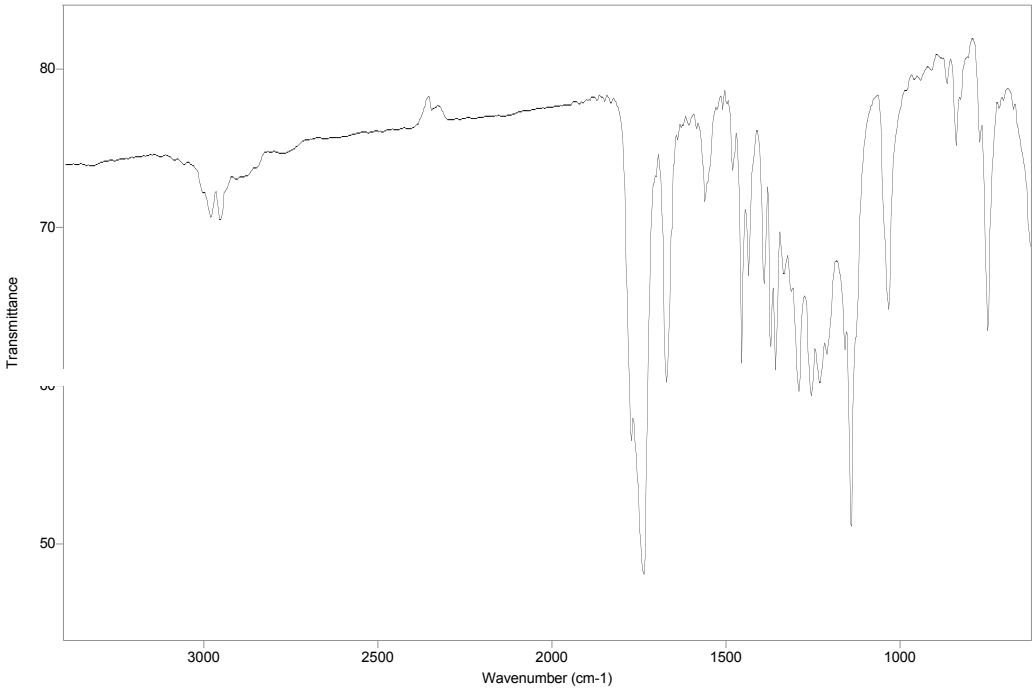

Figure A.1.8 FTIR spectrum (NaCl/thin film) of compound **33**

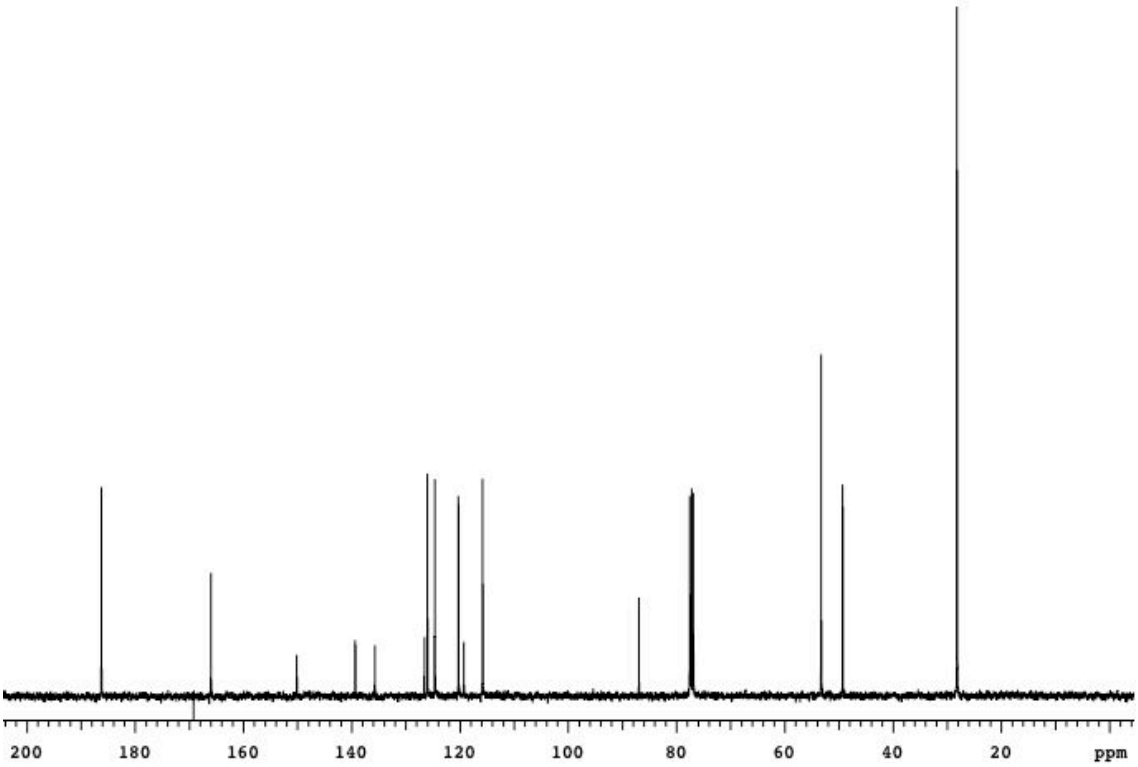

Figure A.1.9 ^{13}C spectrum (100 MHz, $CDCl_3$) of compound **33**

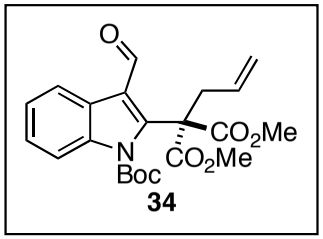

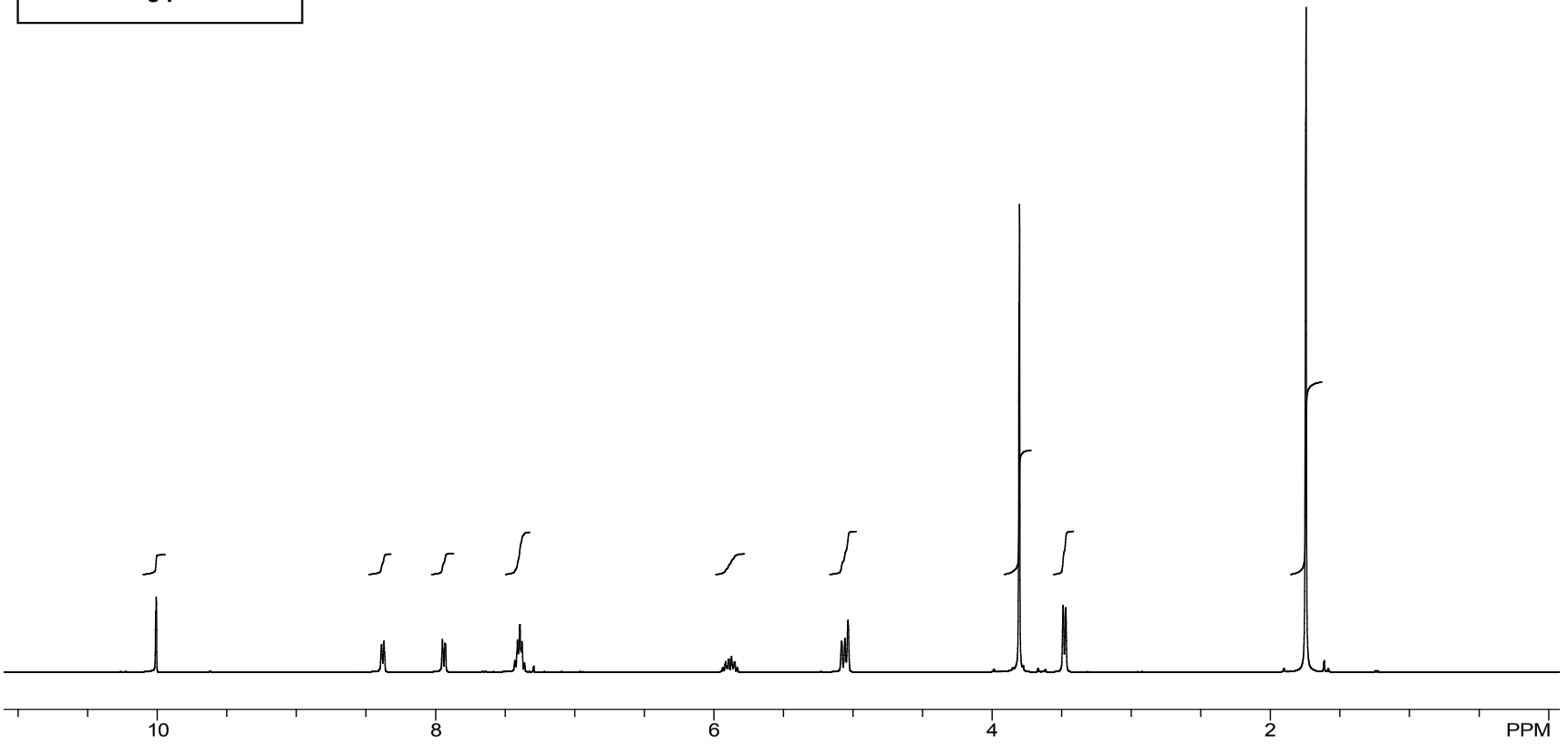

Figure A.1.10 ^{1}H NMR spectrum (400 MHz, $CDCl_3$) of compound **34**

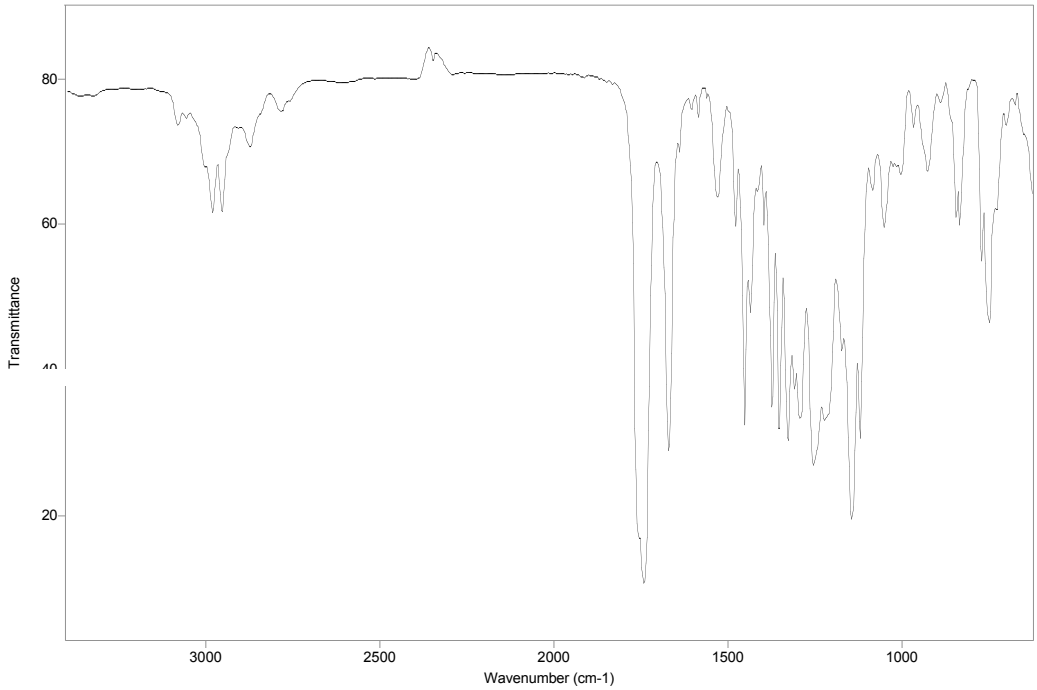

Figure A.1.11 FTIR spectrum (NaCl/thin film) of compound **34**

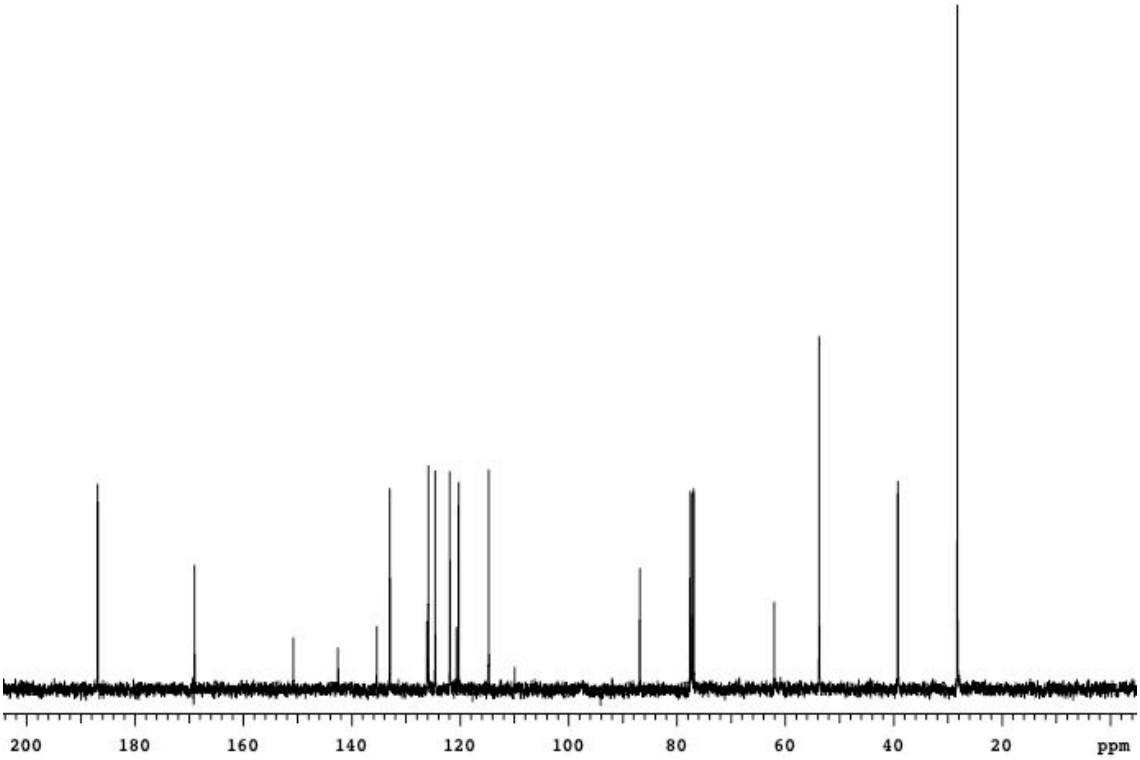

Figure A.1.12 ^{13}C spectrum (100 MHz, $CDCl_3$) of compound **34**

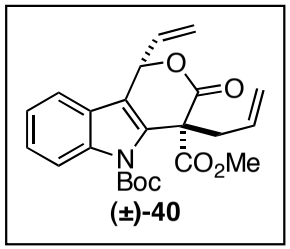

(±)-40

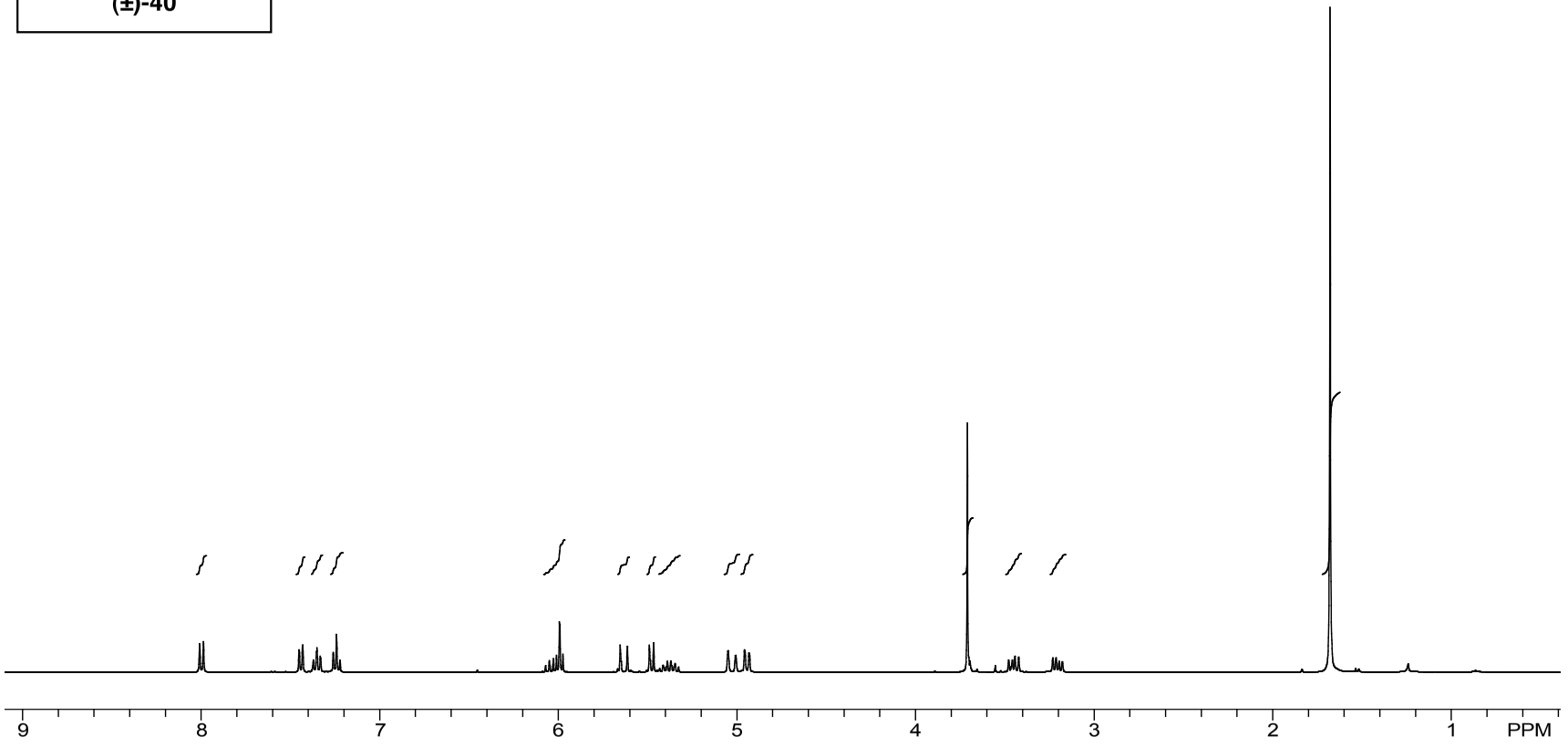

Figure A.1.13 ^{1}H NMR spectrum (400 MHz, $CDCl_3$) of compound **40**

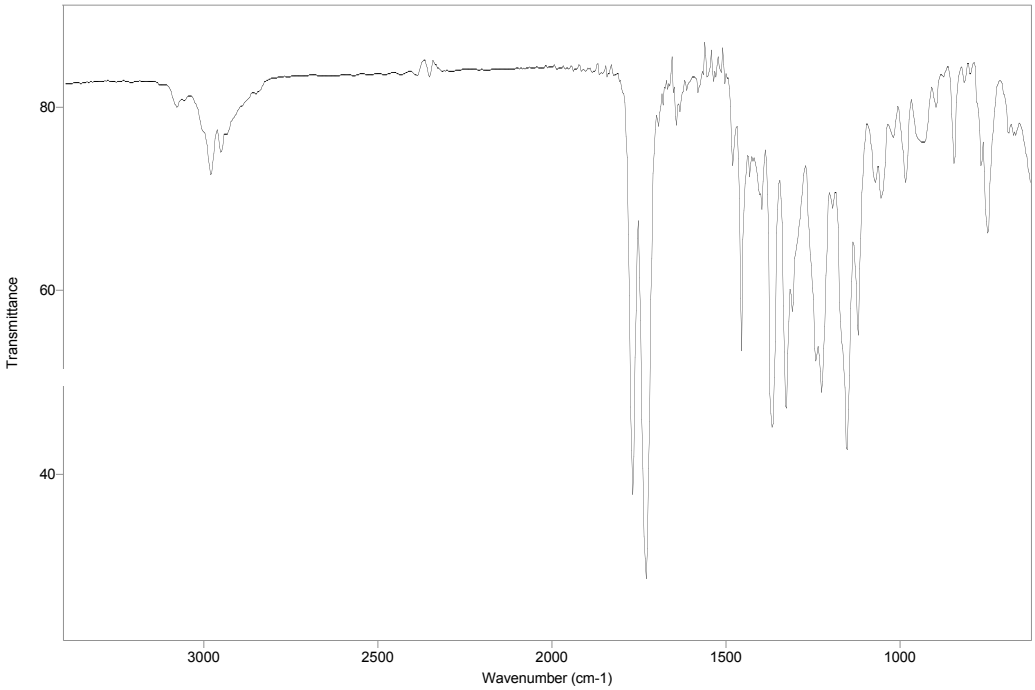

Figure A.1.14 FTIR spectrum (NaCl/thin film) of compound **40**

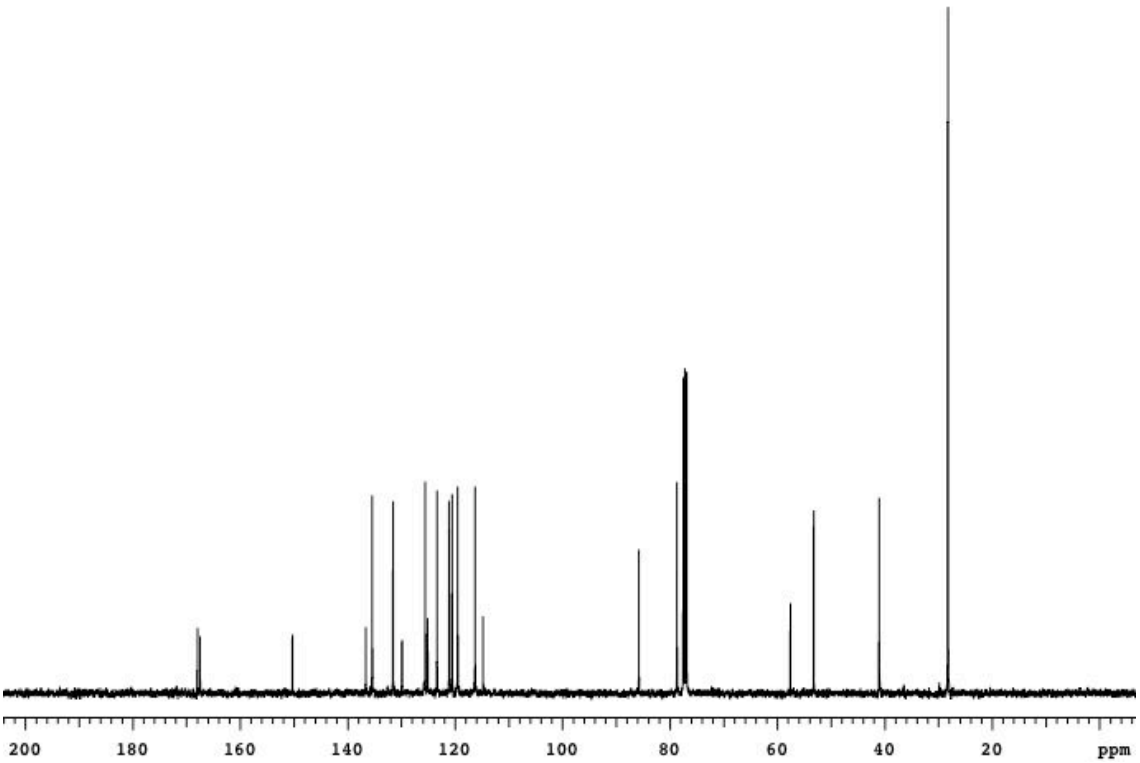

Figure A.1.15 ^{13}C spectrum (100 MHz, $CDCl_3$) of compound **40**

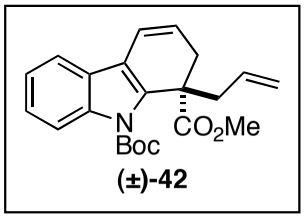

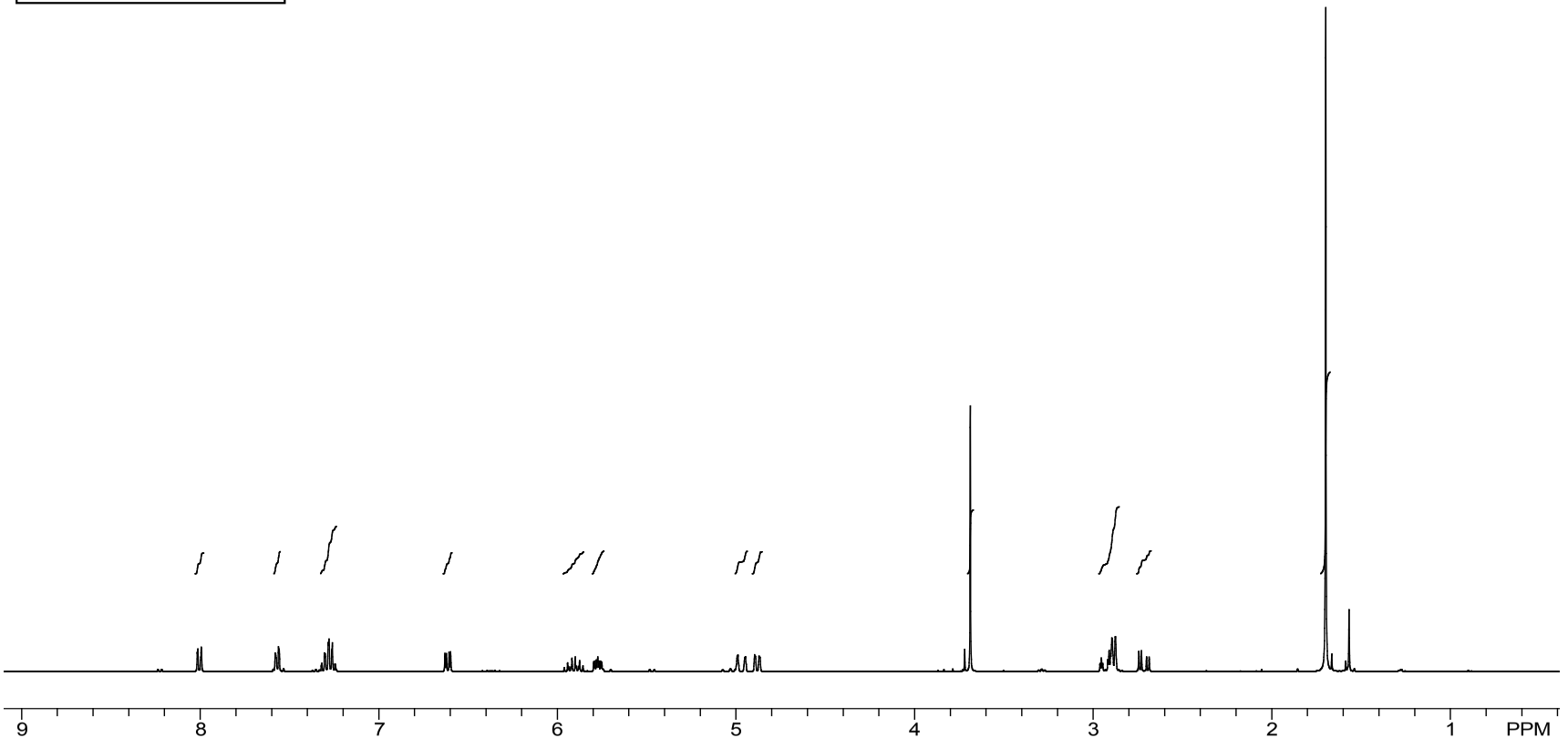

Figure A.1.16 ^{1}H NMR spectrum (400 MHz, $CDCl_3$) of compound **42**

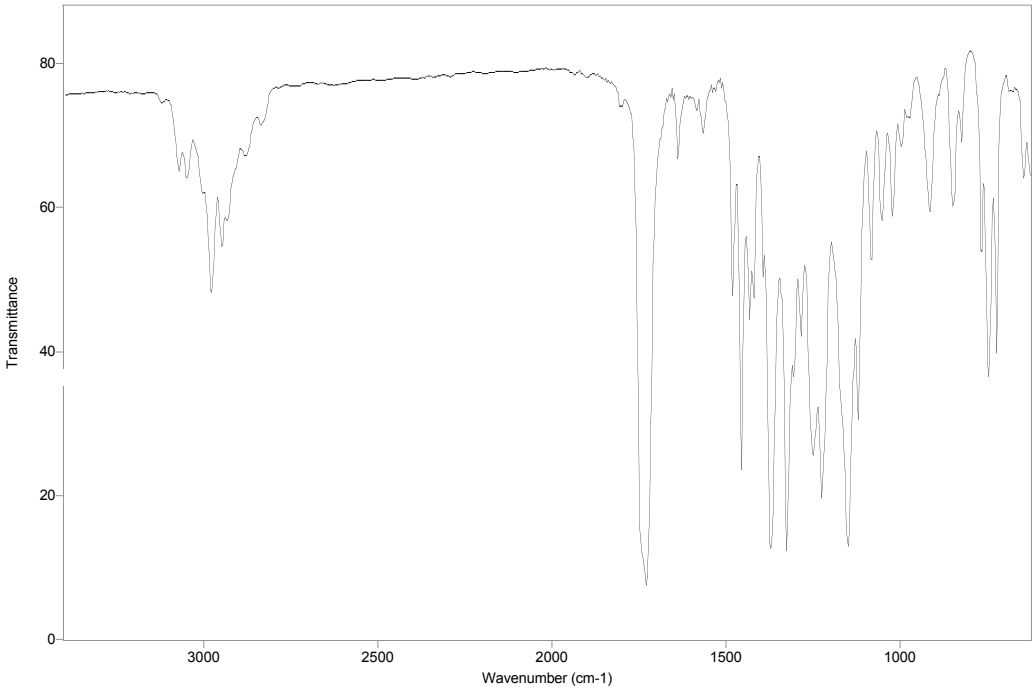

Figure A.1.17 FTIR spectrum (NaCl/thin film) of compound **42**

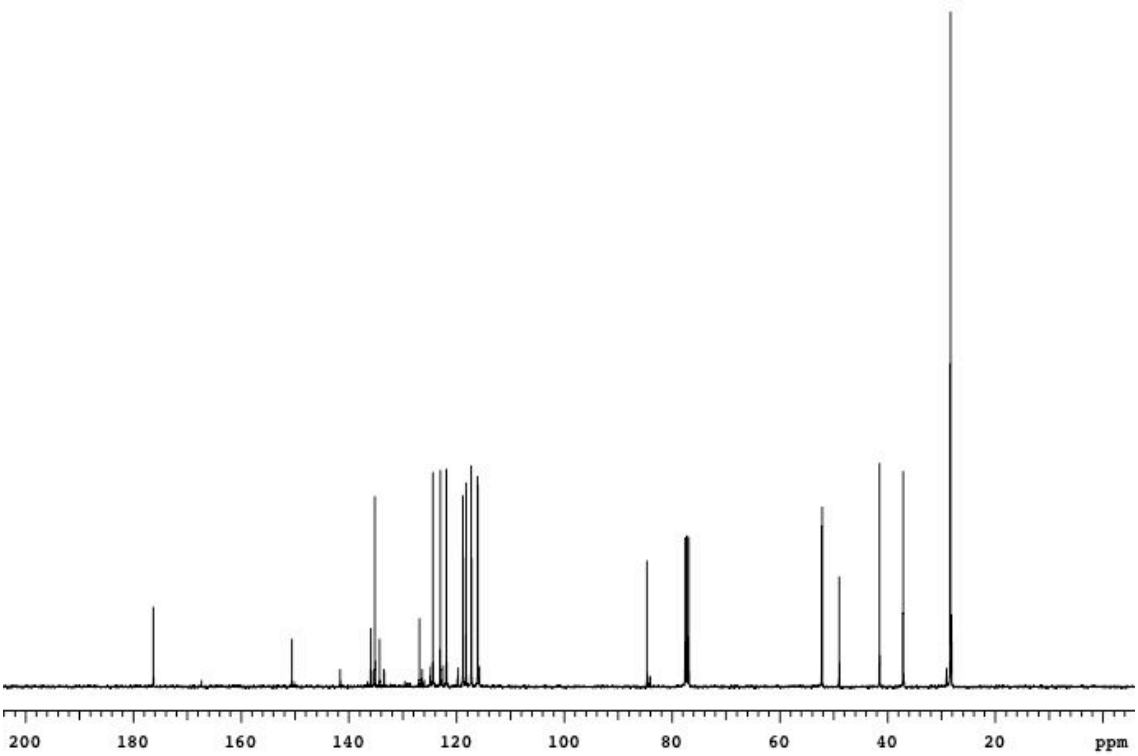

Figure A.1.18 ^{13}C spectrum (100 MHz, $CDCl_3$) of compound **42**

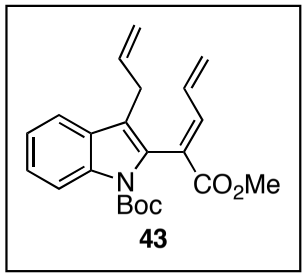

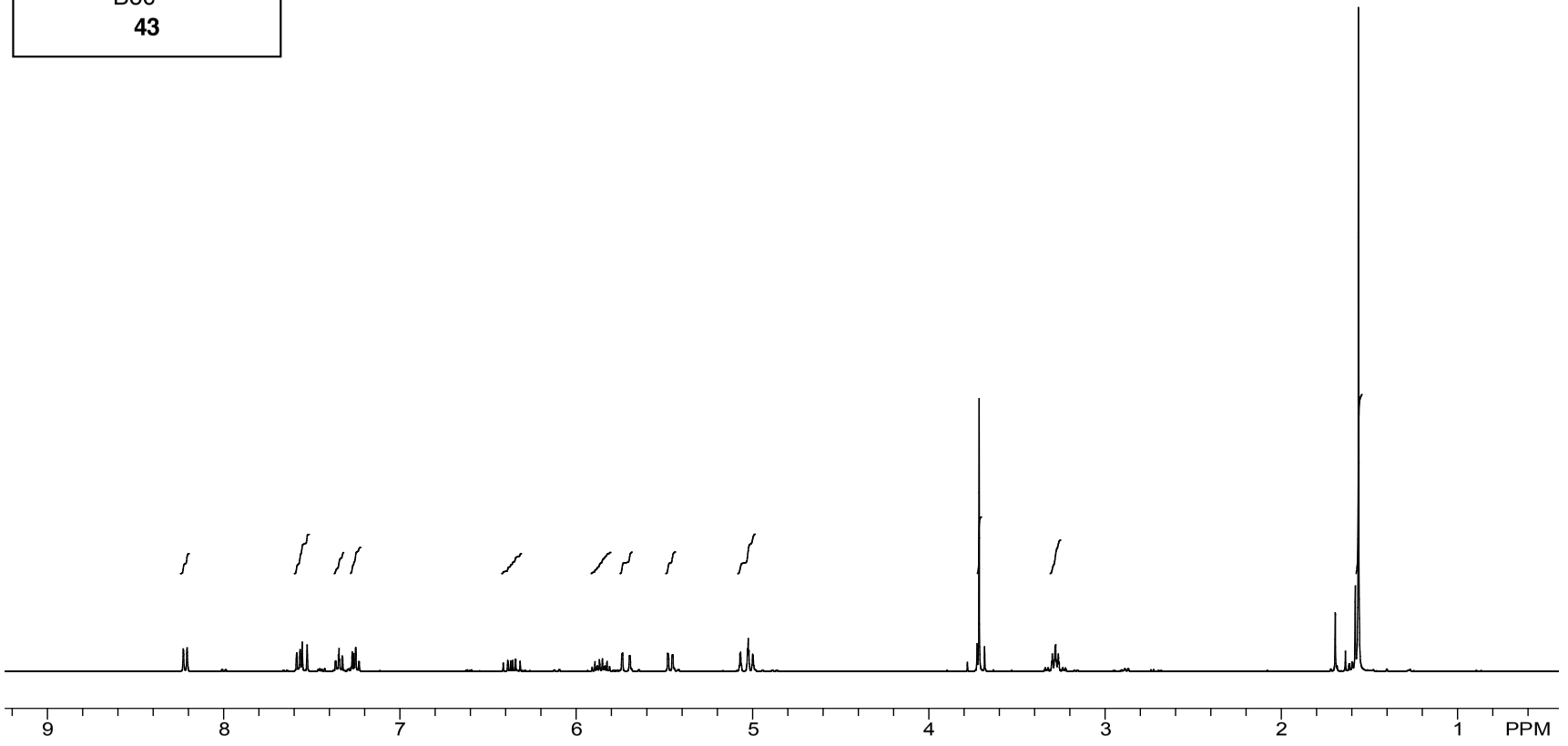

Figure A.1.19 ^{1}H NMR spectrum (400 MHz, $CDCl_3$) of compound **43**

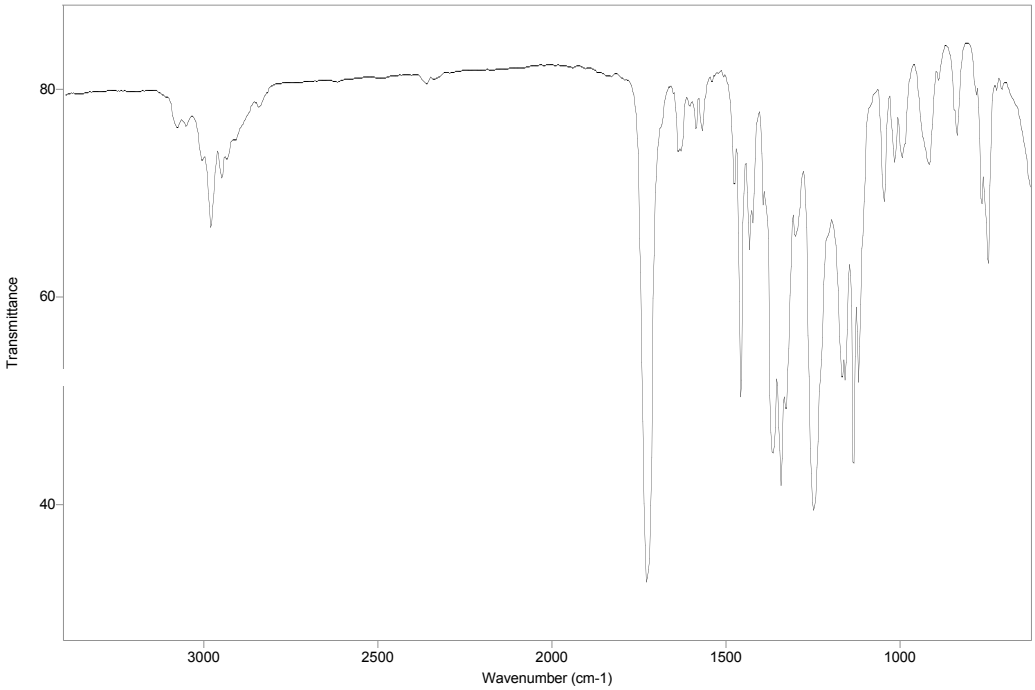

Figure A.1.20 FTIR spectrum (NaCl/thin film) of compound **43**

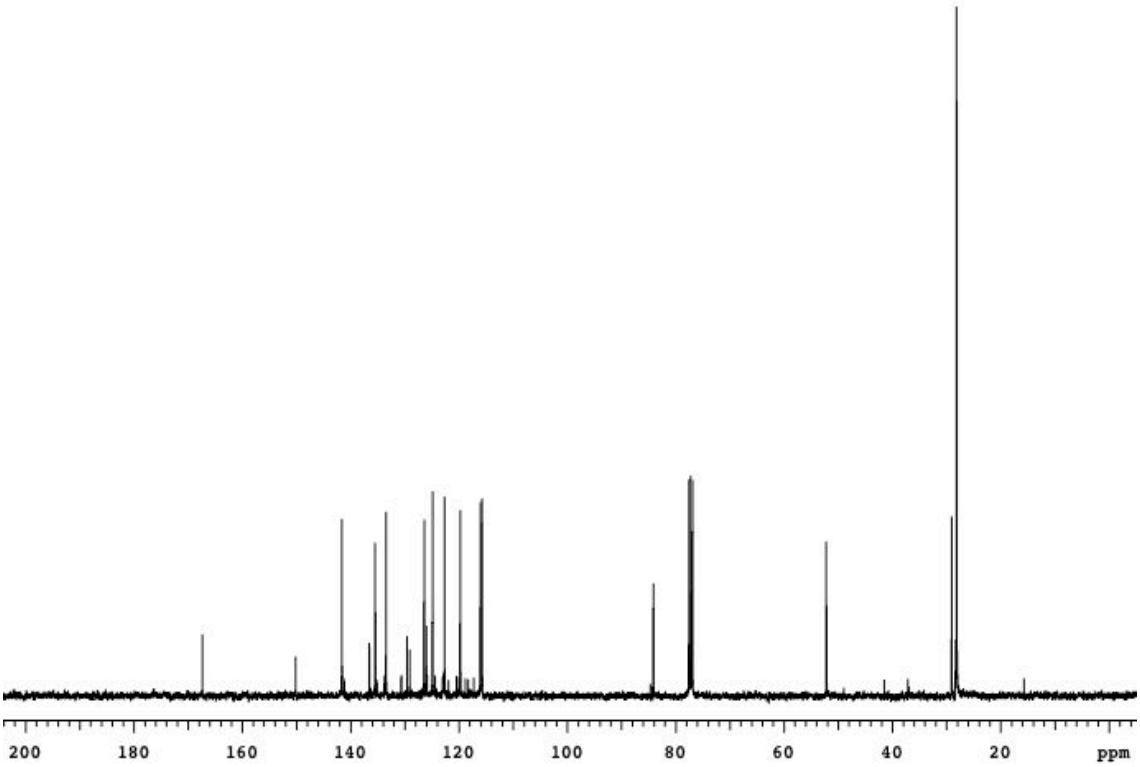

Figure A.1.21 ^{13}C spectrum (100 MHz, $CDCl_3$) of compound **43**

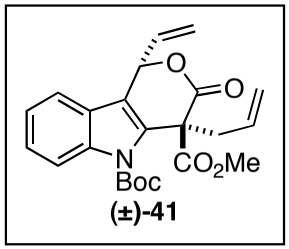

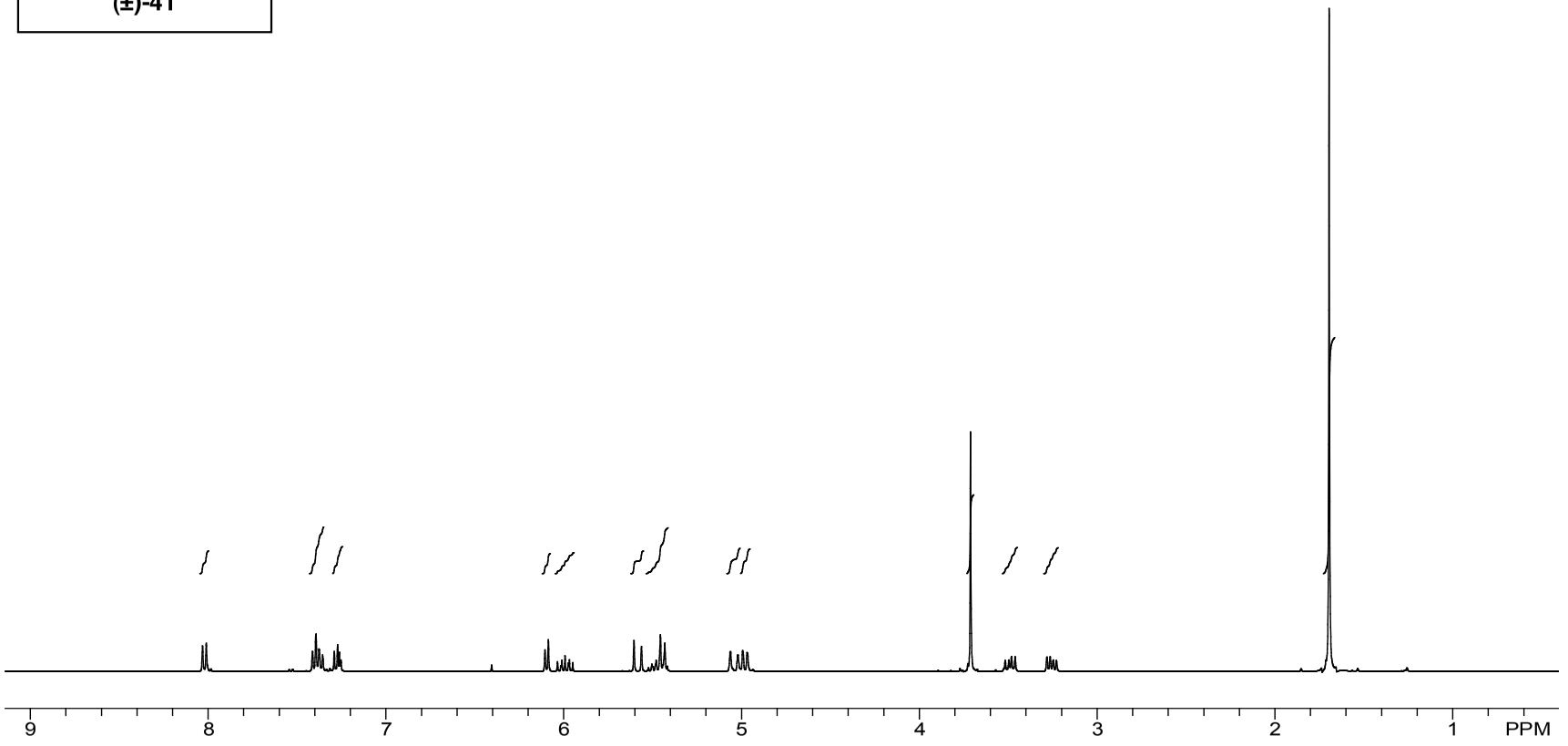

Figure A.1.22 ^{1}H NMR spectrum (400 MHz, $CDCl_3$) of compound **41**

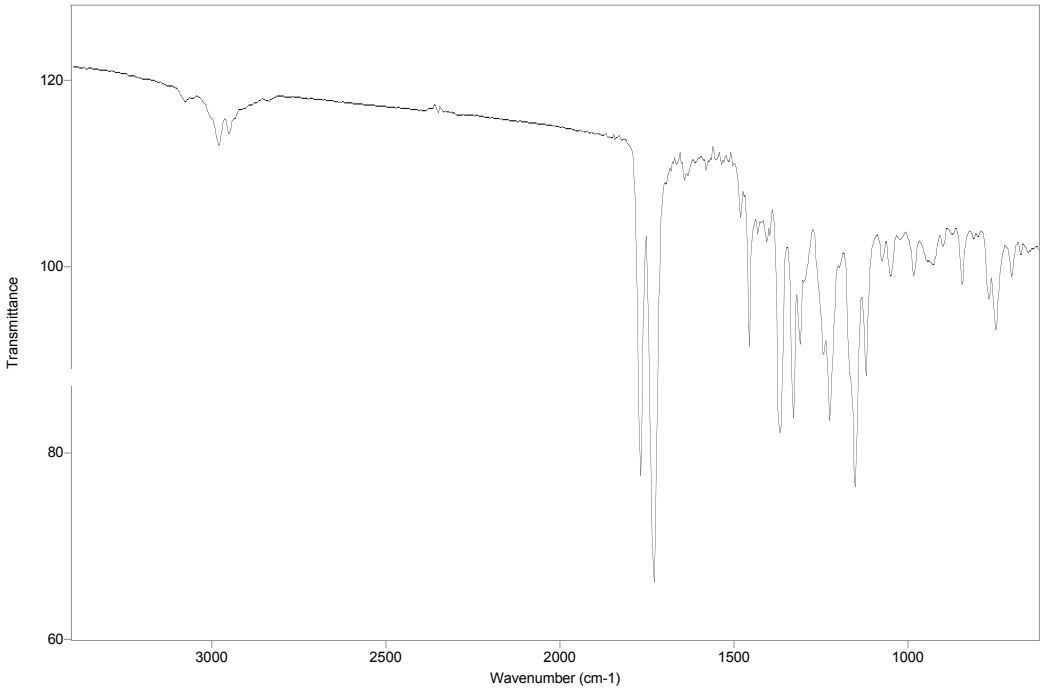

Figure A.1.23 FTIR spectrum (NaCl/thin film) of compound **41**

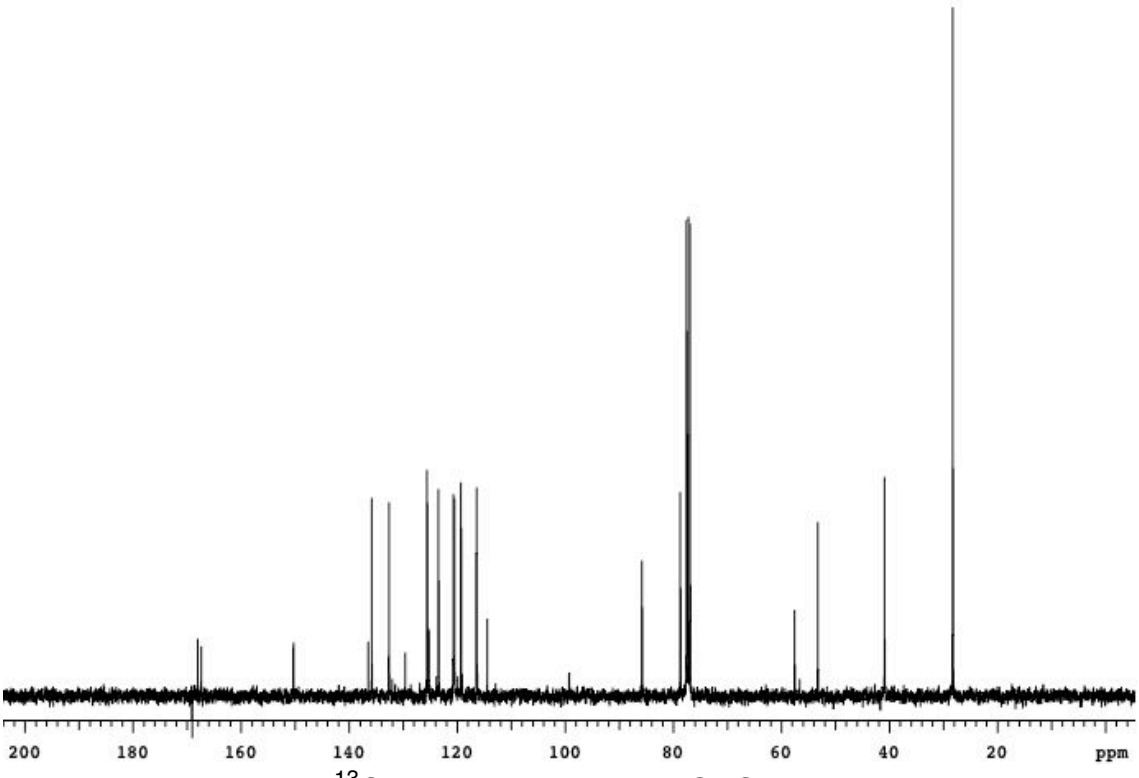

Figure A.1.24 ^{13}C spectrum (100 MHz, $CDCl_3$) of compound **41**

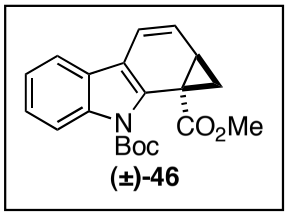

(±)-46

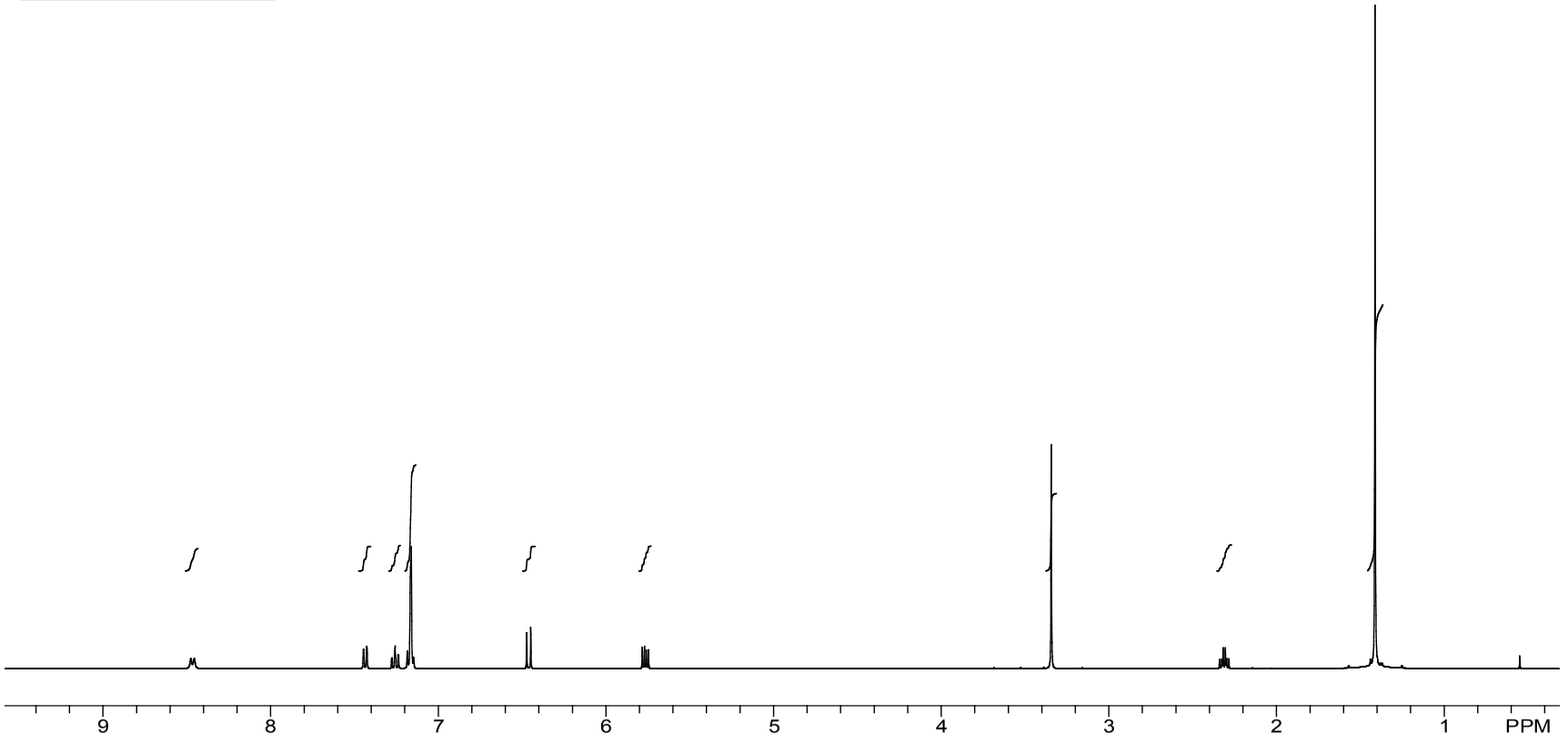

Figure A.1.25 ^{1}H NMR spectrum (400 MHz, Benzene-d_6) of compound **46**

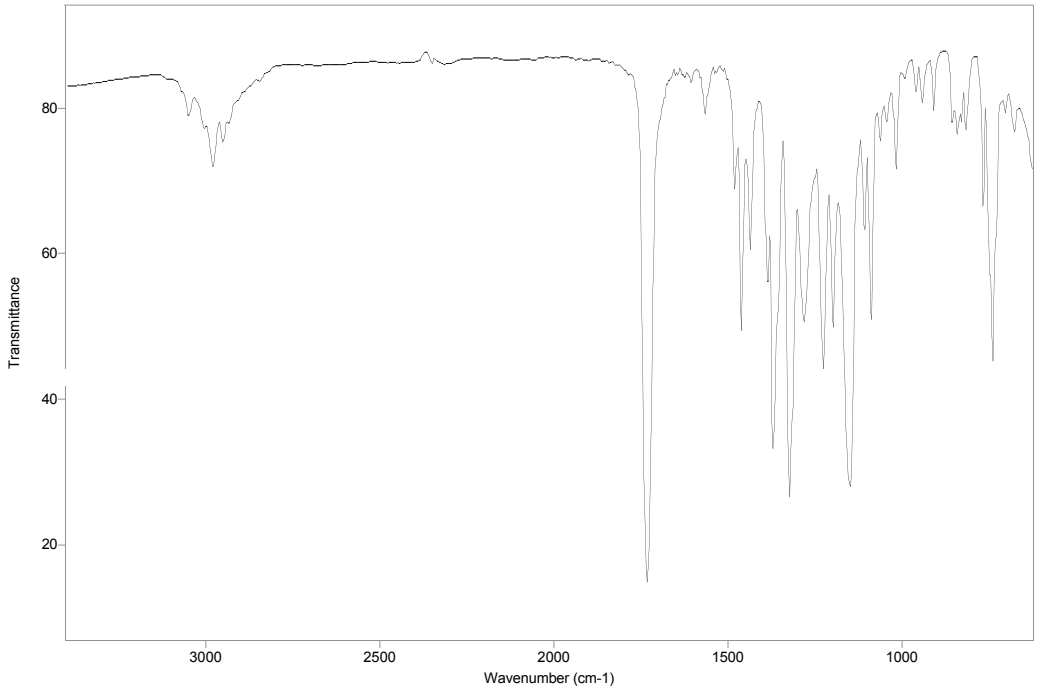

Figure A.1.26 FTIR spectrum (NaCl/thin film) of compound **46**

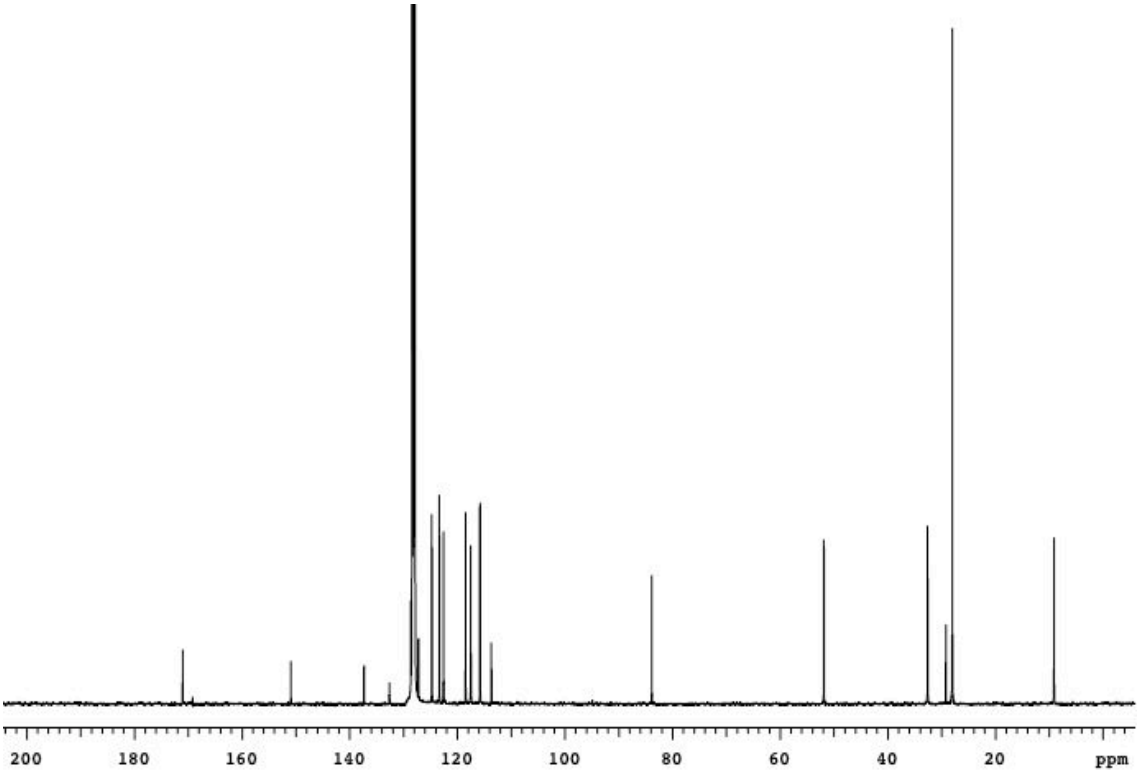

Figure A.1.27 ^{13}C spectrum (100 MHz, Benzene-d_6) of compound **46**

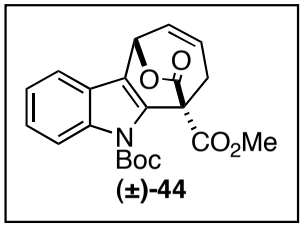

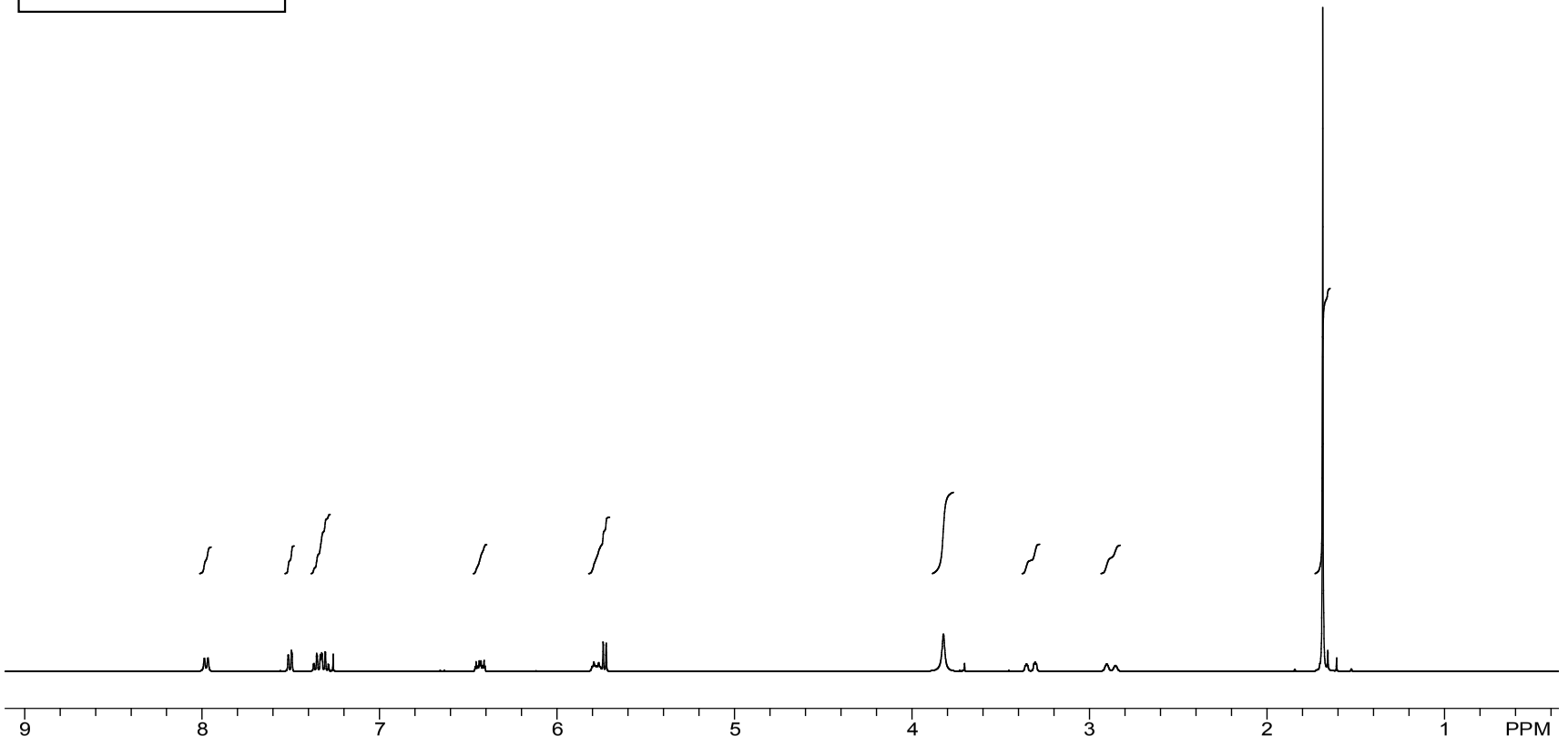

Figure A.1.28 ^{1}H NMR spectrum (400 MHz, $CDCl_3$) of compound **44**

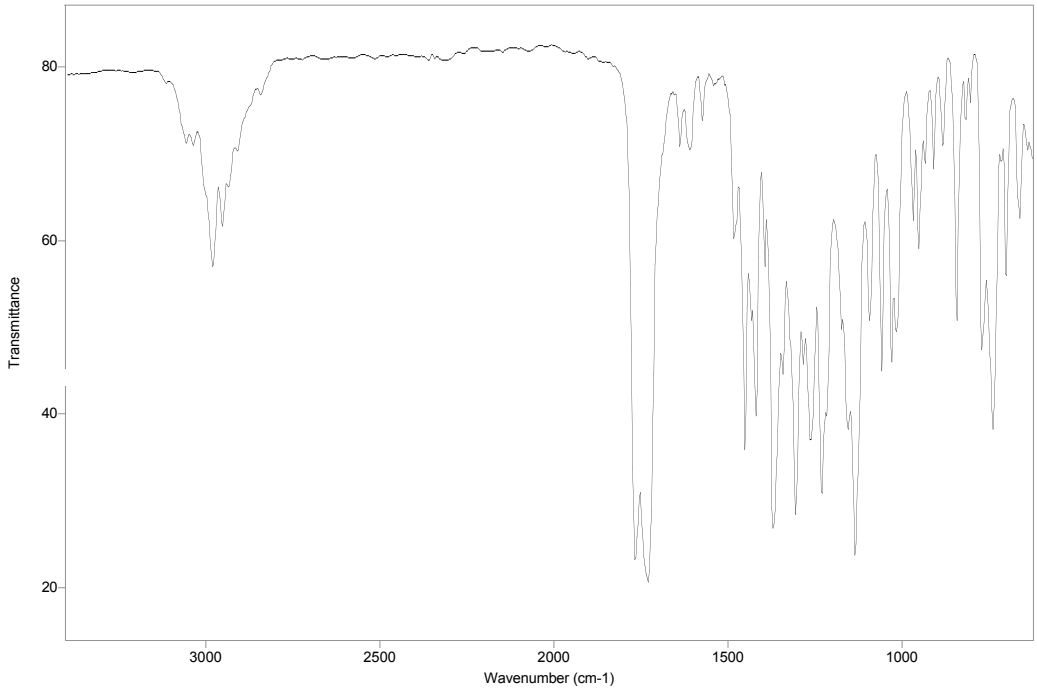

Figure A.1.29 FTIR spectrum (NaCl/thin film) of compound **44**

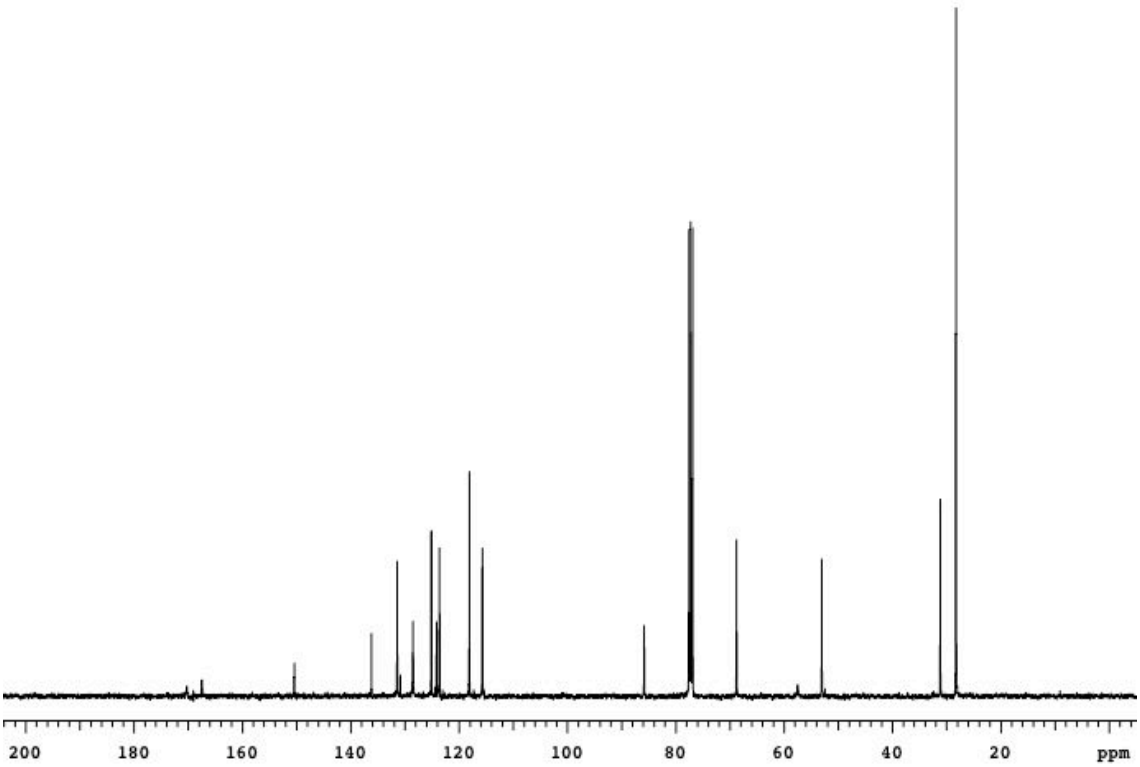

Figure A.1.30 ^{13}C spectrum (100 MHz, $CDCl_3$) of compound **44**

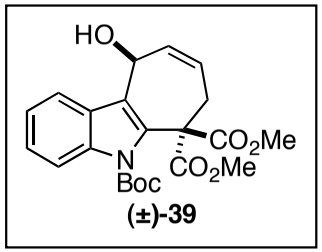

(±)-39

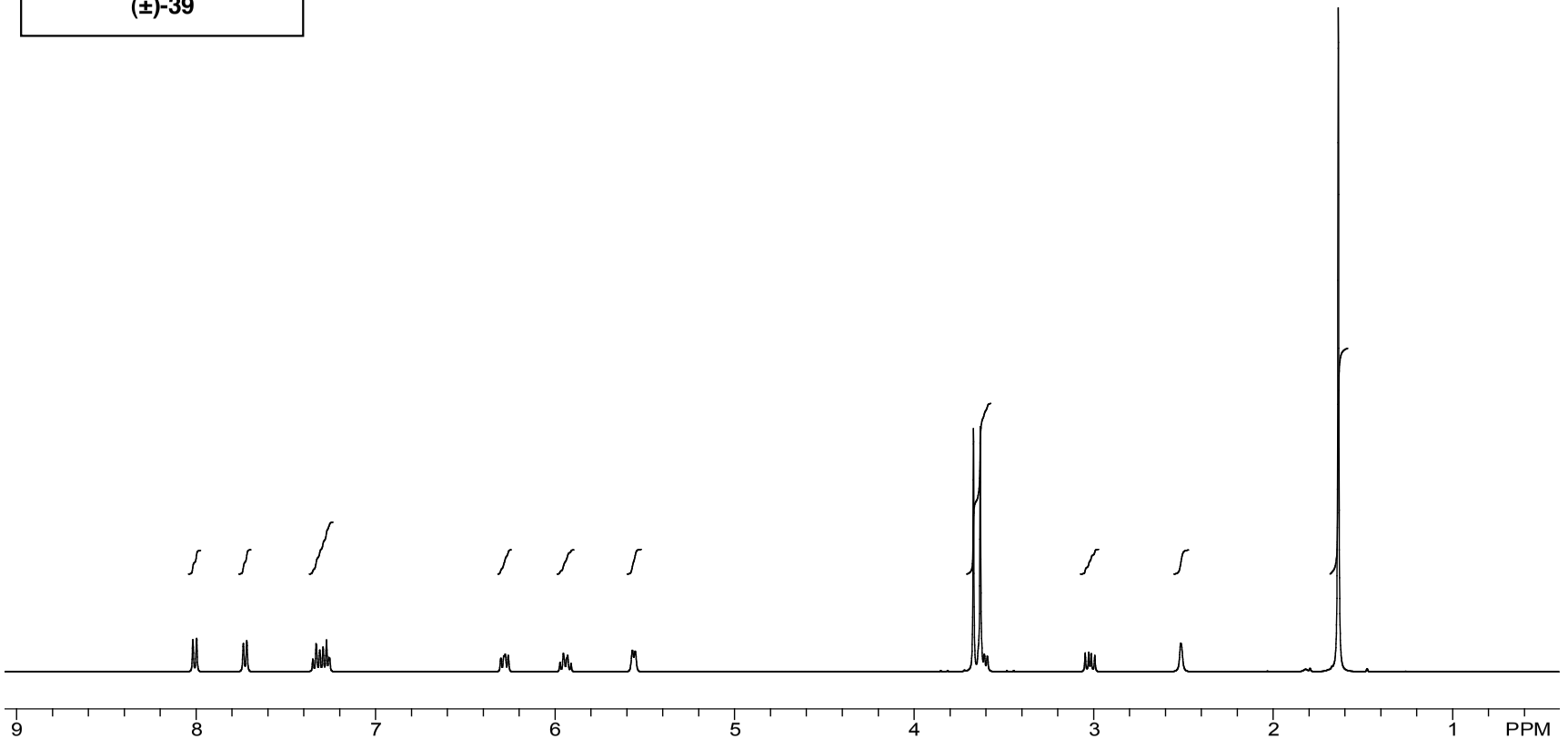

Figure A.1.31 ^{1}H NMR spectrum (400 MHz, $CDCl_3$) of compound **39**

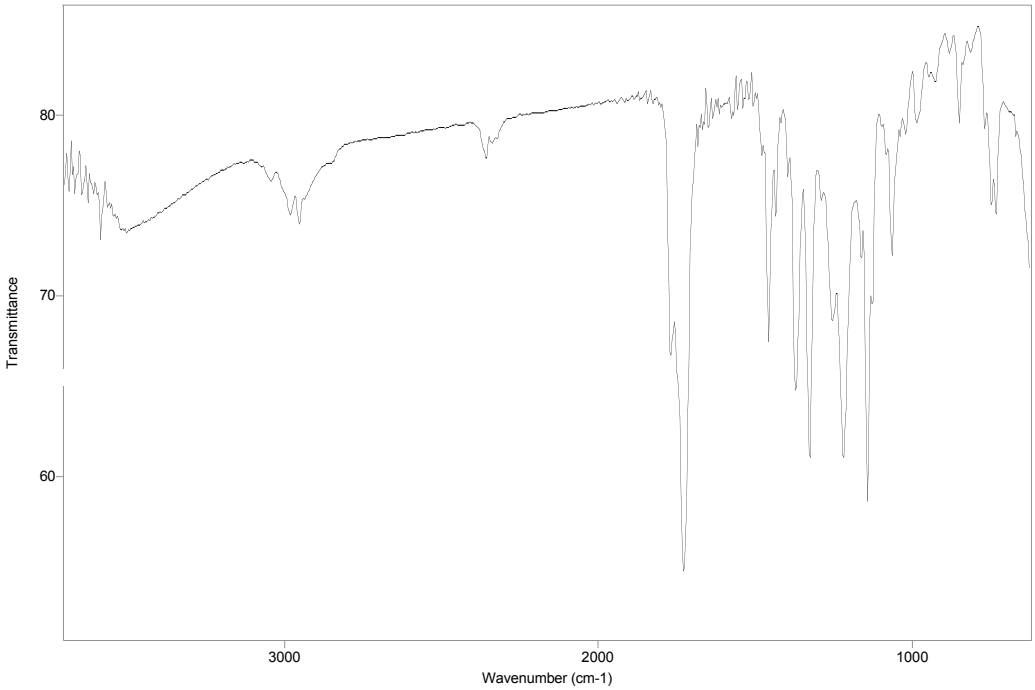

Figure A.1.32 FTIR spectrum (NaCl/thin film) of compound **39**

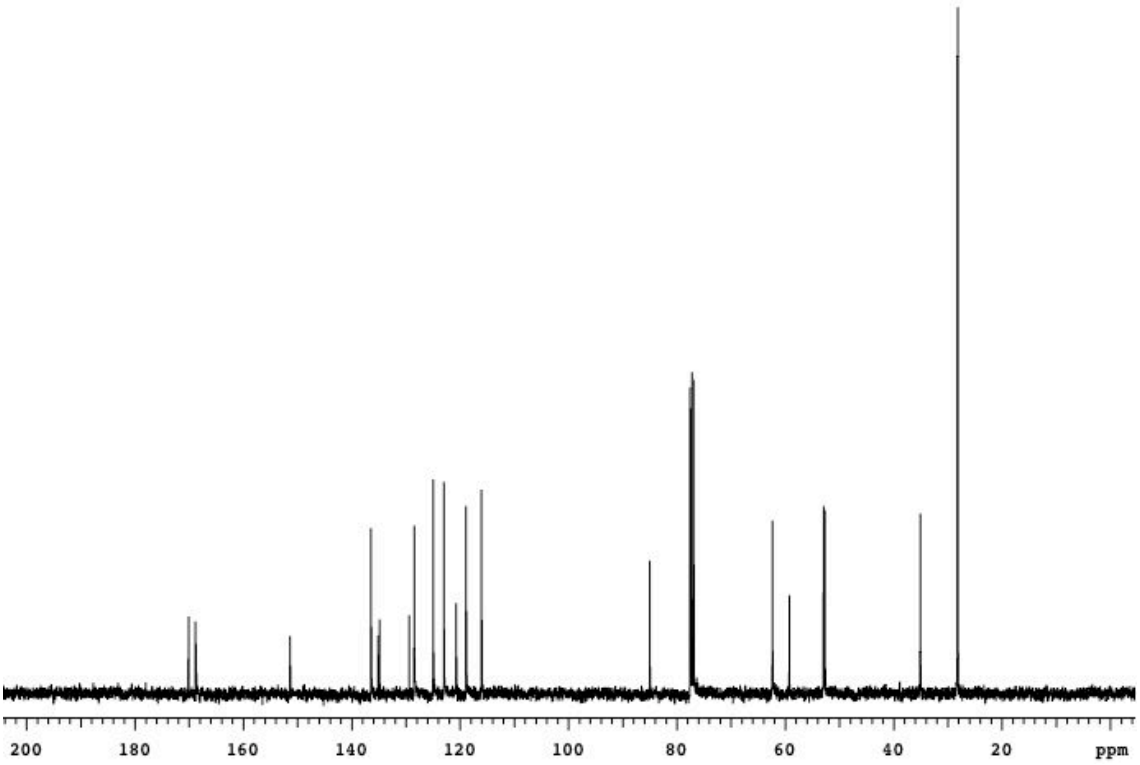

Figure A.1.33 ^{13}C spectrum (100 MHz, $CDCl_3$) of compound **39**

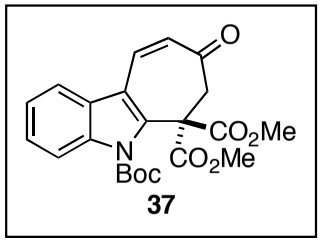

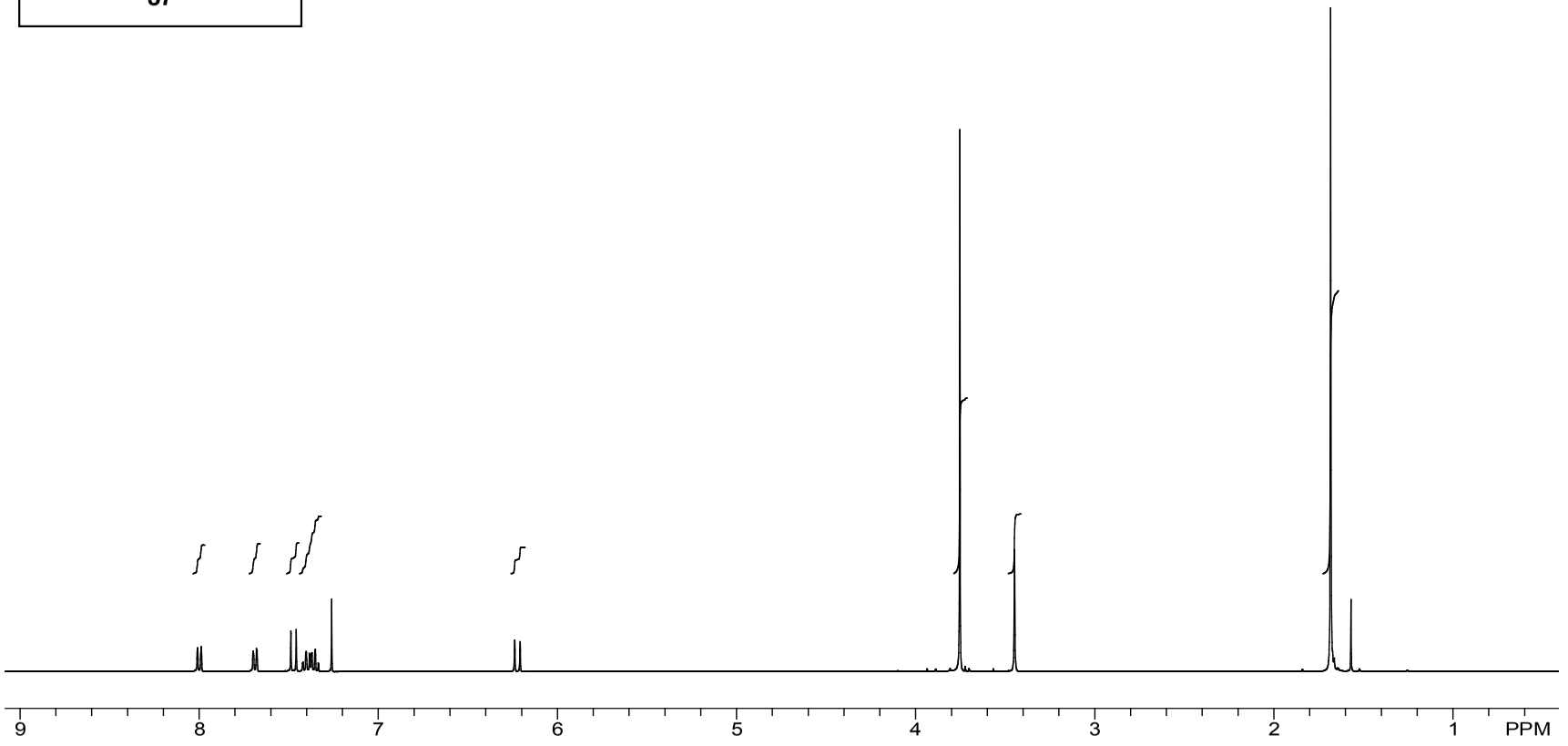

Figure A.1.34 ^{1}H NMR spectrum (400 MHz, $CDCl_3$) of compound **37**

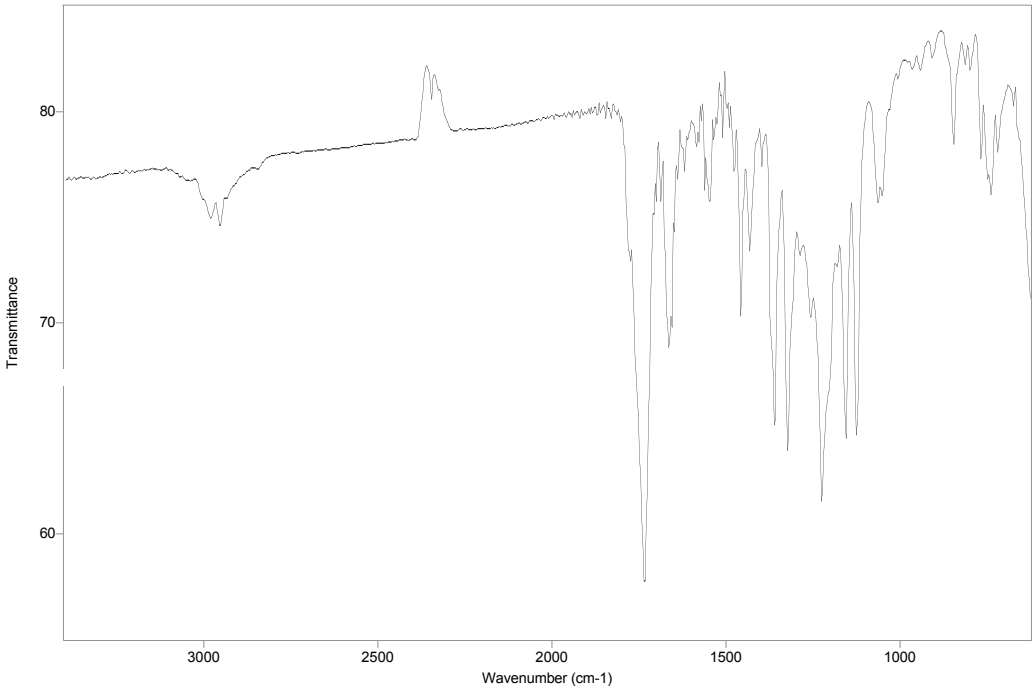

Figure A.1.35 FTIR spectrum (NaCl/thin film) of compound **37**

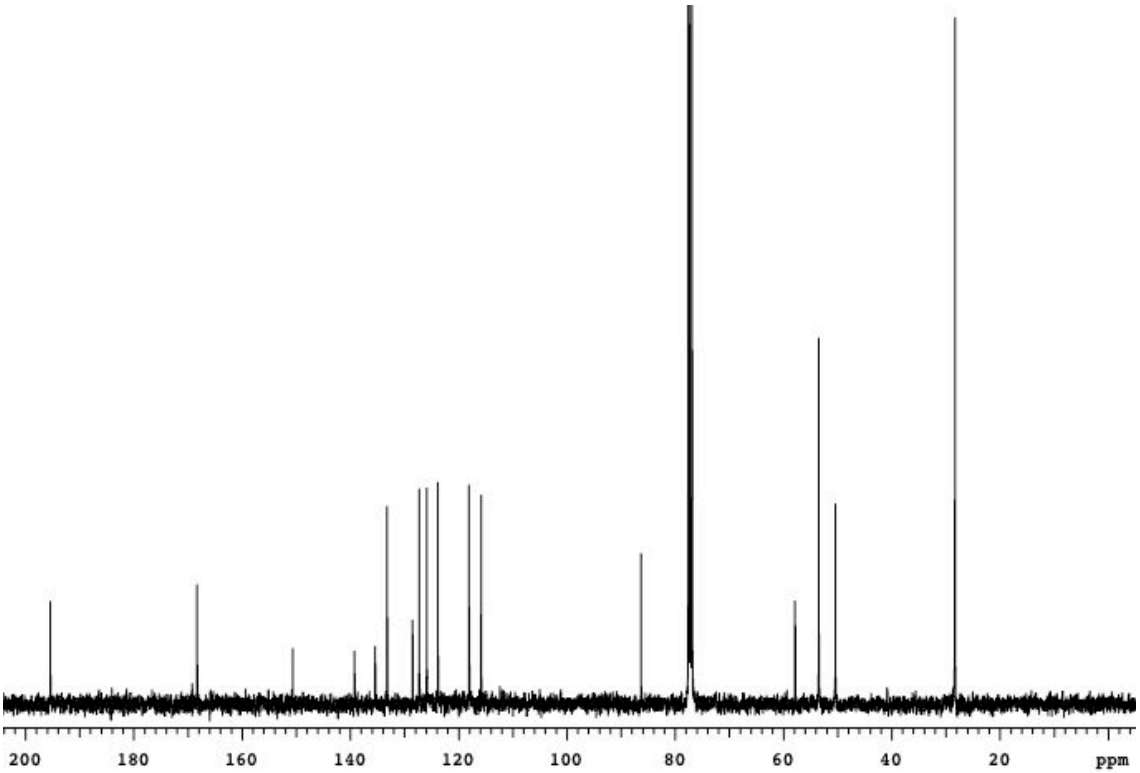

Figure A.1.36 ^{13}C spectrum (100 MHz, $CDCl_3$) of compound **37**

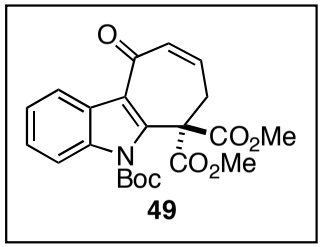

49

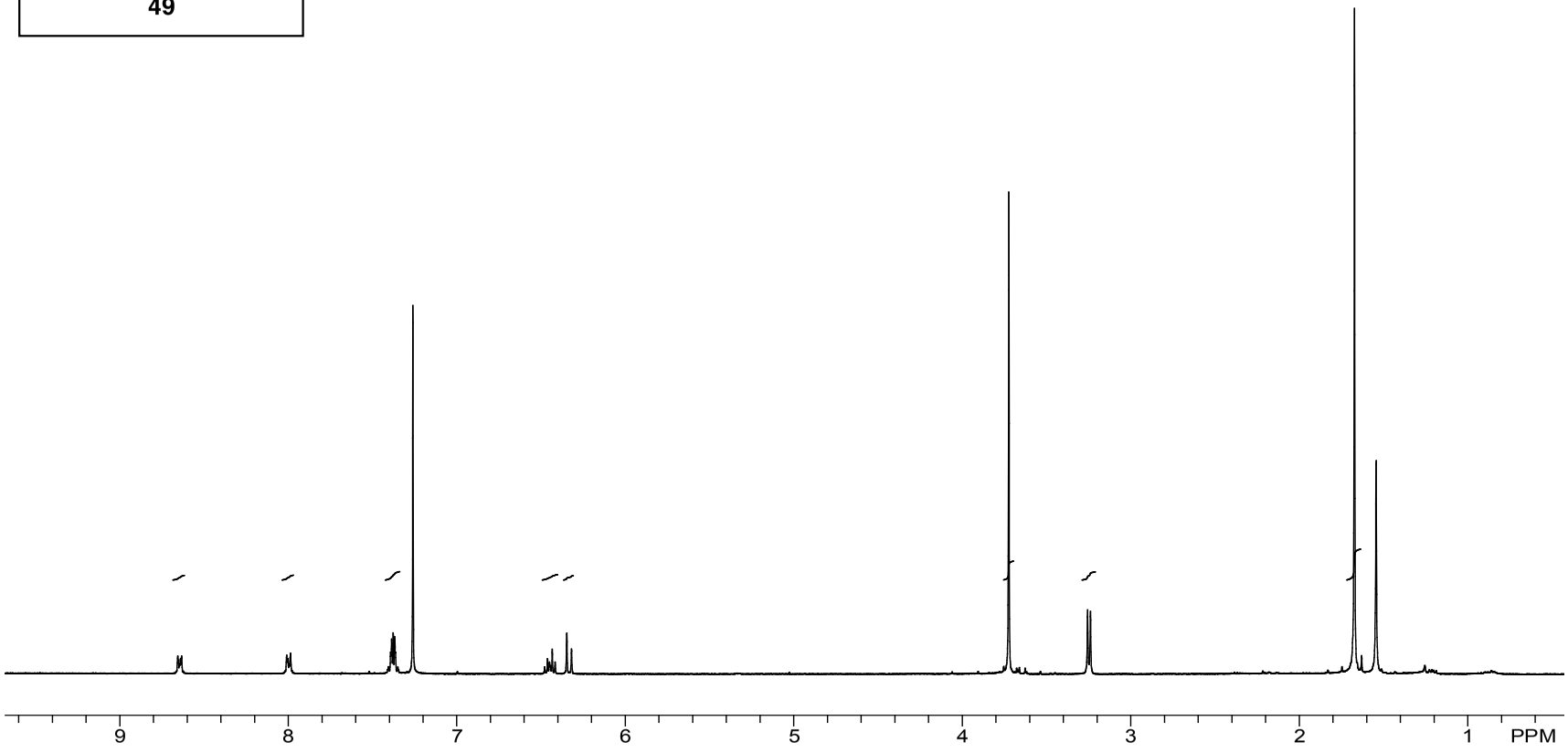

Figure A.1.37 ^{1}H NMR spectrum (400 MHz, $CDCl_3$) of compound **49**

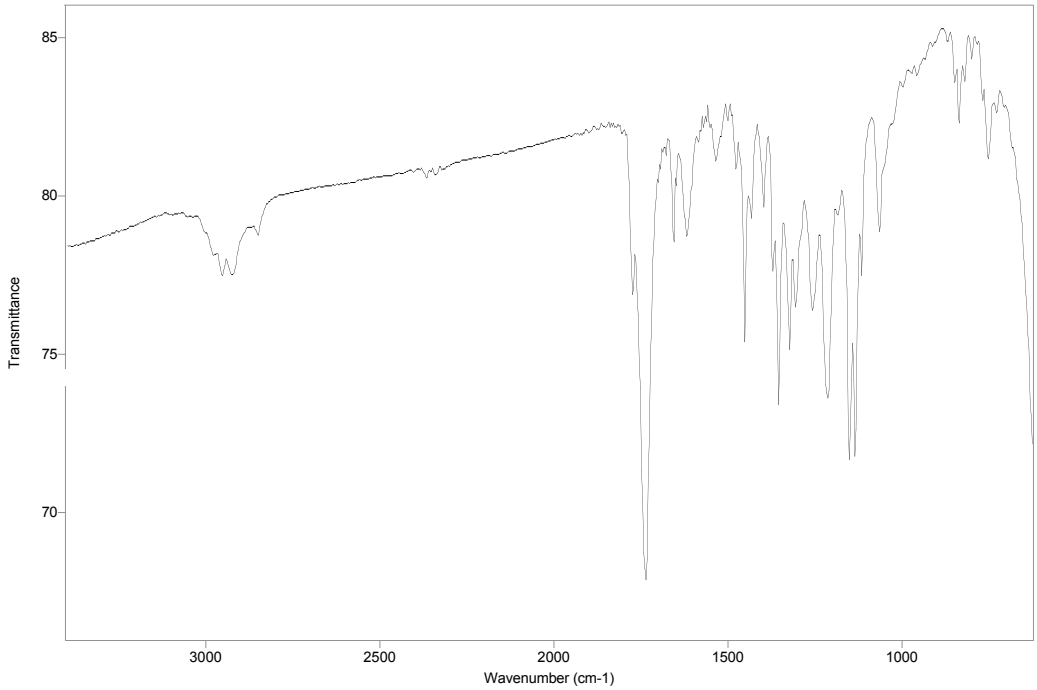

Figure A.1.38 FTIR spectrum (NaCl/thin film) of compound **49**

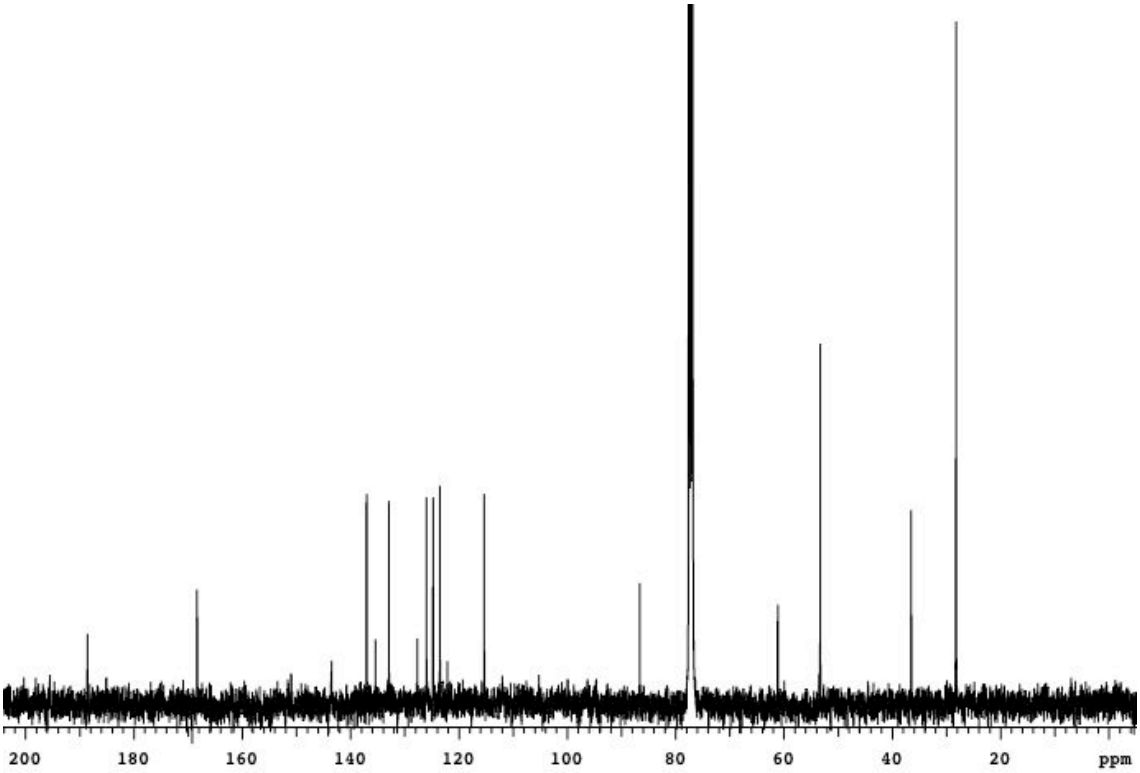

Figure A.1.39 ^{13}C spectrum (100 MHz, $CDCl_3$) of compound **49**

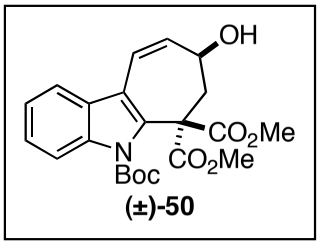

(±)-50

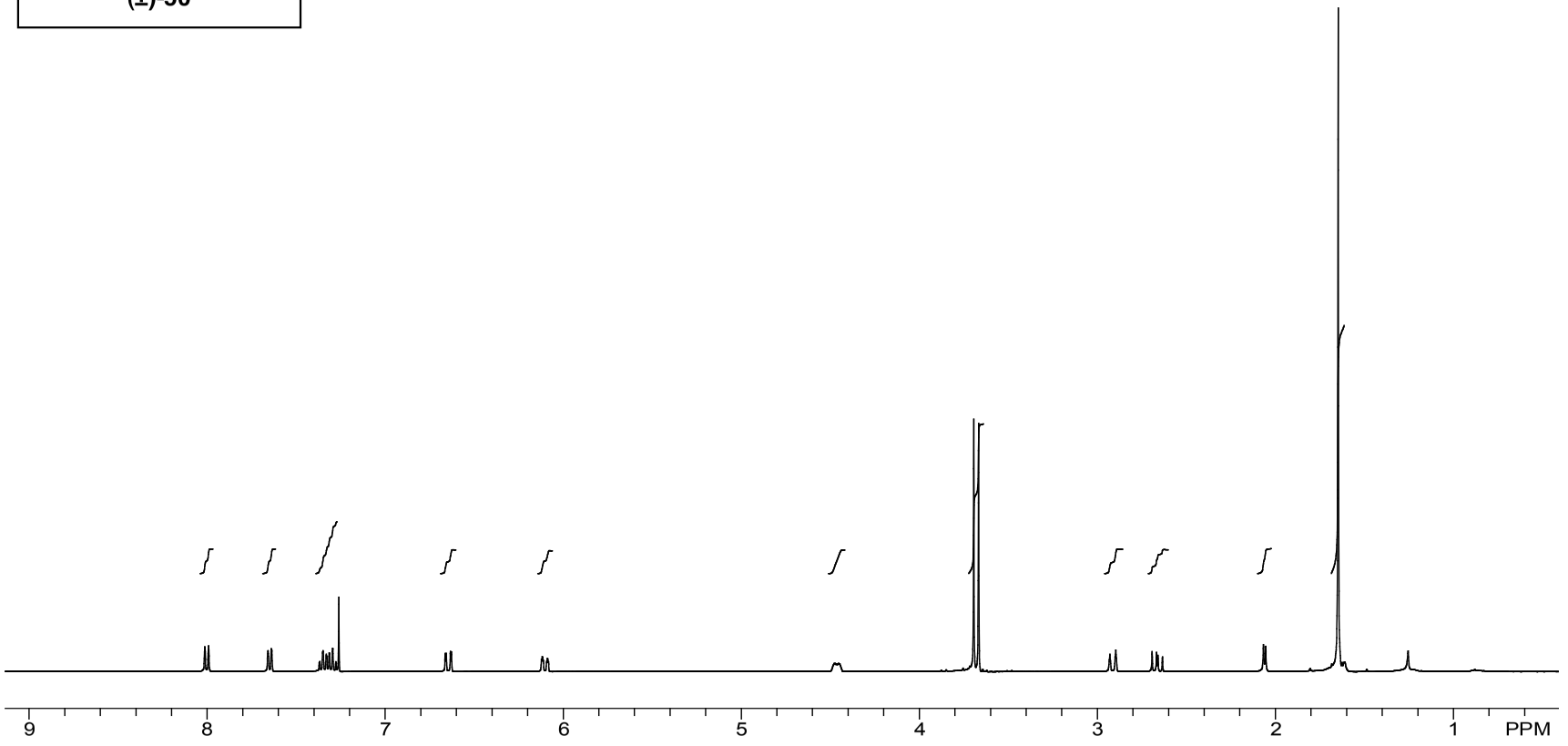

Figure A.1.40 ^{1}H NMR spectrum (400 MHz, $CDCl_3$) of compound **50**

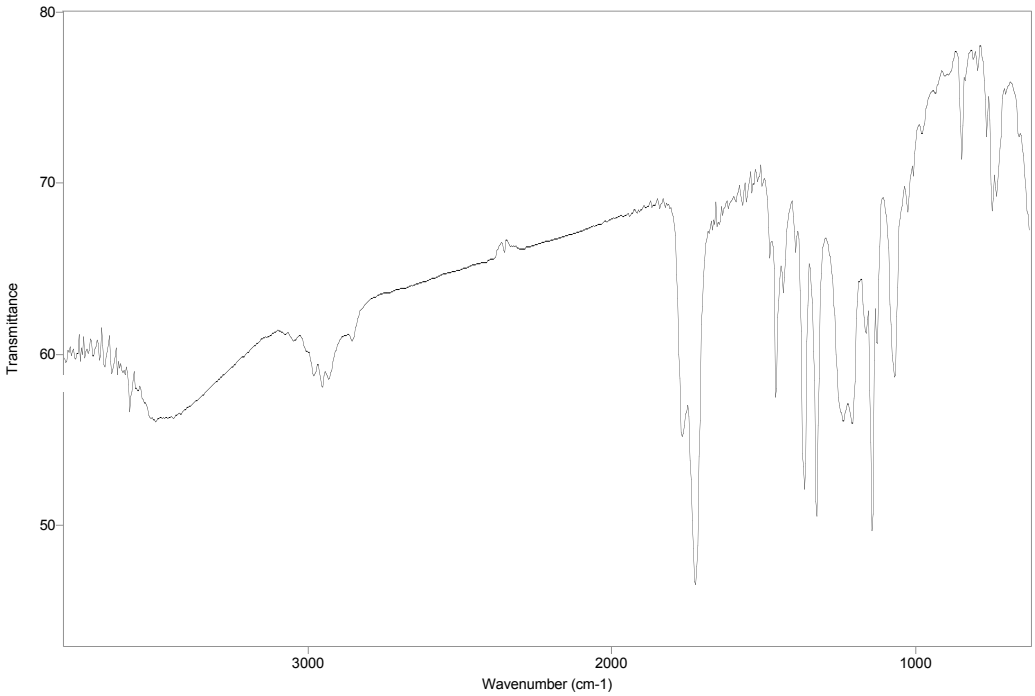

Figure A.1.41 FTIR spectrum (NaCl/thin film) of compound **50**

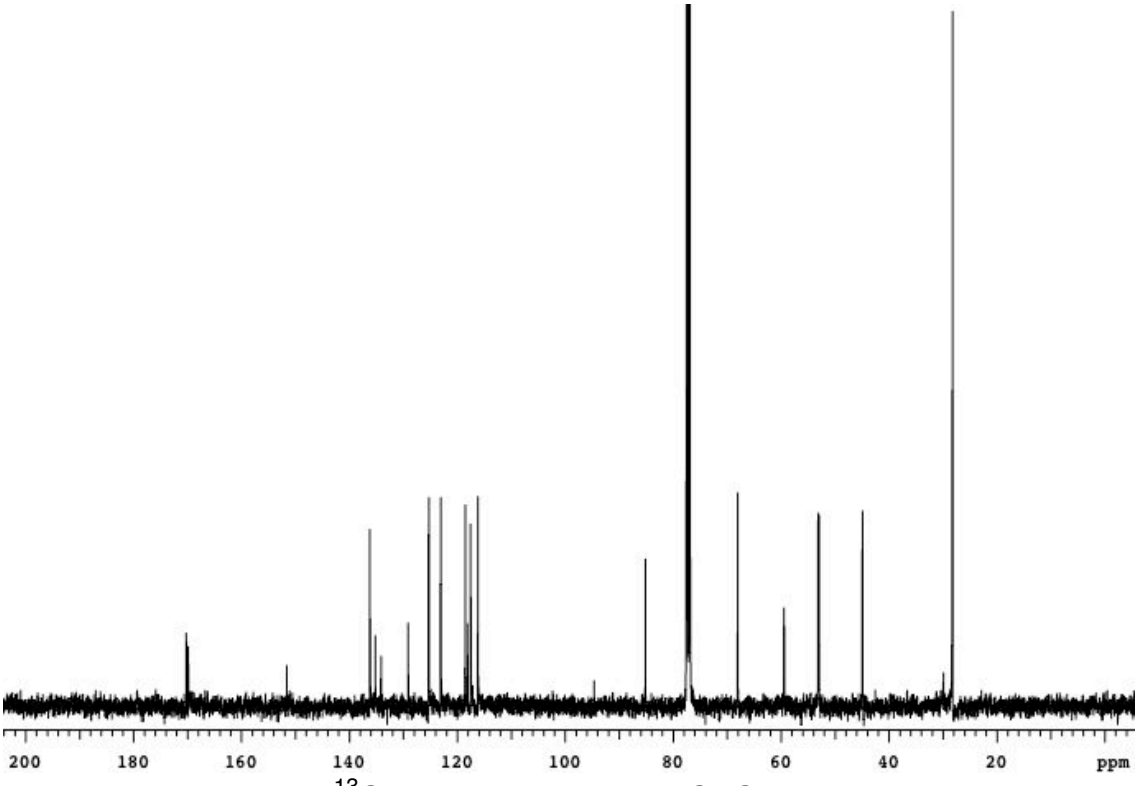

Figure A.1.42 ^{13}C spectrum (100 MHz, $CDCl_3$) of compound **50**

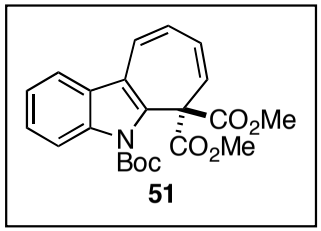

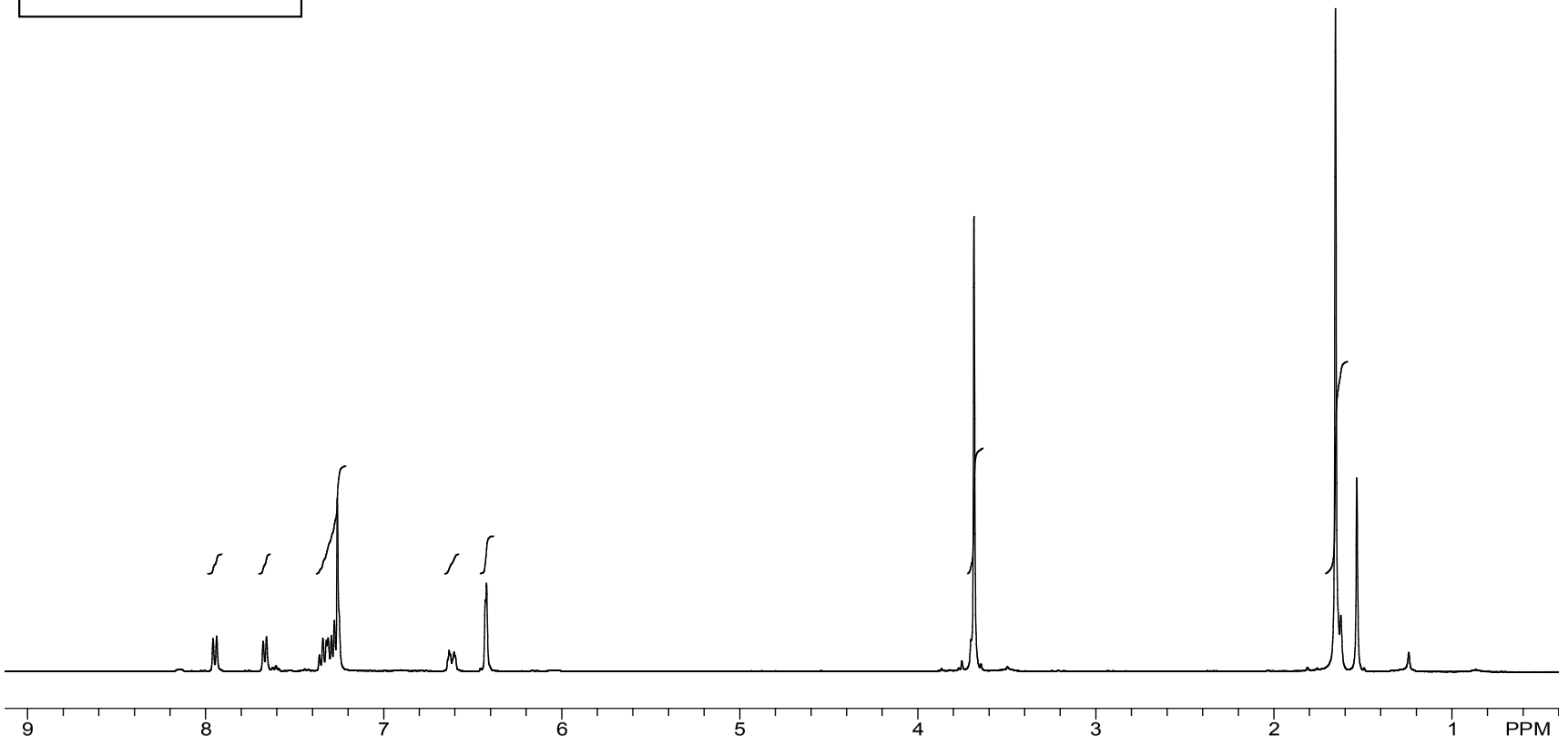

Figure A.1.43 ^{1}H NMR spectrum (400 MHz, $CDCl_3$) of compound **51**

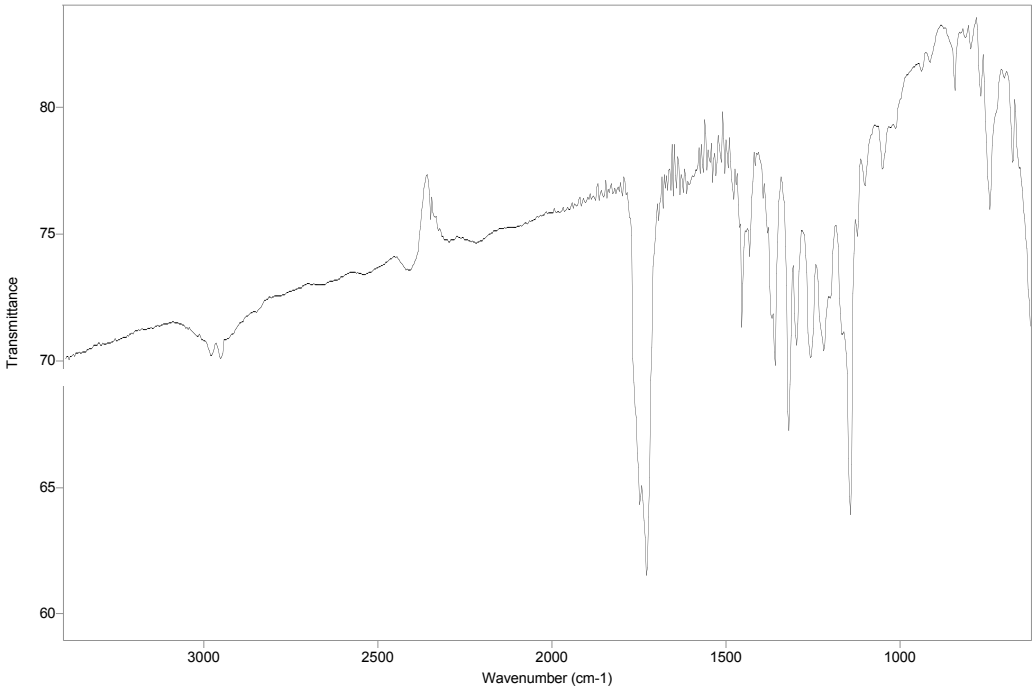

Figure A.1.44 FTIR spectrum (NaCl/thin film) of compound **51**

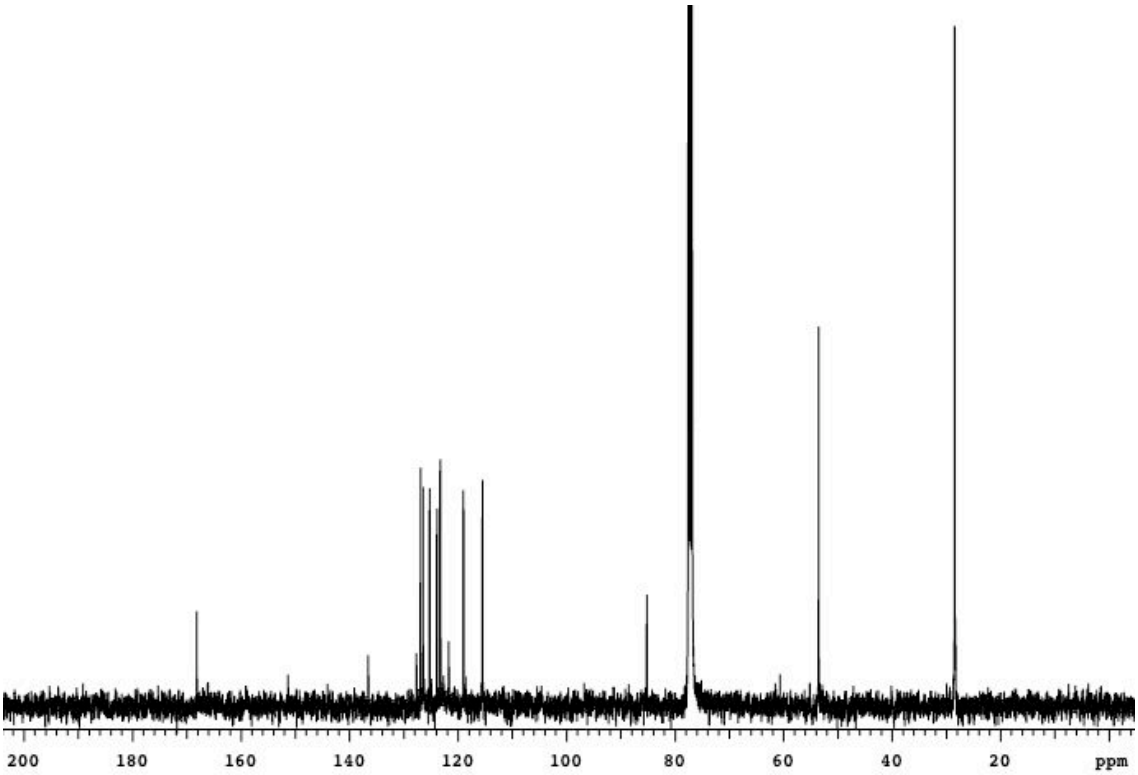

Figure A.1.45 ^{13}C spectrum (100 MHz, $CDCl_3$) of compound **51**

CHAPTER THREE

Synthesis of an Advanced Intermediate Possessing All Requisite Carbon Atoms

3.1 Preventing Lactone Formation

3.1.1 Use of Di-*tert*-butyl Malonate to Increase Steric Bulk

The original Michael addition/alkylation strategy was hampered by the inefficient synthesis of allylic alcohol **39** (see Scheme 2.1.4.2). To alleviate this problem a slightly modified route was devised, which sought to employ bulkier ester functionality on the malonate moiety. Sterically encumbering *t*-Bu esters were chosen not only for the size of the *t*-Bu group, but also due to the commercial availability of the corresponding malonate. With this in mind, simple substitution of dimethyl malonate for di-*t*-Bu malonate provided indolecarboxaldehyde **52** (Scheme 3.1.1.1) following the aforementioned addition-elimination sequence (*cf.* Scheme 2.1.2.1). Tsuji-Trost Pd-catalyzed allylation furnished intermediate **53** in 95% yield.[1] At this point experimentation began to test the feasibility of vinyl Grignard addition *without* lactone formation.

Scheme 3.1.1.1

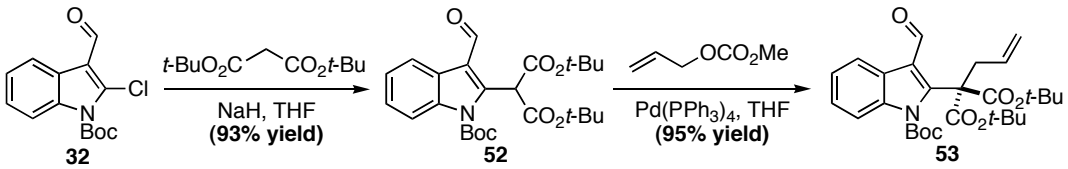

The allylated malonate **53** underwent treatment with vinyl magnesium bromide at –78 °C. As expected, the bulky *t*-Bu esters suppressed lactone formation, keeping the allylic alcohol and malonate moieties intact, which delivered diene **54** in 66% yield (Scheme 3.1.1.2). Seven-membered ring formation proceeded with the Grubbs 2nd generation catalyst providing an efficient route to allylic alcohol **55**.[2]

Scheme 3.1.1.2

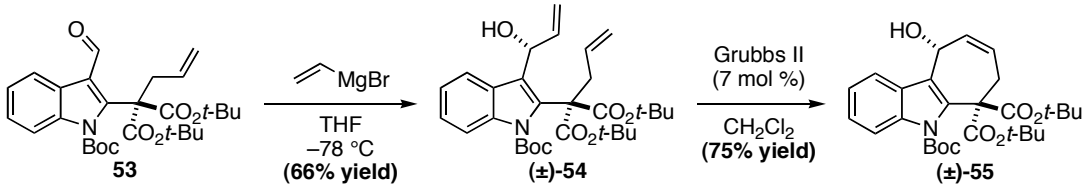

Following this success, intermediate **55** was exposed to the previously established PCC-mediated oxidative transposition reaction conditions. Although lactone **56** was found to be the major product (Scheme 3.1.1.3), it was encouraging to learn that the amount of transposed enone-*t*-Bu **57** increased relative to non-transposed **58** (**57**:**58** = 1:11). Lactone formation presumably occured due to nucleophilic attack of a *t*-Bu ester onto an activated alyllic and

benzylic alcohol, followed by loss of the *t*-Bu group (Scheme 3.1.1.4).[3]

Scheme 3.1.1.3

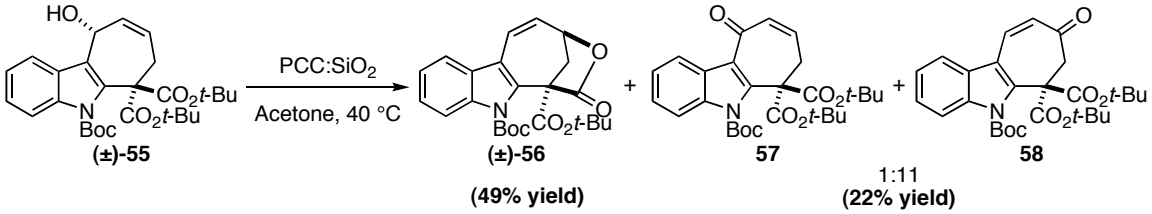

Attempts to elaborate lactone **56** proved fruitless. Undeterred, it was reasoned that an advanced intermediate derived from di-*i*-Pr malonate would suppress lactone formation by providing steric bulk during vinyl Grignard addition and provide greater functional group stability during the oxidative transposition step. The *i*-Pr ester functionality was anticipated to have increased resistance to acid-mediated side reactions.

Scheme 3.1.1.4

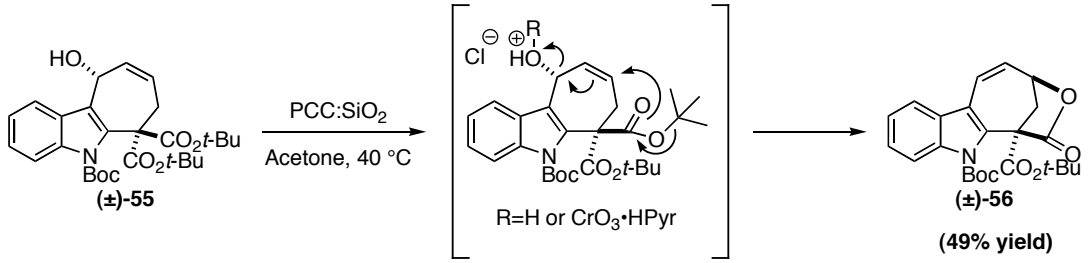

3.1.2 Finding a Balance Between Steric Bulk and Reactivity

To test this hypothesis di-*i*-Pr malonate **59** was subjected to the established reaction sequence (Scheme 3.1.2.1). The synthesis commenced with addition of the sodium salt of di-*i*-Pr malonate to Boc-2-chloroindole **32** which formed indolemalonate **59**. Allyl indolemalonate **60** was isolated following exposure to Tsuji-Trost Pd-catalyzed allylation conditions.[1] Allylated malonate **60** underwent vinyl magnesium bromide addition with minor lactone formation (*circa* 15 mol %) providing diene **61**. Ring-closing metathesis proceeded as expected with the Grubbs 1st generation catalyst affording allylic alcohol **62**.[2]

Scheme 3.1.2.1

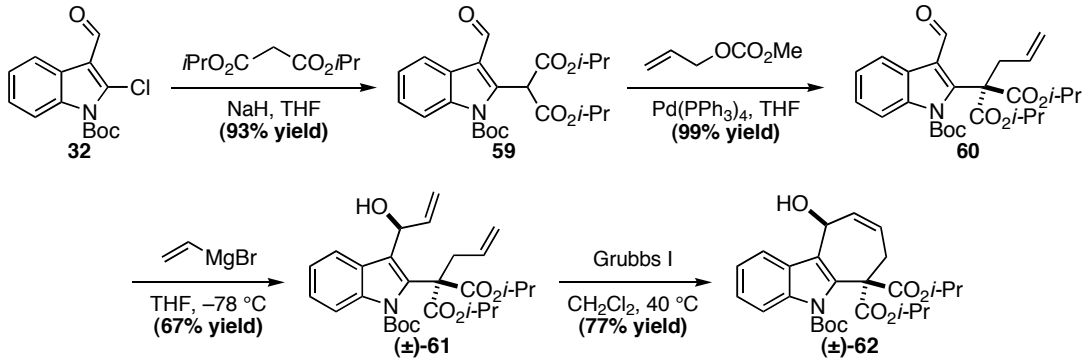

The use of di-*i*-Pr malonate did prevent lactone formation during the course of the reaction however; it was observed that flash chromatography purification, by means of initially absorbing the crude reaction material onto silica gel, or running a slow column, provided the *cis* lactone product **63** exclusively

(Scheme 3.1.2.2). Due to this problem, diene **62** was typically loaded onto the silica gel column as a solution in dichloromethane, purified quickly, and the product immediately advanced to the next step.

The *cis* relative stereochemistry of lactone **63** was established only after demonstrating the ability of this compound to undergo ring-closing metathesis with the Grubbs 2nd generation catalyst yielding bicycle **64**. The stability of this compound relative to the methyl ester derivative was not established.

Scheme 3.1.2.2

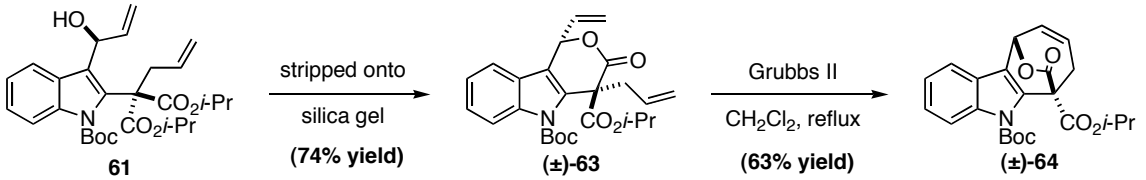

With one hurdle already surpassed, the stage was set for oxidative transposition of **62** with PCC. Pleasingly, after exposure to PCC:SiO_2 the activated allylic alcohol **62** was converted to the transposed enone-*i*-Pr **65** along with regioisomer **66** in a ratio of **65**:**66** = 10:1 (Scheme 3.1.2.3). It is worth noting that solvent, concentration, and temperature all play a key role in transposed product formation. Optimal conditions were found to be syringe pump addition (over 10-12 hr) of allylic alcohol **62** to a solution of PCC:SiO_2 in acetone at 40 °C at a concentration of 0.025 M. Importantly, the streamlined route provided access to gram quantities of enone-*i*-Pr **65**.

Scheme 3.1.2.3

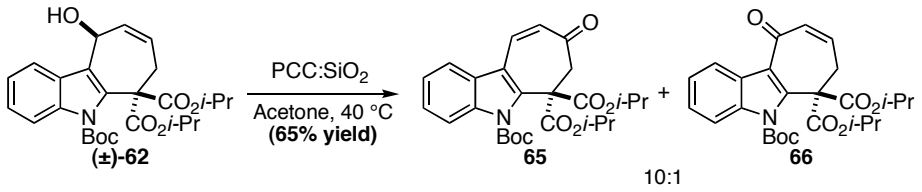

3.1.3 Elaboration of an Advanced Michael Acceptor

Exposure of enone-*i*-Pr **65** to various bifunctional amines did not provide 1,4-addition products. The use of Lewis-acids and/or heat yielded aromatized products as the only isolable compounds, a representative example being that shown in Scheme 3.1.3.1. The aromatization process may proceed *via* the mechanism depicted in Scheme 3.1.3.2. Initial base catalyzed tautomerization produced cycloheptatriene intermediate **67**, which was expected to be in equilibrium with norcaradiene **68**.[4] Carbon–carbon bond scission followed by proton transfer led to an intermediate able to tautomerize providing the isolated aromatized product **69**. Aromatized lactone product **70** was formed upon closure of the phenol oxygen onto the pendant ester functional group.

Scheme 3.1.3.1

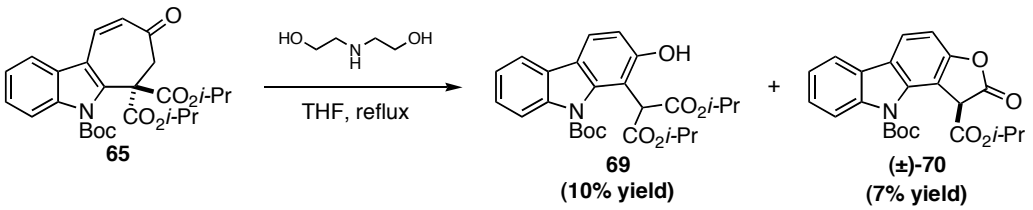

Scheme 3.1.3.2

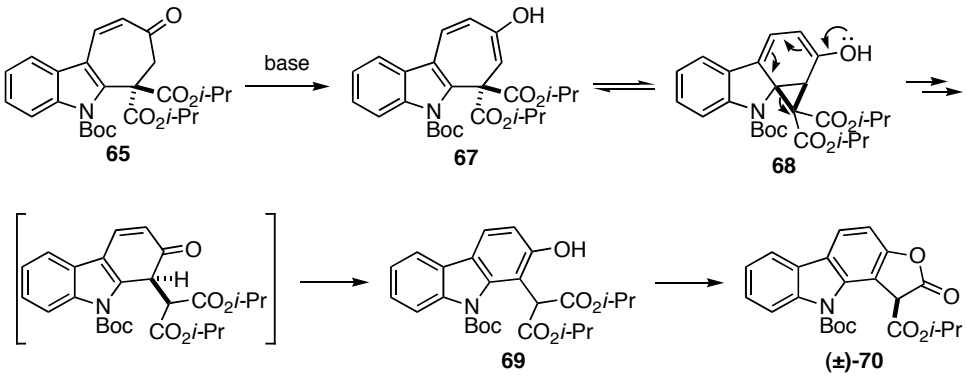

In an attempt to avoid the presumed problematic basicity of nitrogen nucleophiles, our attention turned to a report which detailed initial TBS-OTf mediated arylphosphine 1,4-addition to cyclohexenone, followed by displacement of the generated phosphonium salt with secondary amines.[5,6] This was attractive for our system as the low basicity of triphenylphosphine was expected to suppress norcaradiene formation.[7] Under optimized conditions, exposure of unsaturated ketone **65** to triphenylphosphine and TIPS-OTf generated an intermediate (observed by TLC), which afforded TIPS–enol ether **71** in 80% yield following addition of thiomorpholine at –78 °C and warming to room temperature (Scheme 3.1.3.3). This result represented the first successful *net* amine conjugate addition to enone-*i*-Pr **65**.

Scheme 3.1.3.3

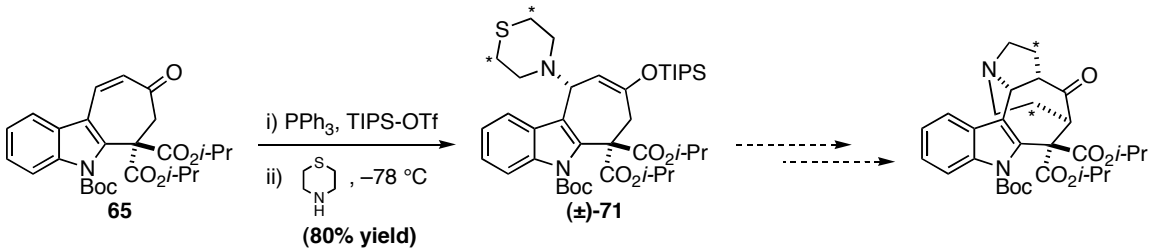

Thiomorpholine was utilized as the amine nucleophile for two reasons: 1) it was found that only cyclic amines worked under the reaction conditions with our substrate and 2) the sulfide functional group provided a possible handle to manipulate the neighboring carbon atoms by means of oxidation (Scheme 3.1.3.4).[8] This was envisioned to occur *via* an iterative process, whereby an oxidation event could occur α to sulfur producing a thionium ion intermediate (**72**), which would be trapped by the pendant silyl enol ether pro-nucleophile, possibly with regeneration of the silyl enol ether if an ene reaction mechanism was involved (**73**).[9] A second round of oxidation (**74**) and carbon–carbon bond formation could follow this step to construct a highly functionalized polycyclic intermediate **75**. The core of actinophyllic acid would be formed following reductive sulfide removal.[10]

Scheme 3.1.3.4

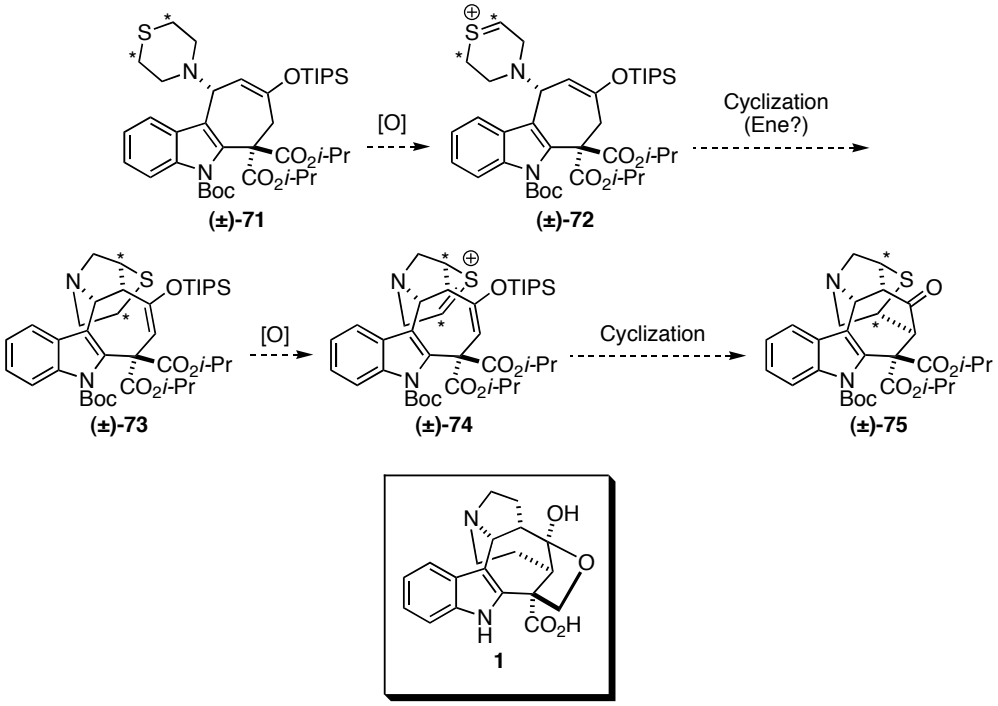

All attempts to form even one carbon–carbon bond through oxidation of sulfide **71** were unsuccessful. When the oxidant was SO_2Cl_2 formation of enone-*i*-Pr **65** was observed by crude ^{1}H NMR in addition to unknown material (Scheme 3.1.3.5). Speculation that thiomorpholine was eliminating due to the presence of trace acid prompted experimentation with milder oxidants less prone to hydrolysis and at lower temperature. Unfortunately, switching to NCS or several other oxidants did not yield the desired product at temperatures below 0 °C.[11] When the reaction temperature was increased to room temperature or higher enone-*i*-Pr **65** was again observed by crude ^{1}H NMR. These results highlighted the difficulties associated with our ambitious plan to oxidize a sulfide in the presence of a TIPS-enol ether and tertiary amine (Scheme 3.1.3.5). Intermediate **71**

represents our most advanced intermediate toward actinophyllic acid utilizing a Michael addition/alkylation strategy.

Scheme 3.1.3.5

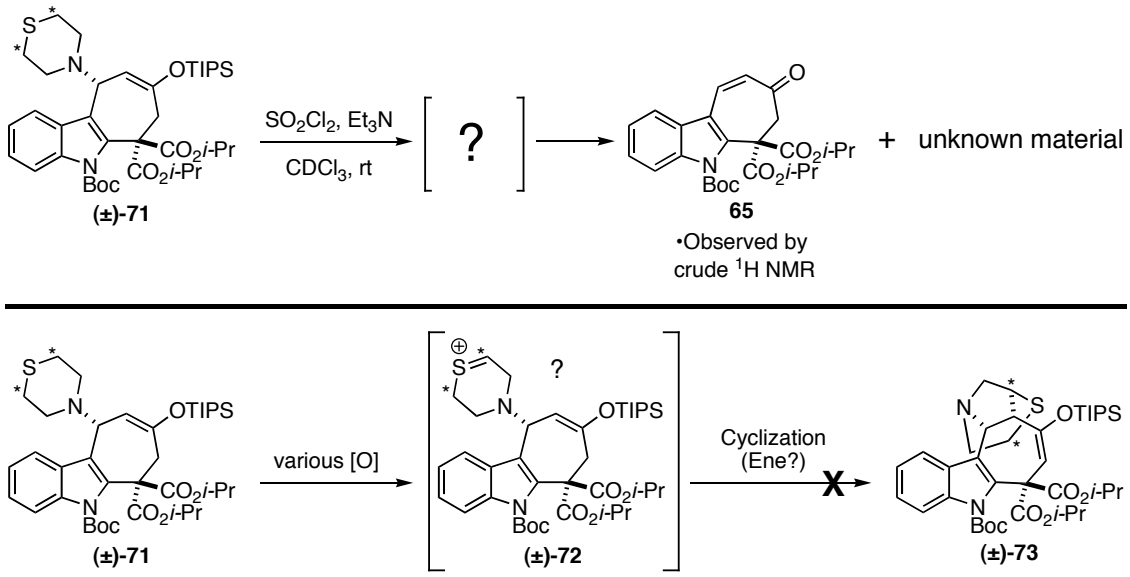

3.2 Conclusion

In summary, the current sequence, starting from commercially available oxindole, rapidly provides gram quantities of enone-*i*-Pr **65**. Highlights from this sequence include a facile nucleophilic aromatic substitution employing malonate nucleophiles, Tsuji-Trost allylation of a congested malonate nucleophile, and an oxidative transposition enabled by PCC which was used to access enone-*i*-Pr **65** in one step from a secondary allylic and benzylic alcohol substrate. The advanced enone intermediate was shown to undergo *net* amine conjugate

addition with the aid of a phosphonium salt intermediate. By choosing thiomorpholine as the amine nucleophile an advanced intermediate was prepared that contained all the atoms and functionality necessary to complete a synthesis of actinophyllic acid. However, all attempts to advance this highly functionalized intermediate were unsuccessful.

3.3 Experimental

3.3.1 Materials and Methods

Unless otherwise sated, reactions were performed under a nitrogen atmosphere using freshly dried solvents. Tetrahydrofuran (THF) was dried either by distillation from sodium/benzophenone or by passing through activated alumina columns. Methylene chloride (CH_2Cl_2), diethyl ether (Et_2O), benzene (PhH), and toluene (PhMe) were dried by passing through activated alumina columns. Dimethylformamide (DMF) was dried over activated molecular sieves or purchased anhydrous from Sigma-Aldrich. MeOH was distilled over magnesium oxide. All other commercially obtained reagents were used as received. All reactions were monitored by thin-layer chromatography using EMD/Merck or Silicycle silica gel 60 F254 pre-coated plates (0.25 mm). Flash chromatography was performed with the indicated solvents using silica gel (particle size 0.040-0.063 mm) purchased from Silicycle. ^{1}H NMR spectra were recorded at 400 MHz

using a Varian Inova 400 instrument. ^{13}C NMR spectra were recorded at 100 MHz using a Varian Inova 400 instrument. Chemical shift are reported relative to internal chloroform (^{1}H, δ = 7.26, ^{13}C, δ = 77.2), dimethyl sulfoxide (^{1}H, δ = 2.50, ^{13}C, δ = 39.5), benzene (^{1}H, δ = 7.16, ^{13}C, δ = 128.1) as indicated. Splitting patterns are reported as such, app = apparent, br = broad, s = singlet, d = doublet, dd = doublet of doublets, ddd = doublet of doublets of doublets, dddd = doublet of doublets of doublets of doublets, t = triplet, q = quartet, m = multiplet, nfom = non-first order multiplet. Infrared spectra were recorded on a Nicolet Avatar 320 FT-IR. Melting points were obtained on a Gallenkamp variable temperature melting point apparatus and are uncorrected. High-resolution mass spectra were acquired at the Colorado State University CIF using an Agilent 6210 TOF LCMS.

3.3.2 Preparative Procedures

Preparation of Indolemalonate-t-Bu **52**

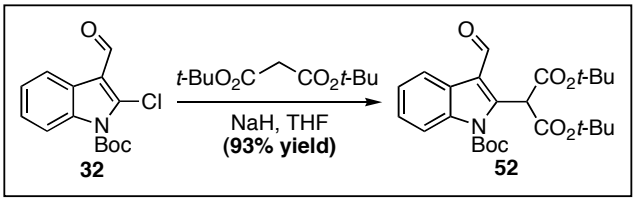

To a flame dried flask containing Boc-2-chloroindole-3-carboxaldehyde **32** (5.0 g, 17.8 mmol) was added anhydrous THF (75 mL) followed by 60% NaH (1.5 g, 39.0 mmol). This solution was cooled to 0 °C followed by addition of di-*tert*-

butyl malonate (4.2 mL, 18.7 mmol) dropwise *via* addition funnel. The reaction was stirred at 0 °C for 1 h followed by an additional 1 h at room temperature. The reaction was quenched by addition of 1N HCl until the solution color turned yellow. Following dilution with H_2O the mixture was transferred to a separatory funnel and extracted with EtOAc (3 x 100 mL). The combined organic layers were washed once with brine and dried over $MgSO_4$. Filtration followed by concentration under reduced pressure and silica gel chromatography (10% EtOAc/Hexanes) loaded as a solution in PhH provided indolemalonate-*t*-Bu **52** (7.6 g, 93% yield) as a white amorphous solid.

Indolemalonate-*t*-Bu 52: m.p. = 125.9 °C (decomposition); FTIR (thin film/NaCl) 2975 (m), 2934 (w), 2868 (w), 1736 (s), 1669 (s), 1557 (w), 1475 (w) 1454 (m) cm^{-1}; ^1H NMR (400 MHz, $CDCl_3$) δ 10.33 (s, 1H), 8.31–8.33 (nfom, 1H), 7.98–8.00 (nfom, 1H), 7.32–7.38 (nfom, 1H and nfom, 1H), 5.99 (s, 1H), 1.71 (s, 9H), 1.47 (s, 18H); ^{13}C NMR (100 MHz, $CDCl_3$) δ 186.9, 165.0, 149.9, 141.6, 135.6, 126.3, 125.7, 124.5, 121.4, 120.0, 115.4, 86.3, 83.1, 51.9, 28.2, 28.0; HRMS (TOF LCMS) calc'd for $C_{25}H_{33}NNaO_7$ $[M+Na]^+$ 482.2149, found 482.2157.

Preparation of Allyl indolemalonate-t-Bu **53**

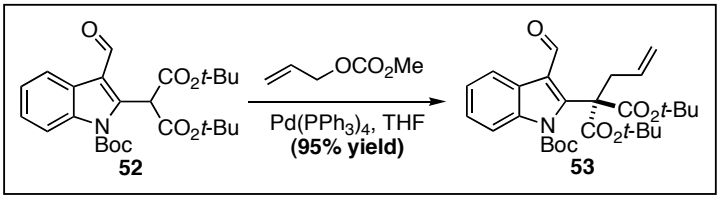

To a solution of indolemalonate-*t*-Bu **52** (981.6 mg, 2.14 mmol) in THF (20 mL) was added allyl methyl carbonate (260 μL, 2.28 mmol) followed by $Pd(PPh_3)_4$ (24.5 mg, 0.021 mmol) at room temperature under N_2. The reaction was stirred 1.5 hrs before it was diluted with Et_2O (50 mL) and filtered through a pad of Celite/SiO_2 (7 cm dia. fritted funnel, 1 cm Celite, 1.5 cm SiO_2). The crude material was eluted with Et_2O (100 mL) and concentrated under reduced pressure. Purification by silica gel chromatography (10% EtOAc/Hexanes) provided allylindolemalonate-*t*-Bu **53** (1.015 g, 95% yield) as a white amorphous solid.

Allylindolemalonate-*t*-Bu 53: m.p. = 115.4 °C (decomposition); FTIR (thin film/NaCl) 3083 (w), 3057 (w), 2975 (s, br), 2934 (s), 2878 (m), 2786 (w), 1746 (s, br), 1669 (s), 1603 (w), 1582 (w), 1531 (m), 1475 (s), 1449 (s) cm^{-1}; ^1H NMR (400 MHz, $CDCl_3$) δ 10.09 (s, 1H), 8.43–8.45 (nfom, 1H), 7.91–7.93 (nfom, 1H), 7.31–7.38 (nfom, 1H and nfom, 1H), 5.81 (dddd, *J* = 17.2, 9.9, 7.3, 7.3 Hz, 1H), 5.06 (d, *J* = 17.1 Hz, 1H), 5.00 (d, *J* = 10.1 Hz, 1H), 3.41 (d, *J* = 7.3 Hz, 1H), 1.71 (s, 9H), 1.48 (s, 18H); ^{13}C NMR (100 MHz, $CDCl_3$) δ 188.1, 167.6, 150.5, 144.3, 135.6, 133.6, 125.8, 125.4, 124.2, 122.3, 121.0, 119.5, 114.5, 86.0, 83.7, 63.5, 38.9, 28.3, 27.8; HRMS (TOF LCMS) calc'd for $C_{28}H_{37}NNaO_7$ $[M+Na]^+$ 522.2462, found 522.2468.

Preparation of Diene-t-Bu **54**

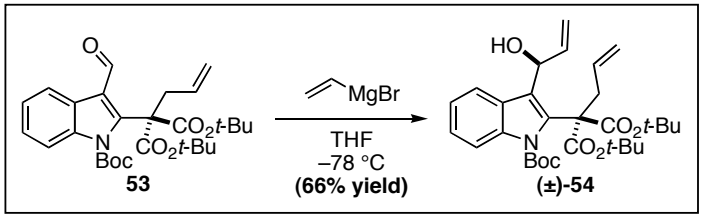

To a solution of allylindolemalonate-*t*-Bu **53** (1.015 g, 2.03 mmol) in anhydrous THF (20 mL) cooled to –78 °C was added vinyl magnesium bromide (6.0 mL of a 1 M soln. in THF, 6.0 mmol) dropwise *via* syringe. The reaction was stirred at –78 °C for 2.7 hrs before it was quenched by addition of saturated aqueous NH_4Cl (6 mL). The contents of the flask were transferred to a separatory funnel and the layers were separated. The aqueous layer was extracted with EtOAc (3 x 50 mL) and the combined organic layers were washed once with brine and dried over Na_2SO_4. Filtration of the solids followed by concentration under reduced pressure and silica gel chromatography (10% EtOAc/Hexanes) provided diene-*t*-Bu **54** (706.7 mg, 66% yield) as a colorless oil.

Diene-*t*-Bu 54: FTIR (thin film/NaCl) 3554 (w, br), 3436 (w, br), 3078 (w), 2975 (m), 2934 (w), 1726 (s), 1475 (w), 1454 (m) cm^{-1}; ^1H NMR (400 MHz, $CDCl_3$) δ 7.89 (d, J = 8.38 Hz, 1H), 7.84 (d, J = 7.75 Hz, 1H), 7.23–7.27 (nfom, 1H), 7.14–7.18 (nfom, 1H), 6.12 (ddd, J = 17.3, 10.7, 3.3 Hz, 1H), 5.87 (dddd, J = 17.2, 10.0, 7.2, 7.2 Hz, 1H), 5.59 (ddd, J = 17.3, 2.0, 2.0 Hz, 1H), 5.29 (ddd, J = 10.7, 2.0, 2.0 Hz, 1H), 5.14 (ddd, J = 5.4, 2.2, 2.2 Hz, 1H), 5.04 (dd, J = 17.1, 1.8 Hz, 1H), 4.98 (dd, J = 10.1, 1.9 Hz, 1H), 3.24 (d, J = 8.0 Hz, 2H), 2.78 (br s, 1H), 1.67 (s, 9H), 1.51 (s, 9H), 1.50 (s, 9H); ^{13}C NMR (100 MHz, $CDCl_3$) δ 169.3,

168.4, 151.4, 137.8, 137.0, 134.5, 134.3, 128.0, 124.7, 124.4, 122.3, 122.1, 118.5, 115.1, 115.0, 84.4, 83.6, 82.6, 67.1, 62.6, 39.8, 28.4, 28.0; HRMS (TOF LCMS) calc'd for $C_{30}H_{41}NNaO_7$ $[M+Na]^+$ 550.2775, found 550.2784.

Preparation of Allylic alcohol-t-Bu **55**

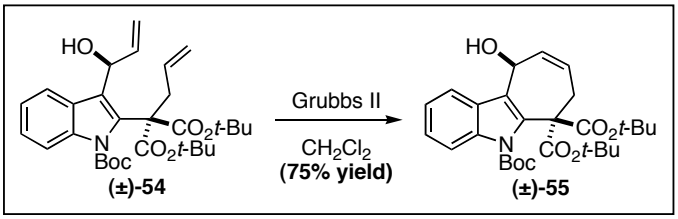

To a solution of diene-*t*-Bu **54** (110.0 mg, 0.208 mmol) in CH_2Cl_2 (10 mL) was added the Grubbs 2nd generation catalyst (12.6 mg, 0.0148 mmol) at room temperature under N_2. The reaction was stirred 16 hrs before it was concentrated under reduced pressure and purified by silica gel chromatography (gradient elution, 10 → 20% EtOAc/Hexanes) to provide allylic alcohol-*t*-Bu **55** (78.0 mg, 75% yield) as a white amorphous solid.

Allylic alcohol-*t*-Bu 55: m.p. = 138.9 °C; FTIR (thin film/NaCl) 3452 (w, br), 3042 (w), 2975 (m), 2929 (w), 1731 (s, br), 1480 (w), 1454 (m) cm^{-1}; ^1H NMR (400 MHz, $CDCl_3$) δ 7.98–8.00 (nfom, 1H), 7.68–7.70 (nfom, 1H), 7.22–7.29 (nfom, 1H and nfom, 1H), 6.31 (ddd, *J* = 9.7, 6.8, 1.1 Hz, 1H), 6.02 (ddd, *J* = 9.7, 7.5, 7.5 Hz, 1H), 5.59 (dd, *J* = 6.6, 3.8 Hz, 1H), 3.61 (ddd, *J* = 13.3, 6.8, 1.5 Hz, 1H), 3.02 (dd, *J* = 13.3, 8.0 Hz, 1H), 2.05 (d, *J* = 4.0 Hz, 1H), 1.66 (s, 9H), 1,42 (s, 9H), 1.36 (s, 9H); ^{13}C NMR (100 MHz, $CDCl_3$) δ 168.6, 167.1, 150.9, 136.9,

135.7, 134.9, 129.5, 129.4, 124.5, 122.6, 119.9, 118.3, 116.2, 84.1, 81.4, 81.4, 62.6, 60.8, 35.1, 28.5, 28.1, 28.0; HRMS (TOF LCMS) calc'd for $C_{28}H_{37}NNaO_7$ $[M+Na]^+$ 522.2462, found 522.2471.

Preparation of Bridged Bicycle-t-Bu **56**, *iso-Enone-t-Bu* **57**, *and Enone-t-Bu* **58**

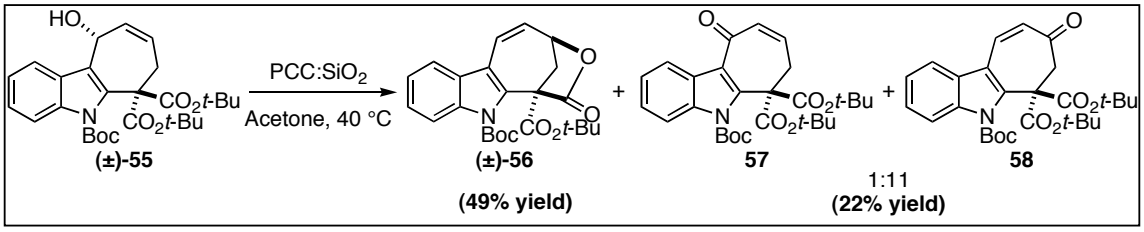

To a solution of SiO_2 (66 mg) in acetone (1.3 mL) was added PCC (35.0 mg, 0.162 mmol) and the heterogeneous solution was pre-warmed to 40 °C before addition of allylic alcohol-*t*-Bu **55** (26 mg, 0.052 mmol) as a solution in acetone (1 mL) *via* syringe pump at a rate of 1.7 mL/hr (ca. 25 min.). The reaction was stirred for an additional 1 h before it was quenched by addition of IPA (200 μL). Stirring for 1 h at room temperature was followed by filtration through Celite and concentration under reduced pressure. The isolated material was purified by silica gel chromatography (10% EtOAc/Hexanes) to provide two products. The first to elute was an 11:1 mixture of enone-*t*-Bu **58**:*iso*-enone-*t*-Bu **57** (5.7 mg, 22% yield) as a colorless oil. The last compound to elute was bridged bicycle-*t*-Bu **56** (10.9 mg, 49% yield) as a colorless oil. Analytical samples of enone-*t*-Bu **58** and *iso*-enone-*t*-Bu **57** were obtained following preparative thin layer chromatography (10% Et_2O/CH_2Cl_2) as colorless oils.

Enone-*t*-Bu 58: FTIR (thin film/NaCl) 2980 (m), 2934 (w), 1731 (s), 1664 (m), 1552 (w), 1480 (w), 1460 (w) cm^{-1}; ^1H NMR (400 MHz, $CDCl_3$) δ 8.00 (d, J = 8.0 Hz, 1H), 7.66 (d, J = 7.2 Hz, 1H), 7.46 (d, J = 12.0 Hz, 1H), 7.29–7.37 (2H), 6.20 (d, J = 12.0 Hz, 1H), 3.37 (s, 2H), 1.67 (s, 9H), 1.43 (s, 18H); ^{13}C NMR (100 MHz, $CDCl_3$) δ 196.2, 166.6, 150.1, 141.0, 135.5, 133.4, 128.7, 126.8, 125.4, 123.4, 117.8, 117.6, 116.1, 85.3, 82.9, 59.2, 50.7, 28.5, 28.0; HRMS (TOF LCMS) calc'd for $C_{28}H_{35}NNaO_7$ $[M+Na]^+$ 520.2306, found 520.2306.

***iso*-Enone-*t*-Bu 57**: FTIR (thin film/NaCl) 2980 (m), 2929 (w), 1736 (s), 1654 (w), 1613 (w), 1454 (m) cm^{-1}; ^1H NMR (400 MHz, $CDCl_3$) δ 8.60–8.62 (nfom, 1H), 7.99–8.02 (nfom, 1H), 7.32–7.35 (nfom, 1H and nfom, 1H), 6.41–6.48 (m, 1H), 6.32 (d, J = 10.7 Hz, 1H), 3.20 (d, J = 7.1 Hz, 2H), 1.68 (s, 9H), 1.38 (s, 18H); ^{13}C NMR (100 MHz, $CDCl_3$) δ 189.3, 166.4, 150.6, 145.7, 136.7, 135.3, 133.1, 127.7, 125.5, 124.4, 123.1, 121.7, 115.6, 85.7, 82.4, 62.5, 36.3, 28.5, 28.0; HRMS (TOF LCMS) calc'd for $C_{28}H_{35}NNaO_7$ $[M+Na]^+$ 520.2306, found 520.2305.

Bridged bicycle-*t*-Bu 56: m.p. = 89.2 °C (decomposition); FTIR (thin film/NaCl) 3047 (w), 2970 (m), 2929 (w), 1787 (s), 1726 (s), 1480 (w), 1454 (m) cm^{-1}; ^1H NMR (400 MHz, $CDCl_3$) δ 7.95 (d, J = 8.4 Hz, 1H), 7.62 (d, J = 7.4 Hz, 1H), 7.32–7.36 (nfom, 1H), 7.26–7.30 (nfom, 1H), 6.98 (dd, J = 11.1, 0.9 Hz, 1H), 6.30 (dd, J = 11.1, 6.6 Hz, 1H), 5.00 (app ddd, J = 7.0, 7.0, 0.7 Hz, 1H), 2.94 (dd, J = 12.6, 8.1 Hz, 1H), 2.70 (d, J = 12.7 Hz, 1H), 1.72 (s, 9H), 1.57 (s, 9H); ^{13}C

NMR (100 MHz, $CDCl_3$) δ 168.3, 167.3, 150.3, 135.8, 133.6, 127.9, 126.9, 125.5, 124.9, 123.1, 118.6, 118.1, 115.4, 85.4, 83.1, 70.5, 54.7, 37.6, 28.6, 28.1; HRMS (TOF LCMS) calc'd for $C_{24}H_{27}NNaO_6$ $[M+Na]^+$ 448.1731, found 448.1728.

Preparation of Indolemalonate-i-Pr **59**

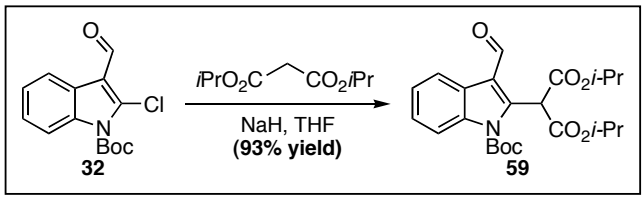

To a flame dried 1 L flask was added Boc-2-chloroindole-3-carboxaldehyde **32** (30.0 g, 107.3 mmol) followed by 60% NaH (10.7 g, 267.5 mmol). The solids were dissolved in anhydrous THF (150 mL) and stirred while cooling the mixture to 0 °C. At this time a 25 mL addition funnel was charged with di-*iso*-propyl malonate (21.4 mL, 112.7 mmol) and 1 mL was added to the stirred contents to initiate the reaction. After gas evolution was observed the addition of di-*iso*-propyl malonate was continued at such a rate that gas evolution and venting was manageable. Following complete addition the ice-water bath was removed and the reaction stirred at room temperature until consumption of starting material (ca. 1 h) judged by TLC. The reaction was quenched upon addition of 1N HCl (200 mL) at 0 °C followed by dilution with H_2O until the crude product precipitated out of solution. The crude solid was filtered and washed with copious amounts of H_2O and dried under high vacuum. The dry material was rinsed with hexanes (2 x ca. 100 mL) and decanted to afford crude

indolemalonate-*i*-Pr **59** (43.0 g, 93% yield) as a beige amorphous solid and pure by ^{1}H NMR.

Indolemalonate-*i*-Pr 59: m.p. = 114.5 °C (decomposition); FTIR (thin film/NaCl) 2986 (m), 2934 (w), 2873 (w), 1751 (s, br), 1669 (s), 1547 (w), 1444 (m) cm^{-1}; ^{1}H NMR (400 MHz, $CDCl_3$) δ 10.34 (s, 1H), 8.27–8.29 (nfom, 1H), 8.00–8.02 (nfom, 1H), 7.34–7.41 (nfom, 1H and nfom, 1H), 6.10 (s, 1H), 5.10 (septet, *J* = 6.3 Hz, 2H), 1.70 (s, 9H), 1.26 (d, *J* = 6.3 Hz, 6H), 1.23 (d, *J* = 6.3 Hz, 6H); ^{13}C NMR (100 MHz, $CDCl_3$) δ 186.4, 165.3, 149.9, 140.4, 135.6, 126.3, 125.8, 124.5, 120.9, 119.8, 115.5, 86.5, 70.2, 50.2, 28.2, 21.7; HRMS (TOF LCMS) calc'd for $C_{23}H_{30}NO_7$ $[M+H]^+$ 432.2017, found 432.2024.

Preparation of Allylindolemalonate-i-Pr **60**

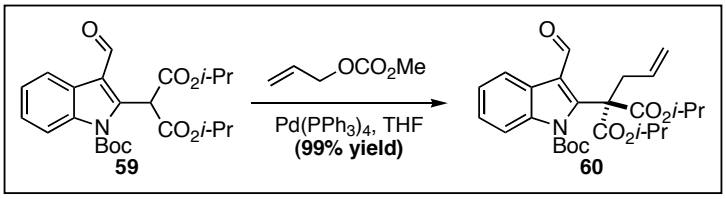

To a solution of indolemalonate-*i*-Pr **59** (1.4102 g, 3.27 mmol) in THF (7 mL) was added allyl methyl carbonate (400 μL, 3.52 mmol) followed by $Pd(PPh_3)_4$ (18.7 mg, 0.0162 mmol) at room temperature under N_2. The reaction was stirred 2.5 hrs before it was concentrated under reduced pressure and passed through a plug of SiO_2 (4 cm dia. x 3.5 cm) as a solution in 15% EtOAc/Hexanes and minimal PhH. The product was eluted with 15% EtOAc/Hexanes (ca. 250 mL) to furnish allylindolemalonate-*i*-Pr **60** (1.5260 g, 99% yield) as a light yellow oil,

which solidified upon standing at room temperature to a light yellow amorphous solid.

Allylindolemalonate-*i*-Pr 60: m.p. = 105.7 °C (decomposition); FTIR (thin film/NaCl) 3078 (w), 3052 (w), 2980 (m), 2924 (w), 2878 (w), 2781 (w), 1751 (s), 1675 (s), 1531 (w), 1454 (m) cm^{-1}; ^1H NMR (400 MHz, $CDCl_3$) δ 9.99 (s, 1H), 8.39–8.41 (nfom, 1H), 7.89–7.91 (nfom, 1H), 7.31–7.39 (nfom, 1H and nfom, 1H), 5.83 (dddd, *J* = 17.2, 9.9, 7.4, 7.4 Hz, 1H), 5.08 (septet, *J* = 6.3 Hz, 2H), 5.04 (dd, *J* = 17.1, 1.9 Hz, 1H), 5.01 (dd, *J* = 10.0, 1.8 Hz, 1H), 3.45 (d, *J* = 7.4 Hz, 2H), 1.70 (s, 9H), 1.27 (d, *J* = 6.3 Hz, 6H), 1.21 (d, *J* = 6.3 Hz, 6H); ^{13}C NMR (100 MHz, $CDCl_3$) δ 187.4, 168.0, 150.6, 143.3, 135.4, 133.3, 125.9, 125.5, 124.3, 122.2, 120.6, 120.0, 114.4, 86.4, 70.8, 62.4, 38.7, 28.2, 21.5, 21.4; HRMS (TOF LCMS) calc'd for $C_{26}H_{34}NO_7$ $[M+H]^+$ 472.2330, found 472.2330.

Preparation of Diene-i-Pr **61** *and Lactone-i-Pr* **63**

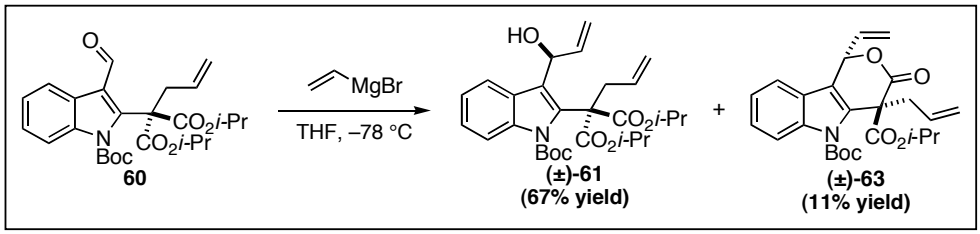

To a solution of allylindolemalonate-*i*-Pr **60** (10.0 g, 21.2 mmol) in THF (50 mL) cooled to –78 °C was added vinyl magnesium bromide (42.0 mL of a 1.0 M soln. in THF, 42 mmol) dropwise *via* addition funnel (ca. 15 min.) under N_2. The reaction was stirred 1 h before it was quenched by addition of 1 M AcOH in THF

(40 mL). The reaction mixture warmed naturally to room temperature and was subsequently transferred to a separatory funnel and washed with H_2O (100 mL). The aqueous layer was extracted with EtOAc (3 x 100 mL) and the combined organic layers were washed with brine and dried over Na_2SO_4. Filtration of the solids followed by concentration under reduced pressure and silica gel chromatography (10% EtOAc/Hexanes) provided a 5.3:1 mixture of diene-*i*-Pr **61**: lactone-*i*-Pr **63** (8.2 g, 78% yield) as a colorless oil, which corresponded to a 67% yield of diene-*i*-Pr **61**.

Diene-*i*-Pr 61: FTIR (thin film/NaCl) 3549 (w, br), 3431 (w, br), 3083 (w), 3052 (w), 2975 (m), 2934 (w), 2847 (w), 1736 (s), 1460 (m) cm^{-1}; ^1H NMR (400 MHz, $CDCl_3$) δ 7.81 (d, J = 8.4 Hz, 1H), 7.75–7.77 (nfom, 1H), 7.16–7.20 (nfom, 1H), 7.07–7.11 (nfom, 1H), 6.06 (ddd, J = 17.3, 10.7, 3.6 Hz, 1H), 5.84 (dddd, J = 16.9, 10.2, 8.2, 6.8 Hz, 1H), 5.48 (ddd, J = 17.3, 1.9, 1.9 Hz, 1H), 5.21 (ddd, J = 10.7, 2.0, 2.0 Hz, 1H), 4.92–5.09 (5H), 3.25 (dd, J = 14.3, 6.5 Hz, 1H), 3.15 (dd, J = 14.4, 8.2 Hz, 1H), 2.65 (d, J = 2.1 Hz, 1H), 1.57 (s, 9H), 1.22 (d, J = 6.3 Hz, 3H), 1.20 (d, J = 6.3 Hz, 6H), 1.15 (d, J = 6.2 Hz, 3H); ^{13}C NMR (100 MHz, $CDCl_3$) δ 169.5, 168.7, 151.4, 137.7, 136.9, 134.1, 133.3, 128.3, 127.7, 124.7, 124.6, 122.3, 122.0, 118.8, 115.3, 114.8, 84.7, 70.4, 69.9, 67.4, 61.5, 39.5, 28.2, 21.6, 21.5; HRMS (TOF LCMS) calc'd for $C_{28}H_{37}NNaO_7$ $[M+Na]^+$ 522.2462, found 522.2457.

Lactone-*i*-Pr 63: see below for characterization

Preparation of Lactone-i-Pr **63**

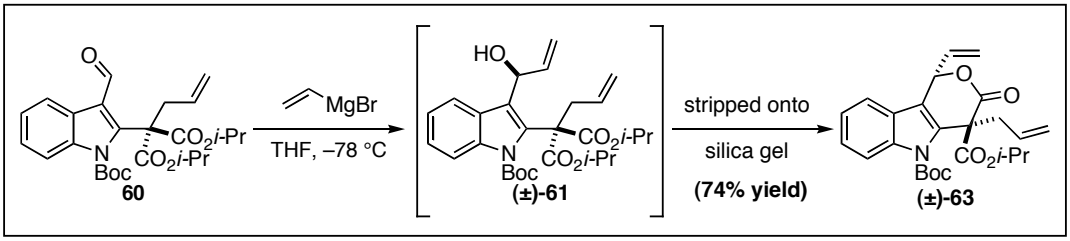

To a solution of allylindolemalonate-*i*-Pr **60** (369 mg, 0.782 mmol) in anhydrous THF (8 mL) cooled to –78 °C was added vinyl magnesium bromide (4.0 mL of a 1.0 M soln. in THF, 4.0 mmol) dropwise *via* syringe under N_2. The reaction was stirred 1 h before it was quenched by addition of saturated aqueous $NaHCO_3$ (12 mL). The layers were separated and the aqueous layer was extracted with EtOAc (3 x 25 mL). The combined organic layers were washed once with brine and dried over Na_2SO_4. Filtration of the solids followed by concentration under reduced pressure and silica gel chromatography (1% EtOAc/PhH) provided lactone-*i*-Pr **63** (255 mg, 74% yield) as a white amorphous solid.

Lactone-*i*-Pr 63: m.p. = 151.3 °C (decomposition); FTIR (thin film/NaCl) 3073 (w), 2975 (m), 2929 (w), 1757 (s), 1731 (s), 1449 (m) cm^{-1}; ^1H NMR (400 MHz, $CDCl_3$) δ 8.01 (d, J = 8.5 Hz, 1H), 7.33–7.39 (2H), 7.24 (dd, J = 7.5, 7.5 Hz, 1H), 6.06 (d, J = 7.6 Hz, 1H), 5.96 (ddd, J = 17.0, 9.7, 7.4 Hz, 1H), 5.55 (d, J = 16.8 Hz, 1H), 5.38–5.49 (2H), 4.91–5.09 (3H), 3.44 (dd, J = 14.2, 8.2 Hz, 1H), 3.23 (dd, J = 14.2, 7.4 Hz, 1H), 1.67 (s, 9H), 1.18 (d, J = 6.3 Hz, 3H), 1.14 (d, J = 6.3 Hz, 3H); ^{13}C NMR (100 MHz, $CDCl_3$) δ 167.5, 166.8, 150.0, 136.3, 135.8,

132.8, 129.8, 125.3, 125.2, 123.2, 120.5, 120.0, 119.1, 116.3, 114.3, 85.5, 78.4, 69.8, 57.7, 40.4, 28.2, 21.6, 21.4; HRMS (TOF LCMS) calc'd for $C_{25}H_{29}NNaO_6$ $[M+Na]^+$ 462.1887, found 462.1881.

Preparation of Bicycle-i-Pr **64**

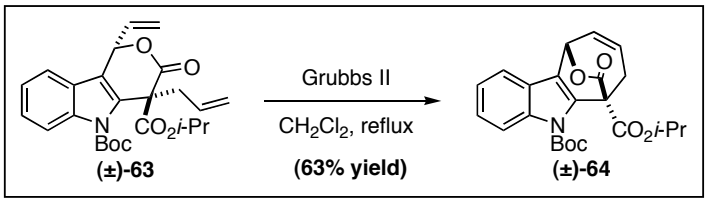

To a solution of lactone-*i*-Pr **63** (102 mg, 0.232 mmol) in anhydrous CH_2Cl_2 (6 mL) was added the Grubbs 2nd generation catalyst (13 mg, 0.0153 mmol) and the contents heated to reflux under N_2. The reaction was stirred 2.5 hrs before it was concentrated under reduced pressure and purified by silica gel chromatography (10% EtOAc/Hexanes) to yield bicycle-*i*-Pr **64** (60 mg, 63% yield) as a white foam.

Bicycle-*i*-Pr 64: FTIR (thin film/NaCl) 3052 (w), 2980 (m), 2934 (w), 1762 (s), 1731 (s, br), 1454 (m), 1419 (m) cm^{-1}; ^1H NMR (400 MHz, $CDCl_3$) δ 8.02 (br d, J = 7.3 Hz, 1H), 7.49–7.51 (nfom, 1H), 7.29–7.37 (nfom, 1H and nfom, 1H), 6.43 (dddd, J = 11.1, 6.7, 2.3, 2.3 Hz, 1H), 5.78 (m, 1H), 5.71 (d, J = 6.7 Hz, 1H), 5.13 (m, 1H), 3.29 (ddd, J = 19.7, 3.9, 2.3 Hz, 1H), 2.86 (br d, J = 19.6 Hz, 1H), 1.67 (s, 9H), 1.28 (br m, 6H); ^{13}C NMR (100 MHz, $CDCl_3$) δ 170.3, 166.4, 150.3, 136.5, 131.6, 131.4, 128.6, 125.0, 124.3, 123.6, 118.1, 115.9, 86.1, 70.1, 68.7,

57.7, 31.1, 28.4, 22.1, 21.3; HRMS (TOF LCMS) calc'd for $C_{23}H_{25}NNaO_6$ $[M+Na]^+$ 434.1574, found 434.1573.

Preparation of Allylic alcohol-i-Pr **62**

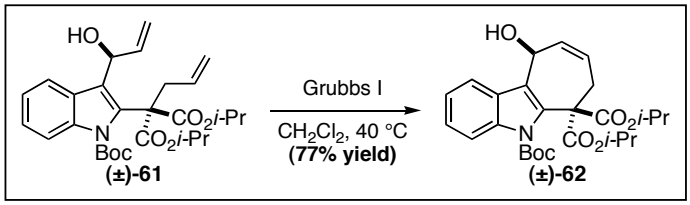

To a solution of diene-*i*-Pr **61** (721.5 mg, 1.44 mmol) in anhydrous CH_2Cl_2 (20 mL) was added the Grubbs 1st generation catalyst (24.0 mg, 0.0292 mmol) and the contents heated to reflux under N_2. The reaction was stirred overnight before it was concentrated under reduced pressure and purified by silica gel chromatography (gradient elution, 15 → 25% EtOAc/Hexanes) to yield allylic alcohol-*i*-Pr **62** (522.0 mg, 77% yield) as a white amorphous solid.

Allylic alcohol-*i*-Pr 62: m.p. = 127.7 °C (decomposition); FTIR (thin film/NaCl) 3467 (w, br), 3262 (w, br), 3047 (w), 2975 (m), 2929 (w), 2868 (w), 1721 (s), 1659 (w), 1454 (m) cm^{-1}; ^1H NMR (400 MHz, $CDCl_3$) δ 8.00–8.02 (nfom, 1H), 7.71–7.73 (nfom, 1H), 7.24–7.33 (nfom, 1H and nfom, 1H), 6.27 (ddd, *J* = 9.9, 6.6, 1.1 Hz, 1H), 5.97 (ddd, *J* = 9.8, 7.4, 7.4 Hz, 1H), 5.57 (dd, *J* = 6.5, 4.4 Hz, 1H), 5.03 (septet, *J* = 6.4 Hz, 1H), 5.01 (septet, *J* = 6.4 Hz, 1H), 3.58 (ddd, *J* = 13.4, 6.8, 1.4 Hz, 1H), 3.02 (dd, *J* = 13.4, 7.9 Hz, 1H), 2.35 (d, *J* = 4.4 Hz, 1H), 1.64 (s, 9H), 1.20 (d, *J* = 6.2 Hz, 3H), 1.16 (d, *J* = 6.3 Hz, 3H), 1.13 (d, *J* = 6.8 Hz, 3H), 1.12 (d, *J* = 6.7 Hz, 3H); ^{13}C NMR (100 MHz, $CDCl_3$) δ 169.1, 167.5,

151.1, 135.8, 134.9, 129.5, 128.8, 124.6, 122.7, 120.3, 118.7, 116.0, 84.5, 69.0, 68.8, 62.6, 59.4, 35.1, 28.3, 21.8, 21.7, 21.6; HRMS (TOF LCMS) calc'd for $C_{26}H_{33}NNaO_7$ $[M+Na]^+$ 494.2149, found 494.2151.

Preparation of Enone-i-Pr **65** *and iso-Enone-i-Pr* **66**

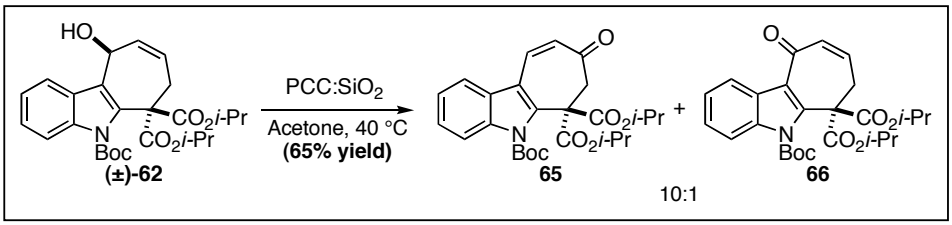

To a solution of SiO_2 (36 g) in acetone (300 mL) was added PCC (3.6 g, 16.8 mmol) and the heterogeneous solution was pre-warmed to 40 °C before addition of allylic alcohol-*i*-Pr **62** (5.3 g, 11.2 mmol) as a solution in acetone (160 mL) dropwise *via* addition funnel (ca. 1.7 hrs). The reaction was stirred for an additional 0.5 h before it was quenched by addition of IPA (10 mL). Stirring for 10 min. at 40 °C was followed by filtration through Celite and concentration under reduced pressure. The isolated material was purified by silica gel chromatography (gradient elution, 10 → 20 → 25% EtOAc/Hexanes) to provide a 10:1 mixture of enone-*i*-Pr **65**:*iso*-enone-*i*-Pr **66** (3.4 g, 65% yield) as a light orange oil. An analytical sample of enone-*i*-Pr **65** and *iso*-enone-*i*-Pr **66** were obtained following preparative thin layer chromatography (10% Et_2O/CH_2Cl_2) as colorless oils.

Enone-*i*-Pr 65: FTIR (thin film/NaCl) 2975 (m), 2939 (w), 2878 (w), 1741 (s, br), 1664 (w), 1547 (w), 1460 (m) cm^{-1}; ^1H NMR (400 MHz, $CDCl_3$) δ 8.00 (d, *J*

= 7.9 Hz, 1H), 7.66–7.68 (nfom, 1H), 7.47 (d, *J* = 12.0 Hz, 1H), 7.33–7.40 (nfom, 1H and nfom, 1H), 6.21 (d, *J* = 12.0 Hz, 1H), 5.07 (septet, *J* = 6.3 Hz, 2H), 3.40 (s, 2H), 1.67 (s, 9H), 1.67 (s, 9H), 1.25 (d, *J* = 6.3 Hz, 6H), 1.22 (d, *J* = 6.3 Hz, 6H); ^{13}C NMR (100 MHz, $CDCl_3$) δ 195.7, 167.1, 150.3, 140.1, 135.5, 133.5, 128.5, 126.9, 125.6, 123.6, 117.9, 117.8, 115.8, 85.9, 70.1, 57.6, 50.5, 28.3, 21.6, 21.6; HRMS (TOF LCMS) calc'd for $C_{26}H_{32}NO_7$ $[M+H]^+$ 470.2173, found 470.2173.

***iso*-Enone-*i*-Pr 66**: FTIR (thin film/NaCl) 2980 (m), 2934 (w), 2873 (w), 1741 (s, br), 1654 (w), 1613 (w), 1454 (m) cm^{-1}; ^{1}H NMR (400 MHz, $CDCl_3$) δ 8.63–8.66 (nfom, 1H), 8.00–8.02 (nfom, 1H), 7.34–7.39 (nfom, 1H and nfom, 1H), 6.45 (dt, *J* = 11.3, 6.8 Hz, 1H), 6.32 (d, *J* = 11.3 Hz, 1H), 5.06 (septet, *J* = 6.3 Hz, 2H), 3.22 (d, *J* = 6.8 Hz, 2H), 1.67 (s, 9H), 1.19 (d, *J* = 6.3 Hz, 6H), 1.17 (d, *J* = 6.3 Hz, 6H); ^{13}C NMR (100 MHz, $CDCl_3$) δ 188.8, 167.0, 150.6, 144.4, 136.6, 135.4, 133.1, 127.7, 125.7, 124.5, 123.3, 121.9, 115.3, 86.2, 69.8, 61.1, 36.4, 28.2, 21.7, 21.6; HRMS (TOF LCMS) calc'd for $C_{26}H_{32}NO_7$ $[M+H]^+$ 470.2173, found 470.2181.

Preparation of Carbazole **69** *and Lactone carbazole* **70**

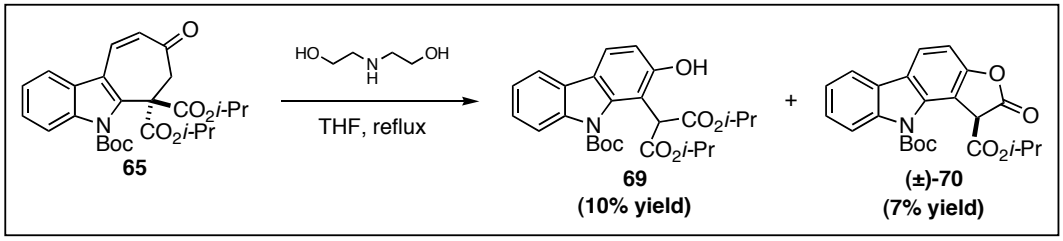

To a solution of 3:1 mixture of enone-*i*-Pr **65** and *iso*-enone-*i*-Pr **66** (68 mg, 0.164 mmol) in THF (2 mL) was added diethanolamine (50 μL, 0.521 mmol) at room temperature under N_2. The reaction was heated to reflux and stirred overnight before it was concentrated under reduced pressure and purified by silica gel chromatography (gradient elution, 10 → 25% EtOAc/Hexanes) to provide two products. The first compound to elute off the column could not be characterized. The second compound to elute was lactone carbazole **70** (5 mg, 7% yield) as a colorless oil. The last compound to elute was carbazole **69** (8 mg, 10% yield) as a colorless oil.

Lactone carbazole 70: FTIR (thin film/NaCl) 2986 (m), 2934 (w), 1808 (s), 1736 (s), 1603 (w), 1449 (s), 1424 (w) cm^{-1}; ^1H NMR (400 MHz, $CDCl_3$) δ 7.98 (d, *J* = 8.5 Hz, 1H), 7.92 (d, *J* = 8.4 Hz, 1H), 7.88 (d, *J* = 7.7 Hz, 1H), 7.37 (dd, *J* = 7.8, 7.8 Hz, 1H), 7.29 (dd, *J* = 7.5, 7.5 Hz, 1H), 7.12 (d, *J* = 8.3 Hz, 1H), 5.47 (s, 1H), 4.98 (septet, *J* = 6.3 Hz, 1H), 1.64 (s, 9H), 1.23 (d, *J* = 6.31 Hz, 3H), 1.18 (d, *J* = 6.2 Hz, 3H); ^{13}C NMR (100 MHz, $CDCl_3$) δ 169.7, 164.7, 154.3, 150.9, 138.3, 135.4, 127.0, 125.7, 123.6, 123.5, 121.1, 119.4, 116.1, 109.7,

107.0, 85.0, 70.4, 53.9, 28.4, 21.8, 21.8; HRMS (TOF LCMS) calc'd for $C_{23}H_{23}NNaO_6$ $[M+Na]^+$ 432.1418, found 432.1412.

Carbazole 69: FTIR (thin film/NaCl) 3395 (m, br), 2980 (m), 2934 (w), 2873 (w), 1726 (s, br), 1623 (w), 1593 (w), 1516 (w), 1449 (m) cm^{-1}; ^1H NMR (400 MHz, $CDCl_3$) δ 8.08 (d, *J* = 8.2 Hz, 1H), 7.91 (d, *J* = 8.3 Hz, 1H), 7.28–7.33 (2H), 7.20 (dd, *J* = 7.5, 7.5 Hz, 1H), 6.63 (d, *J* = 8.4 Hz, 1H), 6.09 (s, 1H), 5.15 (septet, *J* = 6.2 Hz, 2H), 4.99 (s, 1H), 1.70 (s, 9H), 1.29 (d, *J* = 6.3 Hz, 6H), 1.26 (d, *J* = 6.2 Hz, 6H); ^{13}C NMR (100 MHz, $CDCl_3$) δ 169.2, 151.9, 151.5, 139.9, 139.0, 129.3, 126.0, 125.7, 123.4, 122.9, 116.3, 115.4, 114.1, 111.1, 84.4, 69.3, 55.8, 28.3, 21.8, 21.7; HRMS (TOF LCMS) calc'd for $C_{26}H_{31}NNaO_7$ $[M+Na]^+$ 492.1993, found 492.1984.

Preparation of Silyl enol ether **71**

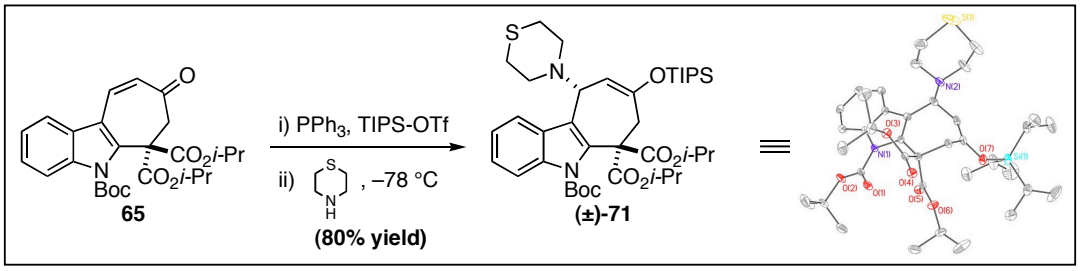

To a round-bottom flask containing a solution of 10:1 enone-*i*-Pr **65**:*iso*-enone-*i*-Pr **66** (182 mg, 0.387 mmol) in CH_2Cl_2 (4 mL) was added triphenylphosphine (112 mg, 0.427 mmol) at room temperature under N_2. The clear yellow solution was cooled to 0 °C in an ice-water bath. At this time TIPS-OTf (320 μL, 1.186 mmol) was added dropwise and the reaction left to stir at 0 °C

(5 min.). The ice-water bath was removed and the clear orange solution was stirred for 1 hr at room temperature. The reaction was cooled to –78 °C, which resulted in a color change from orange to yellow. To the cooled reaction mixture was added thiomorpholine (260 μL, 2.74 mmol) and the reaction was allowed to reach room temperature overnight. The reaction was quenched by addition of silica gel that had been pre-treated with Et_3N (ca. 2 mL). The heterogeneous reaction mixture was concentrated under reduced pressure and purified by silica gel chromatography (1:10:89 Et_3N/EtOAc/Hexanes) to furnish silyl enol ether **71** (225 mg, 80% yield) as a light yellow solid. An analytically pure sample was obtained following recrystallization from MeOH. A crystal proved suitable for x-ray analysis (see Appendix 3, A.3.1).

Silyl enol ether 71: m.p. = 146.4 °C (decomposition); FTIR (thin film/NaCl) 2970 (m), 2939 (m), 2858 (m), 1767 (m), 1726 (s), 1659 (w), 1460 (m) cm^{-1}; ^1H NMR (400 MHz, PhH-d_6) δ 8.24 (d, J = 8.4 Hz, 1H), 7.57 (d, J = 7.8 Hz, 1H), 7.31 (dd, J = 7.3, 8.3 Hz, 1H), 7.22 (d, J = 7.5 Hz, 1H), 5.32 (d, J = 7.7 Hz, 1H), 5.15 (septet, J = 6.2 Hz, 1H), 4.99–5.07 (2H), 4.04 (d, J = 7.7 Hz, 1H), 3.31 (dd, J = 13.1, 1.4 Hz, 1H), 2.93 (m, 2H), 2.75 (m, 2H), 2.47 (m, 4H), 1.40 (s, 9H), 1.13–1.19 (27H), 0.99 (d, J = 6.2 Hz, 3H), 0.95 (d, J = 6.2 Hz, 3H); ^{13}C NMR (100 MHz, PhH-d_6) δ 168.8, 167.3, 153.0, 151.6, 137.1, 134.9, 131.5, 124.7, 122.8, 119.7, 119.3, 116.4, 108.7, 83.9, 68.6, 68.3, 58.3, 56.5, 54.5, 41.4, 28.9, 28.1, 21.9, 21.7, 21.7, 18.2, 18.2, 12.9; HRMS (TOF LCMS) calc'd for $C_{39}H_{60}N_2NaO_7SSi$ $[M+Na]^+$ 751.3783, found 751.3775.

3.4 Notes and References

1. (a) *"Organopalladium Intermediates in Organic Synthesis"*, Trost, B. M. *Tetrahedron* **1977**, *33*, 2615–2649; (b) *"New Synthetic Reactions of Allyl Alkyl Carbonates, Allyl Beta-Keto Carboxylates, and Allyl Vinylic Carbonates Catalyzed by Palladium Complexes"*, Tsuji, J.; Minami, I. *Acc. Chem. Res.* **1987**, *20*, 140–145.

2. (a) *"Ring-Closing Metathesis and Related Processes in Organic Synthesis"*, Grubbs, R. H.; Miller, S. J.; Fu, G. C. *Acc. Chem. Res.* **1995**, *28*, 446–452; (b) *"The Development of L_2X_2Ru=CHR Olefin Metathesis Catalysts: An Organometallic Success Story"*, Trnka, T. M.; Grubbs, R. H. *Acc. Chem. Res.* **2001**, *34*, 18–29.

3. (a) *"Access to Guaianolides: Highly Efficient Stereocontrolled Total Synthesis of (±)-Geigerin"*, Carret, S.; Depres, J.-P. *Angew. Chem. Int. Ed.* **2007**, *46*, 6870–6873; (b) *"Synthetic Studies on the DEF-Rings of FR182877 and Hexacyclinic Acid"*, Clarke, P. A.; Grist, M.; Ebden, M.; Wilson, C.; Blake, A. J. *Tetrahedron* **2005**, *61*, 353–363; (c) *"Total Synthesis of Quadrone and Terrecyclic Acid A"*, Wender, P. A.; Wolanin, D. J. *J. Org. Chem.* **1985**, *50*, 4418–4420.

4. (a) *"Cycloheptatriene-Norcaradiene Equilibrium"*, Balci, M. *Turk. J. Chem.* **1992**, *16*, 42–90; (b) *"7,7-Dicarbomethoxycycloheptatriene"*, Berson, J. A.;

Harter, D. R.; Klinger, H.; Grubb, P. W. *J. Org. Chem.* **1968**, *33*, 1669–1671.

5. *"Facile Nucleophilic Substitution of 3-tert-butyl-Dimethylsilyloxyalk-2-enylphosphonium Salts"*, Lee, P. H.; Cho, M.; Han, I.-S.; Kim, S. *Tetrahedron Lett.* **1999**, *40*, 6975–6978.

6. *"Nucleophilicity of Phosphines"*, Henderson, W. A., Jr.; Buckler, S. A. *J. Am. Chem. Soc.* **1960**, *82*, 5794–5800.

7. *"Basicity of Phosphines"*, Henderson, W. A., Jr.; Streuli, C. A. *J. Am. Chem. Soc.* **1960**, *82*, 5791–5794.

8. *"Chlorination of Unsymmetrical Sulfides"*, Tuleen, D. L.; Stephens, T. B. *J. Org. Chem.* **1969**, *34*, 31–35.

9. *"Lewis Acid Promoted Ene-like Reactions of Enol Ethers with Aldehydes"*, Shoda, H.; Nakamura, T.; Tanino, K.; Kuwajima, I. *Tetrahedron Lett.* **1993**, *34*, 6281–6284.

10. *"A Short Synthesis of (–)-(4R,5S)-Sitophilure Using the Regio- and Stereoselective Reduction of 3-Acyltetrahydrothiopyran-4-ones with Baker's Yeast"*, Fujisawa, T.; Mobele, B. I.; Shimizu, M. *Tetrahedron Lett.* **1992**, *33*, 5567–5570.

11. Oxidants that were screened include: NCS, NBS, *m*-CPBA, Benzoyl peroxide, Selectfluor™, SO_2Cl_2, and Sulfuryl diimidazole.

Appendix 2: Characterization Spectra Relevant to Chapter Three

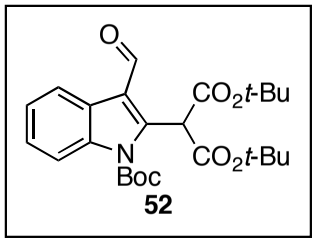

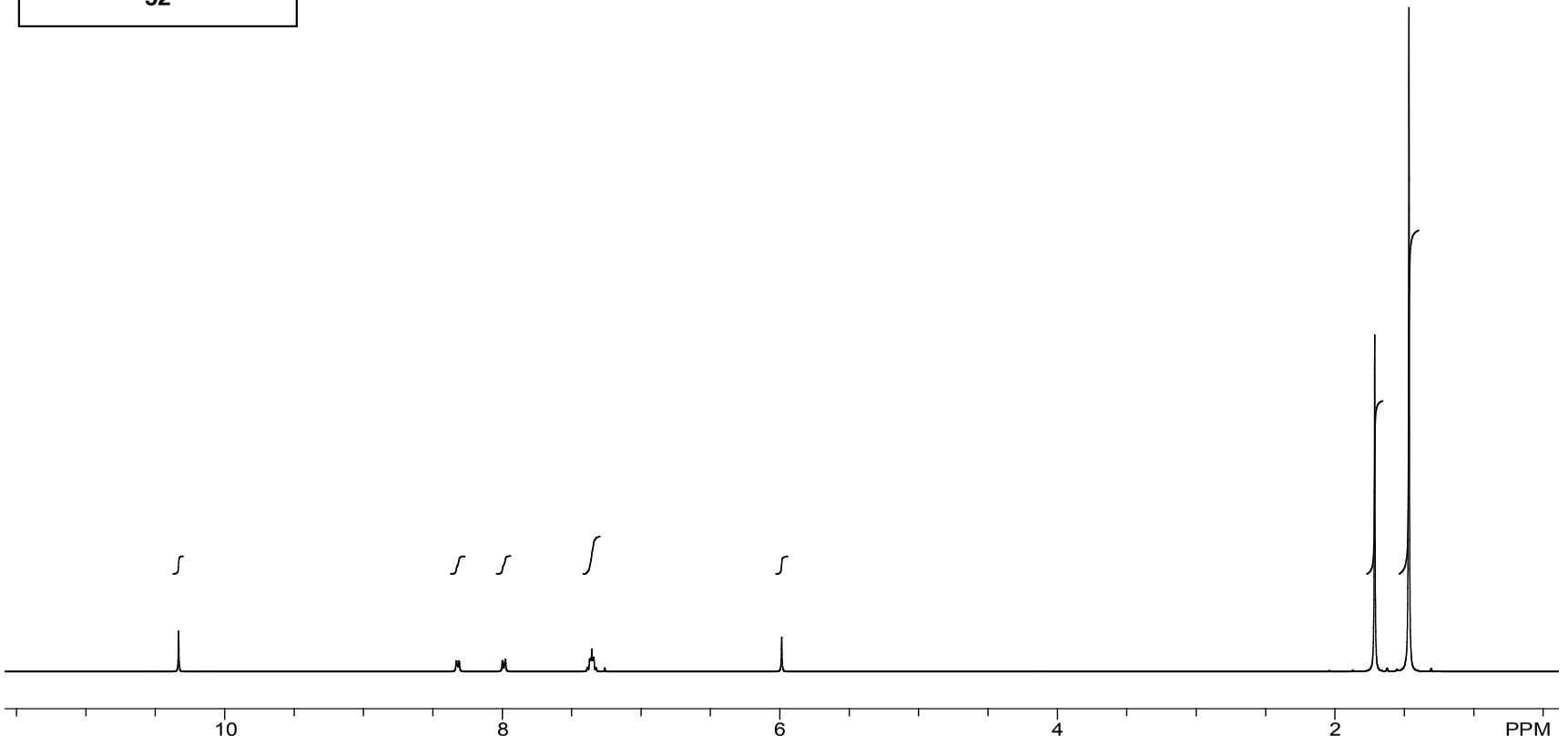

Figure A.2.1 ^{1}H NMR spectrum (400 MHz, $CDCl_3$) of compound **52**

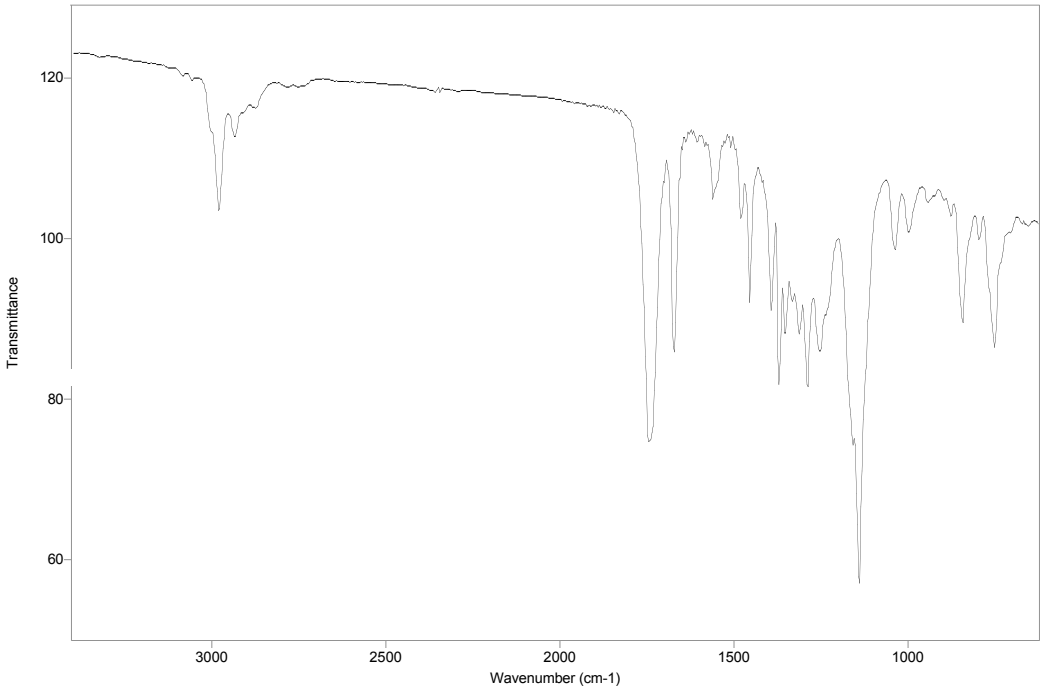

Figure A.2.2 FTIR spectrum (NaCl/thin film) of compound **52**

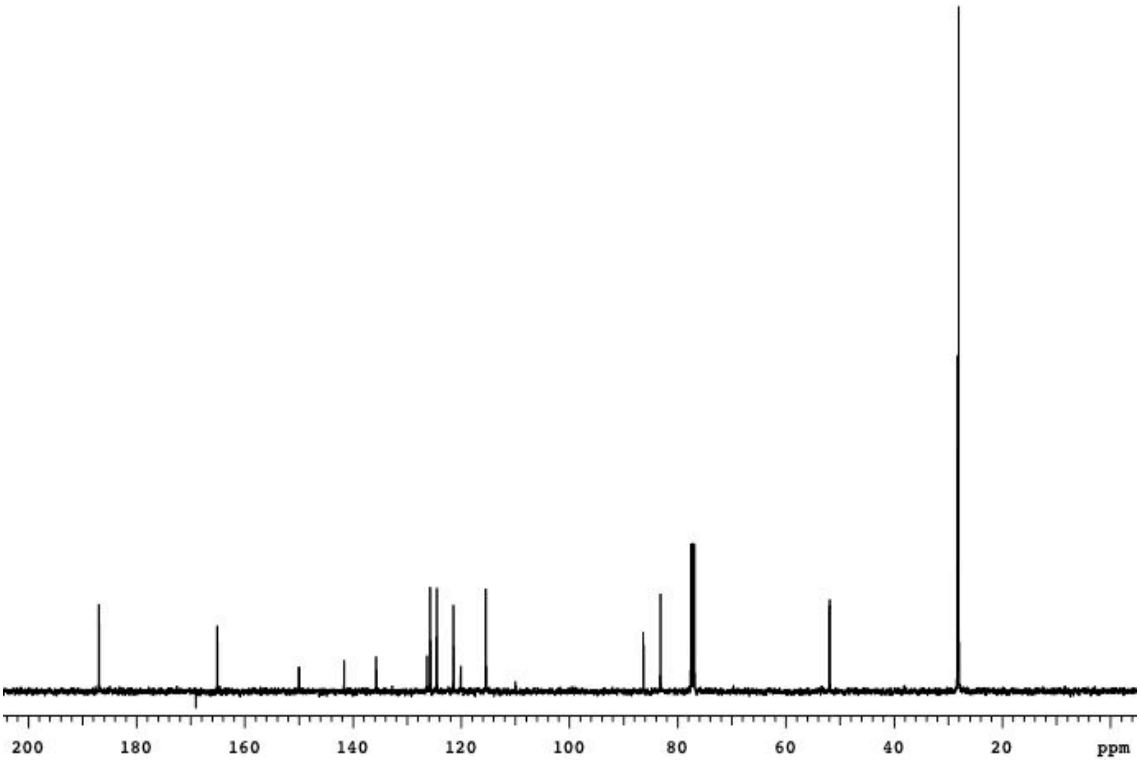

Figure A.2.3 ^{13}C spectrum (100 MHz, $CDCl_3$) of compound **52**

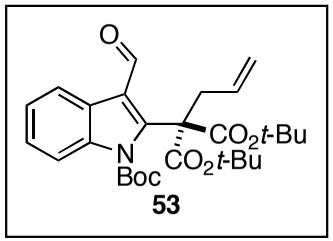

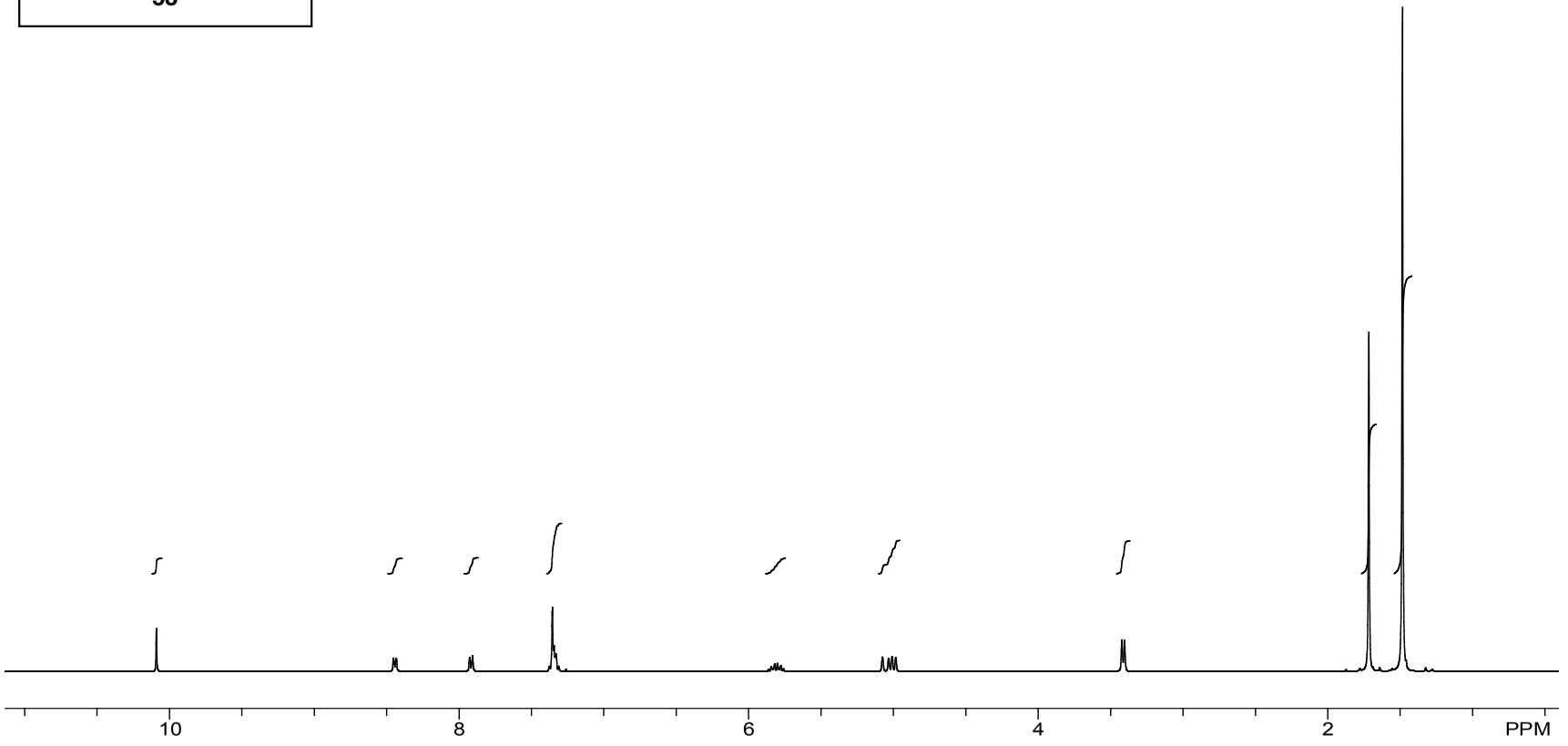

Figure A.2.4 ^{1}H NMR spectrum (400 MHz, $CDCl_3$) of compound **53**

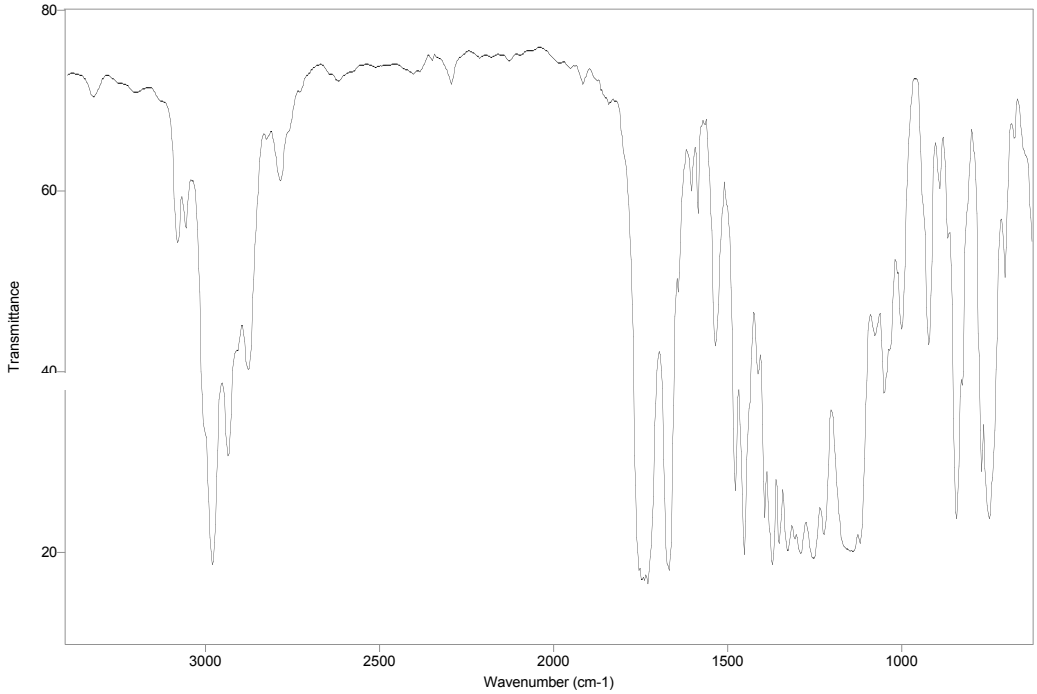

Figure A.2.5 FTIR spectrum (NaCl/thin film) of compound **53**

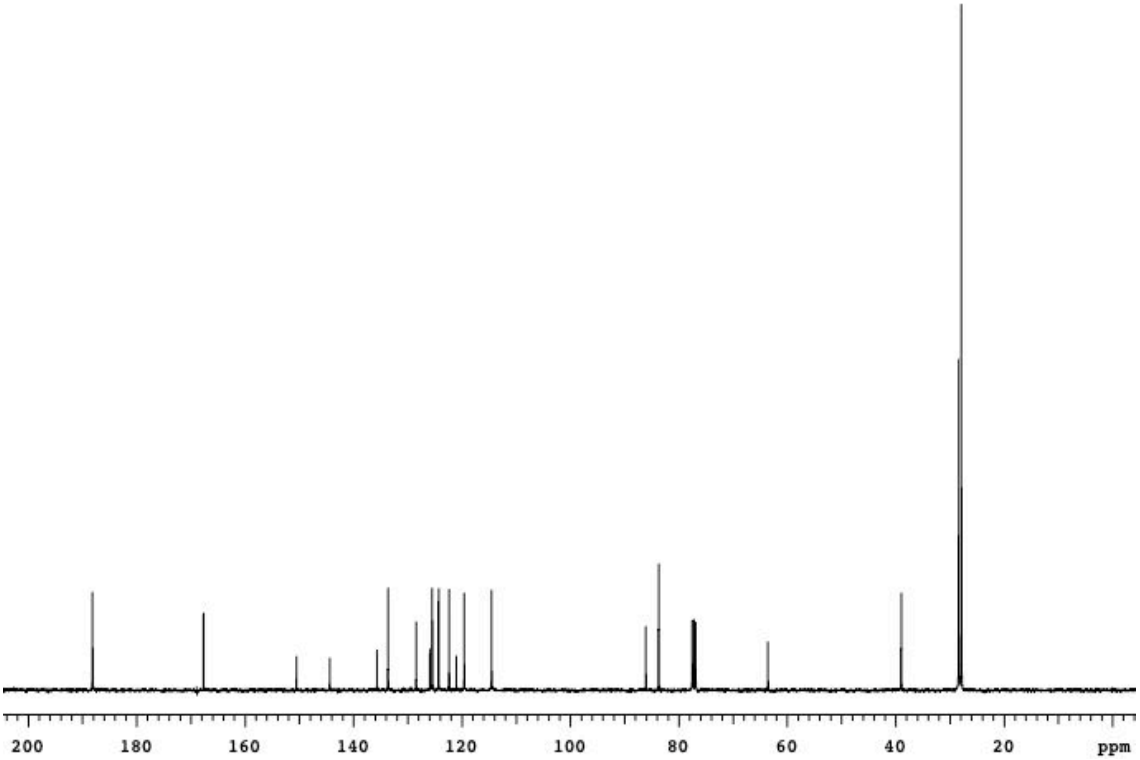

Figure A.2.6 ^{13}C spectrum (100 MHz, $CDCl_3$) of compound **53**

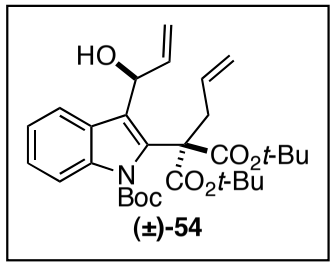

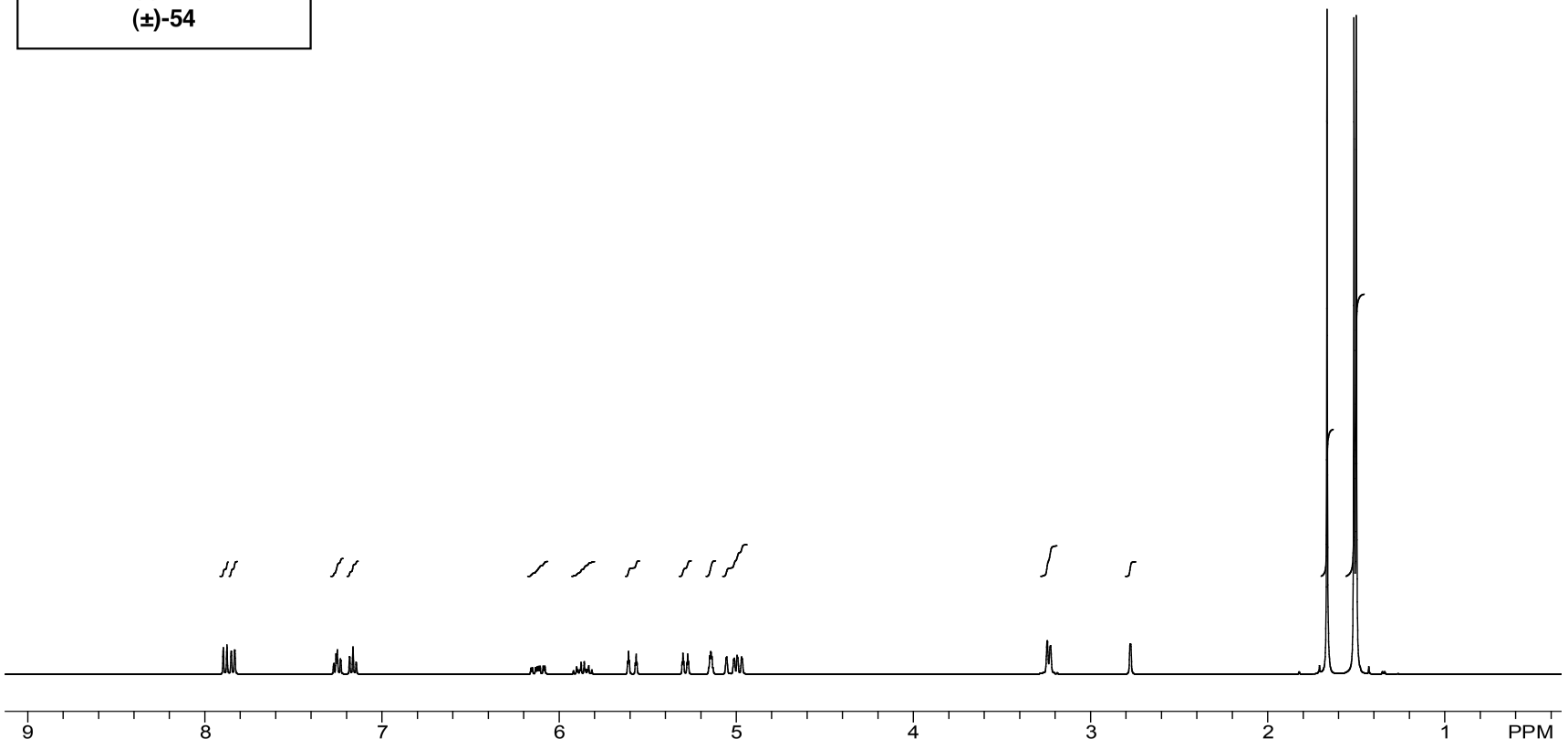

Figure A.2.7 ^{1}H NMR spectrum (400 MHz, $CDCl_3$) of compound **54**

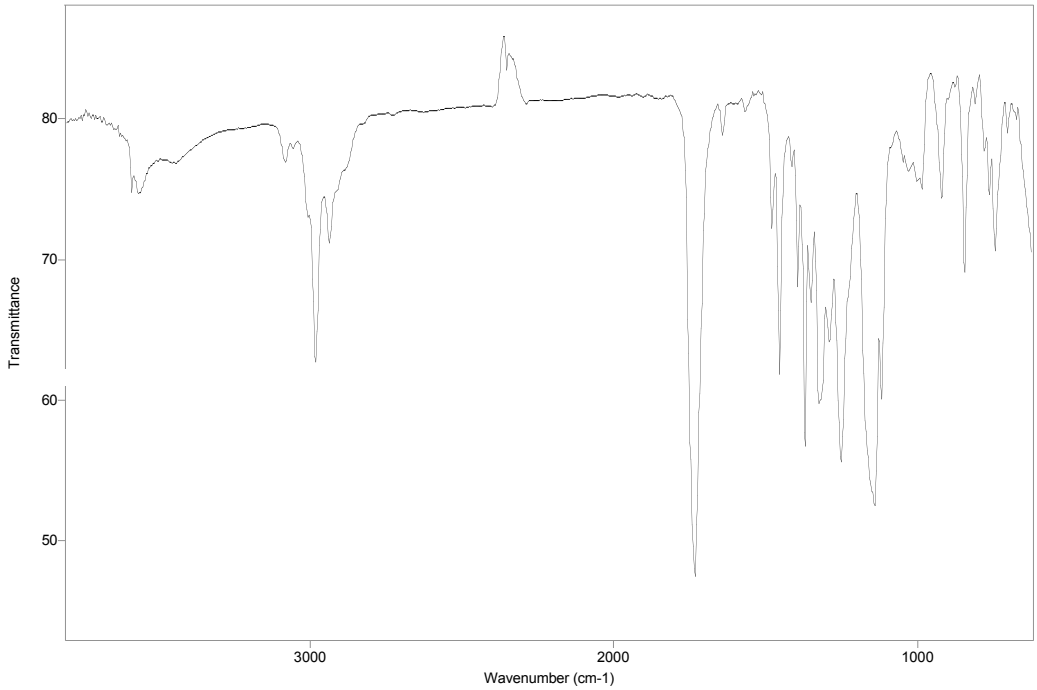

Figure A.2.8 FTIR spectrum (NaCl/thin film) of compound **54**

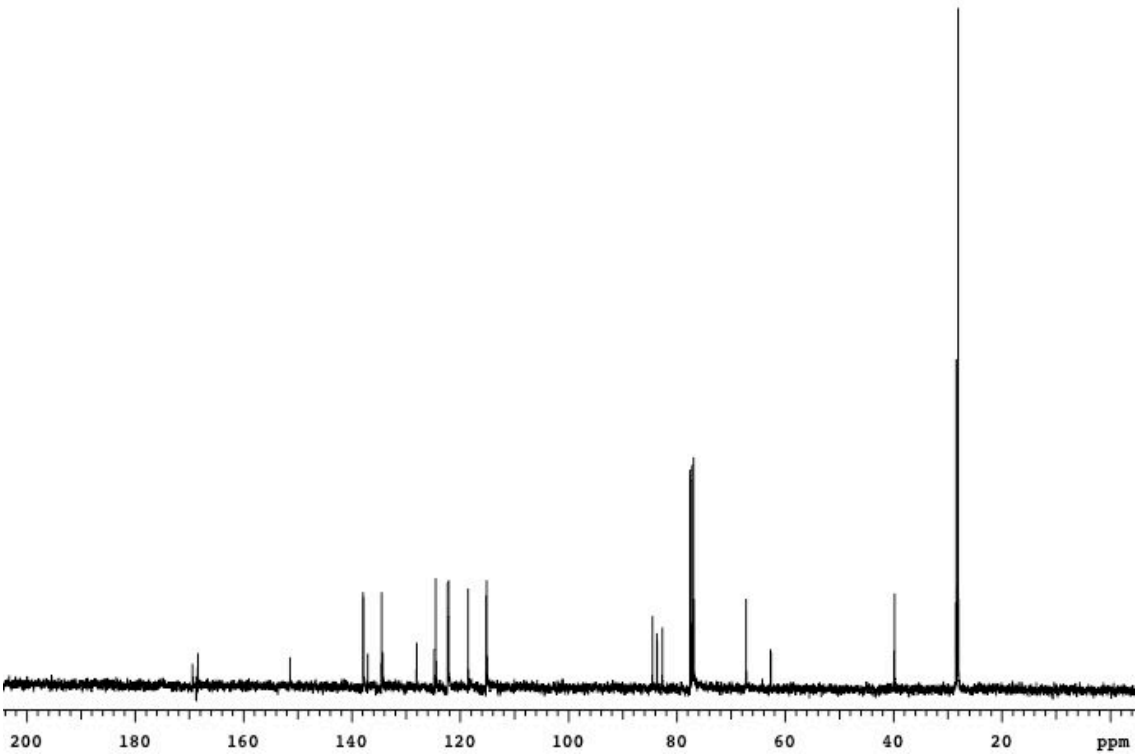

Figure A.2.9 ^{13}C spectrum (100 MHz, $CDCl_3$) of compound **54**

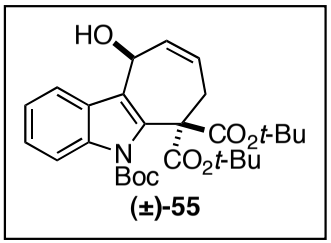

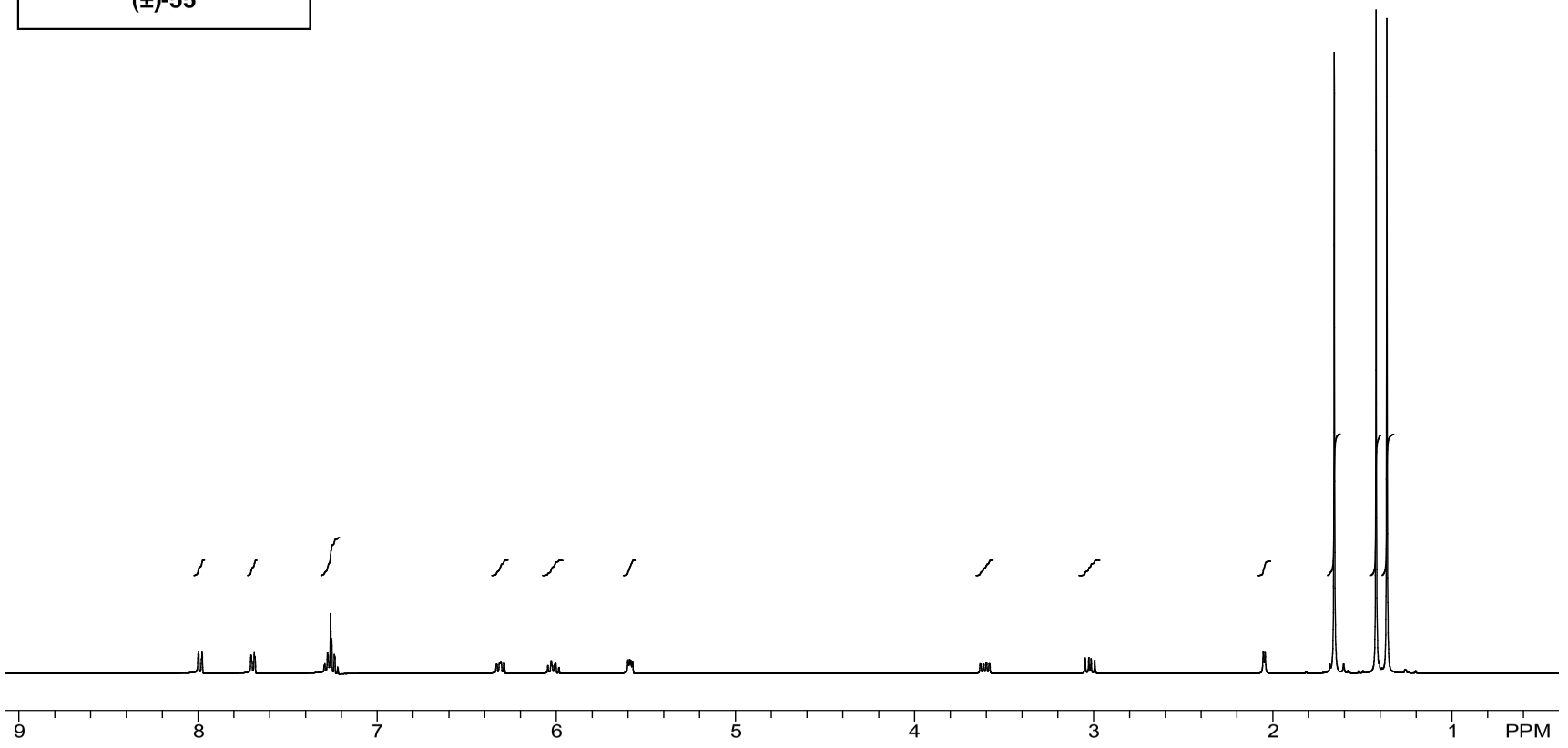

Figure A.2.10 ^{1}H NMR spectrum (400 MHz, $CDCl_3$) of compound **55**

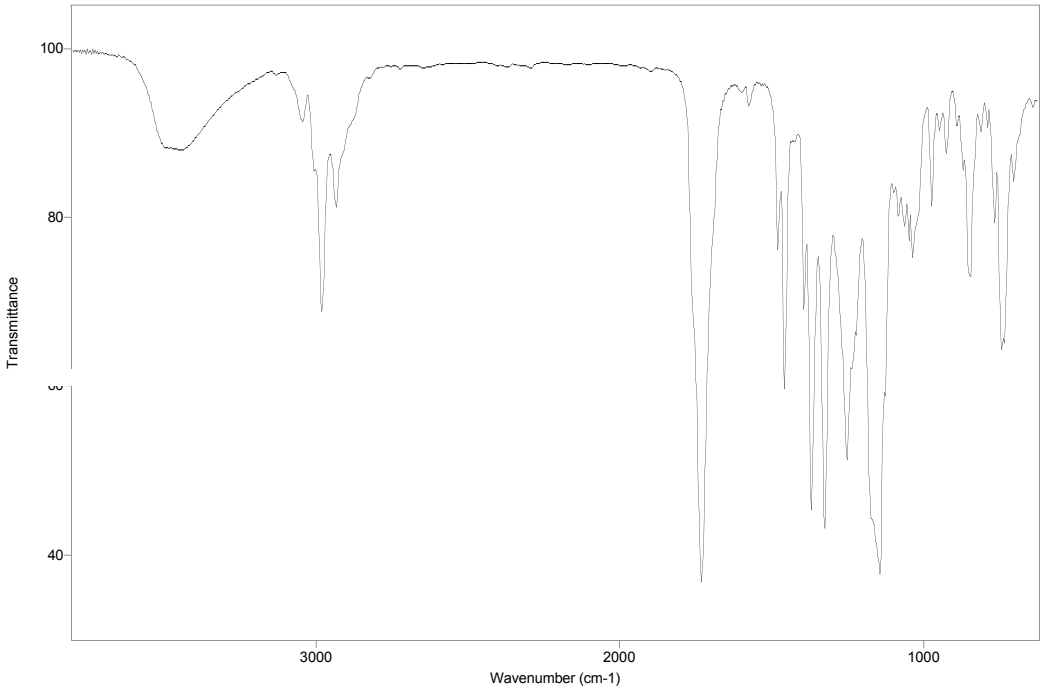

Figure A.2.11 FTIR spectrum (NaCl/thin film) of compound **55**

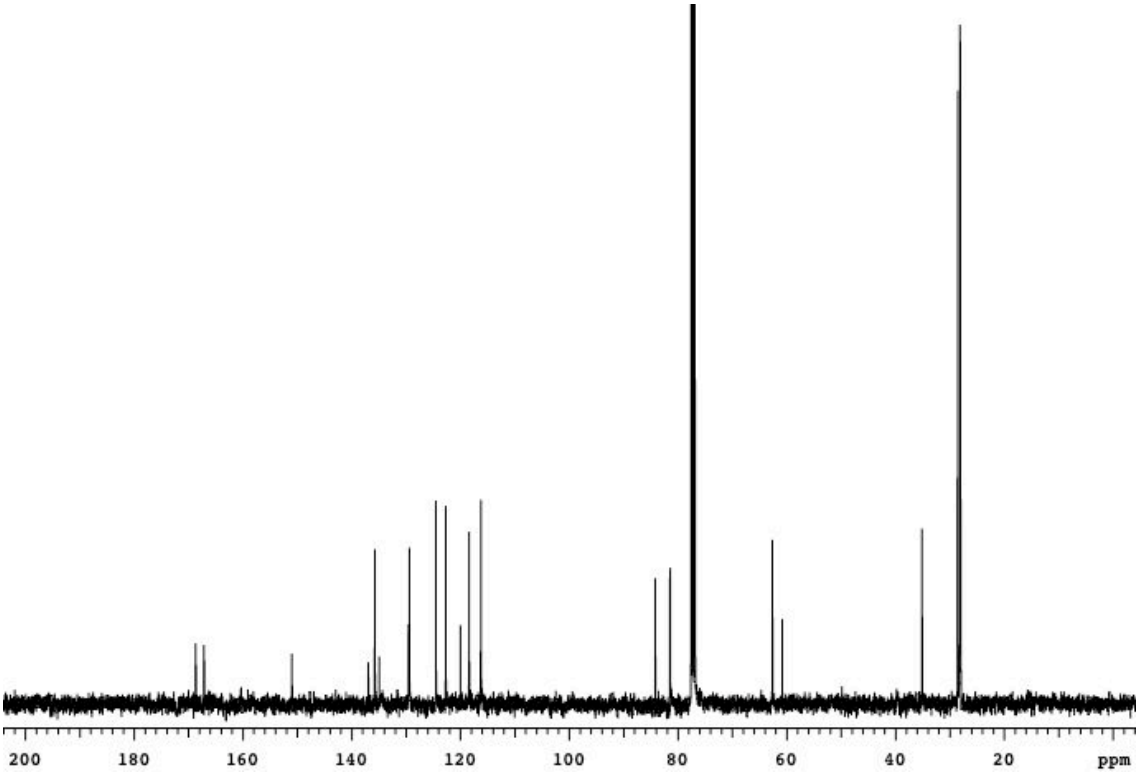

Figure A.2.12 ^{13}C spectrum (100 MHz, $CDCl_3$) of compound **55**

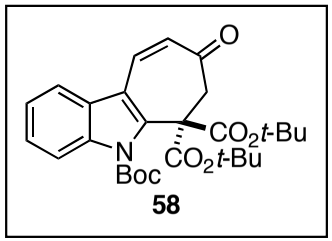

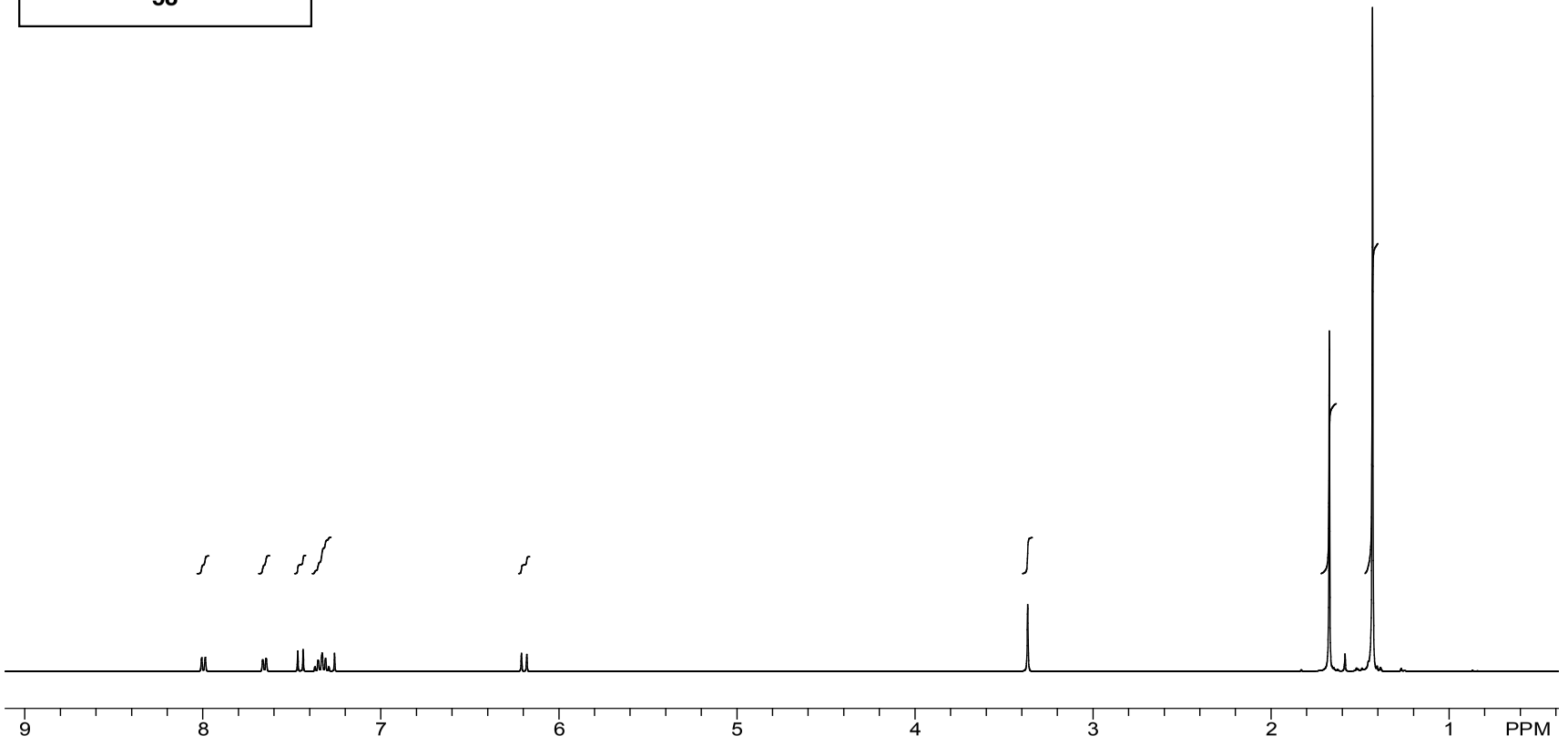

Figure A.2.13 ^{1}H NMR spectrum (400 MHz, $CDCl_3$) of compound **58**

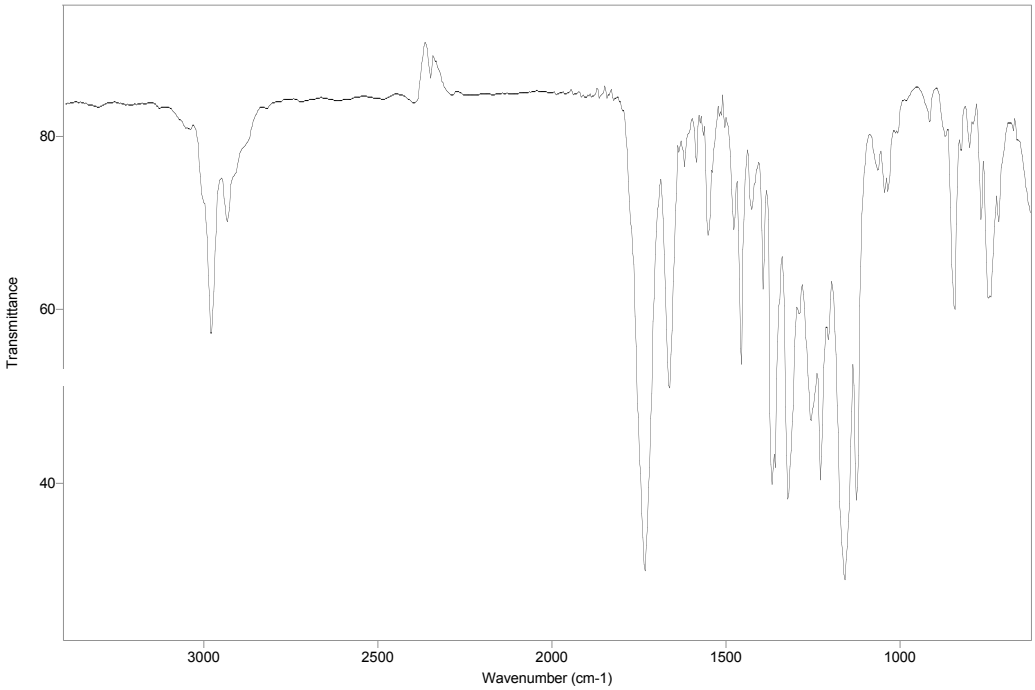

Figure A.2.14 FTIR spectrum (NaCl/thin film) of compound **58**

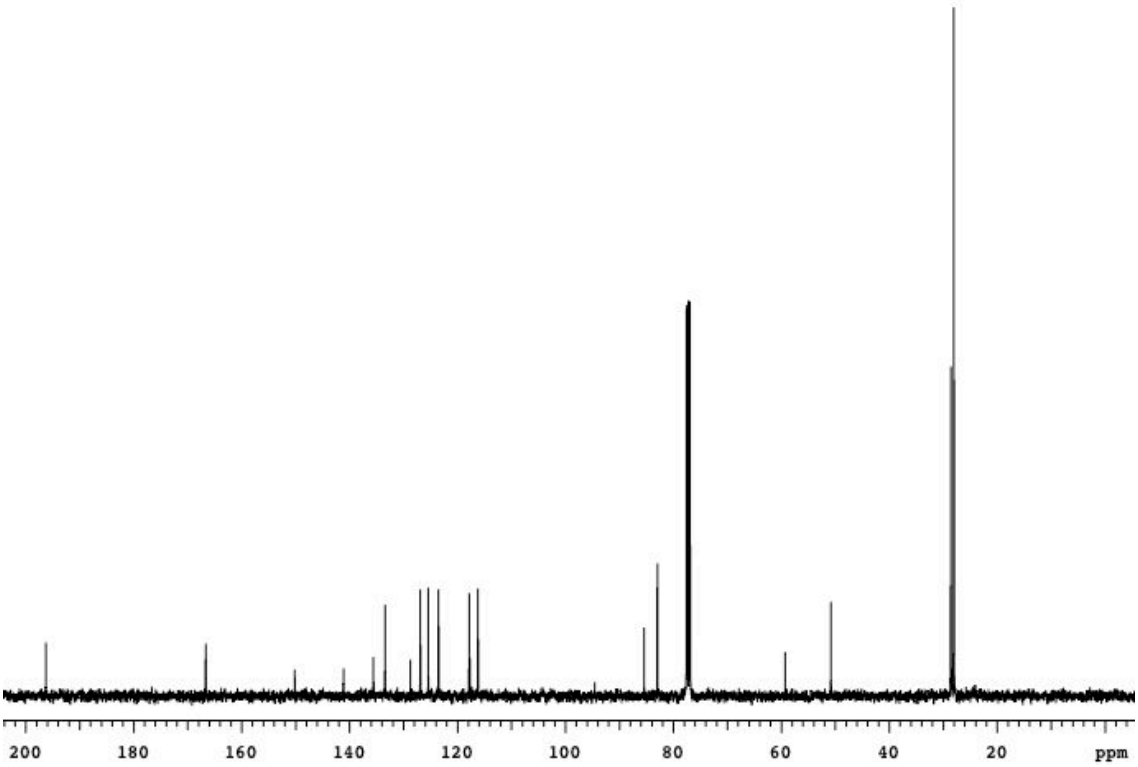

Figure A.2.15 ^{13}C spectrum (100 MHz, $CDCl_3$) of compound **58**

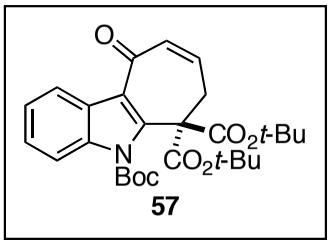

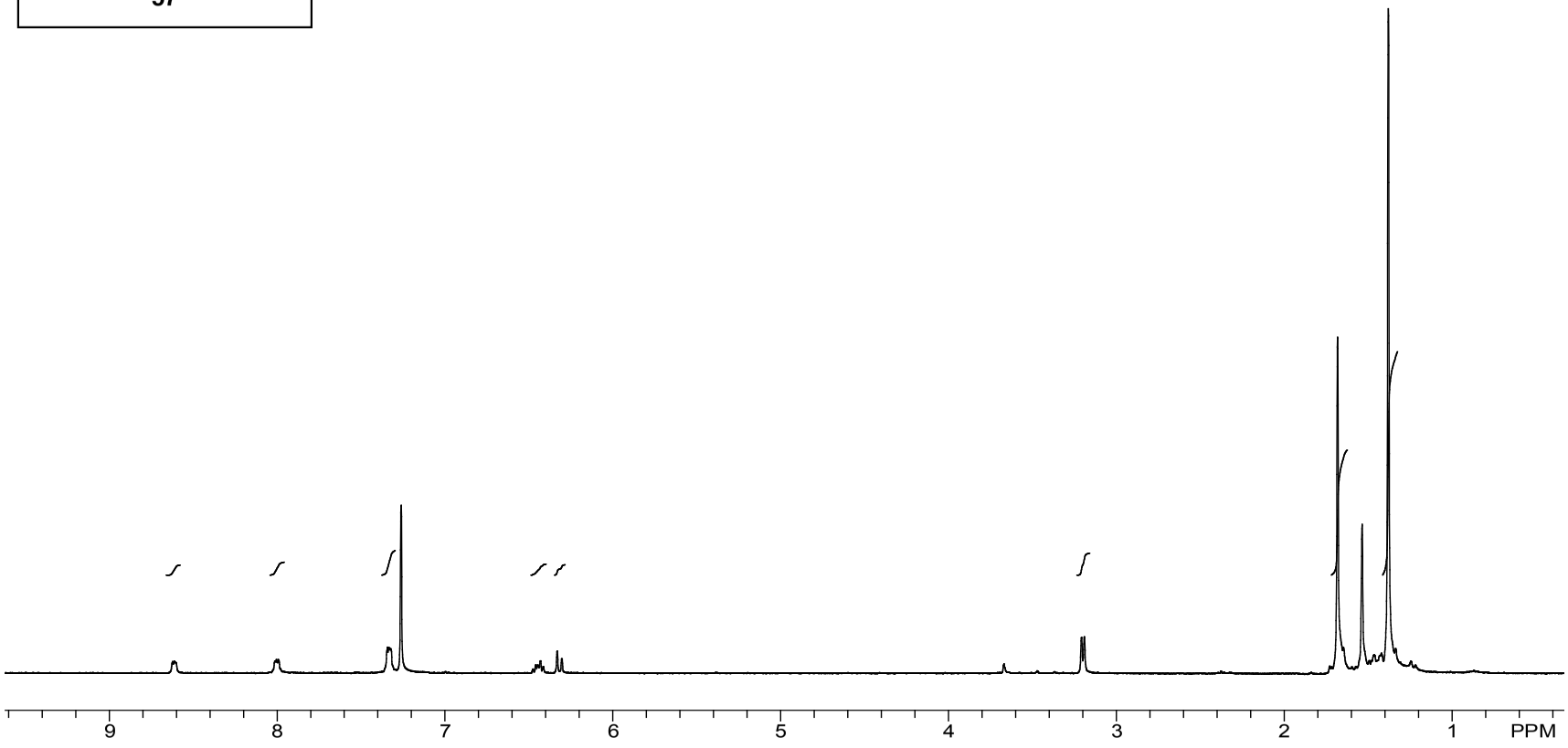

Figure A.2.16 ^{1}H NMR spectrum (400 MHz, $CDCl_3$) of compound **57**

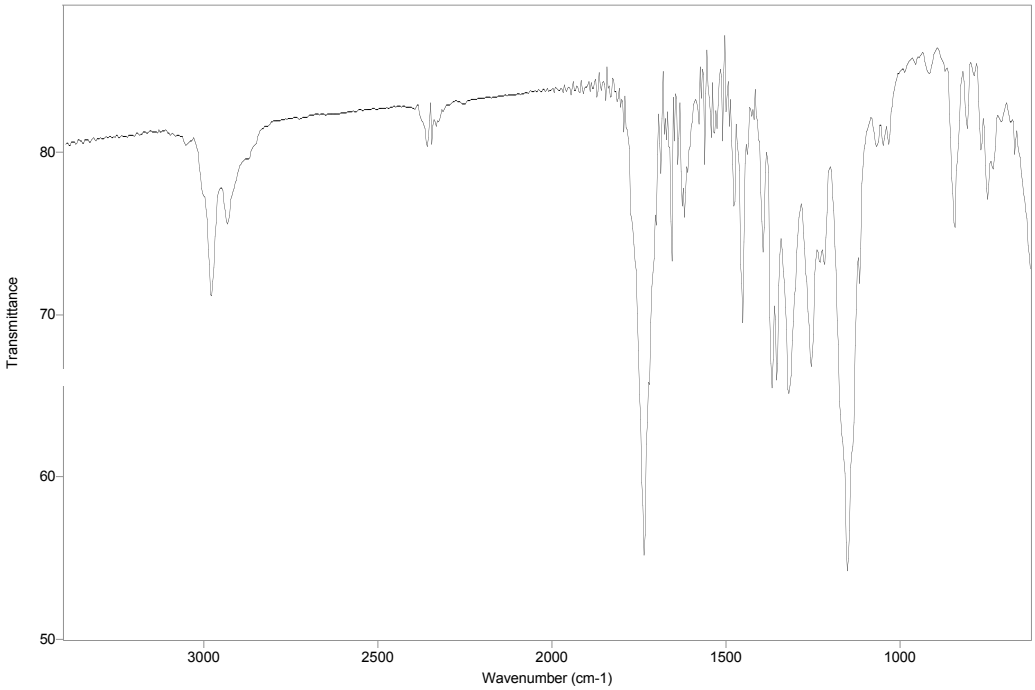

Figure A.2.17 FTIR spectrum (NaCl/thin film) of compound **57**

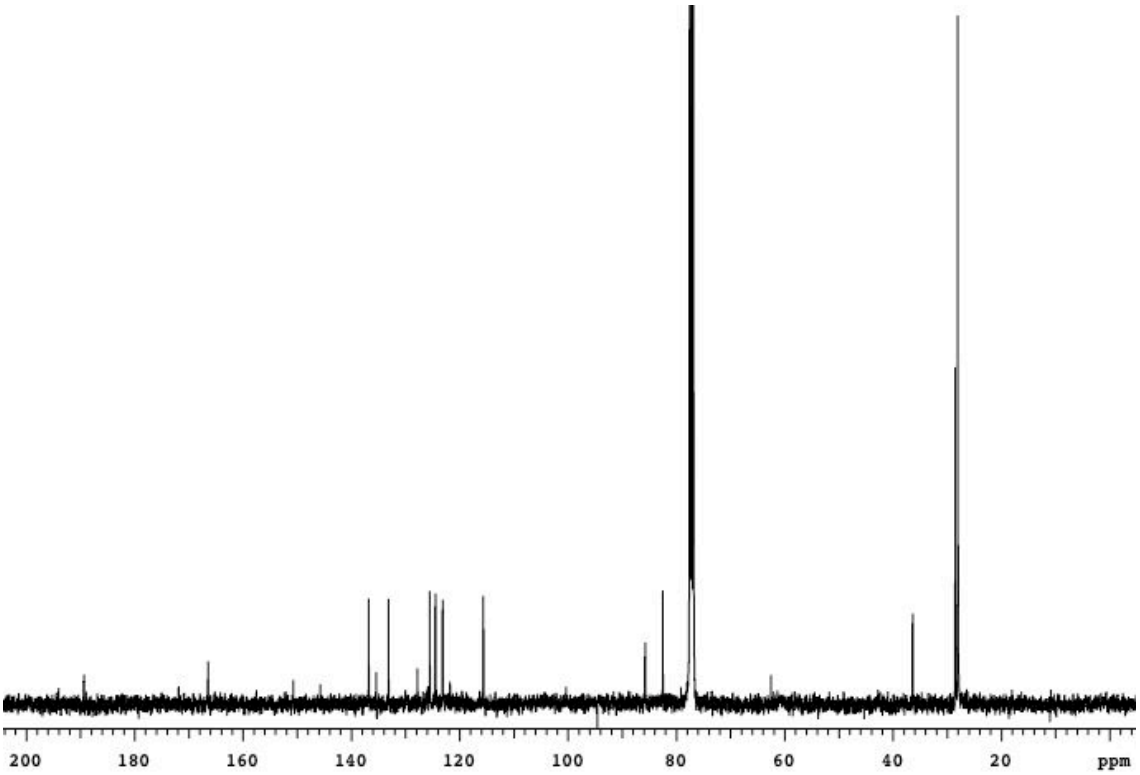

Figure A.2.18 ^{13}C spectrum (100 MHz, $CDCl_3$) of compound **57**

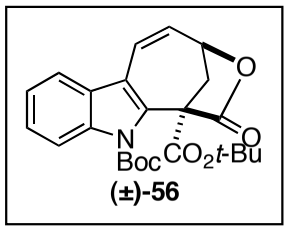

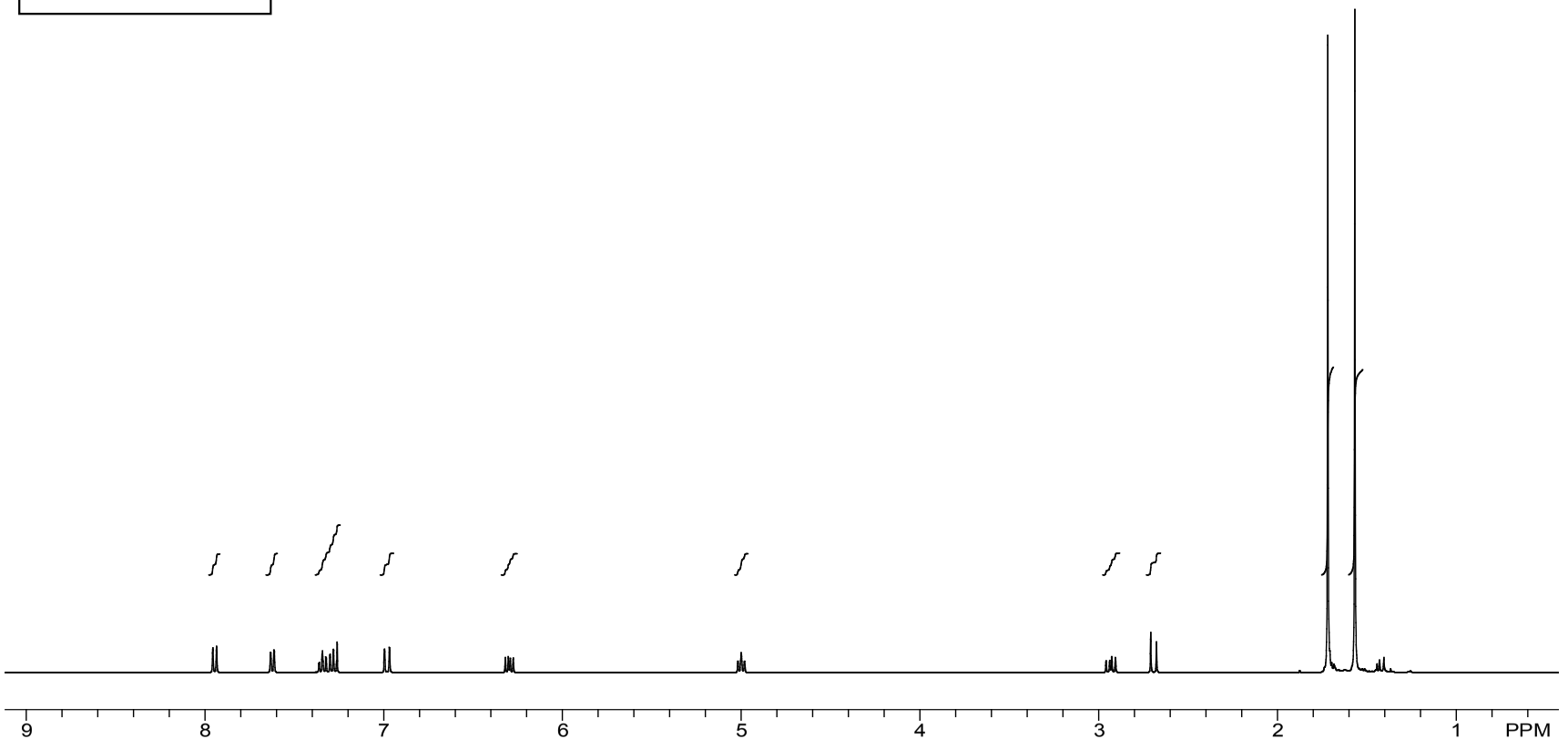

Figure A.2.19 ^{1}H NMR spectrum (400 MHz, $CDCl_3$) of compound **56**

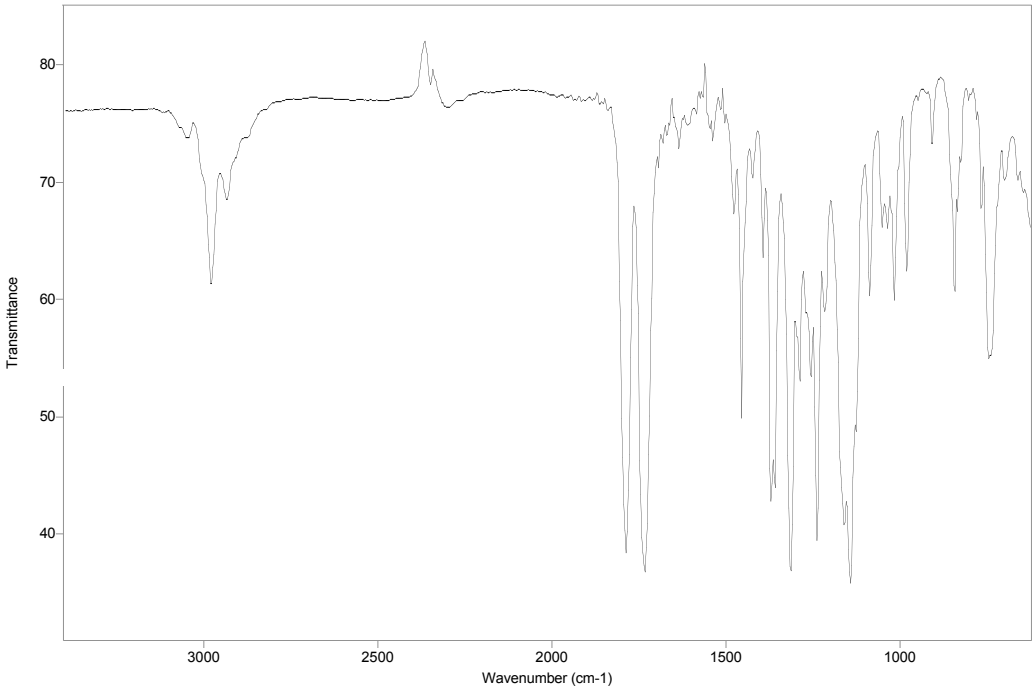

Figure A.2.20 FTIR spectrum (NaCl/thin film) of compound **56**

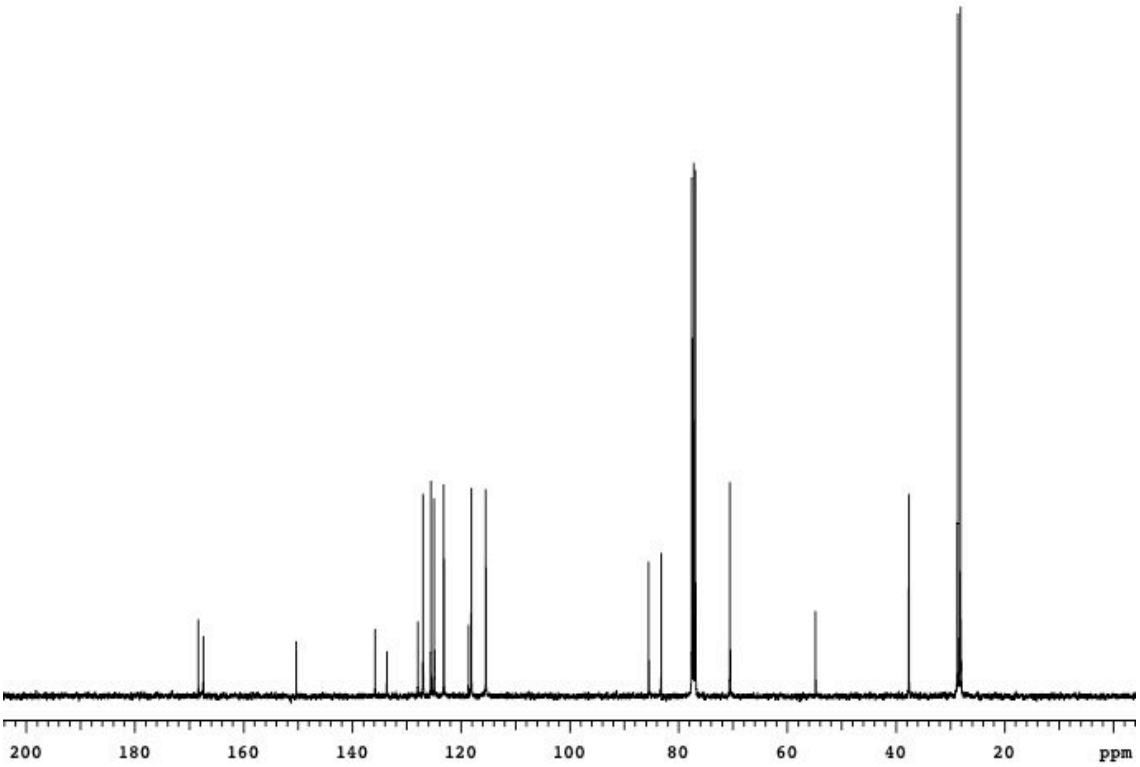

Figure A.2.21 ^{13}C spectrum (100 MHz, $CDCl_3$) of compound **56**

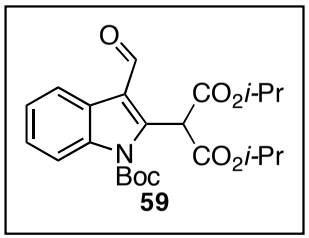

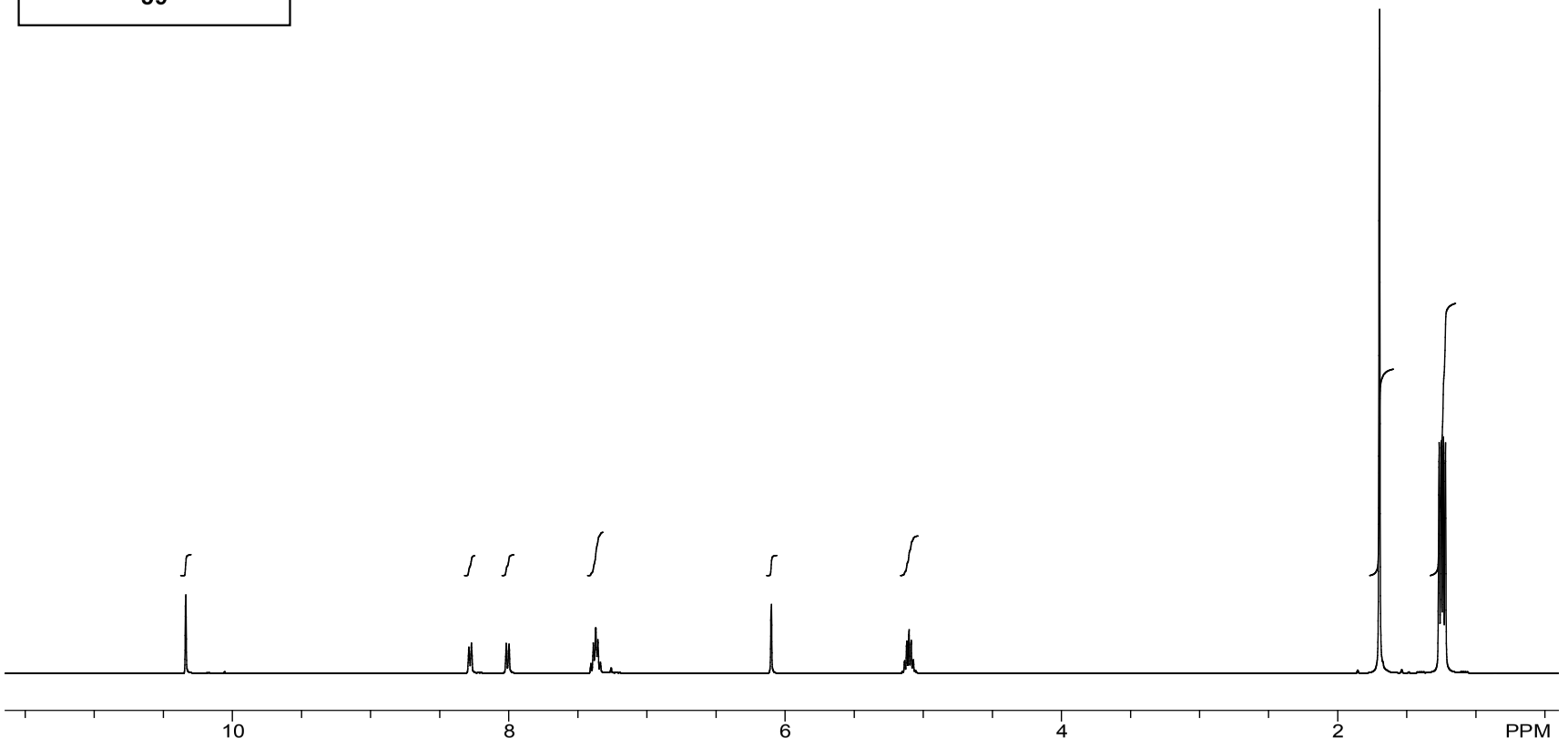

Figure A.2.22 ^{1}H NMR spectrum (400 MHz, $CDCl_3$) of compound **59**

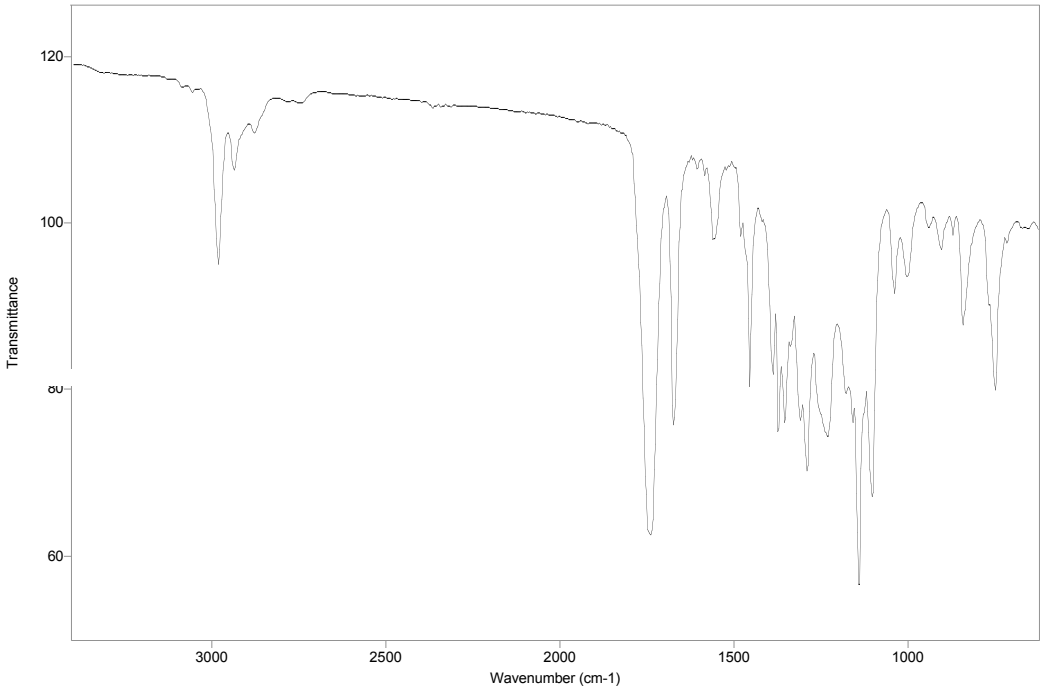

Figure A.2.23 FTIR spectrum (NaCl/thin film) of compound **59**

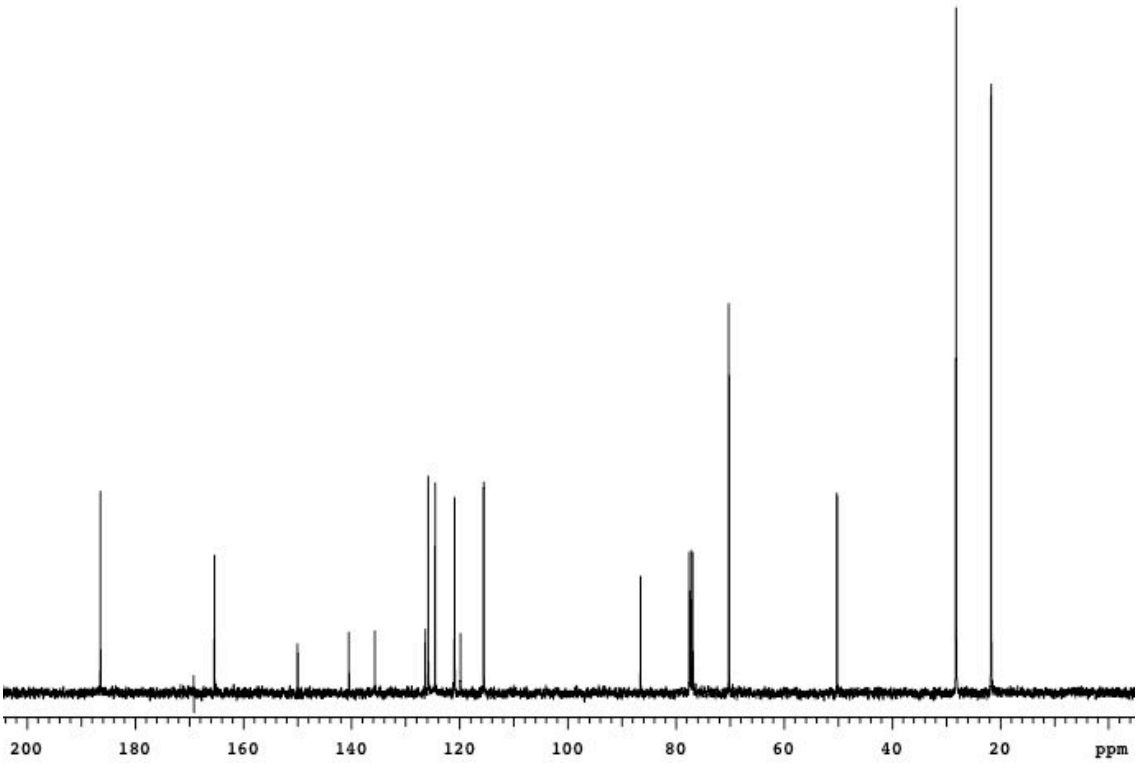

Figure A.2.24 ^{13}C spectrum (100 MHz, $CDCl_3$) of compound **59**

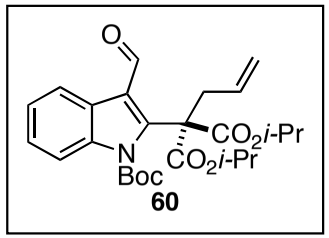

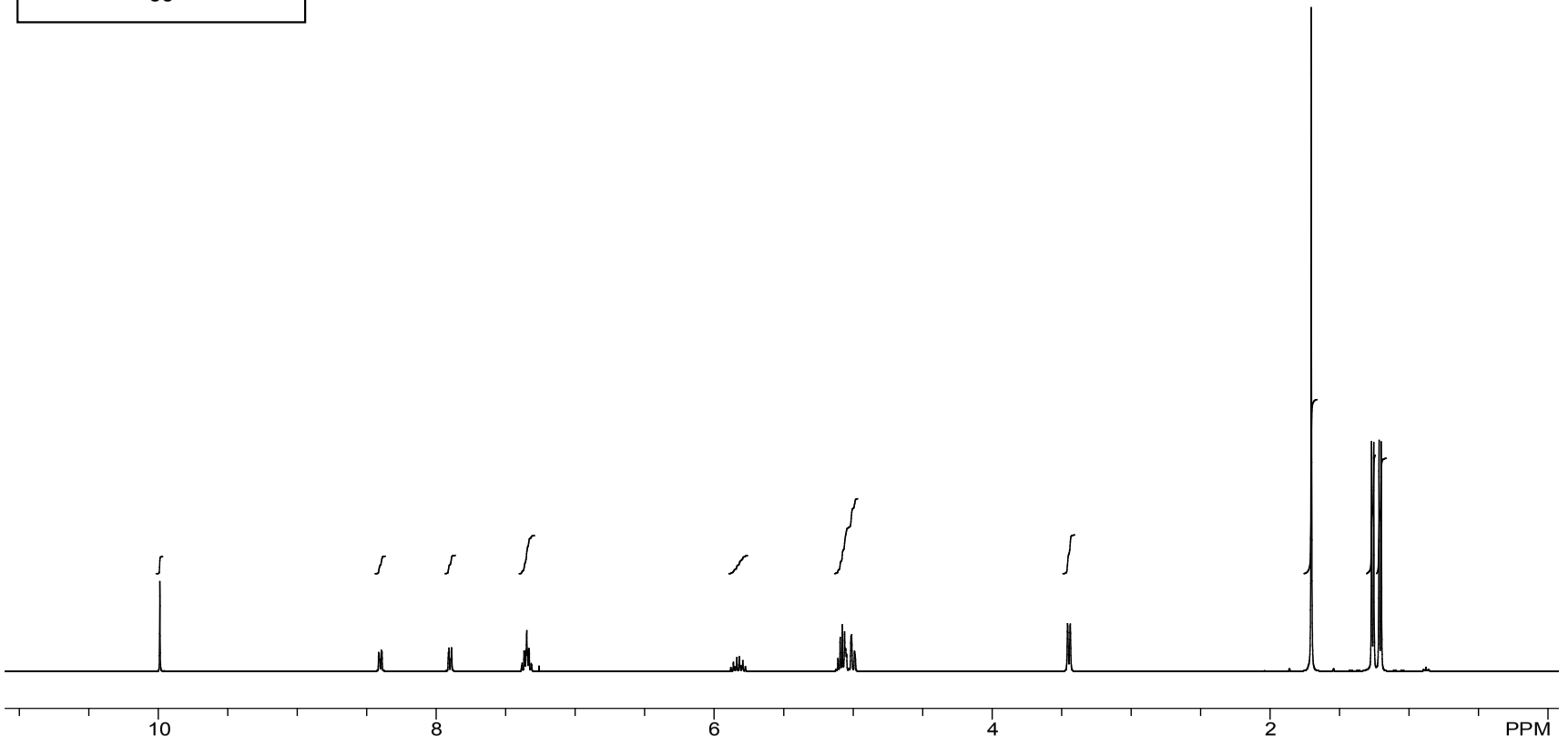

Figure A.2.25 ^{1}H NMR spectrum (400 MHz, $CDCl_3$) of compound **60**

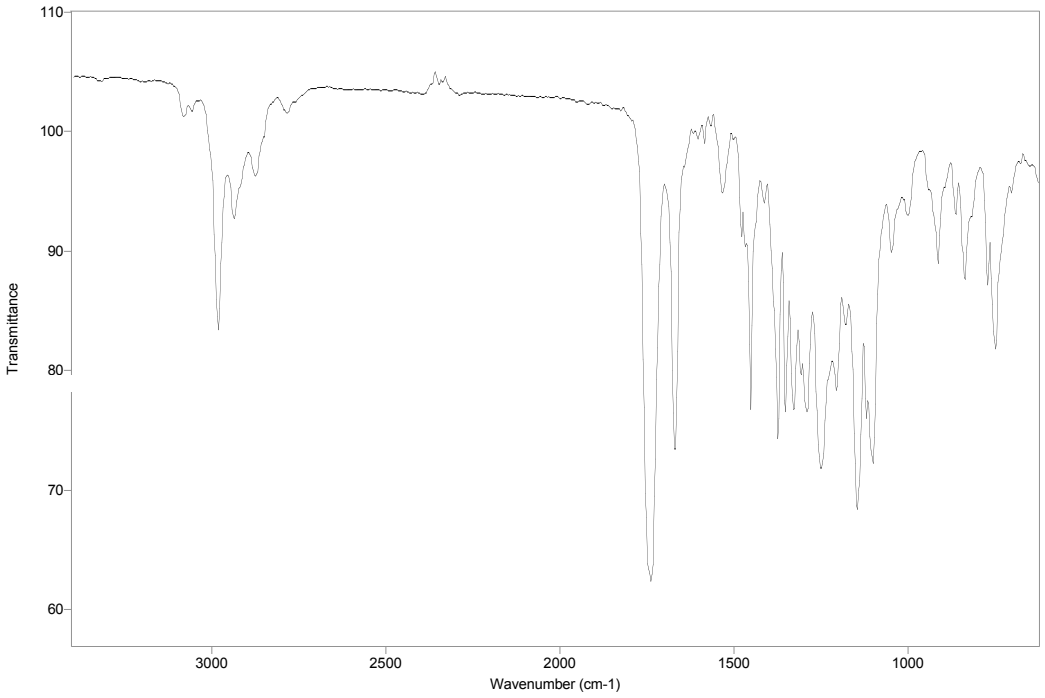

Figure A.2.26 FTIR spectrum (NaCl/thin film) of compound **60**

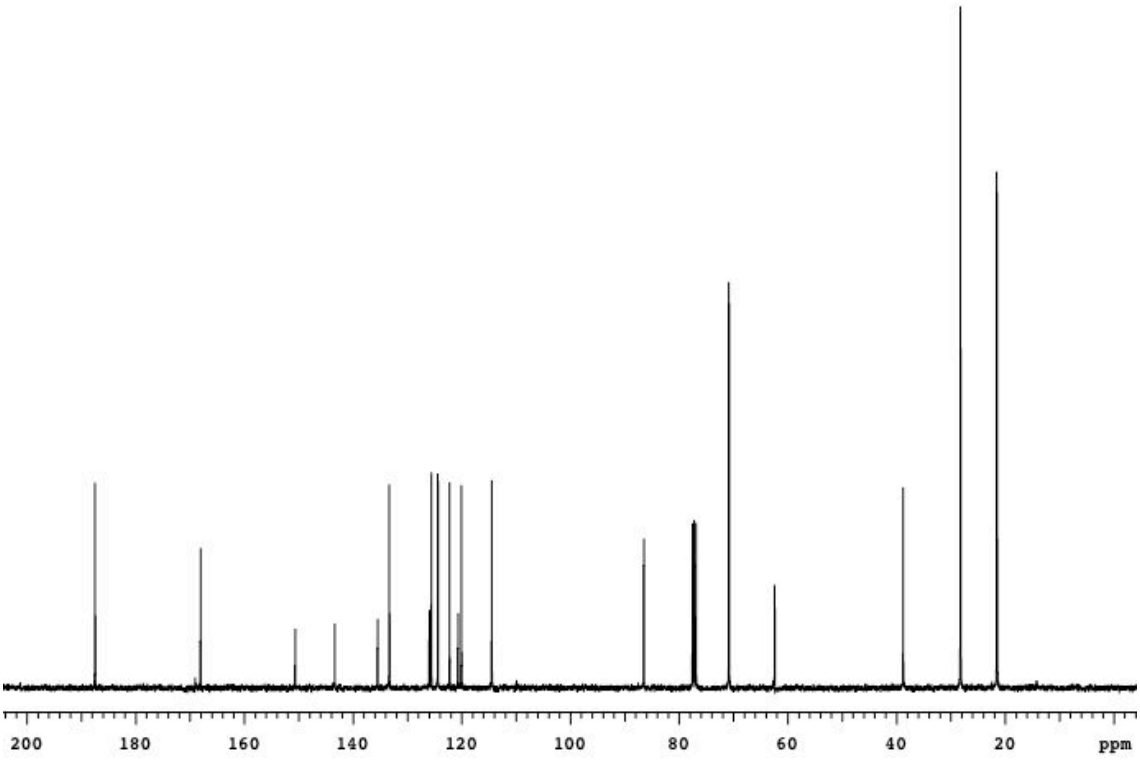

Figure A.2.27 ^{13}C spectrum (100 MHz, $CDCl_3$) of compound **60**

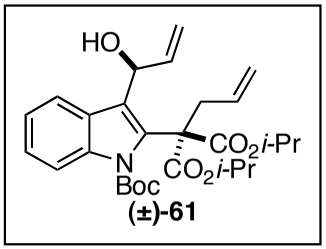

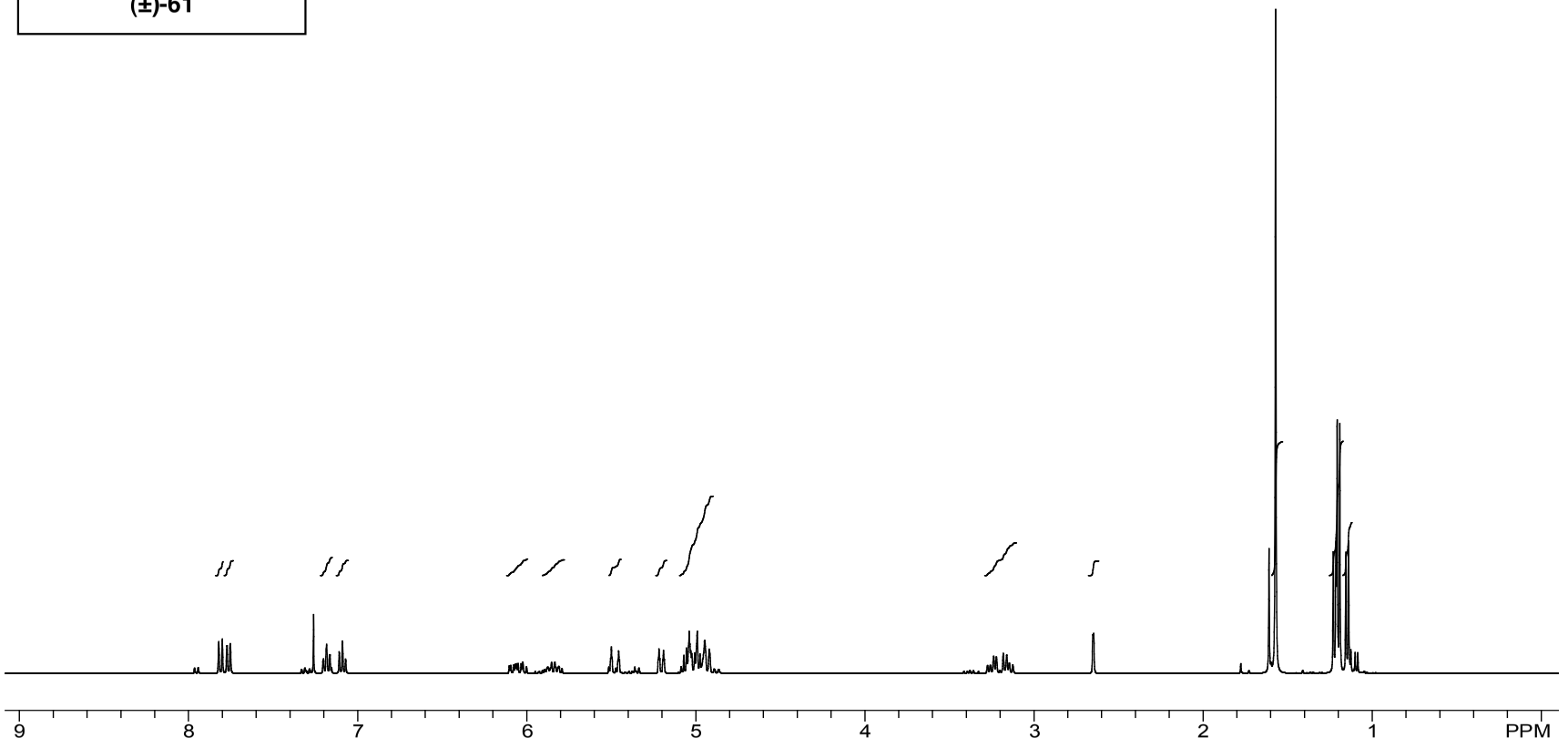

Figure A.2.28 ^{1}H NMR spectrum (400 MHz, $CDCl_3$) of compound **61**

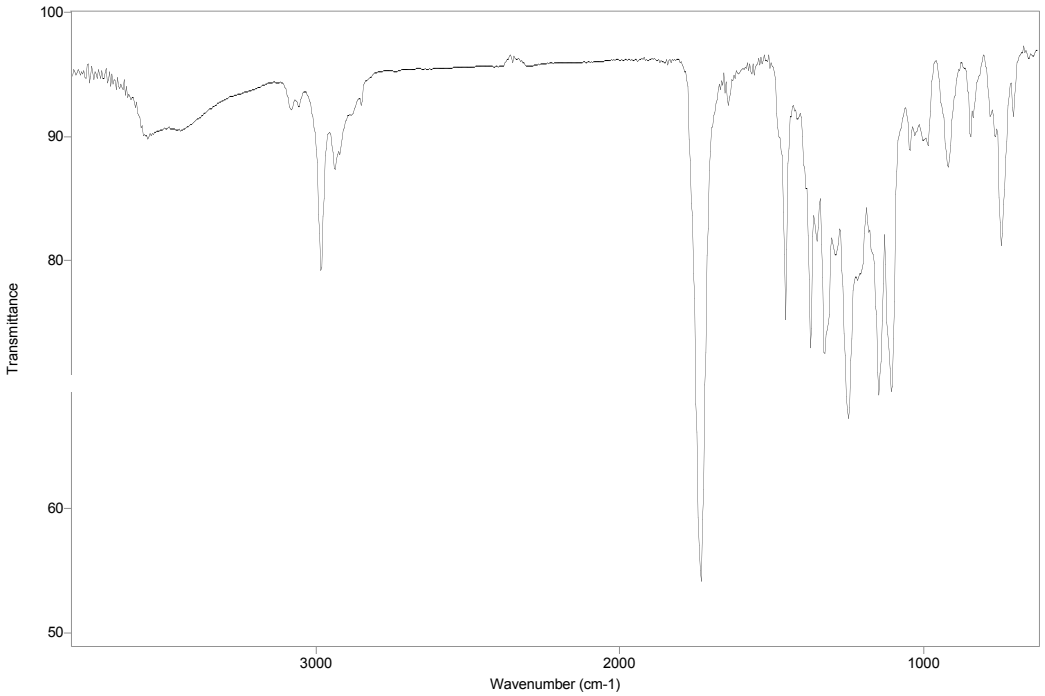

Figure A.2.29 FTIR spectrum (NaCl/thin film) of compound **61**

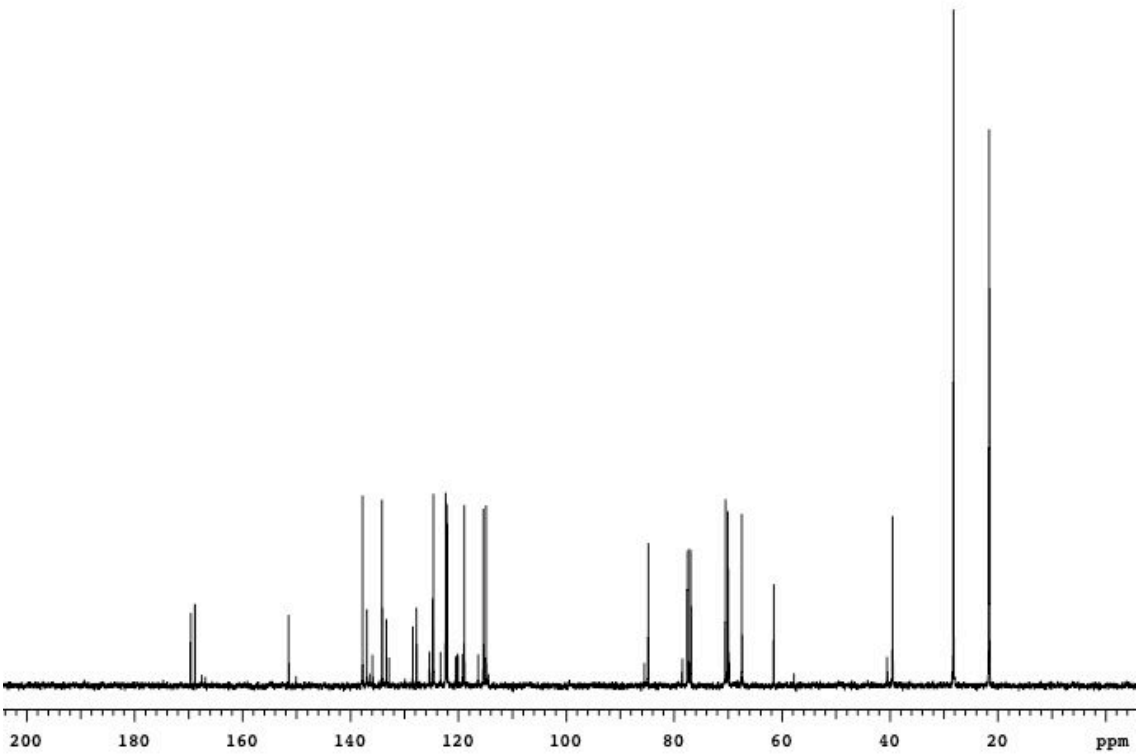

Figure A.2.30 ^{13}C spectrum (100 MHz, $CDCl_3$) of compound **61**

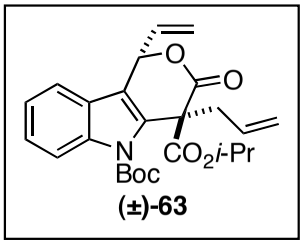

(±)-63

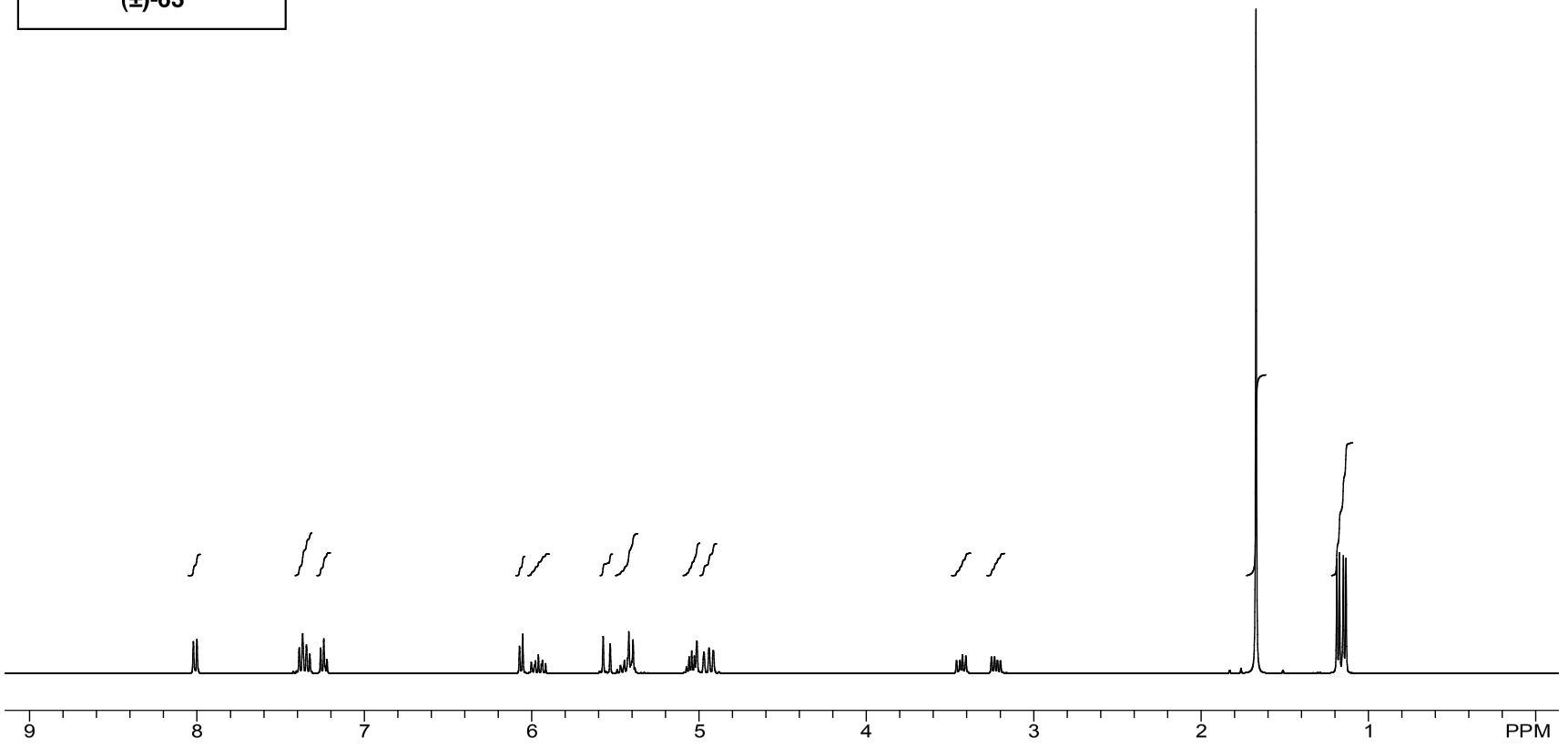

Figure A.2.31 ^{1}H NMR spectrum (400 MHz, $CDCl_3$) of compound **63**

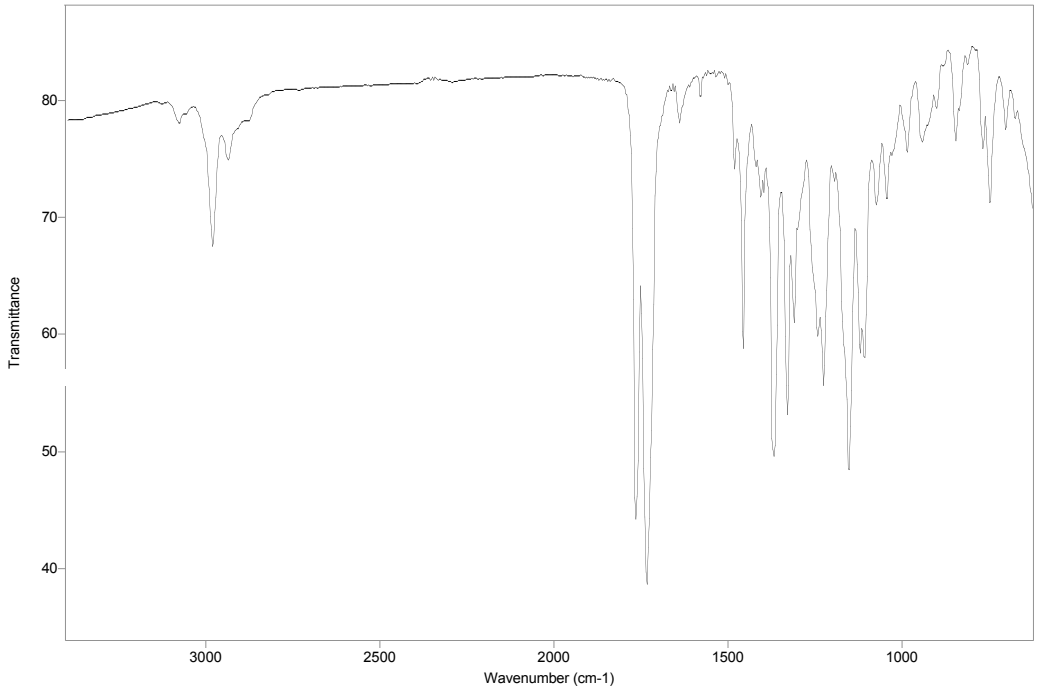

Figure A.2.32 FTIR spectrum (NaCl/thin film) of compound **63**

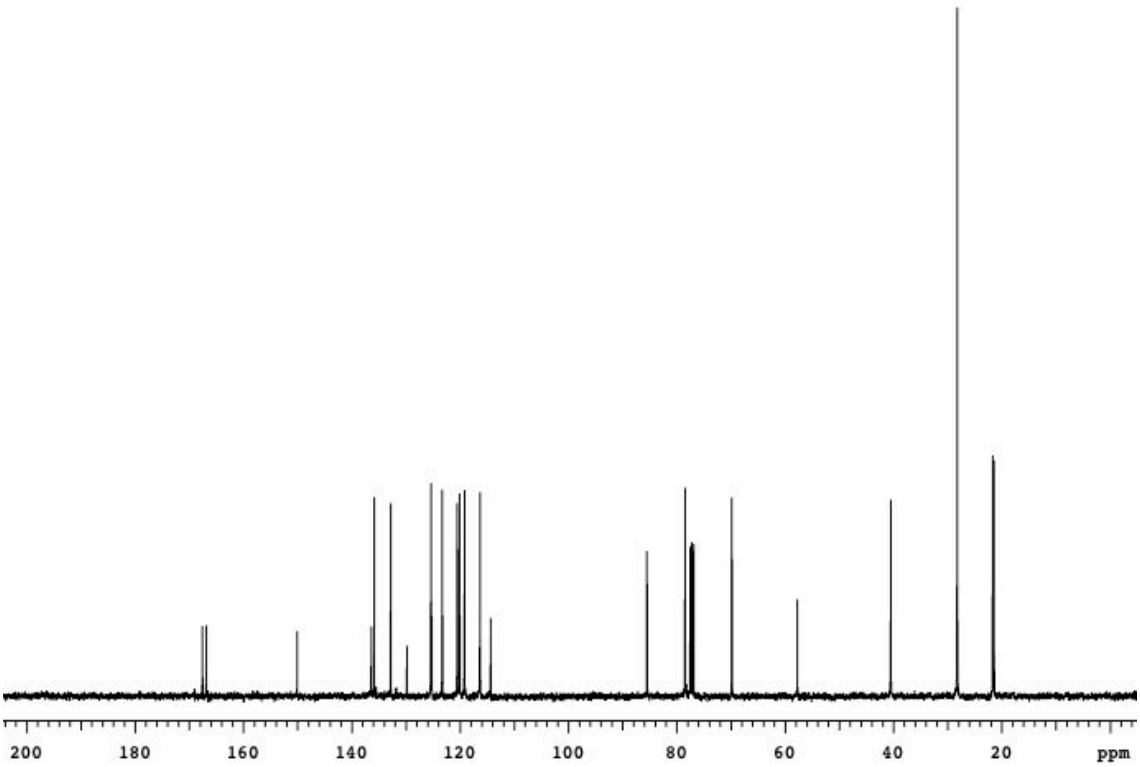

Figure A.2.33 ^{13}C spectrum (100 MHz, $CDCl_3$) of compound **63**

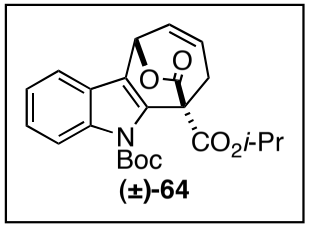

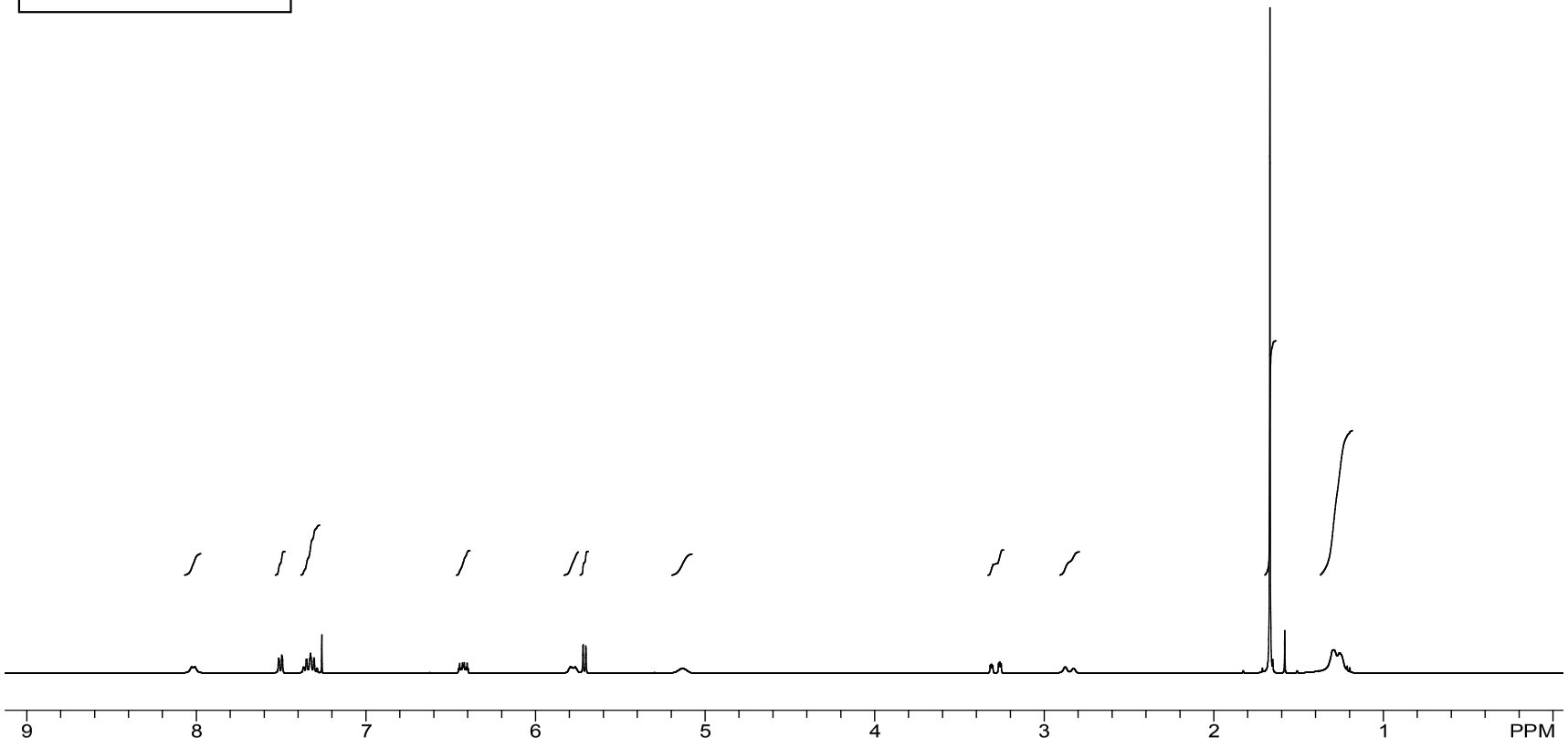

Figure A.2.34 ^{1}H NMR spectrum (400 MHz, $CDCl_3$) of compound **64**

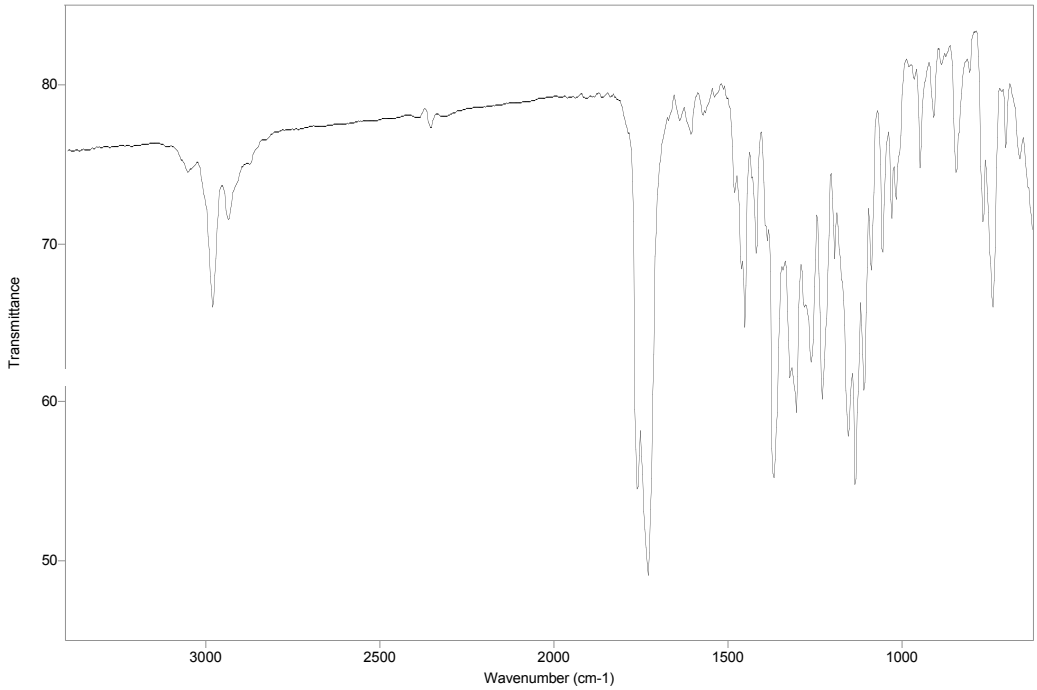

Figure A.2.35 FTIR spectrum (NaCl/thin film) of compound **64**

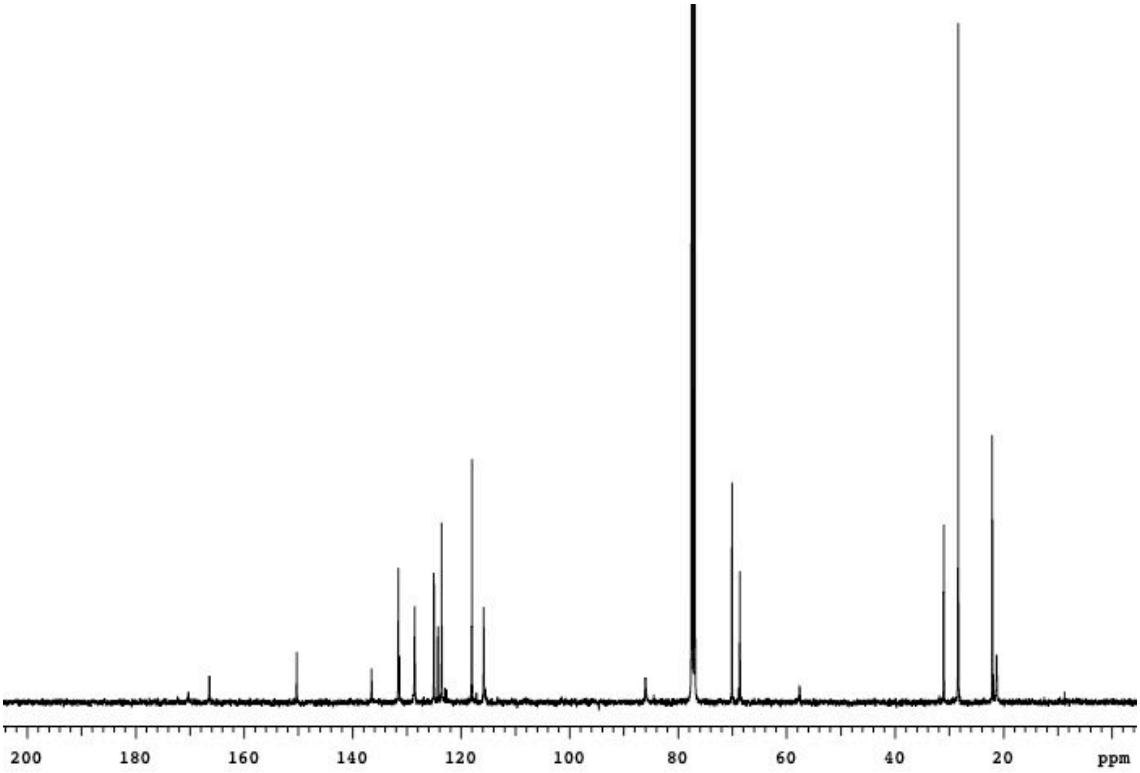

Figure A.2.36 ^{13}C spectrum (100 MHz, $CDCl_3$) of compound **64**

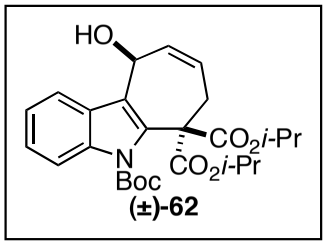

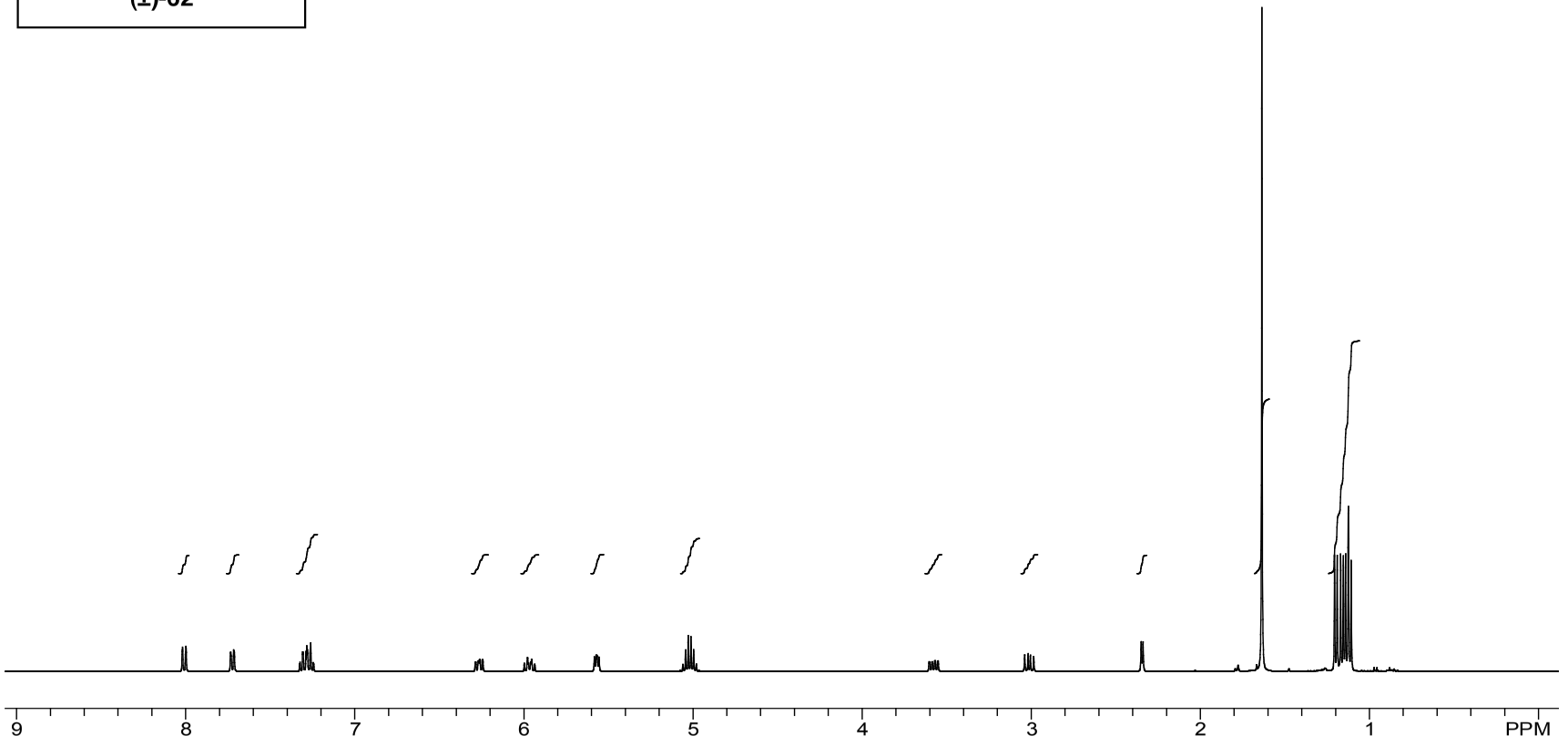

Figure A.2.37 ^{1}H NMR spectrum (400 MHz, $CDCl_3$) of compound **62**

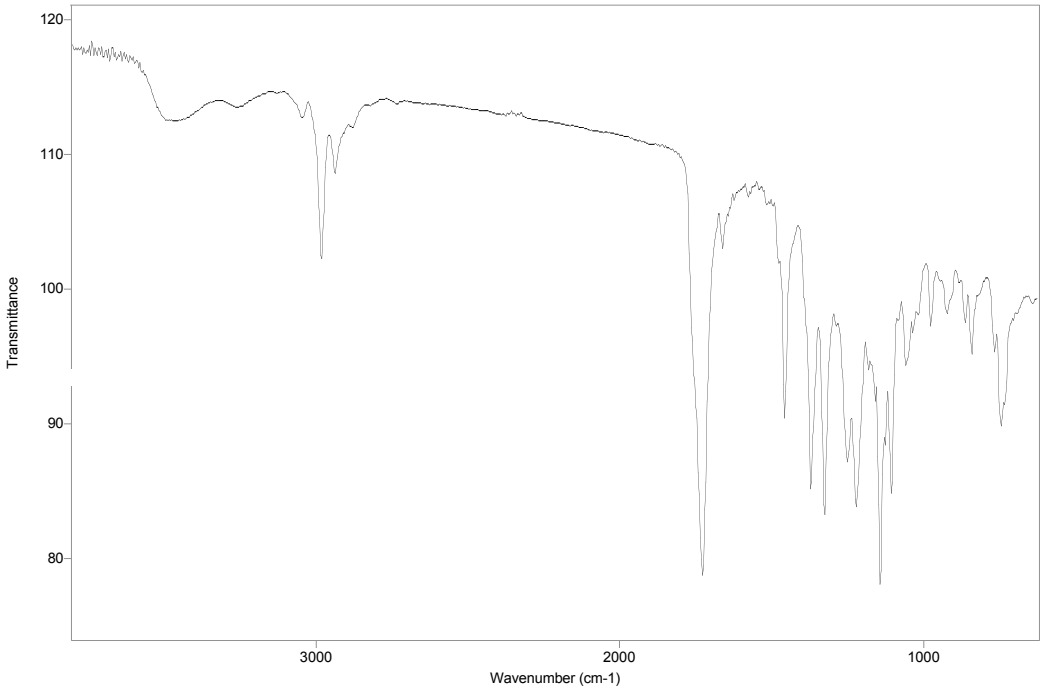

Figure A.2.38 FTIR spectrum (NaCl/thin film) of compound **62**

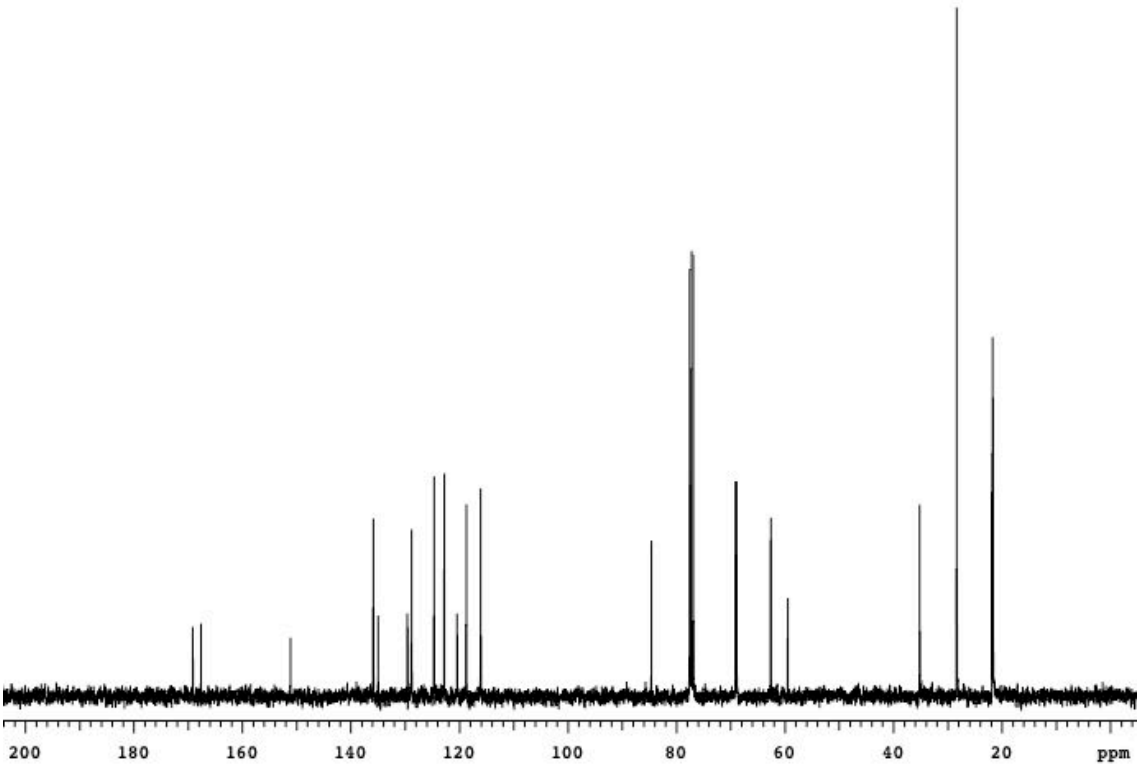

Figure A.2.39 ^{13}C spectrum (100 MHz, $CDCl_3$) of compound **62**

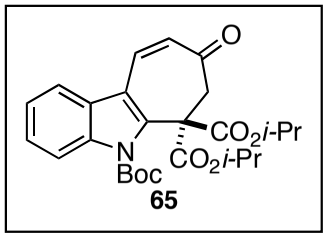

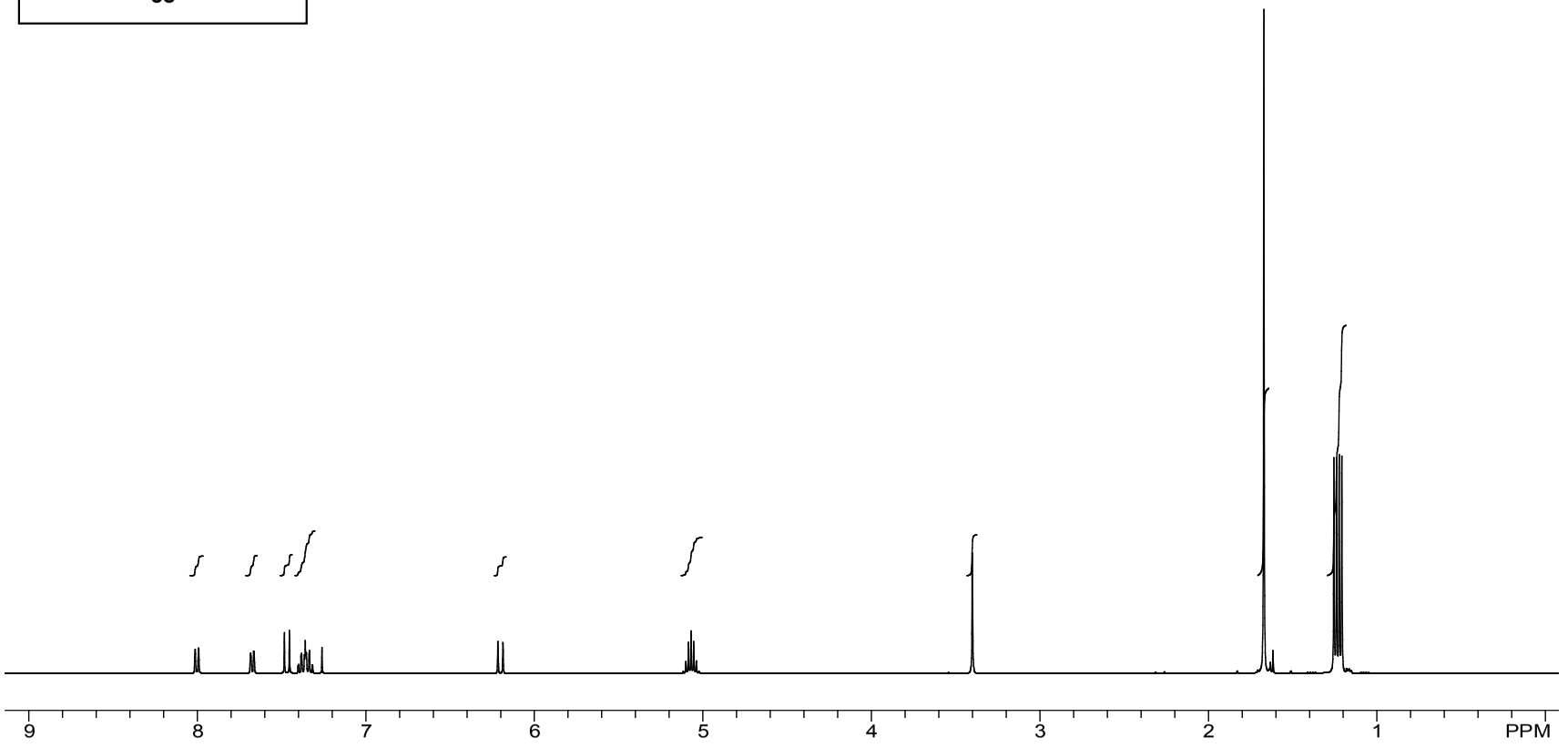

Figure A.2.40 ^{1}H NMR spectrum (400 MHz, $CDCl_3$) of compound **65**

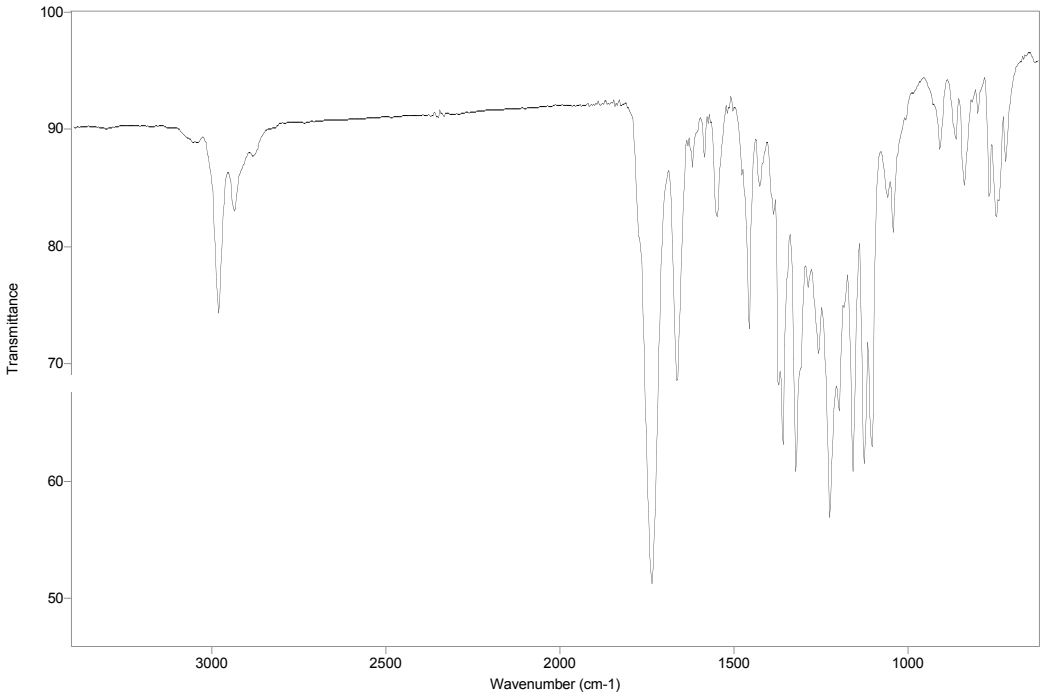

Figure A.2.41 FTIR spectrum (NaCl/thin film) of compound **65**

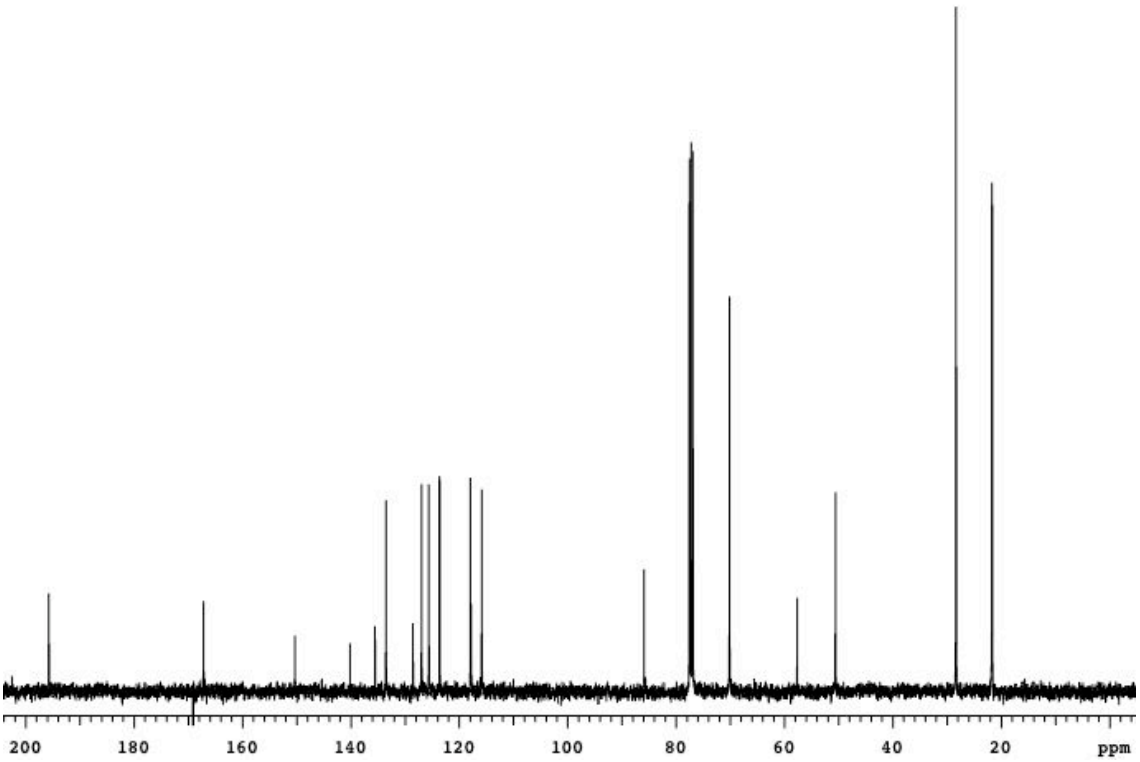

Figure A.2.42 ^{13}C spectrum (100 MHz, $CDCl_3$) of compound **65**

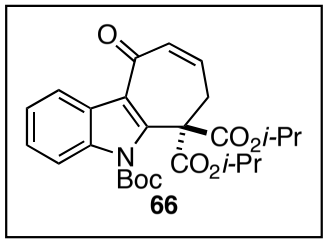

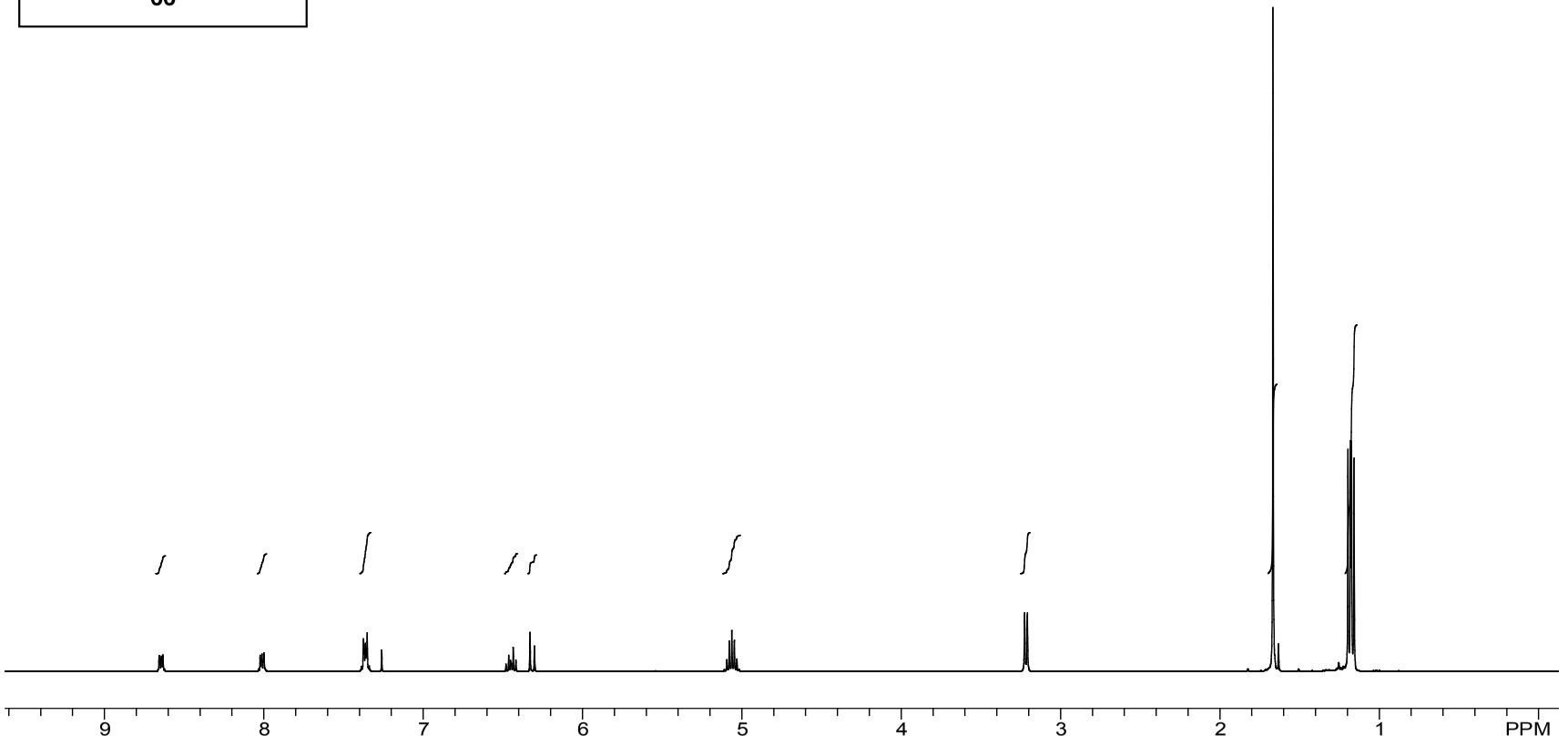

Figure A.2.43 ^{1}H NMR spectrum (400 MHz, $CDCl_3$) of compound **66**

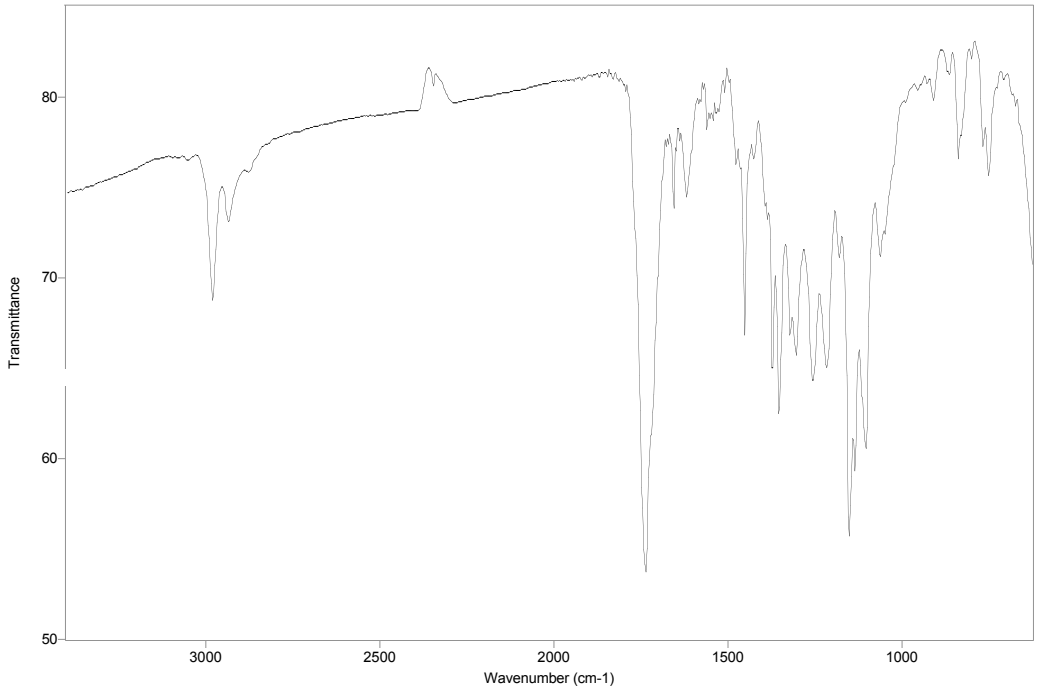

Figure A.2.44 FTIR spectrum (NaCl/thin film) of compound **66**

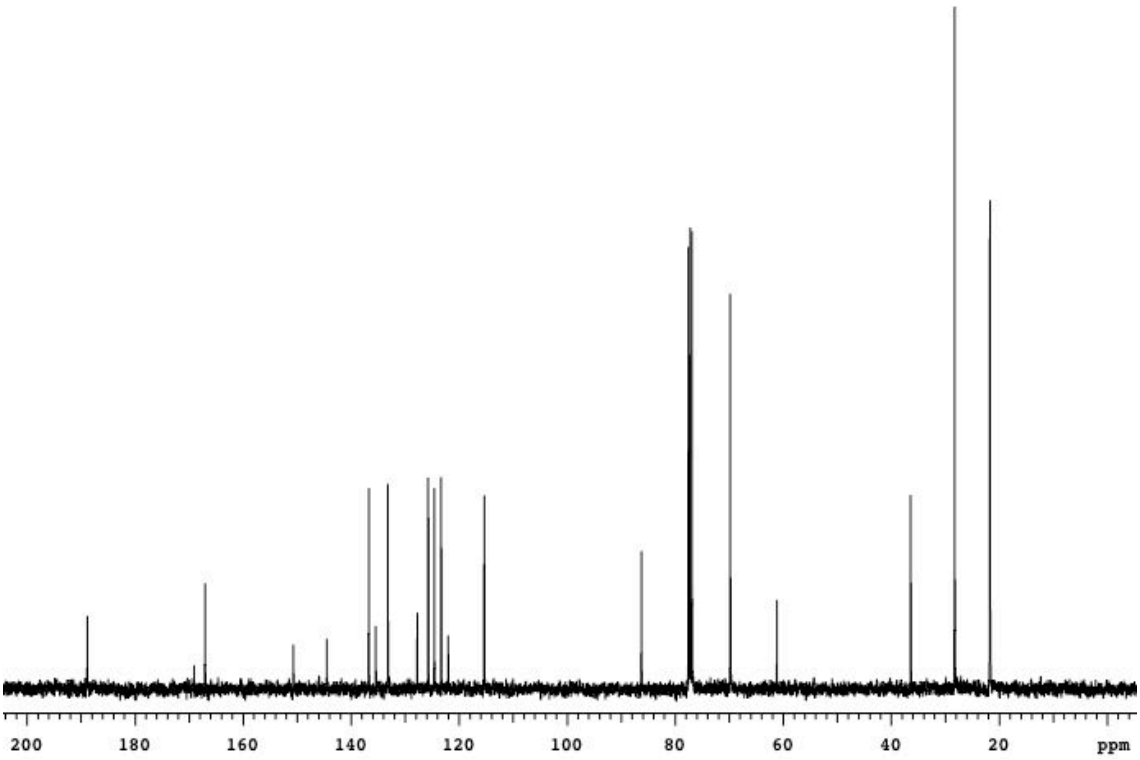

Figure A.2.45 ^{13}C spectrum (100 MHz, $CDCl_3$) of compound **66**

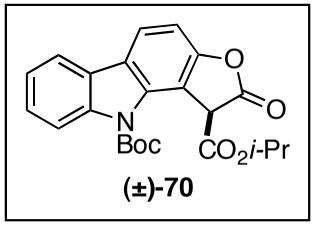

(±)-70

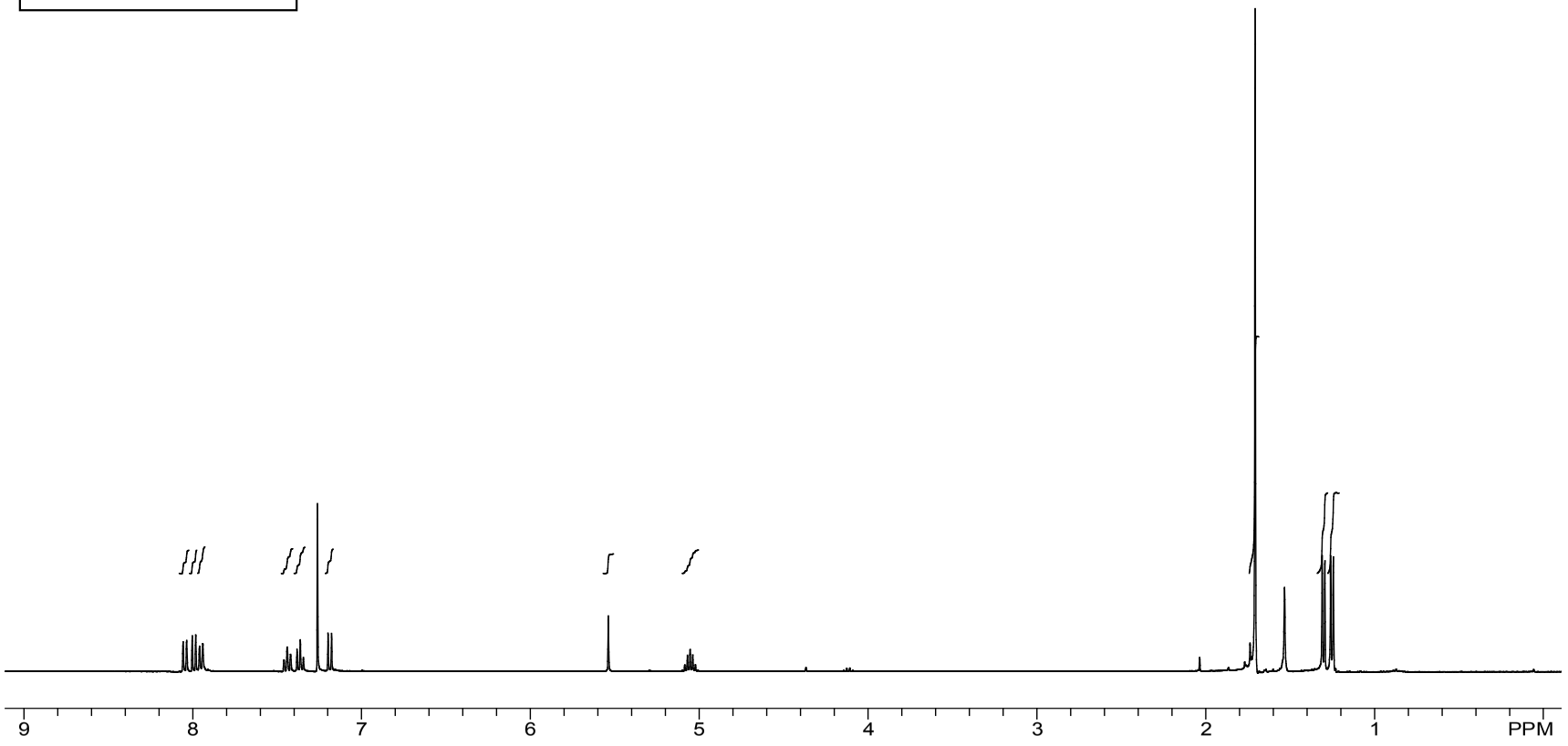

Figure A.2.46 ^{1}H NMR spectrum (400 MHz, $CDCl_3$) of compound **70**

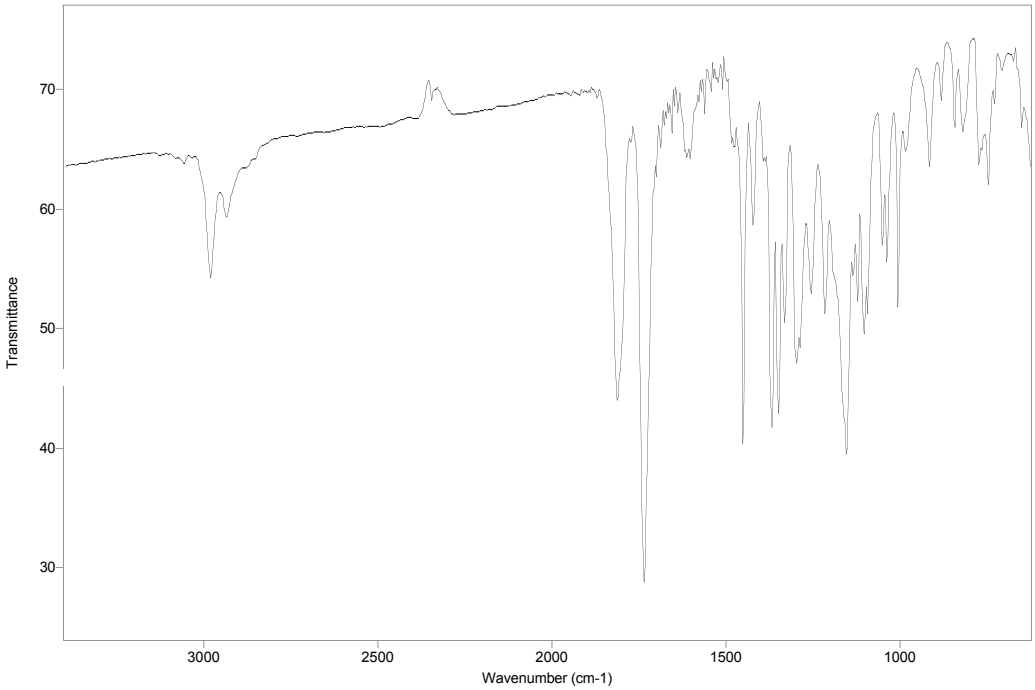

Figure A.2.47 FTIR spectrum (NaCl/thin film) of compound **70**

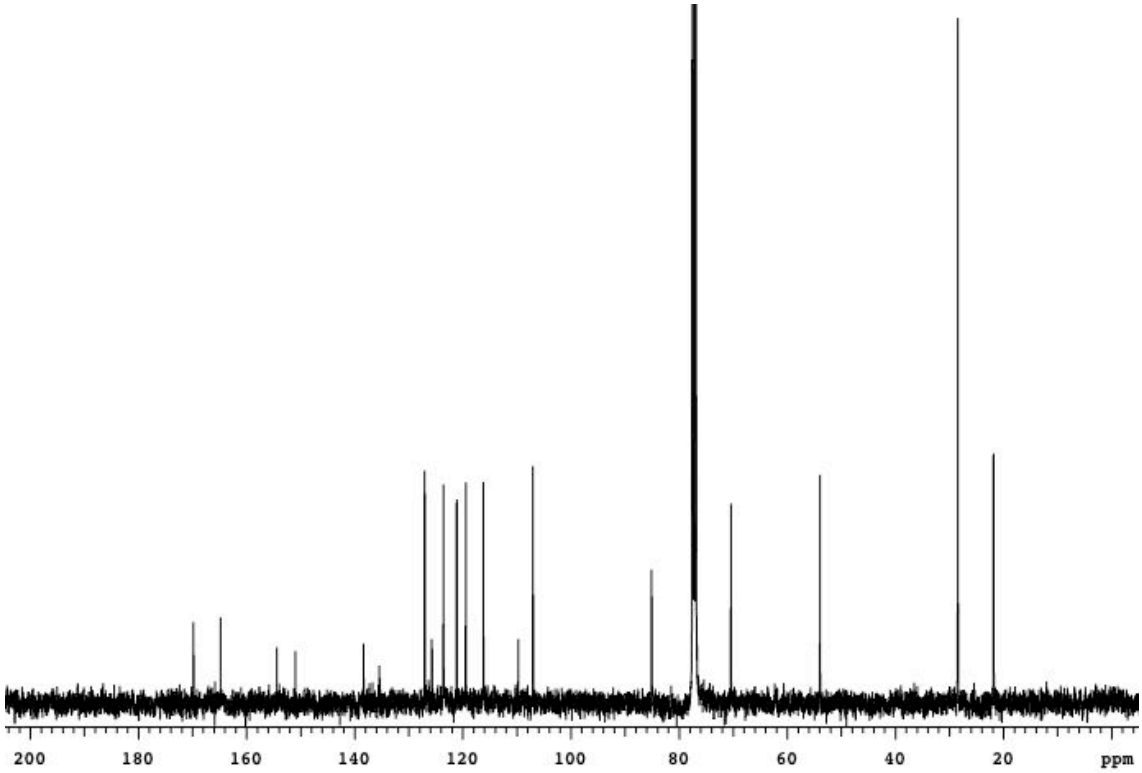

Figure A.2.48 ^{13}C spectrum (100 MHz, $CDCl_3$) of compound **70**

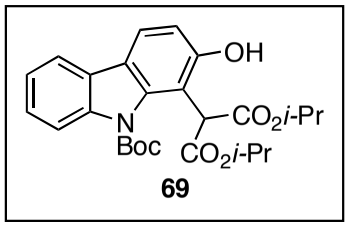

69

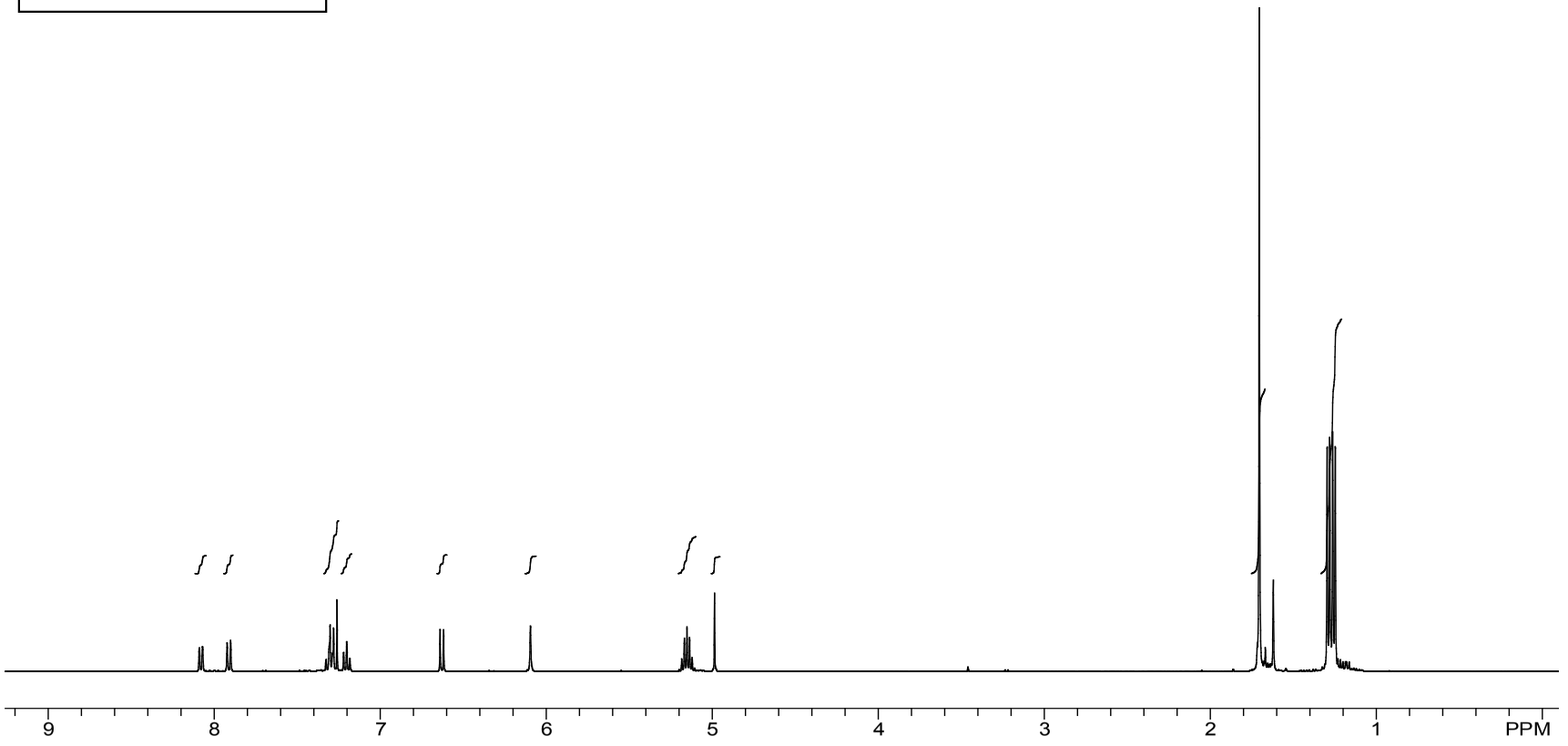

Figure A.2.49 ^{1}H NMR spectrum (400 MHz, $CDCl_3$) of compound **69**

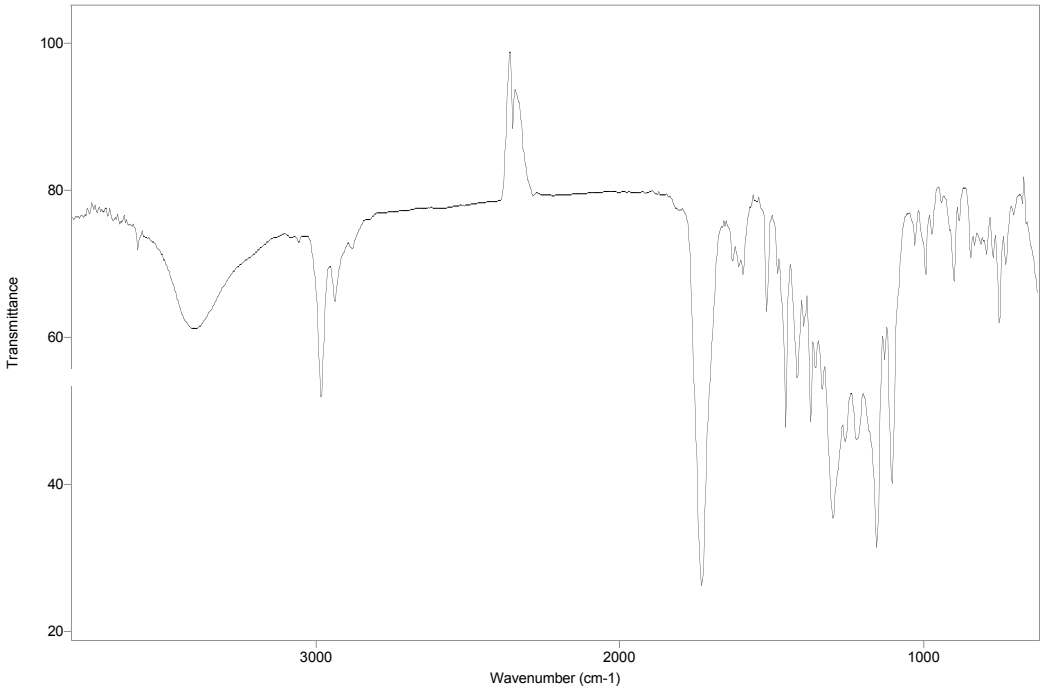

Figure A.2.50 FTIR spectrum (NaCl/thin film) of compound **69**

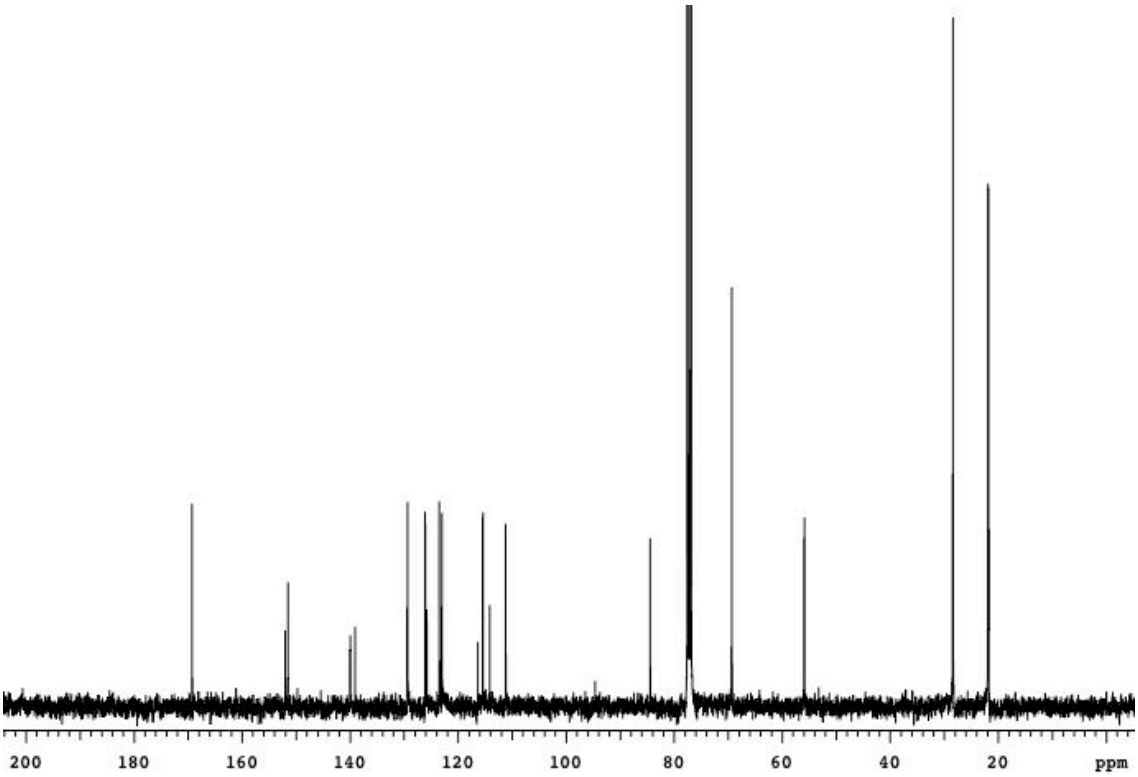

Figure A.2.51 ^{13}C spectrum (100 MHz, $CDCl_3$) of compound **69**

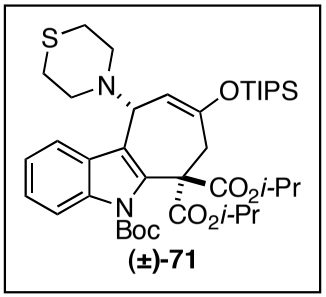

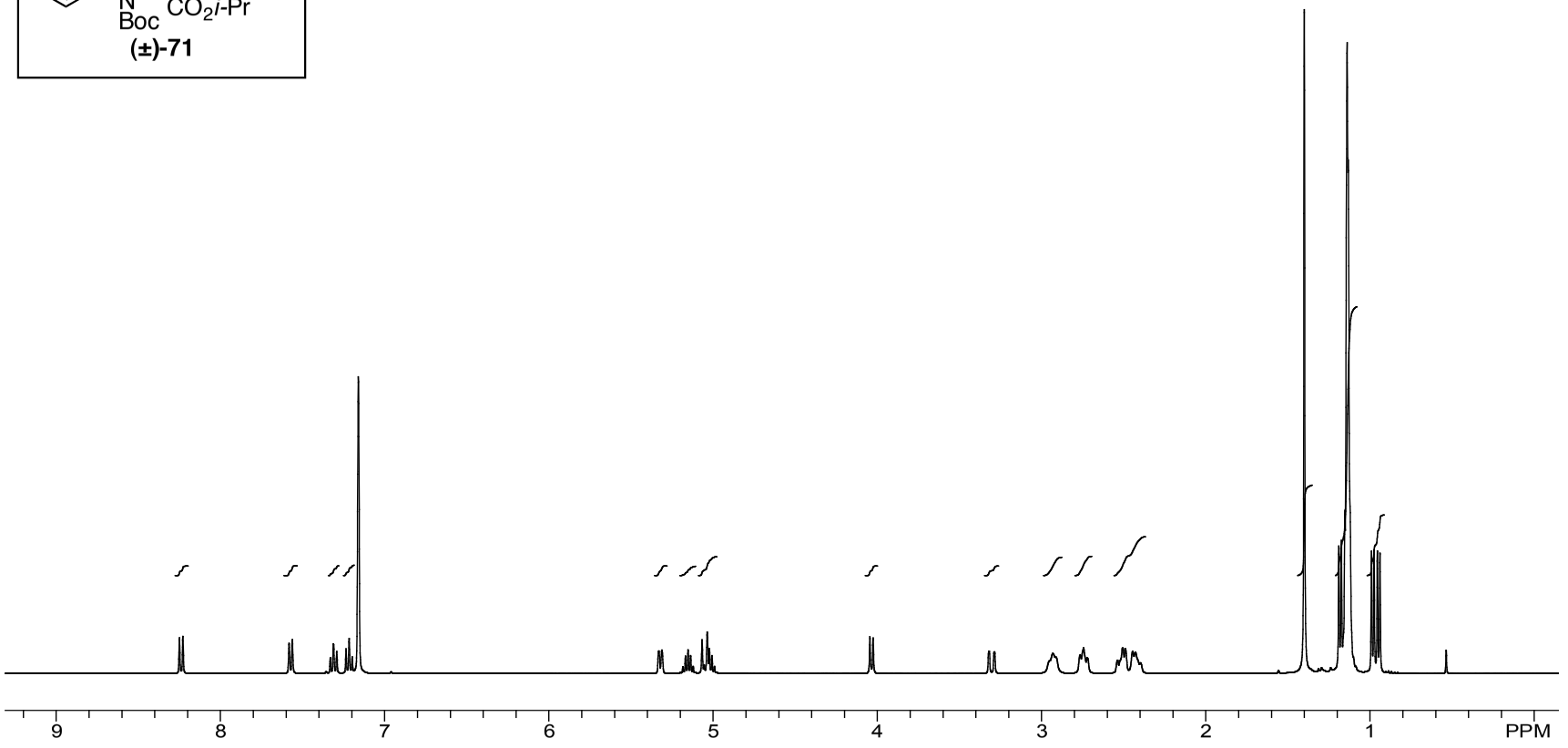

Figure A.2.52 ^{1}H NMR spectrum (400 MHz, Benzene-d_6) of compound **71**

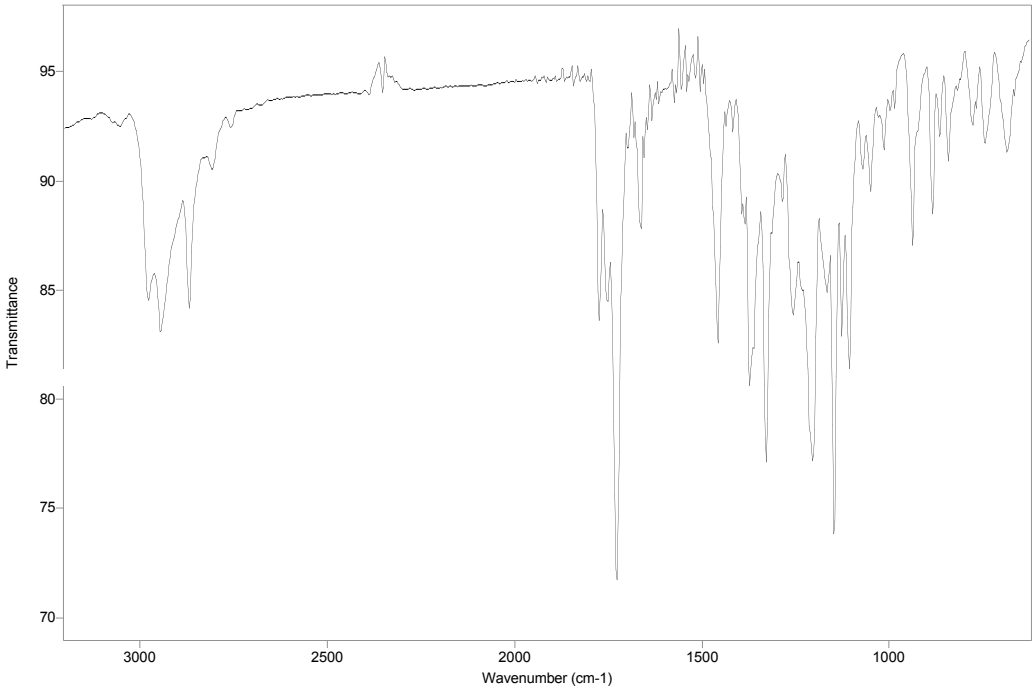

Figure A.2.53 FTIR spectrum (NaCl/thin film) of compound **71**

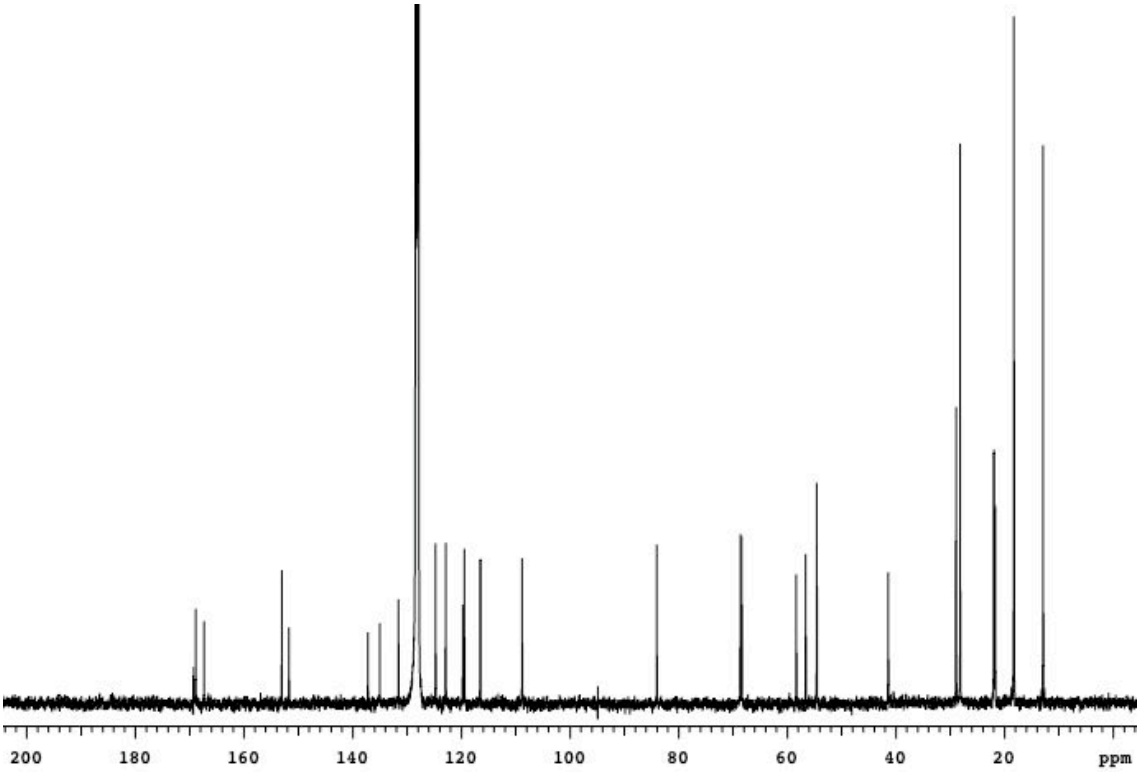

Figure A.2.54 ^{13}C spectrum (100 MHz, Benzene-d_6) of compound **71**

Appendix 3: X-Ray Crystallography Report Relevant to Chapter Three

A.3.1 X-Ray Crystallography Report for Silyl enol ether 71

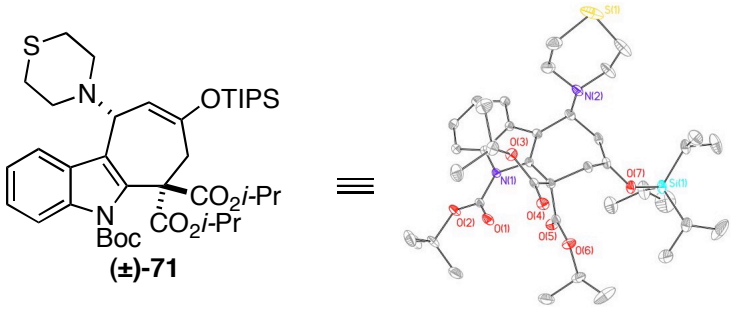

Table A.3.1.1 Crystal data and structure refinement for **71**

Identification code	wood10	
Empirical formula	C39 H60 N2 O7 S Si	
Formula weight	729.04	
Temperature	120(2) K	
Wavelength	0.71073 Å	
Crystal system	Triclinic	
Space group	P-1	
Unit cell dimensions	a = 9.7402(6) Å	a= 81.295(3)°.
	b = 14.6404(9) Å	b= 85.494(2)°.
	c = 14.7683(9) Å	g = 74.288(2)°.
Volume	2002.4(2) Å^3	
Z	2	
Density (calculated)	1.209 Mg/m^3	
Absorption coefficient	0.159 mm^{-1}	
F(000)	788	
Crystal size	0.30 x 0.25 x 0.16 mm^3	
Theta range for data collection	1.88 to 24.71°.	
Index ranges	-11<=h<=11, -17<=k<=17, -17<=l<=17	
Reflections collected	29158	
Independent reflections	6775 [R(int) = 0.0246]	
Completeness to theta = 24.71°	99.1 %	
Absorption correction	Semi-empirical from equivalents	
Max. and min. transmission	0.9751 and 0.9542	
Refinement method	Full-matrix least-squares on F^2	
Data / restraints / parameters	6775 / 0 / 451	

Goodness-of-fit on F^2	1.027
Final R indices [I>2sigma(I)]	R1 = 0.0636, wR2 = 0.1669
R indices (all data)	R1 = 0.0737, wR2 = 0.1758
Largest diff. peak and hole	2.626 and -0.847 e.$Å^{-3}$

Comment: The large diff. peak is due to a partially disordered C39. The disorder was not modeled.

Table A.3.1.2 Atomic coordinates (x 10^4) and equivalent isotropic displacement parameters ($Å^2$x 10^3) for **71**. U(eq) is defined as one third of the trace of the orthogonalized U^{ij} tensor.

	x	y	z	U(eq)
C(1)	-1090(3)	4657(2)	2003(2)	17(1)
C(2)	-2139(3)	6017(2)	862(2)	27(1)
C(3)	-2847(4)	5438(3)	379(2)	39(1)
C(4)	-1403(4)	6616(3)	162(3)	50(1)
C(5)	-3149(4)	6597(2)	1513(2)	43(1)
C(6)	1496(3)	4418(2)	2324(2)	17(1)
C(7)	1839(3)	5252(2)	1912(2)	21(1)
C(8)	3230(3)	5305(2)	1979(2)	23(1)
C(9)	4246(3)	4560(2)	2450(2)	25(1)
C(10)	3897(3)	3739(2)	2868(2)	23(1)
C(11)	2499(3)	3664(2)	2807(2)	18(1)
C(12)	1816(3)	2915(2)	3156(2)	19(1)
C(13)	438(3)	3212(2)	2901(2)	16(1)
C(14)	2640(3)	1942(2)	3615(2)	22(1)
C(15)	2383(3)	1151(2)	3161(2)	24(1)
C(16)	1070(3)	1045(2)	3133(2)	22(1)
C(17)	-195(3)	1671(2)	3592(2)	20(1)
C(18)	-737(3)	2700(2)	3062(2)	17(1)
C(19)	-1216(3)	2576(2)	2127(2)	20(1)
C(20)	-2885(3)	2072(2)	1361(2)	32(1)
C(21)	-3524(4)	2977(3)	726(3)	49(1)
C(22)	-3929(5)	1481(4)	1697(3)	61(1)
C(23)	-1957(3)	3201(2)	3696(2)	18(1)
C(24)	-2519(3)	4256(2)	4841(2)	25(1)
C(25)	-1653(4)	4406(3)	5571(2)	38(1)
C(26)	-3408(4)	5184(2)	4342(2)	38(1)
C(27)	2484(4)	2576(2)	5070(2)	35(1)
C(28)	2021(4)	2451(3)	6077(2)	42(1)
C(29)	3338(4)	876(3)	5005(2)	42(1)
C(30)	2952(4)	568(3)	6000(3)	51(1)
C(31)	350(3)	-1175(2)	2055(2)	33(1)

C(32)	-597(5)	-546(3)	1330(3)	62(1)
C(33)	825(5)	-2200(3)	1869(5)	92(2)
C(34)	2839(3)	-1339(2)	3347(2)	32(1)
C(35)	1916(4)	-1404(3)	4227(2)	41(1)
C(36)	3749(5)	-2337(3)	3199(3)	55(1)
C(37)	2976(4)	-320(3)	1349(3)	47(1)
C(38)	2383(4)	691(3)	836(3)	48(1)
C(39)	3515(7)	-1069(5)	785(4)	97(2)
N(1)	206(2)	4141(2)	2389(2)	16(1)
N(2)	2355(2)	1783(2)	4629(2)	25(1)
O(1)	-2202(2)	4455(1)	2222(1)	25(1)
O(2)	-905(2)	5371(1)	1380(1)	26(1)
O(3)	-1493(2)	3758(1)	4175(1)	22(1)
O(4)	-3114(2)	3048(1)	3812(1)	23(1)
O(5)	-491(2)	2635(2)	1437(1)	27(1)
O(6)	-2434(2)	2312(2)	2195(1)	27(1)
O(7)	720(2)	380(1)	2705(1)	25(1)
S(1)	3113(1)	1399(1)	6734(1)	56(1)
Si(1)	1763(1)	-626(1)	2351(1)	26(1)

Table A.3.1.3 Bond lengths [Å] and angles [°] for **71**

C(1)-O(1)	1.206(3)
C(1)-O(2)	1.326(3)
C(1)-N(1)	1.398(3)
C(2)-O(2)	1.495(3)
C(2)-C(5)	1.503(5)
C(2)-C(3)	1.510(5)
C(2)-C(4)	1.517(5)
C(6)-C(7)	1.392(4)
C(6)-C(11)	1.403(4)
C(6)-N(1)	1.413(3)
C(7)-C(8)	1.390(4)
C(8)-C(9)	1.396(4)
C(9)-C(10)	1.380(4)
C(10)-C(11)	1.407(4)
C(11)-C(12)	1.442(4)
C(12)-C(13)	1.358(4)
C(12)-C(14)	1.519(4)
C(13)-N(1)	1.422(3)
C(13)-C(18)	1.516(4)
C(14)-N(2)	1.497(4)
C(14)-C(15)	1.508(4)
C(15)-C(16)	1.334(4)
C(16)-O(7)	1.365(3)
C(16)-C(17)	1.504(4)
C(17)-C(18)	1.562(4)
C(18)-C(19)	1.542(4)
C(18)-C(23)	1.546(4)
C(19)-O(5)	1.199(3)
C(19)-O(6)	1.337(3)
C(20)-O(6)	1.462(4)
C(20)-C(21)	1.514(5)
C(20)-C(22)	1.515(5)
C(23)-O(4)	1.201(3)
C(23)-O(3)	1.339(3)

C(24)-O(3)	1.472(3)
C(24)-C(25)	1.495(4)
C(24)-C(26)	1.516(4)
C(27)-N(2)	1.451(4)
C(27)-C(28)	1.518(5)
C(28)-S(1)	1.808(4)
C(29)-N(2)	1.470(4)
C(29)-C(30)	1.518(5)
C(30)-S(1)	1.791(5)
C(31)-C(32)	1.497(5)
C(31)-C(33)	1.507(5)
C(31)-Si(1)	1.879(3)
C(34)-C(36)	1.527(4)
C(34)-C(35)	1.527(5)
C(34)-Si(1)	1.881(3)
C(37)-C(39)	1.437(7)
C(37)-C(38)	1.538(5)
C(37)-Si(1)	1.897(3)
O(7)-Si(1)	1.678(2)

O(1)-C(1)-O(2)	126.4(2)
O(1)-C(1)-N(1)	123.0(2)
O(2)-C(1)-N(1)	110.6(2)
O(2)-C(2)-C(5)	109.0(2)
O(2)-C(2)-C(3)	110.1(2)
C(5)-C(2)-C(3)	112.6(3)
O(2)-C(2)-C(4)	101.7(2)
C(5)-C(2)-C(4)	113.1(3)
C(3)-C(2)-C(4)	109.8(3)
C(7)-C(6)-C(11)	121.7(2)
C(7)-C(6)-N(1)	131.6(2)
C(11)-C(6)-N(1)	106.6(2)
C(8)-C(7)-C(6)	117.4(3)
C(7)-C(8)-C(9)	121.7(3)
C(10)-C(9)-C(8)	120.7(3)
C(9)-C(10)-C(11)	118.8(3)

C(6)-C(11)-C(10)	119.7(2)
C(6)-C(11)-C(12)	108.3(2)
C(10)-C(11)-C(12)	132.1(3)
C(13)-C(12)-C(11)	108.0(2)
C(13)-C(12)-C(14)	129.4(2)
C(11)-C(12)-C(14)	122.3(2)
C(12)-C(13)-N(1)	108.6(2)
C(12)-C(13)-C(18)	130.1(2)
N(1)-C(13)-C(18)	121.3(2)
N(2)-C(14)-C(15)	111.2(2)
N(2)-C(14)-C(12)	113.7(2)
C(15)-C(14)-C(12)	110.7(2)
C(16)-C(15)-C(14)	120.9(3)
C(15)-C(16)-O(7)	125.2(3)
C(15)-C(16)-C(17)	121.7(3)
O(7)-C(16)-C(17)	113.1(2)
C(16)-C(17)-C(18)	114.1(2)
C(13)-C(18)-C(19)	108.9(2)
C(13)-C(18)-C(23)	111.6(2)
C(19)-C(18)-C(23)	114.6(2)
C(13)-C(18)-C(17)	111.5(2)
C(19)-C(18)-C(17)	106.5(2)
C(23)-C(18)-C(17)	103.7(2)
O(5)-C(19)-O(6)	124.8(3)
O(5)-C(19)-C(18)	122.3(2)
O(6)-C(19)-C(18)	112.6(2)
O(6)-C(20)-C(21)	110.0(3)
O(6)-C(20)-C(22)	104.5(3)
C(21)-C(20)-C(22)	113.8(3)
O(4)-C(23)-O(3)	124.3(2)
O(4)-C(23)-C(18)	125.2(2)
O(3)-C(23)-C(18)	110.1(2)
O(3)-C(24)-C(25)	106.3(2)
O(3)-C(24)-C(26)	108.4(2)
C(25)-C(24)-C(26)	113.2(3)
N(2)-C(27)-C(28)	110.9(3)

C(27)-C(28)-S(1)	113.5(3)
N(2)-C(29)-C(30)	111.9(3)
C(29)-C(30)-S(1)	112.1(3)
C(32)-C(31)-C(33)	111.8(4)
C(32)-C(31)-Si(1)	112.4(2)
C(33)-C(31)-Si(1)	117.2(3)
C(36)-C(34)-C(35)	109.8(3)
C(36)-C(34)-Si(1)	116.1(3)
C(35)-C(34)-Si(1)	111.9(2)
C(39)-C(37)-C(38)	116.0(4)
C(39)-C(37)-Si(1)	114.4(3)
C(38)-C(37)-Si(1)	112.6(2)
C(1)-N(1)-C(6)	127.4(2)
C(1)-N(1)-C(13)	124.0(2)
C(6)-N(1)-C(13)	108.5(2)
C(27)-N(2)-C(29)	111.5(3)
C(27)-N(2)-C(14)	112.1(2)
C(29)-N(2)-C(14)	108.4(2)
C(1)-O(2)-C(2)	120.5(2)
C(23)-O(3)-C(24)	116.7(2)
C(19)-O(6)-C(20)	116.4(2)
C(16)-O(7)-Si(1)	129.86(18)
C(30)-S(1)-C(28)	96.07(16)
O(7)-Si(1)-C(31)	99.59(12)
O(7)-Si(1)-C(34)	107.68(13)
C(31)-Si(1)-C(34)	113.17(15)
O(7)-Si(1)-C(37)	110.11(13)
C(31)-Si(1)-C(37)	114.74(18)
C(34)-Si(1)-C(37)	110.77(17)

Symmetry transformations used to generate equivalent atoms:

Table A.3.1.4 Anisotropic displacement parameters ($Å^2 x\ 10^3$)for **71**. The anisotropic displacement factor exponent takes the form: $-2\pi^2[\ h^2 a^{*2} U^{11} + ... + 2\ h\ k\ a^*\ b^*\ U^{12}\ ]$

	U^{11}	U^{22}	U^{33}	U^{23}	U^{13}	U^{12}
C(1)	15(1)	16(1)	19(1)	-2(1)	-2(1)	-1(1)
C(2)	20(1)	26(2)	26(2)	8(1)	-5(1)	3(1)
C(3)	40(2)	41(2)	30(2)	-1(2)	-15(2)	3(2)
C(4)	40(2)	48(2)	48(2)	26(2)	-7(2)	-6(2)
C(5)	47(2)	29(2)	40(2)	-2(2)	-3(2)	11(2)
C(6)	14(1)	21(1)	16(1)	-5(1)	1(1)	-4(1)
C(7)	20(1)	21(1)	20(1)	-2(1)	-1(1)	-4(1)
C(8)	24(1)	24(2)	25(2)	-5(1)	4(1)	-10(1)
C(9)	16(1)	30(2)	31(2)	-7(1)	2(1)	-8(1)
C(10)	15(1)	24(1)	28(2)	-4(1)	-2(1)	-2(1)
C(11)	15(1)	18(1)	20(1)	-4(1)	1(1)	-2(1)
C(12)	15(1)	19(1)	20(1)	-3(1)	0(1)	-1(1)
C(13)	15(1)	14(1)	17(1)	-2(1)	1(1)	-2(1)
C(14)	14(1)	23(1)	27(2)	2(1)	-1(1)	-1(1)
C(15)	18(1)	16(1)	33(2)	1(1)	1(1)	2(1)
C(16)	23(1)	14(1)	24(1)	0(1)	-1(1)	-1(1)
C(17)	16(1)	17(1)	23(1)	1(1)	0(1)	-3(1)
C(18)	13(1)	17(1)	21(1)	-1(1)	-1(1)	-2(1)
C(19)	16(1)	15(1)	27(2)	0(1)	-2(1)	-2(1)
C(20)	27(2)	38(2)	34(2)	-15(1)	-6(1)	-10(1)
C(21)	45(2)	47(2)	53(2)	-21(2)	-28(2)	7(2)
C(22)	57(3)	91(3)	62(3)	-39(2)	12(2)	-51(3)
C(23)	16(1)	15(1)	20(1)	2(1)	-3(1)	-2(1)
C(24)	20(1)	26(2)	29(2)	-9(1)	7(1)	-5(1)
C(25)	31(2)	47(2)	37(2)	-20(2)	5(1)	-8(2)
C(26)	37(2)	29(2)	41(2)	-8(2)	5(2)	2(1)
C(27)	39(2)	42(2)	29(2)	1(1)	-7(1)	-19(2)
C(28)	52(2)	51(2)	28(2)	0(2)	-6(2)	-25(2)
C(29)	29(2)	41(2)	39(2)	14(2)	-5(1)	7(2)
C(30)	37(2)	52(2)	44(2)	22(2)	-4(2)	6(2)
C(31)	33(2)	24(2)	41(2)	-8(1)	4(1)	-6(1)

C(32)	82(3)	52(2)	60(3)	9(2)	-35(2)	-33(2)
C(33)	51(3)	48(3)	190(7)	-62(4)	-17(3)	-8(2)
C(34)	26(2)	20(2)	45(2)	2(1)	3(1)	-2(1)
C(35)	37(2)	42(2)	37(2)	-2(2)	2(2)	-3(2)
C(36)	57(2)	30(2)	59(3)	6(2)	17(2)	11(2)
C(37)	43(2)	34(2)	53(2)	-2(2)	26(2)	-3(2)
C(38)	54(2)	44(2)	38(2)	4(2)	16(2)	-11(2)
C(39)	107(5)	103(5)	74(4)	-21(3)	25(3)	-21(4)
N(1)	13(1)	16(1)	18(1)	-1(1)	-1(1)	-2(1)
N(2)	20(1)	24(1)	27(1)	4(1)	-7(1)	-2(1)
O(1)	14(1)	25(1)	31(1)	6(1)	-3(1)	-3(1)
O(2)	19(1)	25(1)	27(1)	10(1)	-5(1)	-4(1)
O(3)	16(1)	24(1)	25(1)	-8(1)	5(1)	-5(1)
O(4)	14(1)	26(1)	29(1)	-2(1)	1(1)	-4(1)
O(5)	26(1)	33(1)	23(1)	-4(1)	1(1)	-11(1)
O(6)	21(1)	36(1)	29(1)	-10(1)	-2(1)	-11(1)
O(7)	22(1)	17(1)	34(1)	-5(1)	3(1)	-3(1)
S(1)	36(1)	100(1)	30(1)	19(1)	-12(1)	-25(1)
Si(1)	25(1)	18(1)	32(1)	-4(1)	8(1)	-2(1)

Table A.3.1.5 Hydrogen coordinates (x 10^4) and isotropic displacement parameters ($Å^2$x 10^3) for **71**.

	x	y	z	U(eq)
H(3A)	-3323	5053	834	59
H(3B)	-2124	5013	24	59
H(3C)	-3553	5871	-34	59
H(4A)	-947	6992	479	75
H(4B)	-2109	7050	-251	75
H(4C)	-677	6194	-193	75
H(5A)	-2642	6960	1807	64
H(5B)	-3522	6167	1983	64
H(5C)	-3943	7041	1175	64
H(7A)	1149	5765	1597	25
H(8A)	3496	5863	1697	28
H(9A)	5188	4618	2483	30
H(10A)	4588	3234	3192	27
H(14A)	3678	1914	3514	27
H(15A)	3166	723	2891	29
H(17A)	65	1724	4213	23
H(17B)	-986	1357	3665	23
H(20A)	-2042	1671	1043	38
H(21A)	-2792	3320	532	74
H(21B)	-4316	3387	1049	74
H(21C)	-3877	2811	186	74
H(22A)	-3446	907	2100	92
H(22B)	-4286	1291	1171	92
H(22C)	-4731	1862	2037	92
H(24A)	-3155	3845	5115	30
H(25A)	-1107	3784	5870	57
H(25B)	-2290	4751	6026	57
H(25C)	-995	4781	5295	57
H(26A)	-3953	5041	3876	57
H(26B)	-2778	5571	4046	57

H(26C)	-4067	5540	4781	57
H(27A)	1884	3183	4759	42
H(27B)	3487	2613	5012	42
H(28A)	1019	2411	6128	50
H(28B)	2055	3024	6345	50
H(29A)	4323	950	4960	50
H(29B)	3314	370	4636	50
H(30A)	3586	-71	6208	61
H(30B)	1958	510	6047	61
H(31A)	-285	-1188	2620	40
H(32A)	-1319	-858	1202	93
H(32B)	-23	-436	769	93
H(32C)	-1070	69	1544	93
H(33A)	-4	-2404	1728	138
H(33B)	1274	-2609	2411	138
H(33C)	1514	-2253	1346	138
H(34A)	3521	-970	3457	39
H(35A)	2514	-1778	4729	61
H(35B)	1175	-1717	4139	61
H(35C)	1467	-758	4379	61
H(36A)	4267	-2644	3755	83
H(36B)	4434	-2283	2684	83
H(36C)	3132	-2724	3064	83
H(37A)	3841	-276	1644	56
H(38A)	3046	816	328	72
H(38B)	2272	1164	1259	72
H(38C)	1453	738	595	72
H(39A)	4134	-859	288	145
H(39B)	2715	-1213	525	145
H(39C)	4062	-1644	1159	145

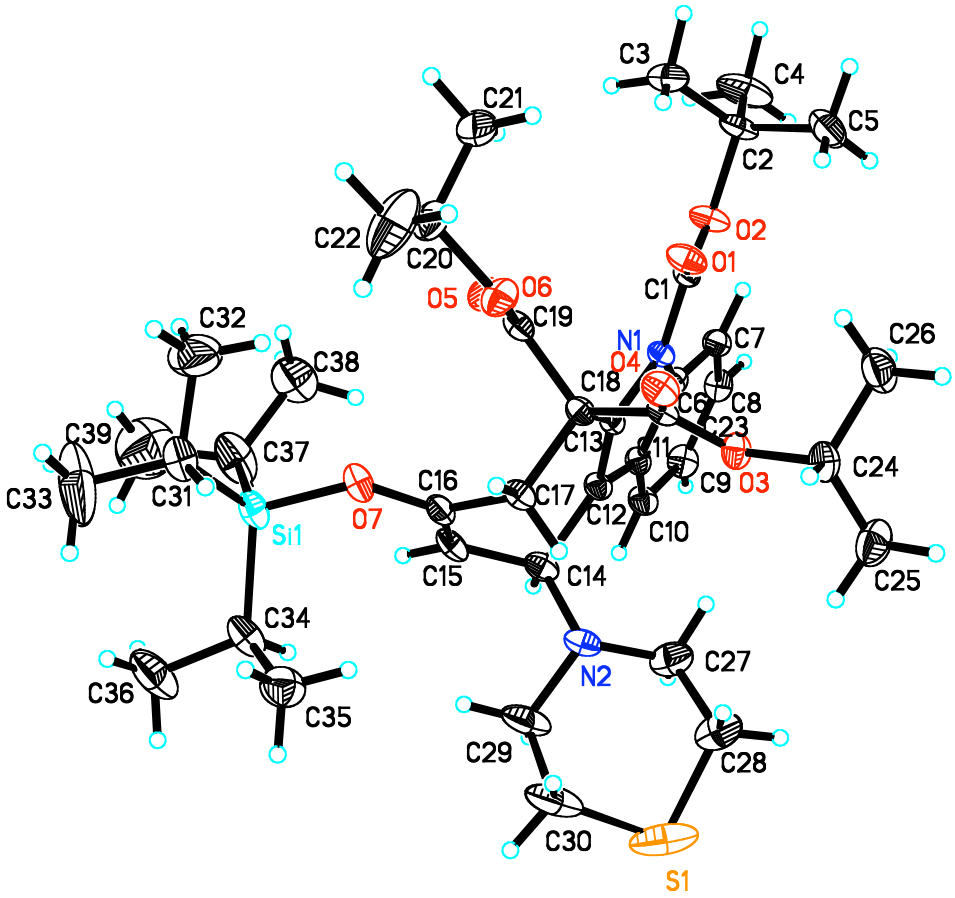
C3
C4
C5
C21
C2
C22
O2
C20
O1
O5
O6
C1
C19
C32
N1
C7
C26
C38
O4
C18
C6
C8
C39
C13
C11
C23
C37
C24
C33
C31
C16
C17
C9
O3
O7
C12
C10
Si1
C15
C14
C25
C34
N2
C27
C36
C35
C29
C28
C30
S1

CHAPTER FOUR

Alternative Approaches to the Complex Framework of Actinophyllic Acid

4.1 Aldehyde Alkylation Strategy

4.1.1 Synthetic Planning

The Michael addition/alkylation strategy, discussed in chapters two and three, relied upon initial allylation of indole malonate **59** (see Scheme 3.1.2.1), followed by alkylation of the aldehyde moiety. An alternative strategy was considered, which switched the order of events. Thus, an initial aldehyde alkylation could be followed by intramolecular carbon–carbon bond formation at the malonate functionality. One advantage of this strategy would be convergence, as the aldehyde coupling partner was envisioned to incorporate all carbon atoms requisite for actinophyllic acid. This is in contrast to the three–carbon unit introduced *via* malonate allylation in the initial strategy. Searching the literature revealed dibutyrolactone as a potential nucleophilic coupling partner, as its carbon framework mapped adequately onto that of actinophyllic acid (Scheme

4.1.1.1). Dibutyrolactone was also realized to possess functionality ideally suited for an intramolecular carbon–carbon bond formation event utilizing radical chemistry (*vide infra*). It was with this information that a retrosynthesis was formulated and synthetic efforts were initiated.

Scheme 4.1.1.1

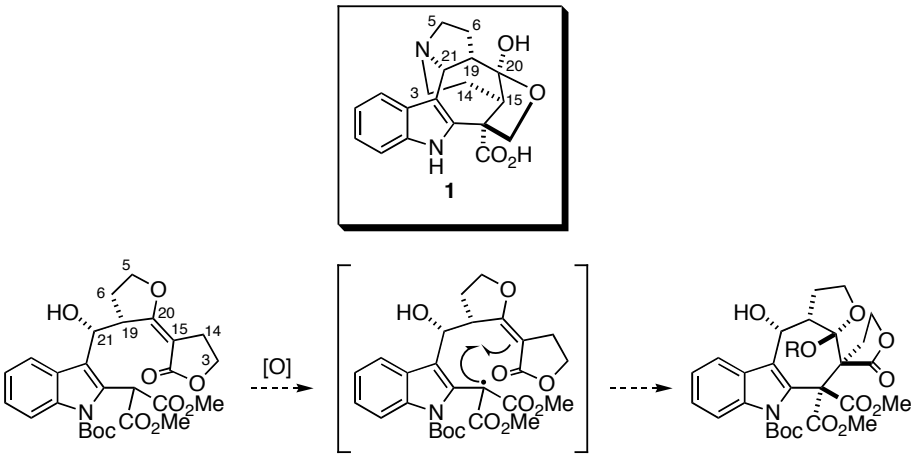

4.1.2 Retrosynthetic Analysis

Once again, the retrosynthetic analysis began with opening of the acetal linkage and oxidation state manipulation at C17. Intermediate **26** was simplified to trichloro ketone **76**, which, in the forward sense, was expected to undergo three consecutive alkylation events upon exposure to an ammonia equivalent (Scheme 4.1.2.1). Trichloro ketone **76** was taken back to an acetal intermediate **77**, itself the result of a proposed malonate radical cyclization onto a pendant olefin providing indolemalonate **78** as a key retrosynthetic intermediate. An aldol

reaction between indolecarboxaldehyde **29** and dibutyrolactone **79** was anticipated to access this compound. This strategy was a starting point for initial experimentation.

Scheme 4.1.2.1

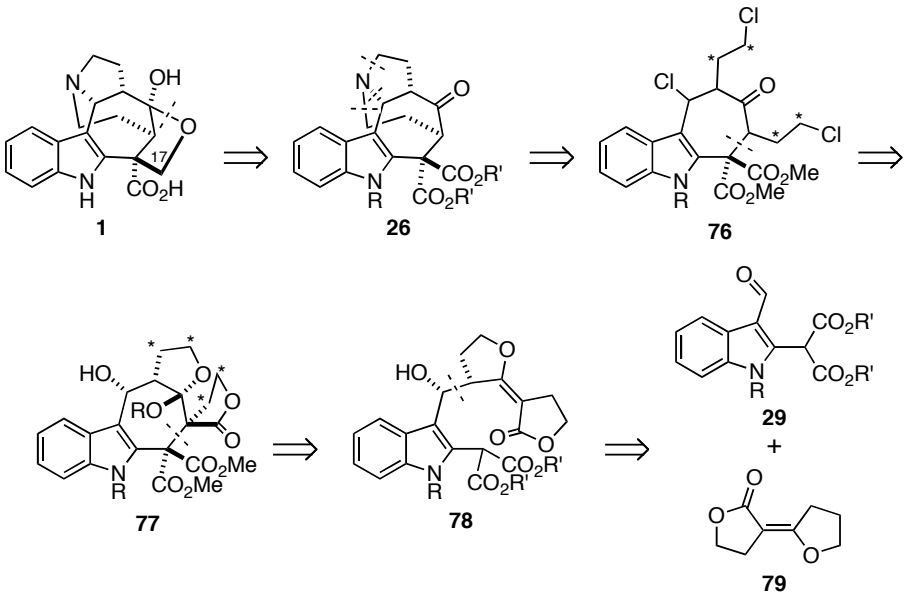

4.1.3 Dibutyrolactone as a Masked Dichloro Ketone

The design of retrosynthetic intermediate **77** was based upon literature precedent, whereby a simple spiro-fused acetal or β-keto ester was exposed to concentrated hydrochloric acid (HCl) to reveal 1,7-dichloroketone (Scheme 4.1.3.1).[1] Our proposed system to access trichloro ketone **76** possessed both an acetal and β-keto ester (**77**), which were expected to form two of the three chlorides upon exposure to HCl. Installation of the first chloride (**80**) from the acetal moiety could start the sequence. The spiro-fused γ-lactone was imagined

to hydrolyze under the acidic conditions (**81**), undergo decarboxylation (**82**), and eventually provide the second chloride (**84**), possibly *via* the intermediate oxocarbenium ion **83** (Scheme 4.1.3.1). The final chloride adjacent to the indole ring was anticipated to form with assistance from the indole nucleus (**85**). Our system was more complex than the literature precedent necessitating synthesis of dibutyrolactone adduct **78** (see Scheme 4.1.2.1) to test this transformation on a more functionalized substrate.

Scheme 4.1.3.1

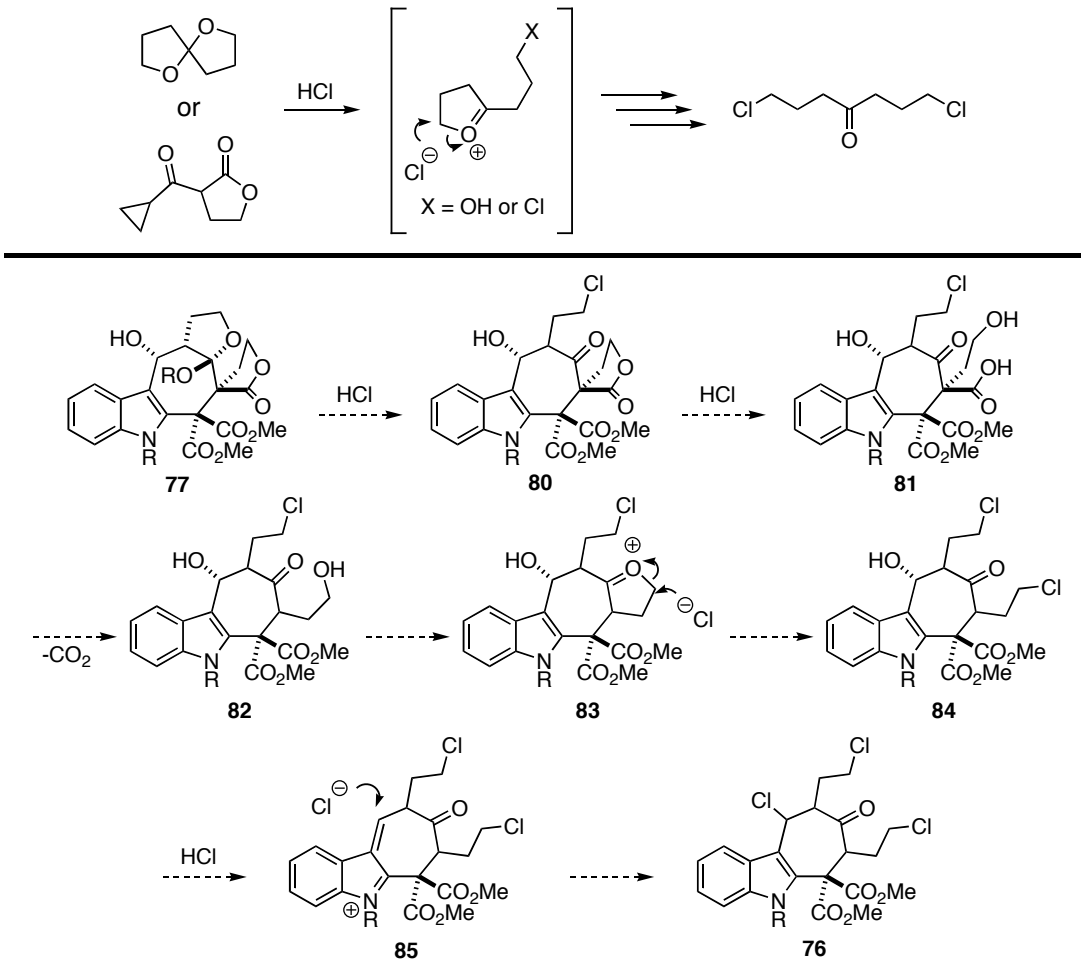

In the forward sense, addition of the extended lithium enolate of dibutyrolactone to indolemalonate **33**, pre-treated with LHMDS to remove the acidic malonate proton, formed the putative lithium alkoxide **86**. Lactone malonate **87** was isolated as the major product after quenching the reaction, as opposed to the desired dibutyrolactone adduct **78** (Scheme 4.1.3.2). Formation of the isolated lactone product **87** was thought to arise *via* attack of the *in situ* generated lithium alkoxide (following aldol addition) onto the pendant vinylogous carbonate functionality followed by expulsion of a primary lithium alkoxide. The relative stereochemistry of the product could not be determined at this stage, but was established after a subsequent step through nOe studies (*vide infra*). The lactonization event, while unexpected, was not a dead end.

Scheme 4.1.3.2

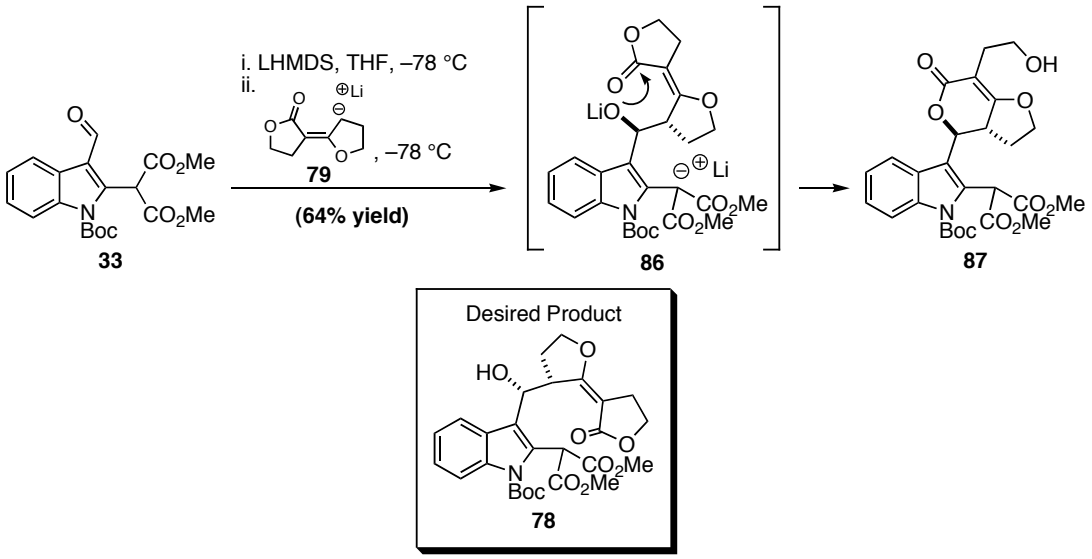

4.1.4 Elaboration of Lactone Malonate 87

We postulated the product isolated from the alkylation reaction could undergo a sequence of transformations, similar to the originally planned route, to arrive at the desired trichloro ketone intermediate (**76**) (Scheme 4.1.4.1). The first challenge was seven-membered ring formation (**88**). Radical cyclization to form seven membered rings is uncommon, however, relevant reports exist in the literature detailing successful ring formation.[2] In addition, 1,3-dicarbonyl functionalities are excellent substrates for producing carbon centered radicals with oxidants such as $Mn(OAc)_3$ and CAN.[3,4] Importantly, electron deficient malonate radicals react with

Scheme 4.1.4.1

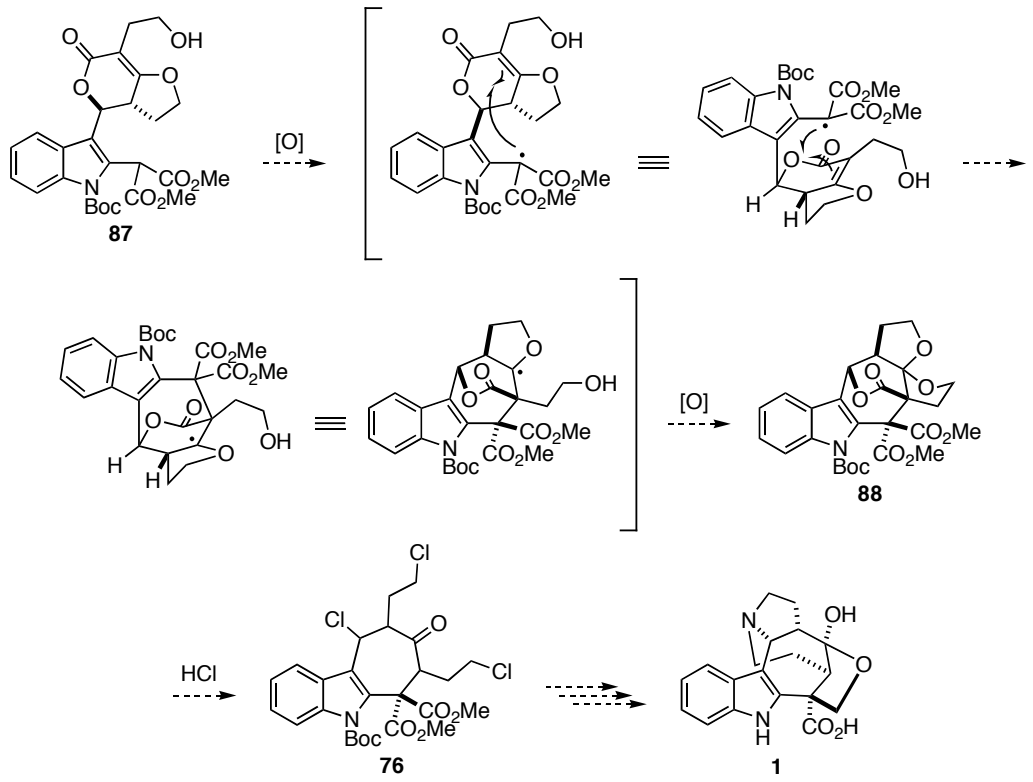

electron rich olefins, which in our case was an enol ether.[4] CAN was chosen to investigate the desired transformation due to its availability and the user-friendly reaction conditions. In the event, exposure of lactonemalonate **87** to a solution of CAN in methanol produced two new products, one of which could be fully characterized. Unfortunately, the isolated product from the reaction was not the desired cyclized product **88**, but rather methoxymalonate **89**. This product was the result of malonate oxidation *without* cyclization (Scheme 4.1.4.2). The second product from the reaction was not investigated further because ^{13}C NMR indicated that the pendant olefin was still intact. It was therefore reasoned that seven-membered ring formation onto a tetra-substituted olefin *via* a carbon-

centered radical was not favorable for our system.

Scheme 4.1.4.2

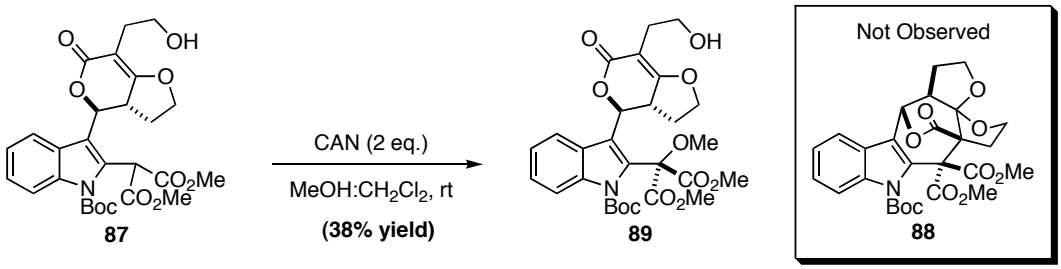

With this result in mind an alternative step was envisioned to access conventional ionic intermediates to produce polycycle **88**. Specifically, exposure of lactone malonate **87** to an electrophilic halogen reagent was expected to form a halonium ion at the vinyl ether functionality (**90**). This could be captured by the pendant malonate nucleophile (**91**).[5] The malonate nucleophile could cyclize to form a six or seven-membered ring. Six-membered ring formation was anticipated to be favored, however, with the aide of the adjacent ether, the malonate moiety could shift one carbon over and displace the bromide leaving group in a subsequent step (**88**) (Scheme 4.1.4.3).[6]

Scheme 4.1.4.3

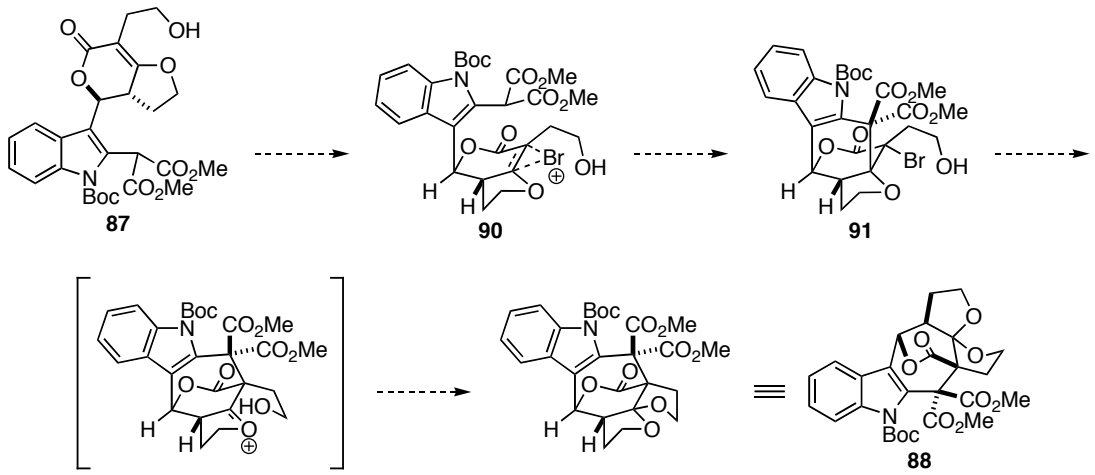

Regrettably, bromomalonate **92** was the major isolated product after exposure of lactonemalonate **87** to NBS in dichloromethane at room temperature. At this point nOe studies revealed the relative stereochemistry of the aldol reaction to be anti (Scheme 4.1.4.4).

Scheme 4.1.4.4

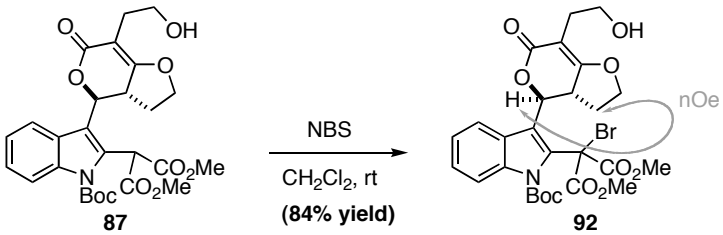

Scheme 4.1.4.5

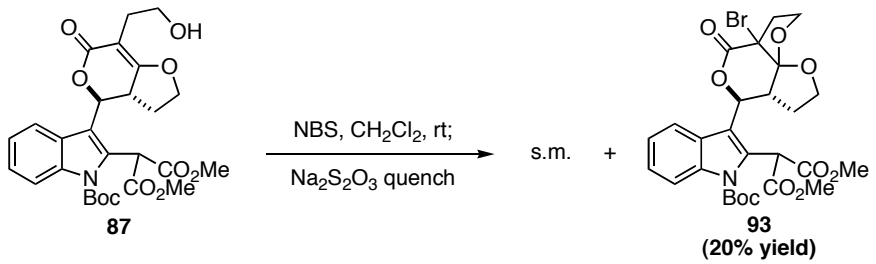

When the bromination reaction was quenched with an aqueous solution of the reducing agent sodium thiosulfate ($Na_2S_2O_3$) and conducted on larger scale bromoacetal **93** was isolated as the only minor product (Scheme 4.1.4.5) in addition to the lactone malonate starting material (**87**). By monitoring the reaction by TLC it was observed that starting material was consumed during the course of the reaction, with the major spot matching an authentic sample of bromomalonate **92** (see Scheme 4.1.4.4), and only reappeared following $Na_2S_2O_3$ quench. Thus, the two products from the reaction were initially brominated at the malonate moiety before the reaction was quenched. The interesting spiro-acetal product **93** was recognized to be a substrate for HCl-mediated trichloro ketone synthesis (*vide supra*). It was exposed to concentrated HCl with the intention of producing tetrahalo intermediate **94**, a substrate envisioned to access a highly functionalized seven-membered ring intermediate (Scheme 4.1.4.6). Unfortunately, the desired transformation was not achieved.[7] It was at this time that our focus turned exclusively to parallel studies, which held the promise of efficiently constructing the carbon skeleton of actinophyllic acid through the use of enamine chemistry. This is discussed in the next section.

Scheme 4.1.4.6

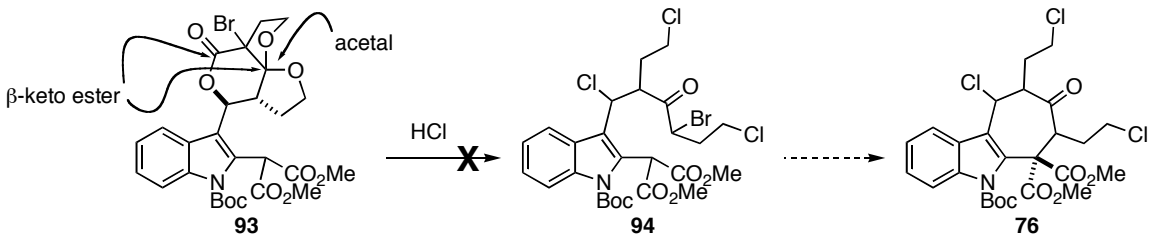

4.2 Late Stage Amine Incorporation Strategy

4.2.1 Initial Considerations and Revised Retrosynthesis

Our failure in advancing the dibutyrolactone addition product necessitated an alternative strategy. As mentioned previously, dibutyrolactone had served as a precursor to 1,7-dichloroketone and while this compound is not viable for intermolecular reactions involving an enolate, it could be elaborated to a compound suitable for an aldol reaction.[1] After consulting the literature it was found that 1,7-dichloroketone is a starting material for preparation of symmetric imine **95**, which was anticipated to be an ideal nucleophilic coupling partner.[8,9] An updated retrosynthesis was prepared to incorporate symmetric imine **95** (Scheme 4.2.1.1) and highlighted an inherent symmetry found within the polycyclic skeleton. The initial retrosynthetic disconnection is identical to previous plans, producing penultimate intermediate **26**. Disconnection of an azacyclooctane ring led us back to symmetric imine **95** and indolecarboxaldehyde **29**.

Scheme 4.2.1.1

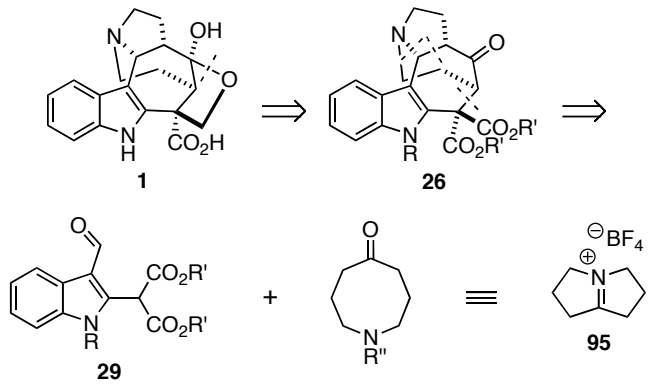

The symmetric imine could alkylate twice on either side of the iminium after deprotonation to its enamine form. Thus, an ideal indolecarboxaldehyde coupling partner must initially possess two electrophilic carbons to match the inherent chemistry of the enamine. Unfortunately, the intermediate indolecarboxaldehyde (**33**) contained one electrophilic position and one nucleophilic position (Figure 4.2.1.1). A solution to this problem and its implementation is addressed in the following two sections.

Figure 4.2.1.1

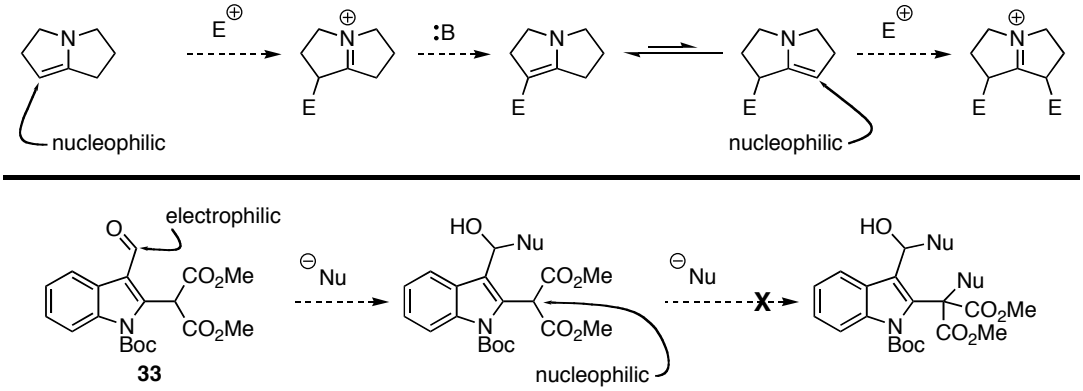

4.2.2 Precedent for Bis-alkylation Strategy

The synthetic literature played a key role in designing substrates for the proposed coupling of indolecarboxaldehyde **33** and imine **95** (Scheme 4.2.2.1). A related symmetric imine **96** had been shown to undergo initial alkylation with a highly reactive quinonemethide intermediate (Scheme 4.2.2.1).[10] The authors did not discuss whether the reaction proceeded stepwise or through a concerted [4+2] mechanism.

Scheme 4.2.2.1

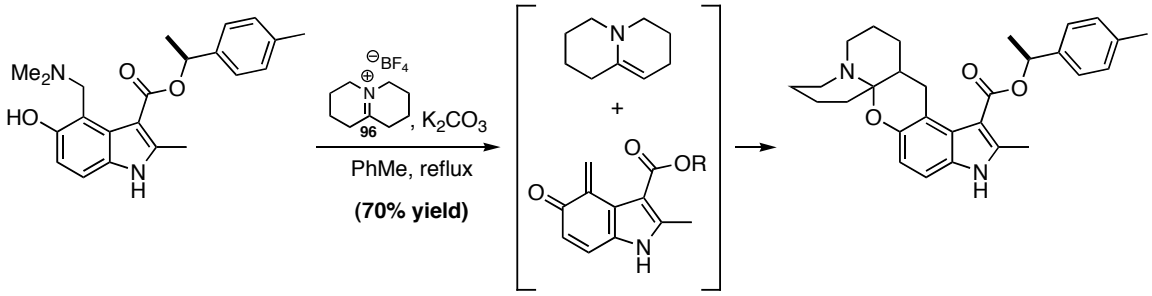

With this in mind an indolecarboxaldehyde intermediate (**97**) was designed which could undergo elimination of a halide, thus generating an electrophilic and highly reactive aza-isobenzofulvene (**98**), which was anticipated to react with enamine **99**, itself generated *in situ* from imine **95** (Scheme 4.2.2.2). In addition, this strategy was attractive because it provided the possibility of forming both carbon–carbon bonds required to access the carbon skeleton of actinophyllic acid in *one step*. After initial enamine alkylation, this was expected to proceed by

Scheme 4.2.2.2

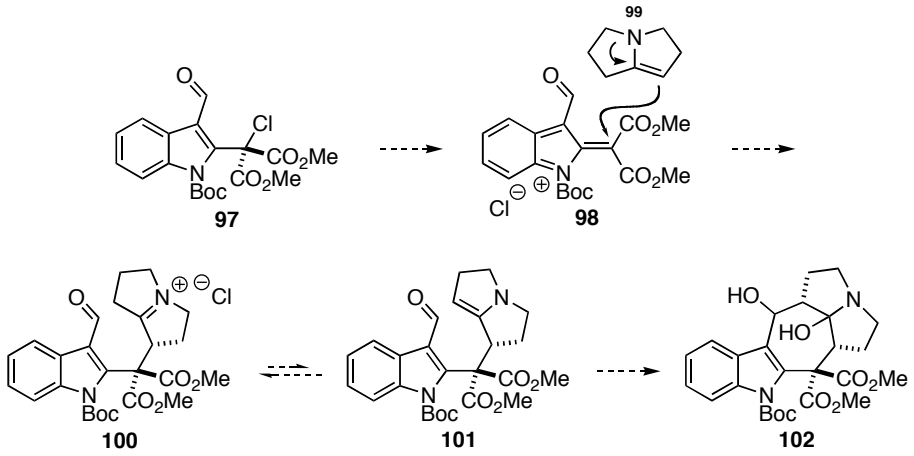

regeneration of an enamine (**101**), from the intermediate imine **100**, followed by attack onto the pendant aldehyde to form a highly functionalized polycyclic product (**102**). It was clear that reformation of the enamine could form either of two intermediates with the tetra-substituted enamine being thermodynamically favored, but undesired for alkylation. Fortunately, an equilibrium could exist between the two enamines and literature precedent suggests that the thermodynamically unfavored, but less sterically hindered enamine undergoes alkylation (Scheme 4.2.2.3).[9] With these encouraging literature results in mind efforts commenced employing the strategy outlined in Scheme 4.2.2.2.

Scheme 4.2.2.3

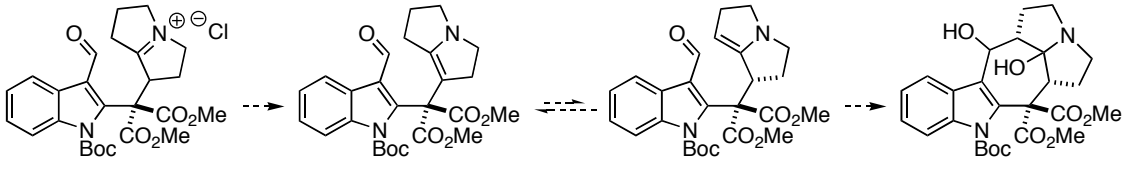

4.2.3 Trapping an Aza-isobenzofulvene Intermediate

Elaboration of previously prepared indole **33** began with chlorination of the malonate moiety (**103**) utilizing household bleach (scheme 4.2.3.1).[11] Removal of the indole Boc protecting group with TFA furnished a substrate (**104**) poised for the key carbon–carbon bond forming cascade with iminium salt **95**.

Scheme 4.2.3.1

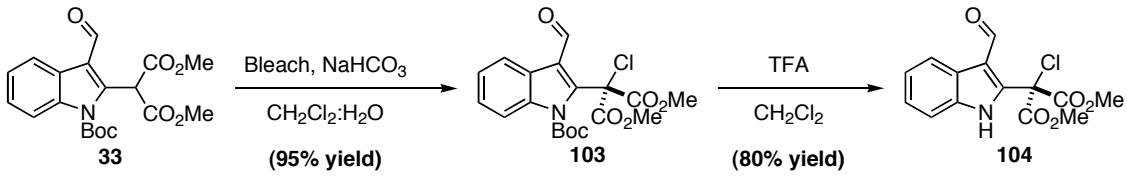

In the event, exposure of **104** to a slight excess of **95** and triethylamine provided not the desired product (**105**) (resulting from two sequential carbon–carbon bond formations), but pentacycle **106** whose structure was confirmed following x-ray analysis (Scheme 4.2.3.2).[12] This structurally complex product was envisioned to arise from initial carbon–carbon bond formation *via* a putative aza-isobenzofulvene intermediate (**107**) followed by closure of the indole nitrogen onto the formed iminium species (**108**) (Scheme 4.2.3.3). All efforts to avoid aminal formation, including use of excess base or alternative bases, were unfruitful.

Scheme 4.2.3.2

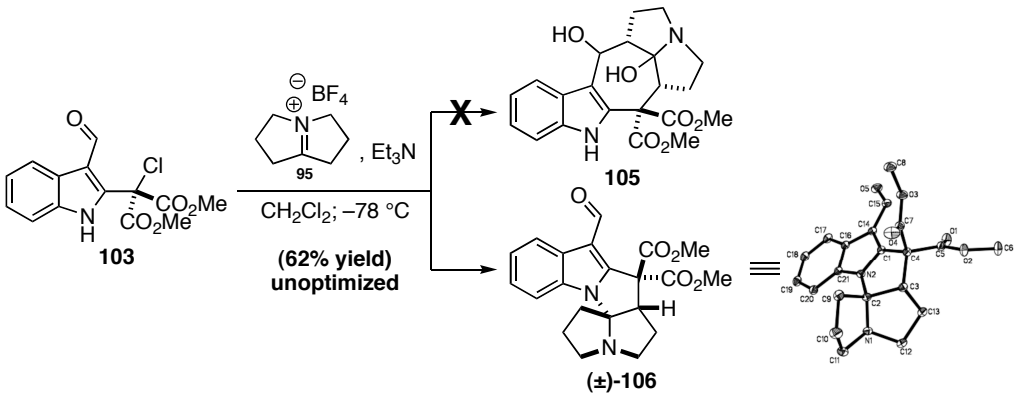

Aminal formation in our system mimicked the result found in the literature for iminium species **96** (*vide supra*). The reaction did not proceed as intended, however, one carbon–carbon bond had been formed, which created a quaternary carbon center.

Scheme 4.2.3.3

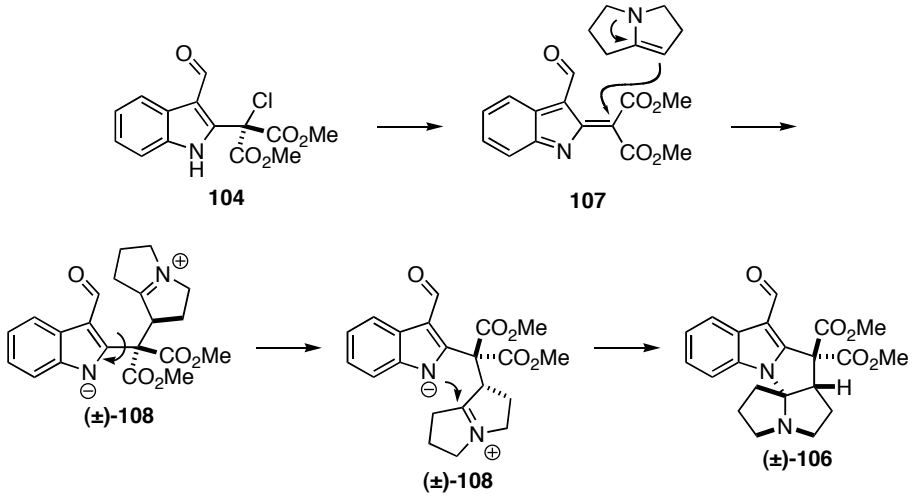

At this stage, our attention focused on elaboration of this unique product. To our surprise, intermediate pentacycle **106** proved difficult to hydrolyze under both acidic and basic conditions.[13] In most cases starting material was re-isolated, decomposed, or produced compounds too polar to purify and characterize. Some insight may be gained from the solid-state crystal structure (Figure 4.2.3.1). It is clear that the tertiary nitrogen lone pair of the aminal moiety cannot overlap with the σ^* orbital of the indole nitrogen–carbon bond. Assuming that the solid-state structure accurately reflects the solution structure, this could explain the difficulties encountered while attempting aminal hydrolysis.

Figure 4.2.3.1

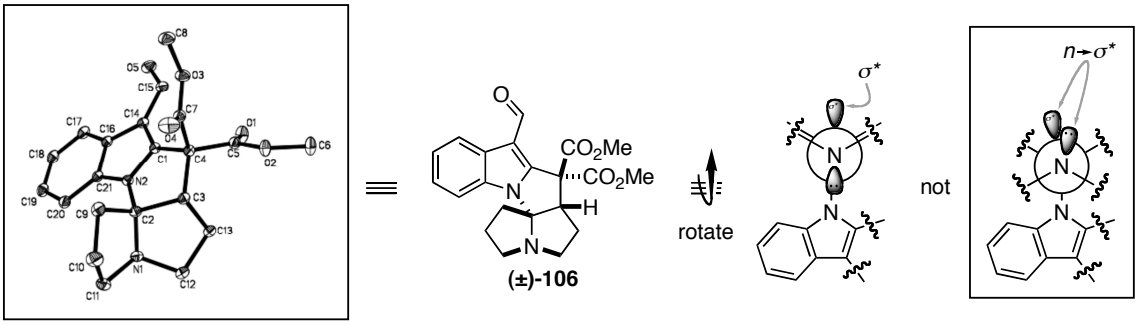

Following this lack of success, attempts were made to open the aminal *via* alternative methods. The stability of the aminal was further established following conversion of this material to azacyclooctane (**109**) upon treatment with methyl chloroformate in benzene at reflux (Scheme 4.2.3.4). The anticipated aminal cleavage under thermal conditions and trapping of the indole nitrogen as the methyl carbamate (**110**) was not a viable strategy.[13] It appeared that under the

reaction conditions acylation of the tertiary amine preceded and likely activated aminal cleavage, which under anhydrous conditions was followed by olefin formation. At this time it is unknown whether this proposed mechanistic pathway can be extended to the aqueous acidic conditions, which upon heating led to decomposition and uncharacterized polar material. It is clear that future effort must focus on mild conditions for aminal hydrolysis or, taken one step back, further screen conditions to avoid aminal formation altogether.

Scheme 4.2.3.4

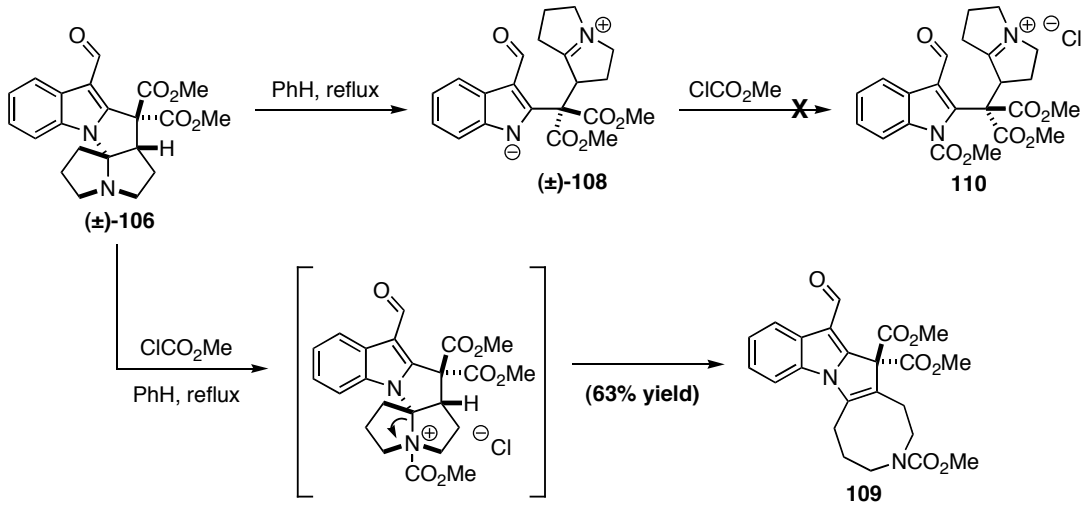

4.3 Conclusions

4.3.1 Summary of Actinophyllic Acid Progress

At this time, pentacyclic intermediate **106** constitutes our most advanced substrate toward an actinophyllic acid total synthesis. Along the way, the Wood laboratory has explored a Michael addition/alkylation sequence to furnish the polycyclic framework of actinophyllic acid. This strategy has resulted in the synthesis of advanced intermediate **71**, possessing all of the carbon atoms necessary for a total synthesis of actinophyllic acid, but none of the structural complexity. A more convergent strategy proposed three late stage amine alkylations to access an advanced polycyclic intermediate. This route furnished lactone intermediate **87**, which was not elaborated further, due to an increasing step count. Lastly, moving from a dibutyrolactone coupling partner to iminium salt **95** provided a highly convergent route, which proposed to utilize both enamine and aza-isobenzofulvene chemistry to rapidly establish the polycyclic framework of actinophyllic acid. Employing this strategy has led to the synthesis of structurally complex pentacyclic intermediate **106**.

4.4 Experimental

4.4.1 Materials and Methods

Unless otherwise sated, reactions were performed under a nitrogen atmosphere using freshly dried solvents. Tetrahydrofuran (THF) was dried either by distillation from sodium/benzophenone or by passing through activated alumina columns. Methylene chloride (CH_2Cl_2), diethyl ether (Et_2O), benzene (PhH), and toluene (PhMe) were dried by passing through activated alumina columns. Dimethylformamide (DMF) was dried over activated molecular sieves or purchased anhydrous from Sigma-Aldrich. MeOH was distilled over magnesium oxide. All other commercially obtained reagents were used as received. All reactions were monitored by thin-layer chromatography using EMD/Merck or Silicycle silica gel 60 F254 pre-coated plates (0.25 mm). Flash chromatography was performed with the indicated solvents using silica gel (particle size 0.040-0.063 mm) purchased from Silicycle. ^{1}H NMR spectra were recorded at 400 MHz using a Varian Inova 400 instrument. ^{13}C NMR spectra were recorded at 100 MHz using a Varian Inova 400 instrument. Chemical shift are reported relative to internal chloroform (^{1}H, δ = 7.26, ^{13}C, δ = 77.2), dimethyl sulfoxide (^{1}H, δ = 2.50, ^{13}C, δ = 39.5), benzene (^{1}H, δ = 7.16, ^{13}C, δ = 128.1) as indicated. Splitting patterns are reported as such, app = apparent, br = broad, s = singlet, d = doublet, dd = doublet of doublets, ddd = doublet of doublets of doublets, dddd = doublet of doublets of doublets of doublets, t = triplet, q = quartet, m = multiplet,

nfom = non-first order multiplet. Infrared spectra were recorded on a Nicolet Avatar 320 FT-IR. Melting points were obtained on a Gallenkamp variable temperature melting point apparatus and are uncorrected. High-resolution mass spectra were acquired at the Colorado State University CIF using an Agilent 6210 TOF LCMS.

4.4.2 Preparative Procedures

Preparation of Vinylogous carbonate **87**

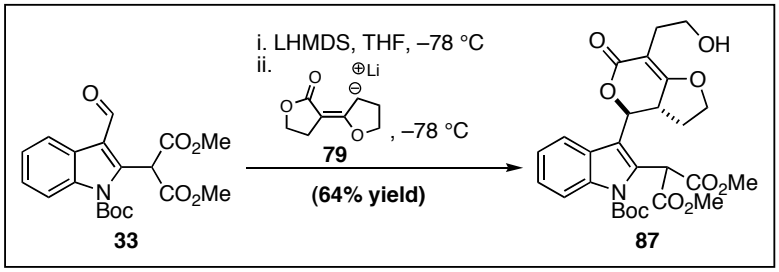

To a flame dried round-bottom flask (*flask a*) containing indolemalonate **33** (1.102 g, 2.93 mmol) was added THF (30 mL) and the solution cooled to –78 °C under N_2. To the stirred solution was added LHMDS (3.0 mL of a 1.0 M soln., 3.0 mmol) dropwise *via* syringe and the reaction aged for 1 h. Concurrent to this, a second flame dried round-bottom flask (*flask b*) was charged with dibutyrolactone **79** (503 mg, 3.26 mmol) followed by THF (30 mL) and the contents cooled to –78 °C. To this solution under N_2 was added LHMDS (3.4 mL of a 1.0 M soln., 3.4 mmol) dropwise *via* syringe and the contents stirred for 1 h. The contents of *flask b* was transferred *via* cannula to *flask a* dropwise at –78 °C with a positive pressure of N_2. *Flask b* was rinsed with THF (5 mL), which was transferred *via*

cannula to *flask a*. The reaction stirred 8 hrs, during which time the temperature reached room temperature, before it was quenched by addition of 1N HCl (6.5 mL) at 0 °C. The reaction was diluted with H_2O (100 mL) and transferred to a separatory funnel where the layers where separated. The aqueous layer was extracted with EtOAc (3 x 100 mL) and the combined organic layers were washed with brine and dried over Na_2SO_4. Filtration of the solids followed by concentration under reduced pressure and silica gel chromatography (gradient elution, 25 → 50% EtOAc/Hexanes → 100% EtOAc) provided Vinylogous carbonate **87** (1.0 g, 64% yield) as a white amorphous solid.

Vinylogous carbonate 87: m.p. > 158.0 °C (decomposition); FTIR (thin film/NaCl) 3436 (m, br), 2975 (m), 2950 (m), 2899 (m), 1736 (s, br), 1675 (s, br), 1475 (w), 1449 (s), 1434 (m) cm^{-1}; ^1H NMR (400 MHz, $CDCl_3$) δ 8.04 (d, *J* = 8.5 Hz, 1H), 7.77 (br d, *J* = 7.6 Hz, 1H), 7.36 (dd, *J* = 7.5, 7.5 Hz, 1H), 7.26 (dd, *J* = 7.5, 7.5 Hz, 1H), 5.31–5.36 (2H), 4.57 (dd, *J* = 8.7 Hz, 1H), 4.25 (ddd, *J* = 11.7, 9.0, 5.2 Hz, 1H), 3.74–3.84 (9H), 2.41–2.70 (3H), 2.01 (ddd, *J* = 12.6, 7.5, 5.2 Hz, 1H), 1.87 (ddd, *J* = 24.0, 12.0, 8.8 Hz, 1H), 1.67 (s, 9H); ^{13}C NMR (100 MHz, $CDCl_3$) δ 173.1, 169.5, 167.1, 166.4, 150.5, 135.9, 130.2, 126.7, 125.3, 123.1, 120.6, 117.7, 116.0, 97.8, 85.6, 76.1, 74.0, 62.2, 53.2, 53.1, 50.0, 43.2, 28.2, 27.8, 27.6; HRMS (TOF LCMS) calc'd for $C_{27}H_{32}NO_{10}$ $[M+H]^+$ 530.2021, found 530.2022.

Preparation of Methoxy indolemalonate **89**

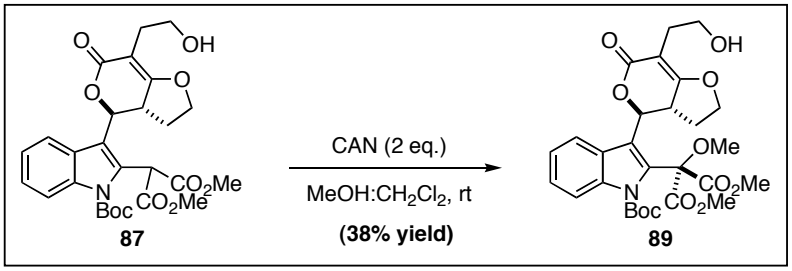

To a solution of Vinylogous carbonate **87** (20 mg, 0.0377 mmol) in a MeOH (300 μl)/CH_2Cl_2 (280 μL) mixed solvent system was added CAN (43 mg, 0.0784 mmol) at 0 °C. The reaction was stirred 10 min. before it was warmed to room temperature and concentrated under reduced pressure following consumption of starting material, judged by TLC. The crude material was dissolved in a minimal amount of CH_2Cl_2 and filtered through Celite. The filtrate was concentrated under reduced pressure and purified by silica gel chromatography (gradient elution, 65 → 75% EtOAc/Hexanes) to provide methoxy indolemalonate **89** (8 mg, 38% yield) as a colorless oil.

Methoxy indolemalonate 89: FTIR (thin film/NaCl) 3431 (m, br), 2980 (m), 2955 (m), 2929 (m), 2904 (m), 2827 (w), 1726 (s), 1680 (s), 1598 (m), 1470 (m), 1434 (m) cm^{-1}; ^1H NMR (400 MHz, PhH-d_6) δ 7.92 (d, *J* = 7.5 Hz, 1H), 7.79 (d, *J* = 8.2 Hz, 1H), 7.12 (dd, *J* = 7.9, 7.9 Hz, 1H), 6.90 (dd, *J* = 7.5, 7.5 Hz, 1H), 5.36 (d, *J* = 12.1 Hz, 1H), 3.74 (m, 2H), 3.61 (dd, *J* = 8.1, 8.1 Hz, 1H), 3.53 (s, 3H), 3.48 (s, 3H), 3.20 (ddd, *J* = 11.3, 8.6, 5.8 Hz, 1H), 2.89 (s, 3H), 2.85 (br s, 1H), 2.55 (m, 2H), 2.24 (m, 2H), 2.04 (ddd, *J* = 12.0, 12.0, 7.5 Hz, 1H), 1.40 (s, 9H); ^{13}C NMR (100 MHz, PhH-d_6) δ 171.1, 167.6, 165.8, 164.7, 150.4, 149.5,

142.8, 130.8, 129.8, 124.8, 116.2, 116.0, 98.0, 89.1, 84.7, 83.7, 73.0, 61.9, 52.5, 52.3, 52.2, 38.4, 28.1, 28.0; HRMS (TOF LCMS) calc'd for $C_{28}H_{34}NO_{11}$ $[M+H]^+$ 560.2126, found 560.2122.

Preparation of Br-Vinylogous carbonate **92**

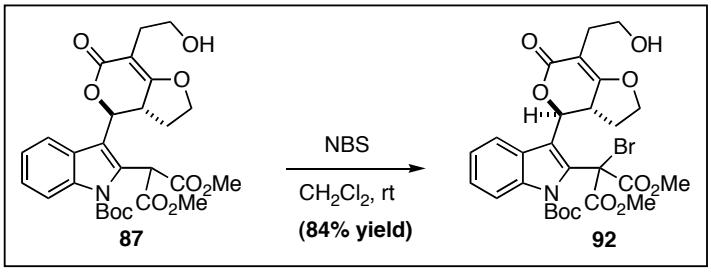

To a solution of vinylogous carbonate **87** (26 mg, 0.0491 mmol) in CH_2Cl_2 (400 μL) was added NBS (10.7 mg, 0.0601 mmol) at room temperature. The reaction was stirred 5 min. before it was quenched by addition of saturated aqueous $NaHCO_3$ (1 mL). The aqueous layer was extracted with CH_2Cl_2 (3 x 5 mL) and the combined organic layers were washed with H_2O (3 x 20 mL), once with brine, and dried over Na_2SO_4. Filtration of the solids followed by concentration under reduced pressure and silica gel chromatography (75% EtOAc/Hexanes) provided Br-vinylogous carbonate **92** (25.3 mg, 84% yield) as a colorless oil.

Br-Vinylogous carbonate 92: FTIR (thin film/NaCl) 3452 (m, br), 2975 (m), 2955 (m), 2929 (m), 1767 (s, br), 1736 (s, br), 1705 (s, br), 1669 (s, br), 1449 (s) cm^{-1}; ^1H NMR (400 MHz, $CDCl_3$) δ 7.96 (d, *J* = 8.5 Hz, 1H), 7.82 (d, *J* = 7.9 Hz, 1H), 7.37–7.41 (nfom, 1H), 7.25–7.29 (nfom, 1H), 5.14 (d, *J* = 11.6 Hz,

1H), 4.57 (m, 1H), 4.22 (ddd, *J* = 17.1, 17.1, 8.9 Hz, 1H), 3.92 (ddd, *J* = 20.8, 20.8, 10.4 Hz, 1H), 3.87 (s, 3H), 3.85 (s, 3H), 3.79 (m, 2H), 2.68 (m, 1H), 2.58 (m, 1H), 2.49 (br s, 1H), 2.01 (m, 2H), 1.70 (s, 9H); ^{13}C NMR (100 MHz, $CDCl_3$) δ 173.2, 169.2, 166.9, 165.7, 150.5, 136.1, 132.1, 126.4, 126.3, 123.4, 121.9, 119.1, 115.3, 97.8, 86.2, 75.4, 74.2, 62.3, 59.1, 55.0, 54.7, 42.7, 28.3, 28.0, 27.6; HRMS (TOF LCMS) calc'd for $C_{27}H_{31}BrNO_{10}$ $[M+H]^+$ 608.1126, found 608.1128.

Preparation of Br-Acetal **93**

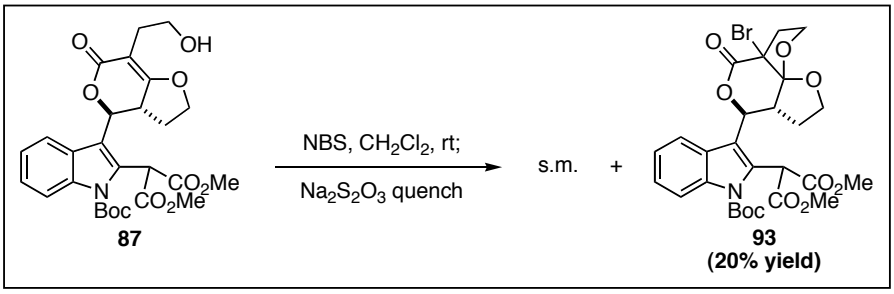

To a solution of vinylogous carbonate **87** (40 mg, 0.0755 mmol) in CH_2Cl_2 (760 μL) was added NBS (17 mg, 0.0955 mmol) at room temperature. The reaction was stirred 10 min. before it was quenched by addition of saturated aqueous $NaHCO_3$ (1 mL) and 10% aqueous $Na_2S_2O_3$ (1 mL). The aqueous layer was extracted with CH_2Cl_2 (3 x 5 mL) and the combined organic layers were washed with H_2O (3 x 20 mL), once with brine, and dried over Na_2SO_4. Filtration of the solids followed by concentration under reduced pressure and silica gel chromatography (gradient elution, 25 → 35 → 45 → 65% EtOAc/Hexanes → 100% EtOAc) provided Br-acetal **93** (9 mg, 20% yield) as a white film and recovered vinylogous carbonate **87** (26 mg, 65% yield).

Br-acetal 93: FTIR (thin film/NaCl) 3052 (w), 2955 (m), 2919 (m), 2852 (w), 1741 (s), 1454 (m) cm^{-1}; ^1H NMR (400 MHz, $CDCl_3$) δ 8.04 (d, J = 8.5 Hz, 1H), 7.67 (d, J = 7.9 Hz, 1H), 7.34–7.38 (nfom, 1H), 7.26–7.29 (nfom, 1H), 5.93 (br d, J = 10.5 Hz, 1H), 5.34 (s, 1H), 4.18 (ddd, J = 8.1, 8.1, 2.4 Hz, 1H), 3.95–4.07 (3H), 3.78 (s, 3H), 3.77 (s, 3H), 3.38 (ddd, J = 12.5, 7.9, 4.3 Hz, 1H and br s, 1H), 2.63 (ddd, J = 12.8, 9.5, 7.8 Hz, 1H), 1.99 (m, 1H), 1.68–1.83 (s, 9H and m, 1H); ^{13}C NMR (100 MHz, $CDCl_3$) δ 167.4, 166.8, 166.4, 150.6, 136.0, 130.4, 126.5, 125.4, 123.3, 120.3, 117.4, 116.1, 111.9, 85.7, 75.2, 68.9, 65.4, 53.4, 53.2, 53.2, 50.1, 47.4, 36.5, 30.0, 28.2; HRMS (TOF LCMS) calc'd for $C_{27}H_{30}BrNNaO_{10}$ $[M+Na]^+$ 630.0951, found 630.0984.

Vinylogous carbonate 87: identical to a characterized sample (^1H NMR, TLC).

Preparation of Boc-Cl-Indolemalonate-Me **103**

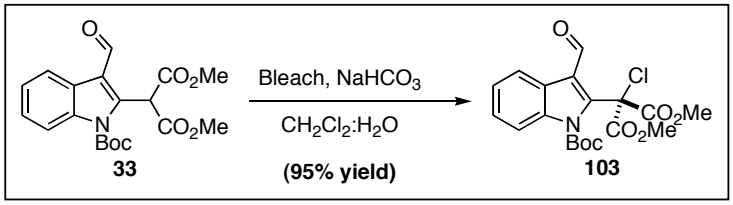

To a solution of indolemalonate-Me **33** (15.0 g, 39.9 mmol) in a biphasic mixture of CH_2Cl_2 (250 mL) and H_2O (150 mL) was added saturated aqueous $NaHCO_3$ (45 mL, ca. 53.5 mmol) at room temperature. The contents stirred 5 min. before household bleach (55 mL of a 6 wt.% soln., 44.3 mmol) was added dropwise *via* addition funnel. The reaction was stirred 2 before it was transferred to a separatory funnel. The layers were separated followed by extraction of the

aqueous layer with CH_2Cl_2 (3 x 150 mL) and the combined organic layers were washed once with brine and dried over Na_2SO_4. Filtration of the solids followed by concentration under reduced pressure provided crude material that was recrystallized from 10% EtOAc/Hexanes yielding pure Boc-Cl-indolemalonate-Me **103** (15.5 g, 95% yield) as colorless crystals that slowly turned light orange over a period of weeks upon storage at room temperature.

Boc-Cl-Indolemalonate-Me 103: m.p. = 109.1 °C (decomposition); FTIR (thin film/NaCl) 3078 (w), 2975 (m), 2950 (m), 2873 (w), 2770 (w), 1741 (s), 1664 (s), 1531 (m), 1454 (s), 1429 (m) cm^{-1}; ^1H NMR (400 MHz, $CDCl_3$) δ 10.38 (s, 1H), 8.29 (d, *J* = 7.6 Hz, 1H), 7.89–7.91 (nfom, 1H), 7.35–7.45 (nfom, 1H and nfom, 1H), 3.88 (s, 6H), 1.70 (2, 9H); ^{13}C NMR (100 MHz, $CDCl_3$) δ 186.3, 165.3, 150.1, 138.7, 135.3, 126.8, 126.0, 124.9, 121.9, 121.0, 114.5, 87.5, 67.6, 54.8, 28.1; HRMS (TOF LCMS) calc'd for $C_{19}H_{20}ClNNaO_7$ $[M+Na]^+$ 432.0821, found 432.0822.

Preparation of Cl-Indolemalonate **104**

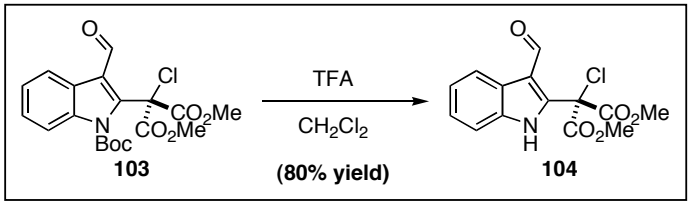

To a solution of Boc-Cl-Indolemalonate-Me **103** (4.0 g, 9.7 mmol) in CH_2Cl_2 (100 mL) was added TFA (10 mL, 129.8 mmol) at room temperature under N_2. The reaction was stirred overnight before it was diluted with CH_2Cl_2

(100 mL) and quenched by slowly pouring onto an ice-water mixture (500 mL) in a separatory funnel. The layers were separated and the aqueous layer was diluted with H_2O (200 mL). The aqueous layer was extracted with CH_2Cl_2 (3 x 100 mL) and the combined organic layers were washed once with saturated aqueous $NaHCO_3$ (200 mL), brine (200 mL), and dried over Na_2SO_4. Filtration followed by concentration under reduced pressure provided Cl-indolemalonate **104** (2.4 g, 80% yield) as a brown solid.

Cl-Indolemalonate 104: m.p. = 150.1 °C (decomposition); FTIR (KBr pellet) 3206 (s, br), 3078 (m), 3021 (w), 2960 (w), 2847 (w), 2827 (w), 1792 (s), 1741 (s), 1618 (s), 1582 (w), 1516 (w), 1485 (s), 1454 (s, br) cm^{-1}; ^1H NMR (400 MHz, DMSO-d_6) δ 12.46 (br s, 1H), 10.13 (s, 1H), 8.15 (d, J = 7.7 Hz, 1H), 7.60 (d, J = 7.7 Hz, 1H), 7.27–7.35 (nfom, 1H and nfom, 1H), 3.87 (s, 6H); ^{13}C NMR (100 MHz, DMSO-d_6) δ 184.6, 164.7, 137.5, 134.8, 126.1, 124.3, 123.1, 120.2, 114.0, 112.9, 66.8, 55.1; HRMS (TOF LCMS) calc'd for $C_{14}H_{13}ClNO_5$ $[M+H]^+$ 310.0477, found 310.0477.

Preparation of Pentacycle **106**

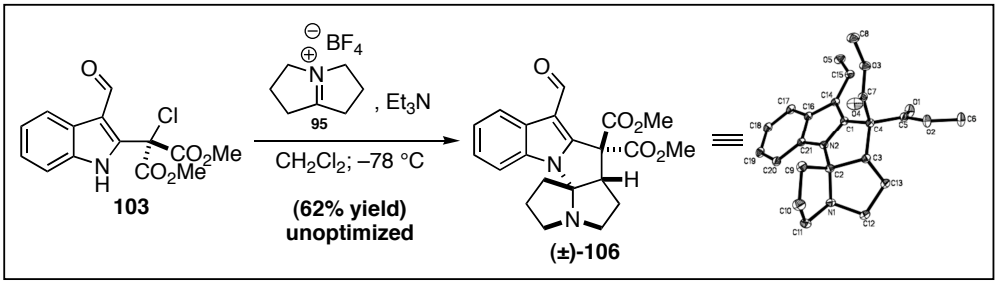

To a solution of iminium **95** (21.4 mg, 0.108 mmol) in CH_2Cl_2 (1 mL) was added Et_3N (40 μL, 0.728 mmol) at room temperature under N_2. The contents were stirred 20 min. before it was cooled to –78 °C. Solid Cl-indolemalonate **104** (30.0 mg, 0.0968 mmol) was added and the reaction stirred 15 hrs, during which time the temperature reached room temperature, before it was quenched by addition of 50% AcOH/H_2O (1 mL). The reaction mixture was transferred to a separatory funnel and the layers were separated. The aqueous layer was extracted with CH_2Cl_2 (3 x 5 mL) and the combined organic layers were washed once with saturated aqueous $NaHCO_3$, brine, and dried over Na_2SO_4. Filtration of the solids followed by concentration under reduced pressure and silica gel chromatography (gradient elution, 25 → 50% EtOAc/Hexanes) provided pentacycle **106** (23.0 mg, 62% yield) as an amorphous solid. A sample suitable for x-ray analysis was obtained following crystallization from THF/Pentanes using the method of vapor diffusion (Appendix 5, A.5.1).

Pentacycle 106: m.p. = 172.0 °C (decomposition); FTIR (thin film/NaCl) 2955 (w), 2868 (w), 2842 (w), 1741 (s), 1654 (s), 1536 (w), 1454 (w) cm^{-1}; ^1H NMR (400 MHz, $CDCl_3$) δ 10.17 (s, 1H), 8.39–8.41 (nfom, 1H), 7.44–7.46 (nfom,

1H), 7.25–7.32 (nfom, 1H and nfom, 1H), 3.86 (s, 3H), 3.76–3.81 (s, 3H and m, 1H), 3.49 (ddd, *J* = 11.0, 7.6, 5.8 Hz, 1H), 3.30 (ddd, *J* = 9.3, 7.5, 1.8 Hz, 1H), 2.88 (m, 2H), 2.60 (m, 1H), 2.03–2.28 (4H), 1.83 (m, 1H); ^{13}C NMR (100 MHz, $CDCl_3$) δ 186.9, 167.7, 167.6, 143.4, 130.7, 130.5, 123.8, 123.4, 123.3, 111.9, 111.3, 97.4, 62.9, 57.6, 55.6, 54.9, 54.1, 53.5, 35.7, 29.1, 26.3; HRMS (TOF LCMS) calc'd for $C_{21}H_{23}N_2O_5$ $[M+H]^+$ 383.1601, found 383.1598.

Preparation of Methyl carbamate **109**

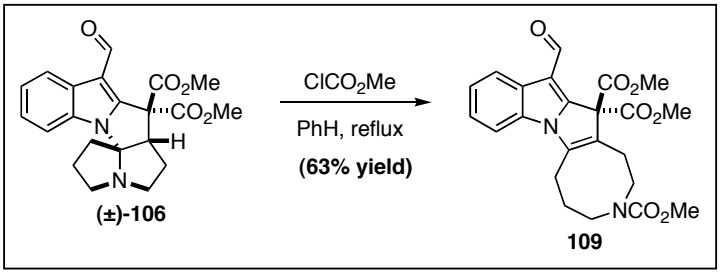

To a solution of pentacycle **106** (33.3 mg, 0.0871 mmol) in PhH (5 mL) was added methyl chloroformate (10 μL, 0.129 mmol) at room temperature under N_2. The reaction was heated to reflux and stirred 1 h before additional methyl chloroformate (50 μL, 0.647 mmol) was added at room temperature. The reaction was heated to reflux and stirred for an additional 1 h before the final addition of methyl chloroformate (50 μL, 0.647 mmol) was added at room temperature and the reaction heated to reflux. The reaction stirred overnight before it was cooled to room temperature, concentrated under reduced pressure, and purified by silica gel chromatography (25% EtOAc/Hexanes) providing methyl carbamate **109** (24 mg, 63% yield) as a white foam.

Methyl carbamate 109: FTIR (thin film/NaCl) 2955 (m), 2852 (w), 1736 (s), 1700 (s), 1659 (s), 1557 (m), 1480 (m), 1454 (s) cm^{-1}; ^1H NMR (400 MHz, $CDCl_3$) δ 10.28 (s, 1H), 8.42–8.44 (nfom, 1H), 7.52–7.57 (nfom, 1H), 7.30–7.37 (nfom, 1H and nfom, 1H), 3.82 (s, 3H), 3.81 (s, 3H), 3.75–3.76 (3H), 3.59 (m, 2H), 3.34 (m, 2H), 2.95 (ddd, *J* = 6.2, 6.2, 6.2 Hz, 2H), 2.73 (ddd, *J* = 10.0, 5.1, 5.1 Hz, 2H), 2.30 (ddd, *J* = 12.0, 5.9, 5.9 Hz, 1H), 2.20 (ddd, *J* = 12.3, 6.1, 6.1 Hz, 1H); ^{13}C NMR (100 MHz, $CDCl_3$, mixture of rotamers) δ 186.0, 166.5, 157.2, 156.4, 145.9, 145.7, 140.4, 140.1, 131.0, 129.2, 129.1, 124.9, 124.8, 123.6, 123.5, 123.4, 123.3, 122.8, 114.4, 110.4, 110.2, 66.3, 54.2, 54.1, 52.9, 52.8, 50.8, 47.7, 46.7, 27.0, 26.7, 26.2, 25.9, 21.6, 21.6; HRMS (TOF LCMS) calc'd for $C_{23}H_{25}N_2O_7$ $[M+H]^+$ 441.1656, found 441.1660.

4.5 Notes and References:

1. (a) *"A Simple Entry to Polycyclopropylated Molecules. Dicyclopropyl Ketone"*, Hart, H.; Curtis, O. E., Jr. *J. Am. Chem. Soc.* **1956**, *78*, 112–116; (b) *"Dicyclopropyl Ketone"*, Curtis, O. E., Jr.; Sandri, J. M.; Crocker, R. E.; Hart, H. *Org. Synth.* **1958**, *38*, 19–21.
2. (a) *"Atom Transfer Cyclization Reactions of α-Iodo Esters, Ketones, and Malonates: Examples of Selective 5-exo, 6-endo, and 7-endo Ring*

Closures", Curran, D. P.; Chang, C. T. *J. Org. Chem.* **1989**, *54*, 3140–3157; (b) *"Lewis Acid Promoted Phenylseleno Group Transfer Tandem Radical Cyclization Reactions"*, Yang, D.; Gao, Q.; Lee, O.-Y. *Org. Lett.* **2002**, *4*, 1239–1241.

3. (a) *"Mechanism of Manganese(III)-Based Oxidation of β-Keto Esters"*, Snider, B. B.; Patricia, J. J.; Kates, S. A. *J. Org. Chem.* **1988**, *53*, 2137–2143; (b) *"Manganese (III) Acetate Initiated Oxidative Free Radical Reaction of 3-Heteroaryl Substituted Malonates"*, Chuang, C.-P.; Wang, S.-F. *Synth. Commun.* **1994**, *24*, 1493–1505.

4. *"Synthesis of 1,4-Dicarbonyl Compounds by the Ceric Ammonium Nitrate Promoted Reaction of Ketones with Vinyl and Isopropenyl Acetate"*, Baciocchi, E.; Giampiero, C.; Ruzziconi, R. *Tetrahedron Lett.* **1987**, *28*, 5357–5360.

5. (a) *"New Cyclization Procedure for Alkenyl-substituted β-Dicarbonyl Compounds using N-Phenylselenophthalimide"*, Jackson, W. P.; Ley, S. V.; Morton, J. A. *J. Chem. Soc., Chem. Commun.* **1980**, 1028–1029; (b) *"Selenium-mediated Cyclization Reactions of Alkenyl-substituted β-Ketoesters"*, Jackson, W. P.; Ley, S. V.; Whittle, A. J. *J. Chem. Soc., Chem. Commun.* **1980**, 1173–1174; (c) *"Novel Intramolecular Cyclopropanation Reaction of Unsaturated β-Keto Esters"*, Yang, D.; Gao, Q.; Lee, C.-S.; Cheung, K.-K. *Org. Lett.* **2002**, *4*, 3271–3274; (d) *"Total Synthesis of Garsubellin A"*, Siegel, D. R.; Danishefsky, S. J. *J. Am.*

Chem. Soc. **2006**, *128*, 1048–1049; (e) *"Differentiation of Nonconventional "Carbanions"–The Total Synthesis of Nemorosone and Clusianone"*, Tsukano, C.; Siegel, D. R.; Danishefsky, S. J. *Angew. Chem. Int. Ed.* **2007**, *46*, 8840–8844.

6. (a) *"An Approach to the Synthesis of Gelsemine: The Intramolecular Reaction of an Allylsilane with an Acyliminium Ion for the Synthesis of One of the Quaternary Centers"*, Clarke, C.; Fleming, I.; Fortunak, J. M. D.; Gallagher, P. T.; Honan, M. C.; Mann, A.; Nuebling, C. O.; Raithby, P. R.; Wolff, J. J. *Tetrahedron Lett.* **1988**, *44*, 3931–3944; (b) *"Base-mediated Hydrolytic Cleavage with Chain Migration of 1-Chloromethyl-tetrahydropyranol[3,4-b]indoles: an Unusual Pathway to 2-Succinoyl Tryptophols"*, Chou, S.-Y.; Chen, C.-H. *Tetrahedron Lett.* **2006**, *47*, 6045–6048 and references therein.

7. At room temperature only starting material was observed by TLC. Decomposition occurred upon heating.

8. (a) *"Studies on 1-Azabicyclo Compounds. XXVII. Synthesis of 1-Methyl-perhydroazocin-5-one from Pyrrolizidine"*, Arata, Y.; Tanaka, K.; Yoshifuji, S.; Kanatomo, S. *Chem. Pharm. Bull.* **1979**, *27*, 981–983; (b) *"A Novel Synthesis of $\Delta^{4(8)}$-Dehydropyrrolizidinium Perchlorate"*, Miyano, S.; Somehara, T.; Nakao, M.; Sumoto, K. *Synthesis* **1978**, 701–702; (c) *"Synthesis of $\Delta^{1[9]}$- and/or $\Delta^{8[9]}$-Dehydroindolizidines and Related Compounds"*, Miyano, S.; Fujii, S.; Yamashita, O.; Toraishi, N.; Sumoto, K.

J. Heterocyclic Chem. **1982**, *19*, 1465–1468; (d) *"1-Azoniabicyclo[3.3.0]oct-1(5)-ene Salt Derivatives and Process for the Preparation of the Same"*, Kurono, M.; Kondo, Y.; Matsumoto, Y.; Oka, M.; Sawai, K. U.S. Patent 5,110,945, May 5, 1992; (e) *"Preparation of 5-Cyanomethyl-1-azabicyclo[3.3.0]octane"*, Kurono, M.; Unno, R.; Inagaki, H.; Baba, Y.; Sawai, K. JP 05286975, November 2, 1993.

9. *"Ring Transformation of 1,2,3,5,6,7-Hexahydropyrrolizinium Perchlorates into 1-Substituted 5-Oxo-perhydroazocines"*, Sumoto, K.; Mibu, N.; Irie, M.; Abe, N.; Miyano, S. *Chem. Pharm. Bull.* **1990**, *38*, 577–580.

10. *"Expedient Synthesis of MLN1251, A CCR5 Antagonist for Treatment of HIV"*, Rönn, M.; McCubbin, Q.; Winter, S.; Veigi, M. K.; Grimster, N.; Alorati, T.; Plamondon, L. *Org. Process Res. Dev.* **2007**, *11*, 241–245.

11. (a) *"Process for Preparing 2-Aryl-2-chloromalonic Diesters"*, Theis, C.; Bordeianu, R.; Latz, W. U.S. Patent 5,777,152, July 7, 1998; (b) *"An Efficacious Method for the Halogenation of β-Dicarbonyl Compounds Under Mildly Acidic Conditions"*, Meketa, M. L.; Mahajan, Y. R.; Weinreb, S. M. *Tetrahedron Lett.* **2005**, *46*, 4749–4751.

12. The crystal structure contained one water molecule.

13. *"N-Mannich Bases of 3-Substituted Indoles and Alkylations with Some N-Indolylmethyltrimethylammonium Iodides"*, Swaminathan, S.; Ranganathan, S.; Sulochana, S. *J. Org. Chem.* **1958**, *23*, 707–711.

Appendix 4: Characterization Spectra Relevant to Chapter Four

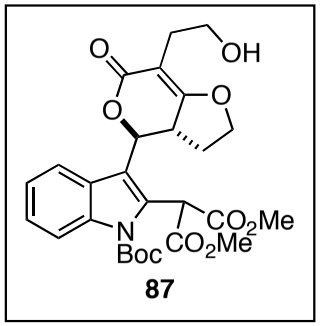

87

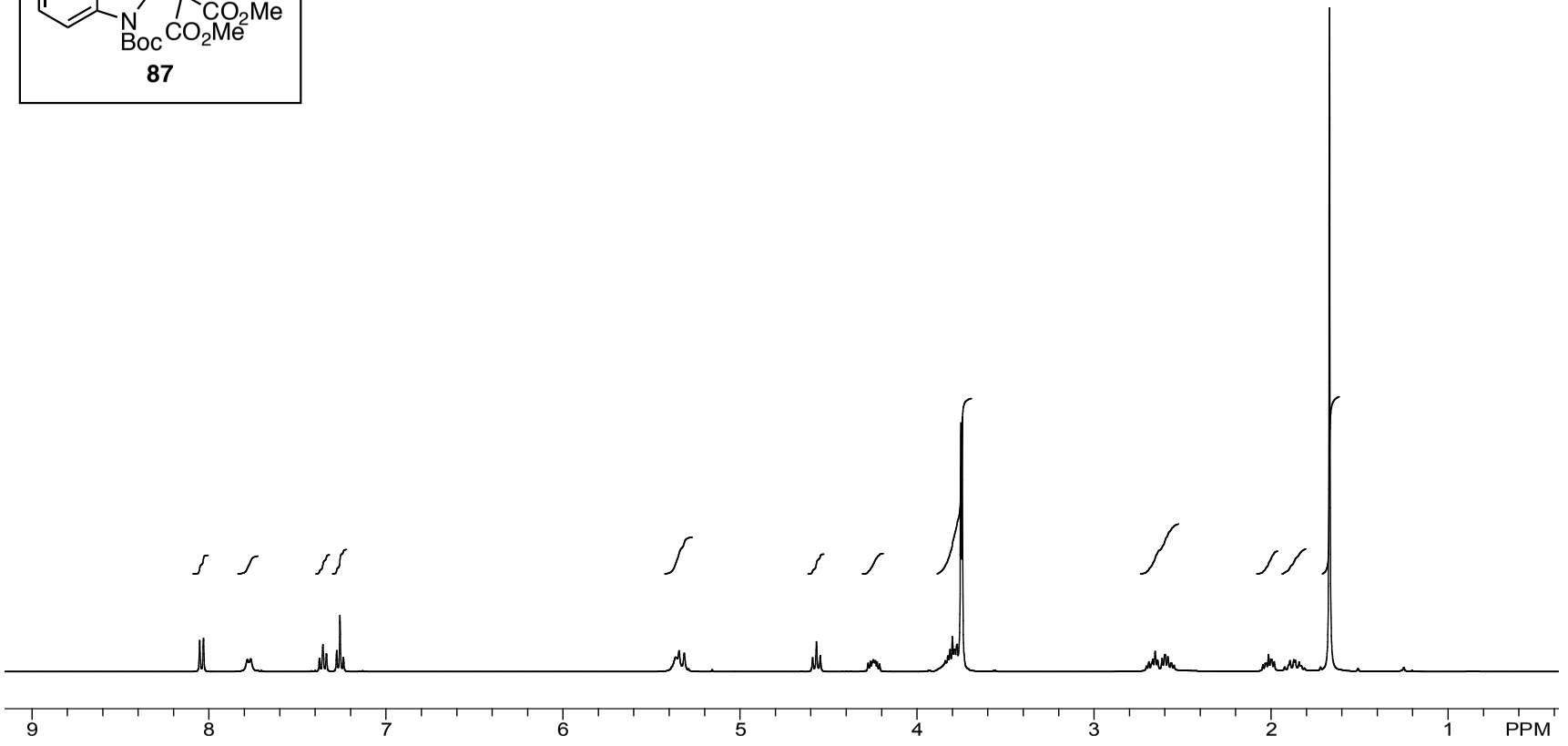

Figure A.4.1 ^{1}H NMR spectrum (400 MHz, $CDCl_3$) of compound **87**

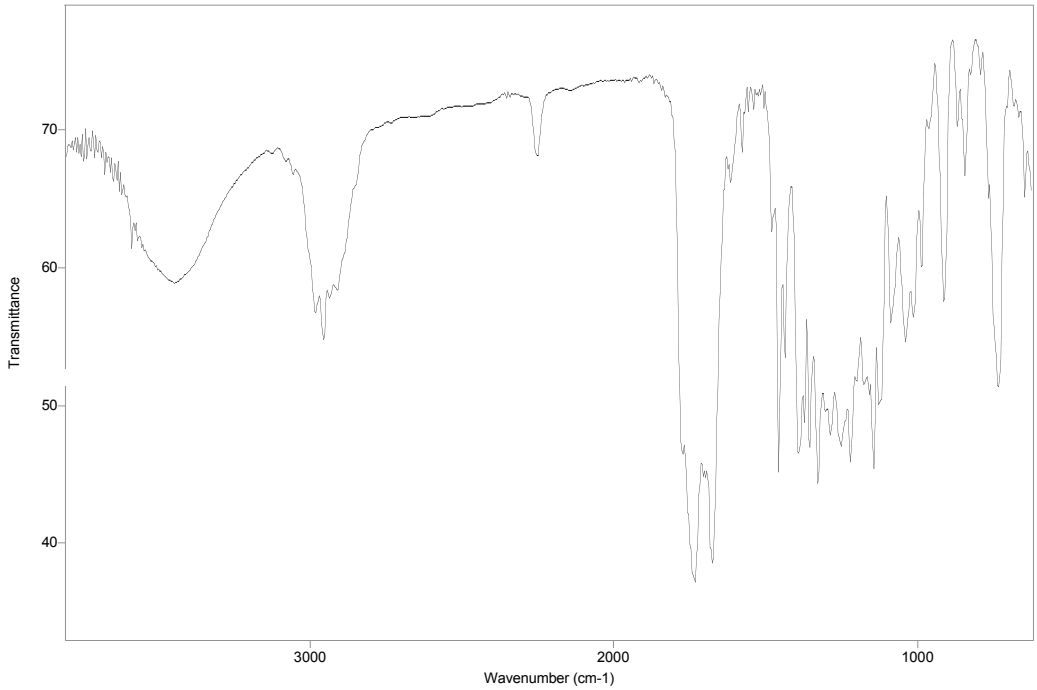

Figure A.4.2 FTIR spectrum (NaCl/thin film) of compound **87**

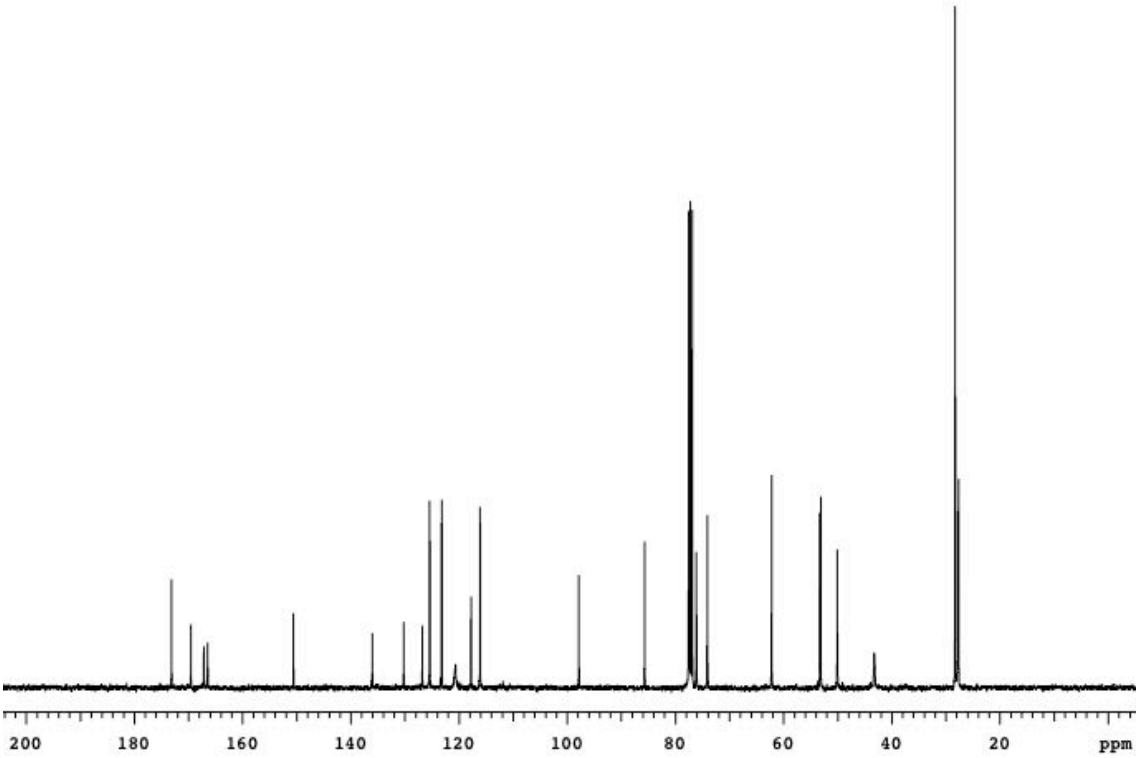

Figure A.4.3 ^{13}C spectrum (100 MHz, $CDCl_3$) of compound **87**

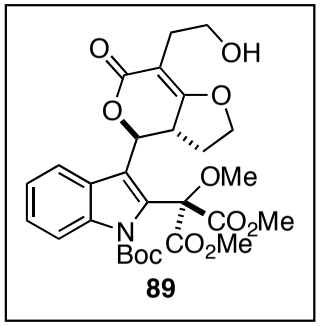

89

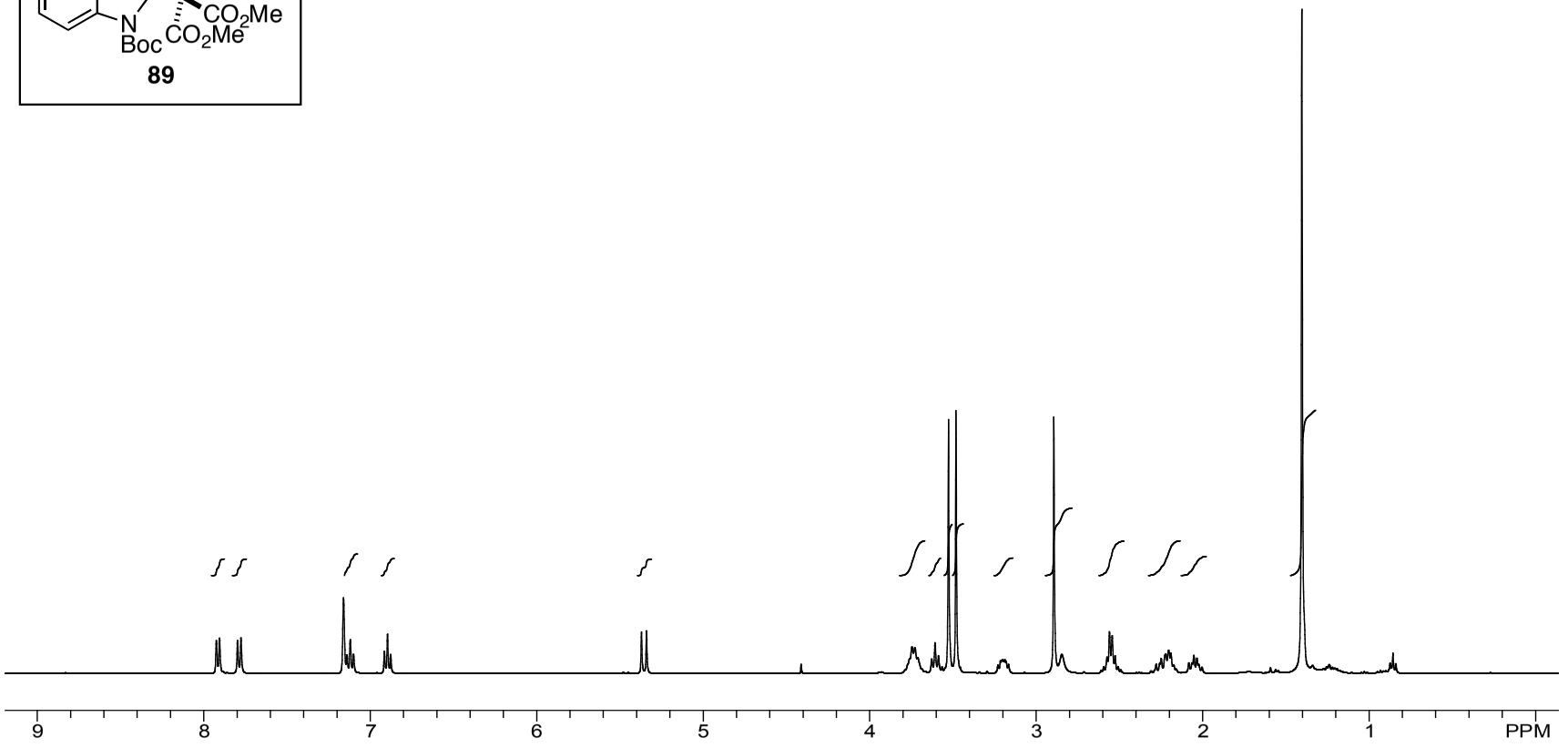

Figure A.4.4 ^{1}H NMR spectrum (400 MHz, Benzene-d_6) of compound **89**

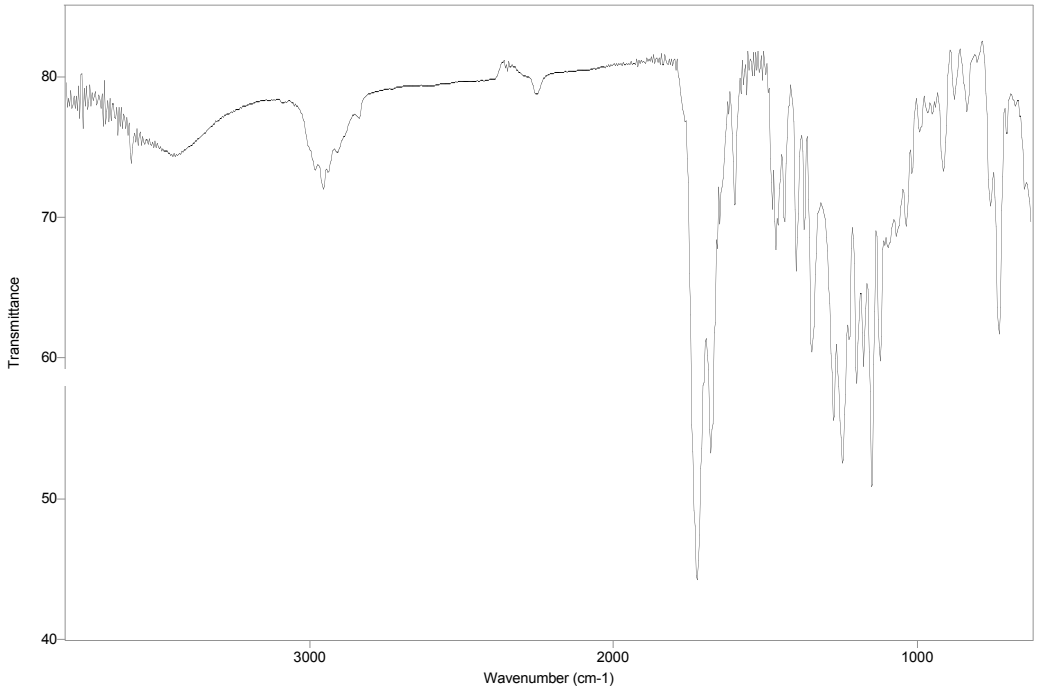

Figure A.4.5 FTIR spectrum (NaCl/thin film) of compound **89**

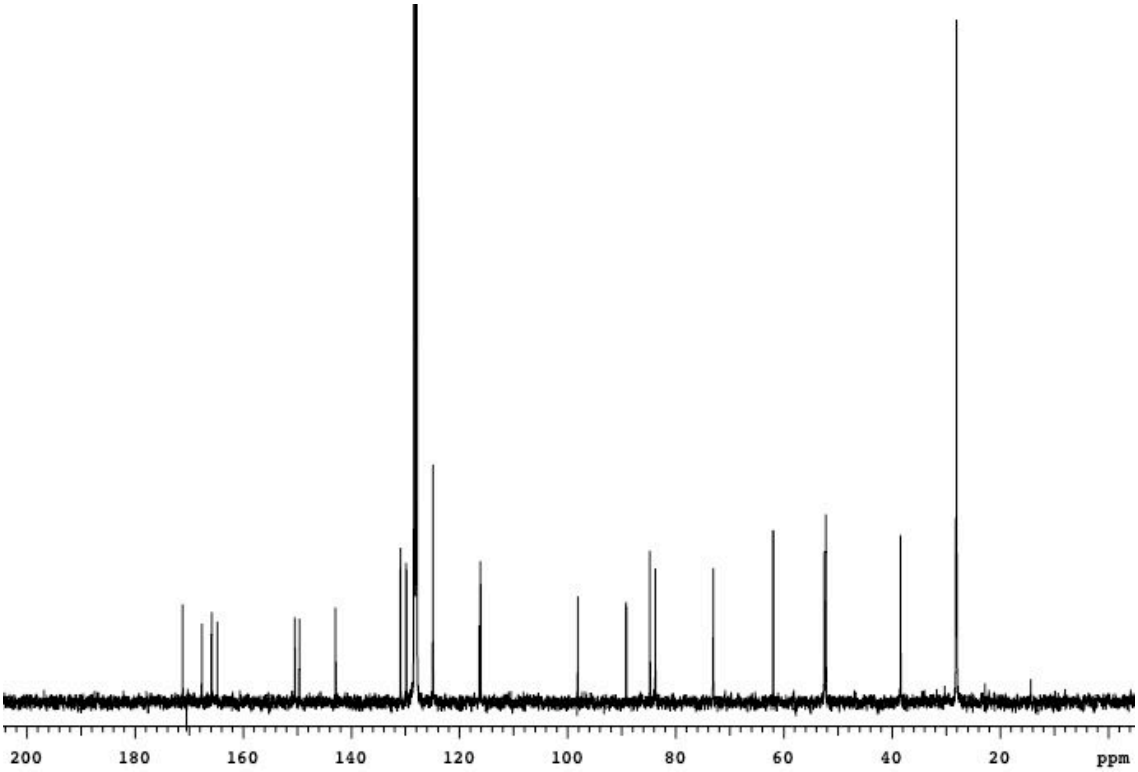

Figure A.4.6 ^{13}C spectrum (100 MHz, Benzene-d_6) of compound **89**

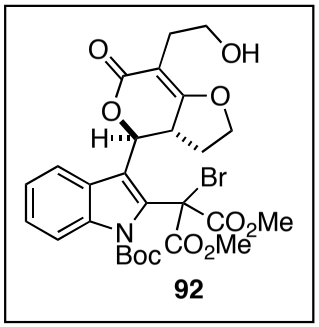

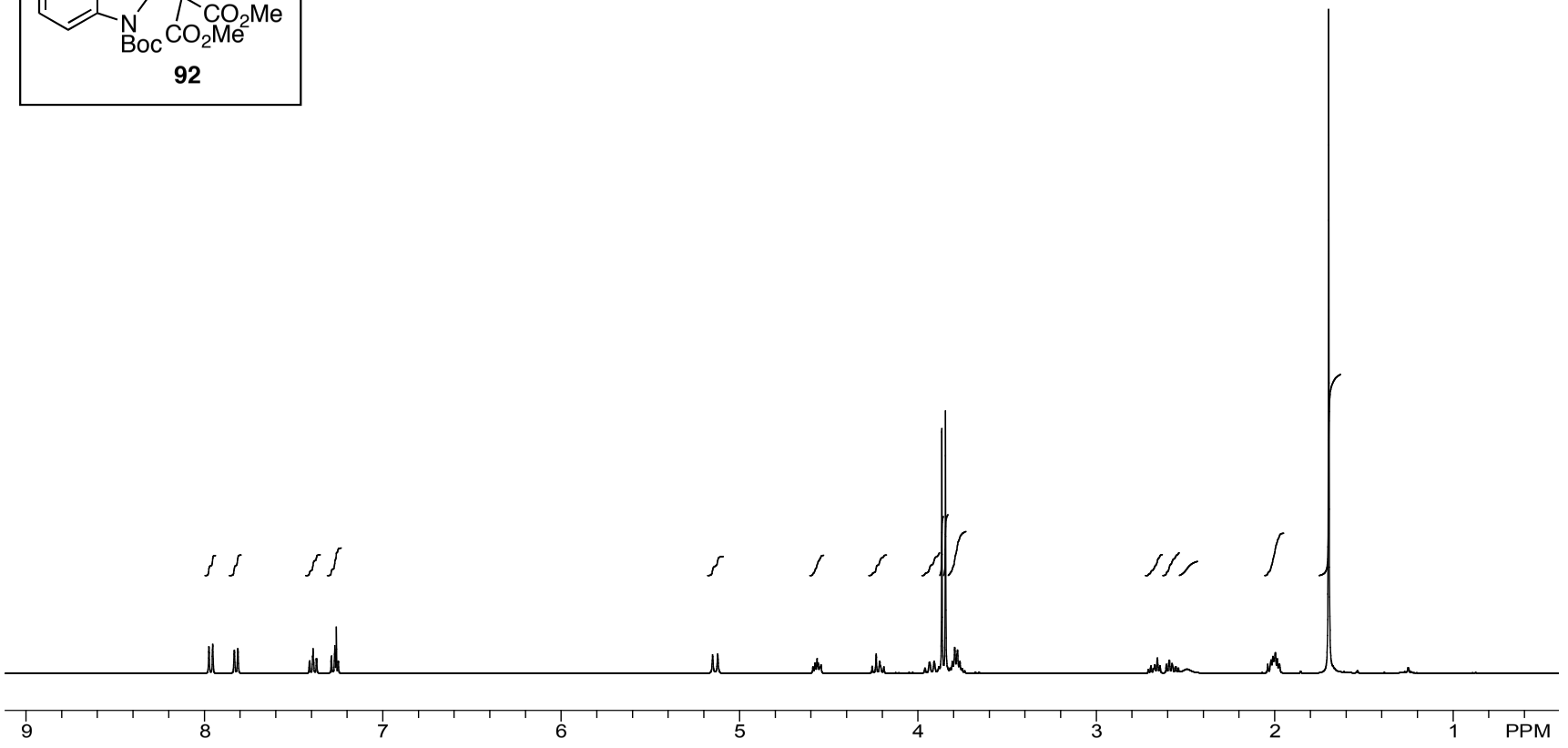

Figure A.4.7 ^{1}H NMR spectrum (400 MHz, $CDCl_3$) of compound **92**

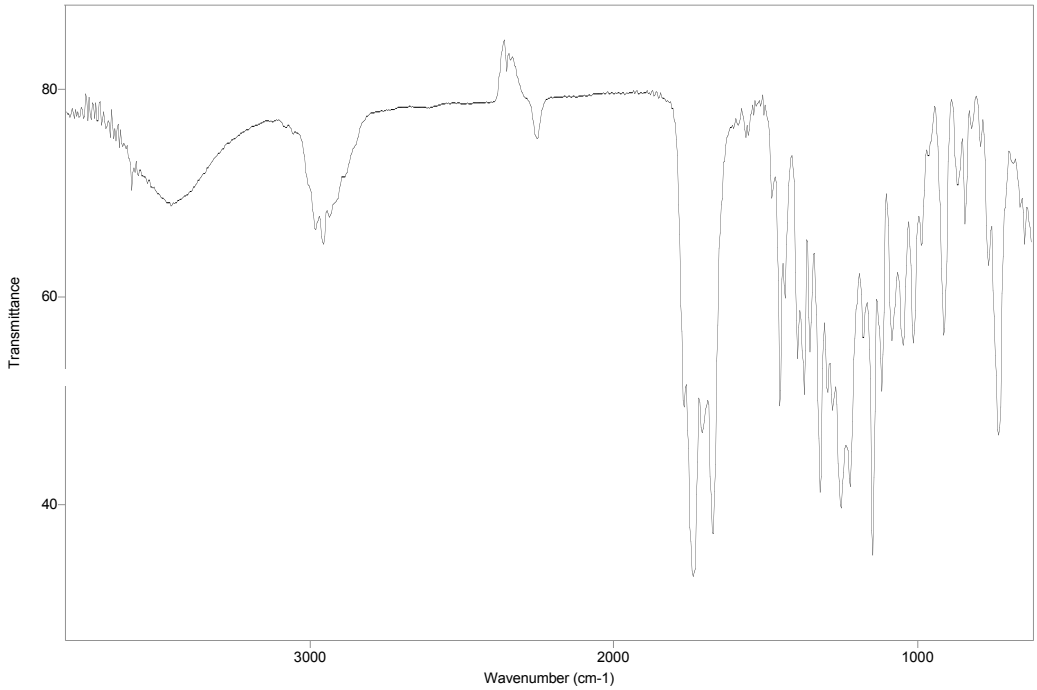

Figure A.4.8 FTIR spectrum (NaCl/thin film) of compound **92**

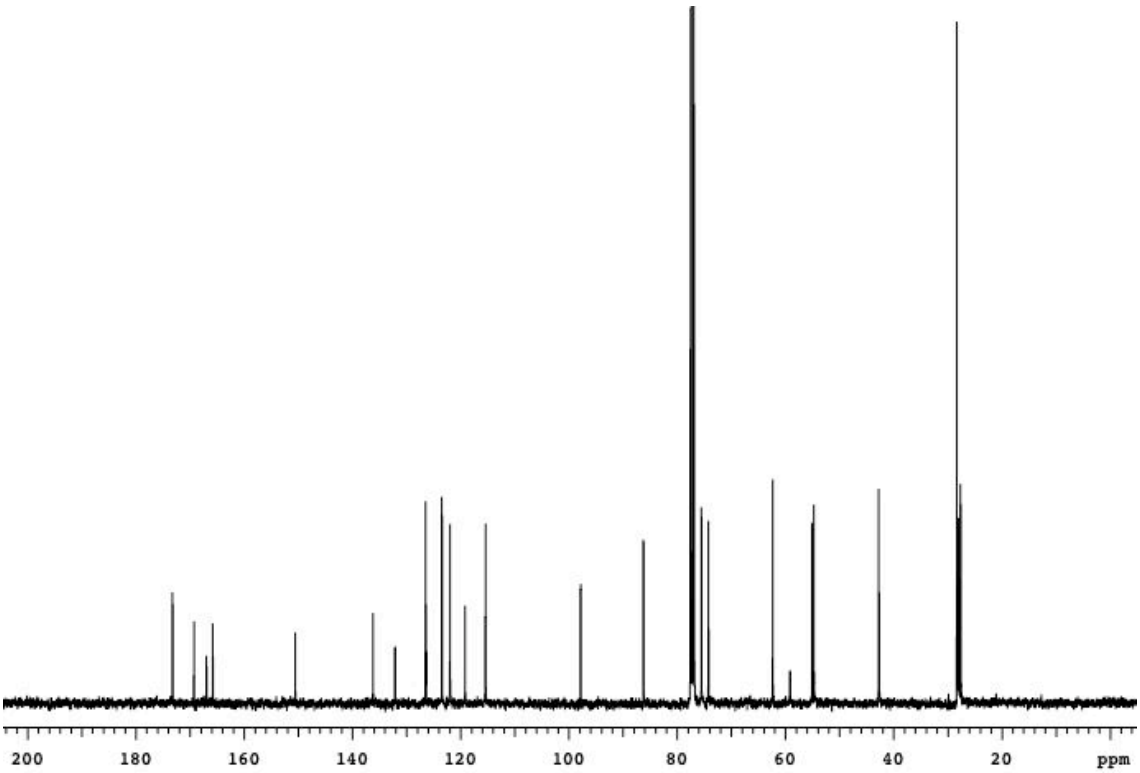

Figure A.4.9 ^{13}C spectrum (100 MHz, $CDCl_3$) of compound **92**

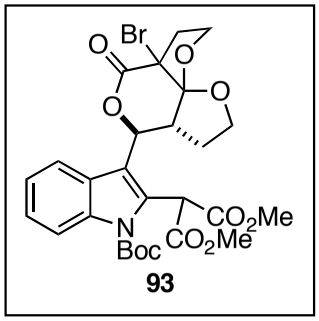

93

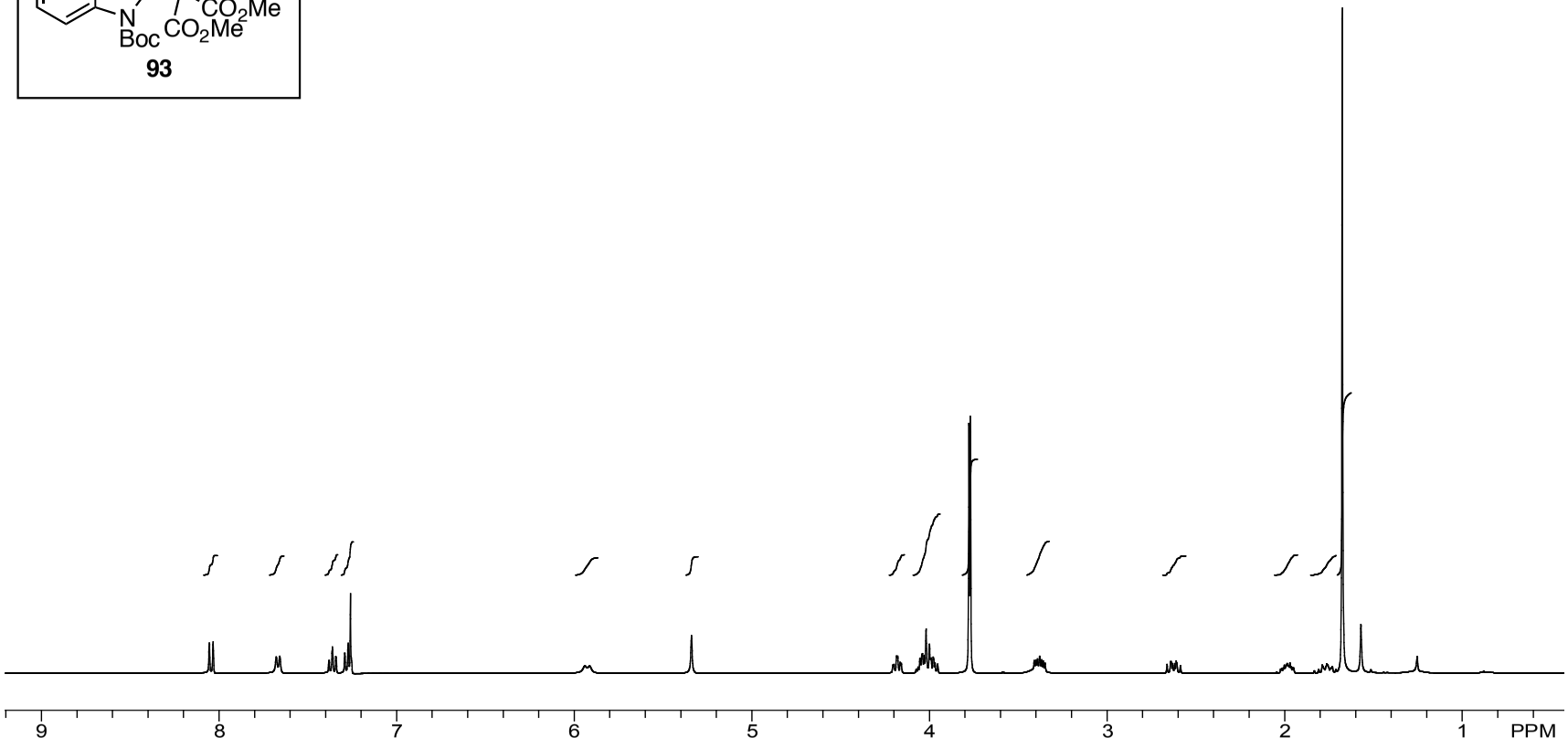

Figure A.4.10 ^{1}H NMR spectrum (400 MHz, $CDCl_3$) of compound **93**

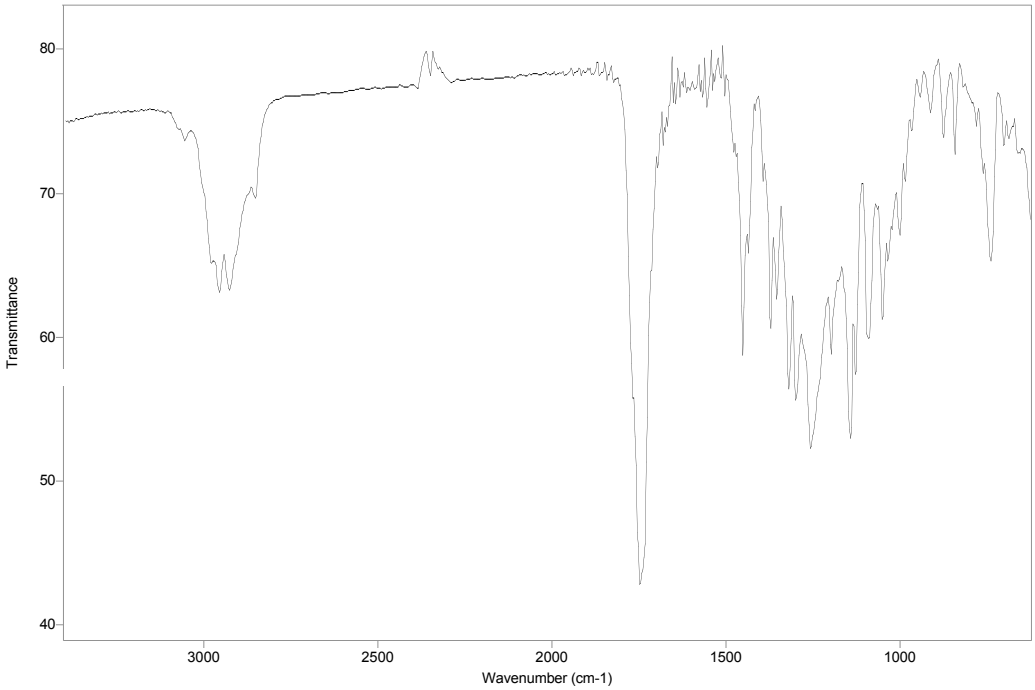

Figure A.4.11 FTIR spectrum (NaCl/thin film) of compound **93**

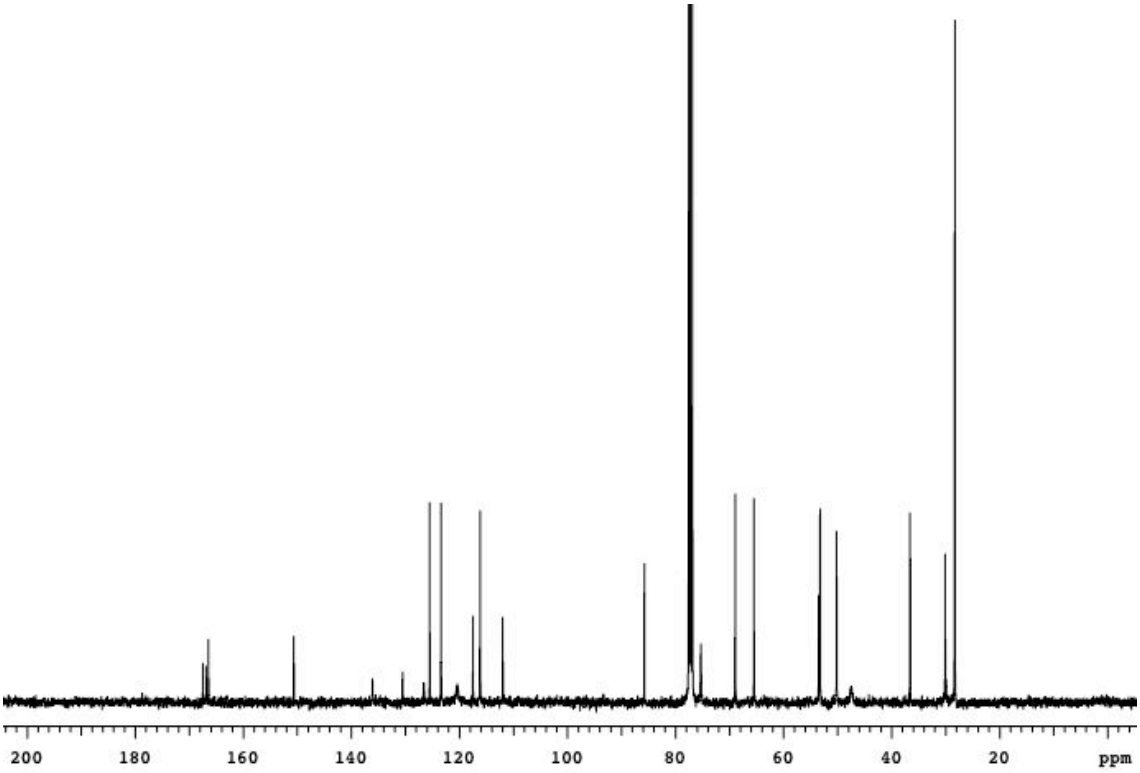

Figure A.4.12 ^{13}C spectrum (100 MHz, $CDCl_3$) of compound **93**

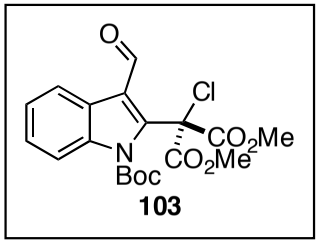

103

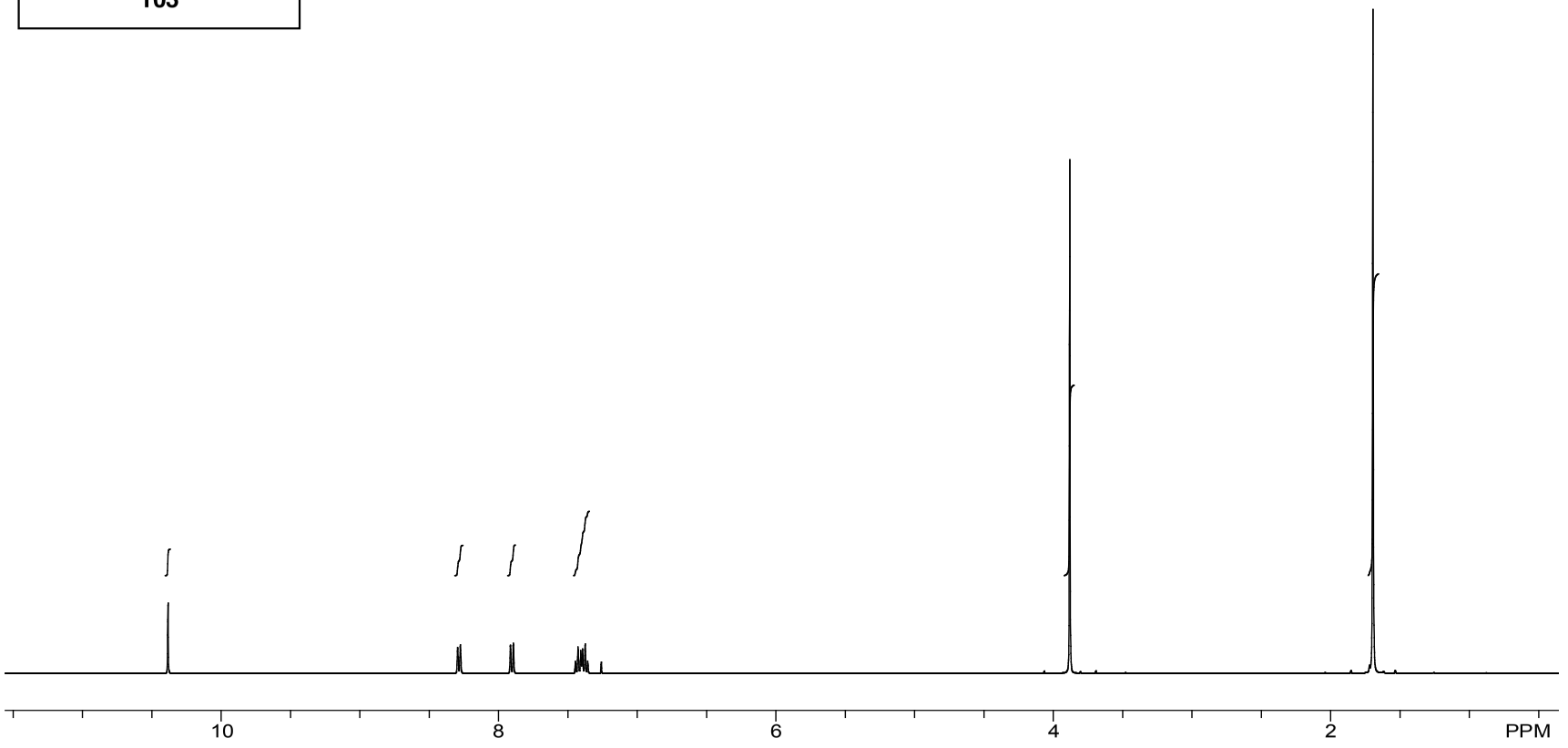

Figure A.4.13 ^{1}H NMR spectrum (400 MHz, $CDCl_3$) of compound **103**

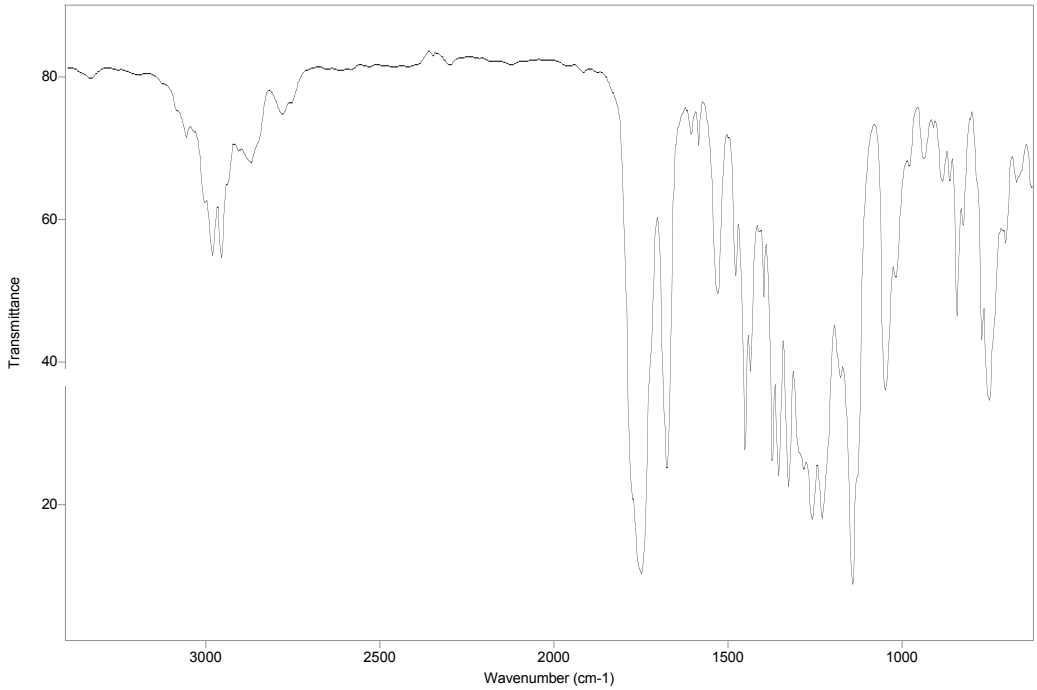

Figure A.4.14 FTIR spectrum (NaCl/thin film) of compound **103**

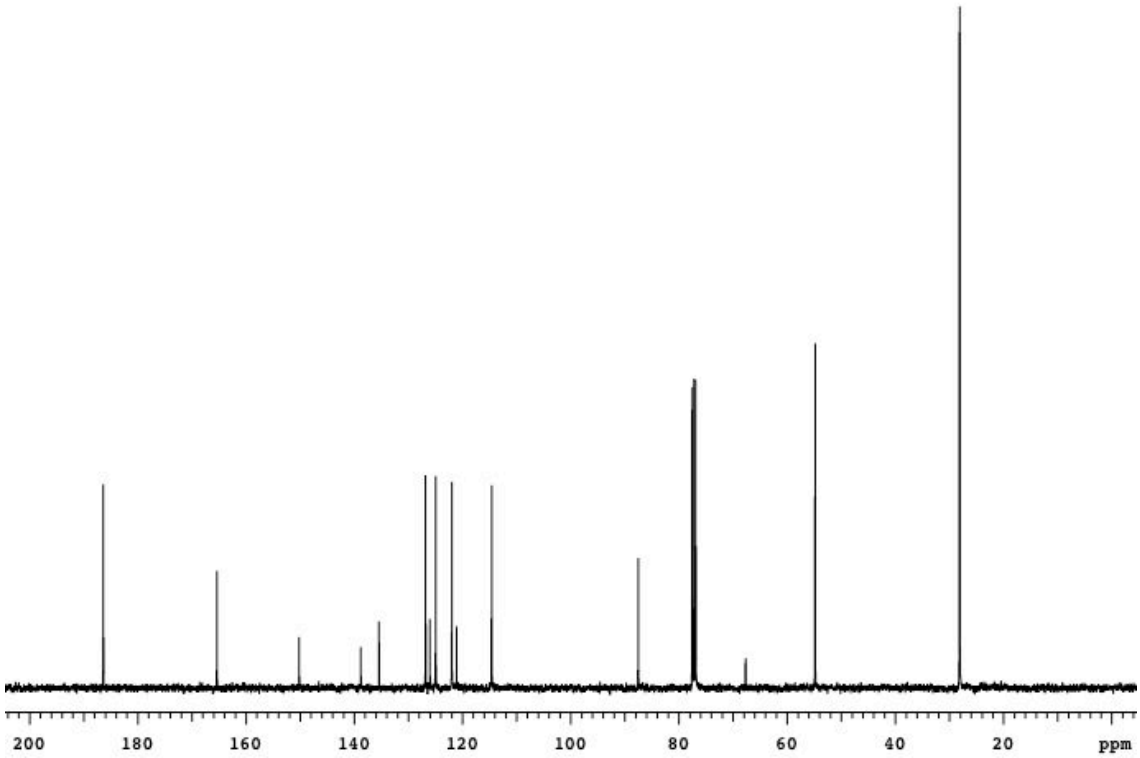

Figure A.4.15 ^{13}C spectrum (100 MHz, $CDCl_3$) of compound **103**

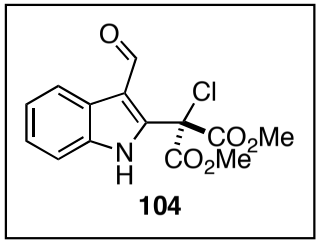

104

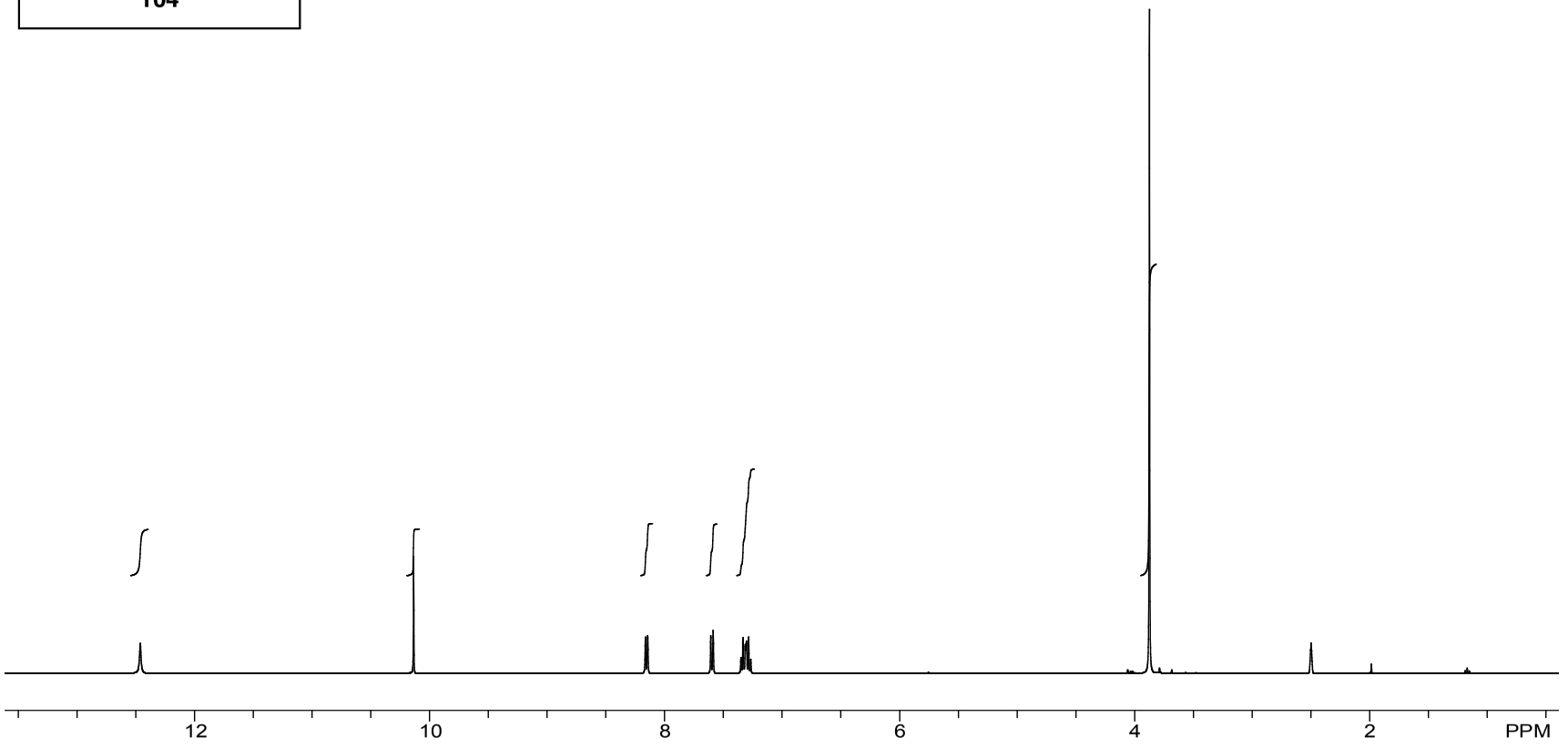

Figure A.4.16 ^{1}H NMR spectrum (400 MHz, DMSO-d_6) of compound **104**

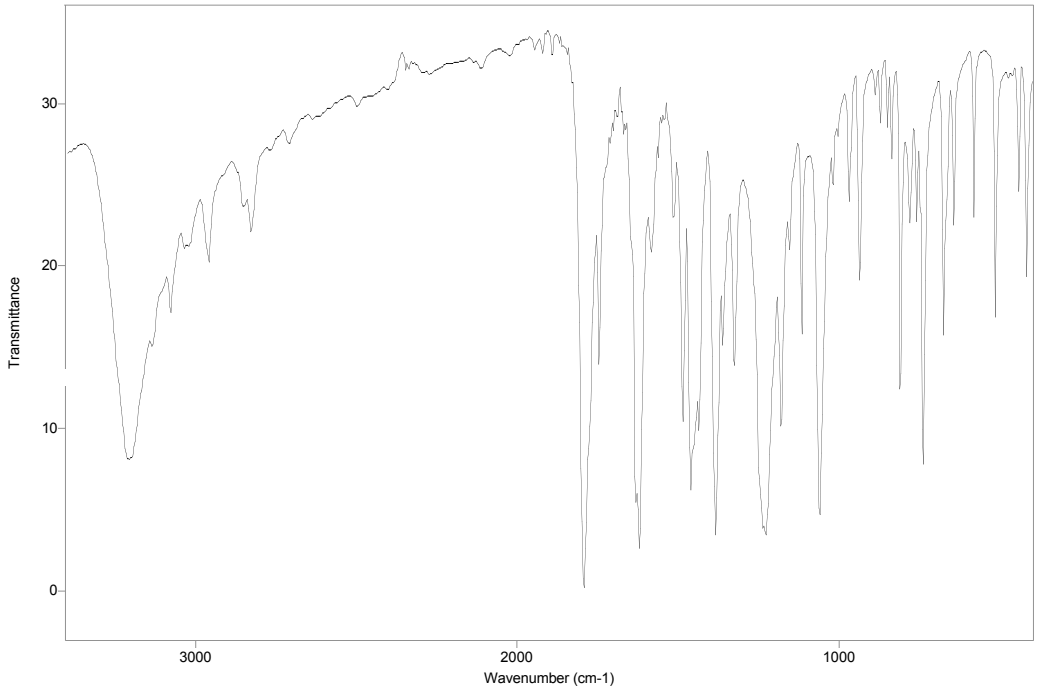

Figure A.4.17 FTIR spectrum (KBr pellet) of compound **104**

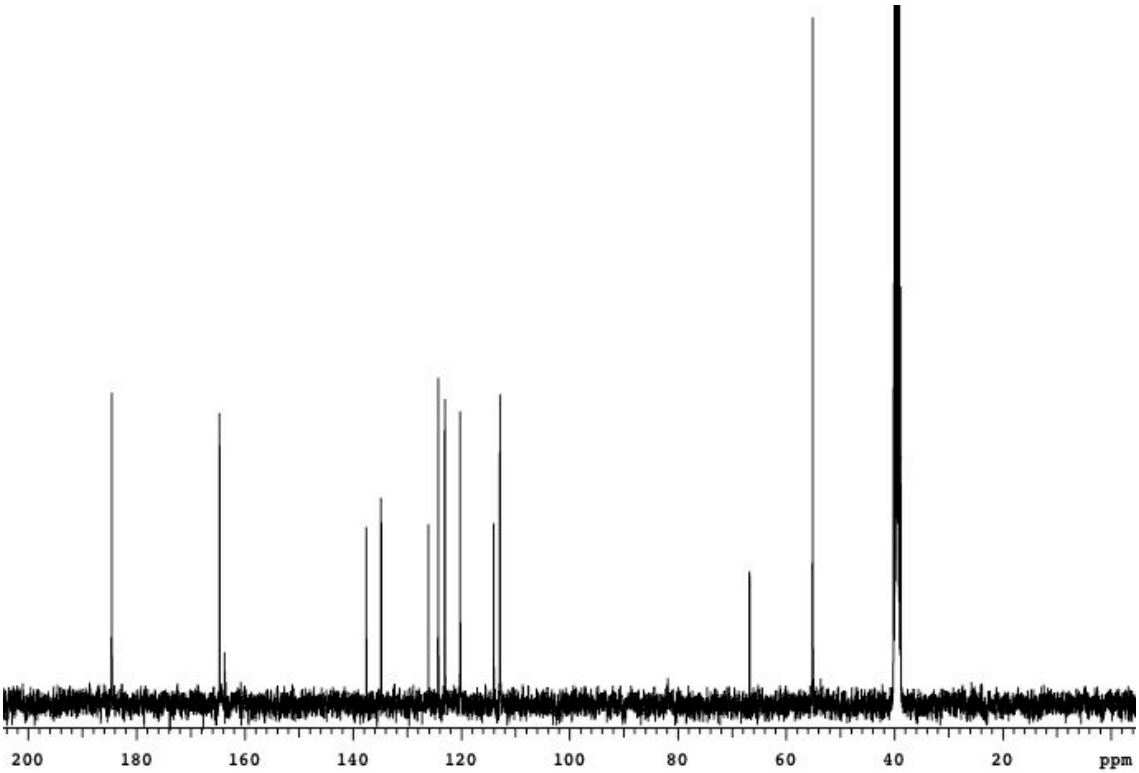

Figure A.4.18 ^{13}C spectrum (100 MHz, DMSO-d_6) of compound **104**

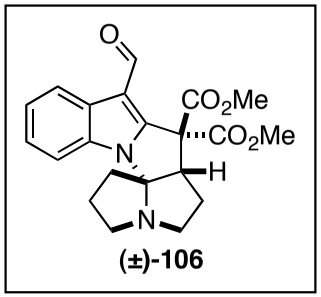

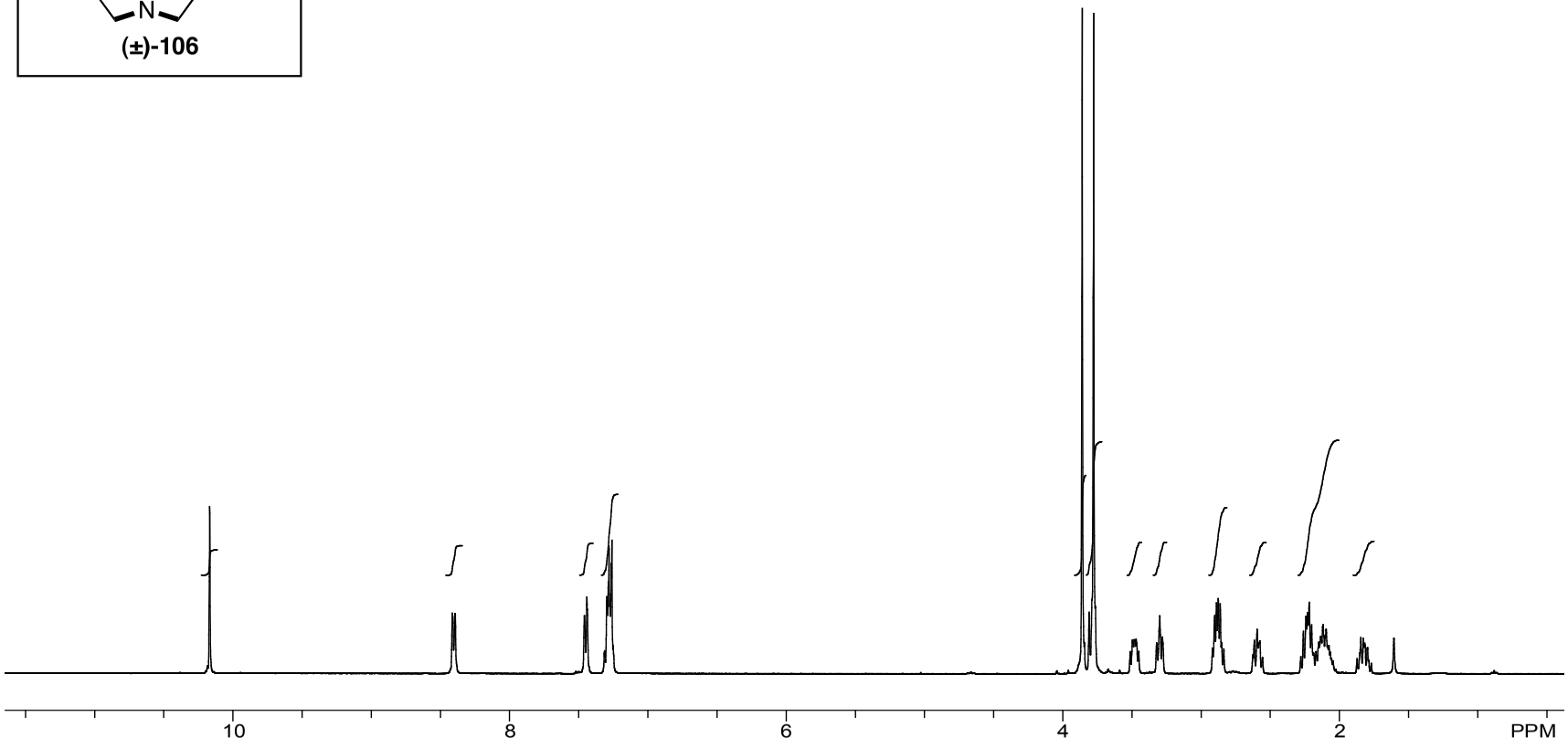

Figure A.4.19 ^{1}H NMR spectrum (400 MHz, $CDCl_3$) of compound **106**

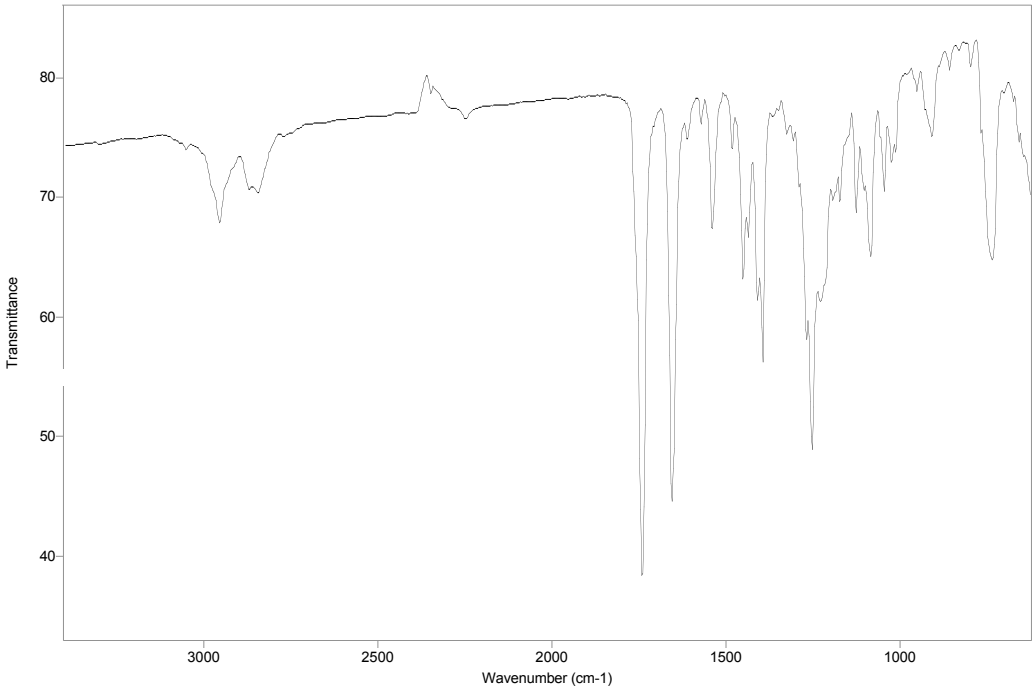

Figure A.4.20 FTIR spectrum (NaCl/thin film) of compound **106**

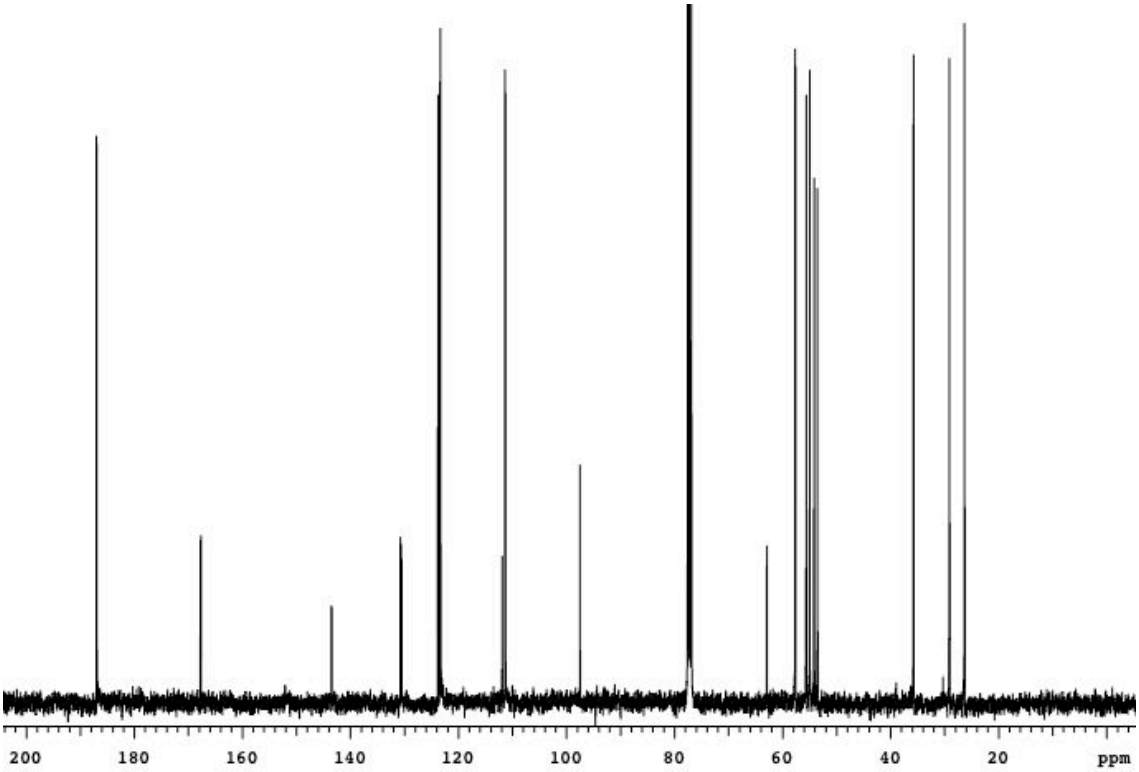

Figure A.4.21 ^{13}C spectrum (100 MHz, $CDCl_3$) of compound **106**

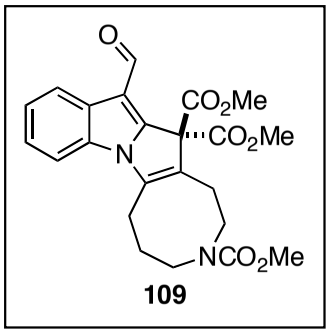

109

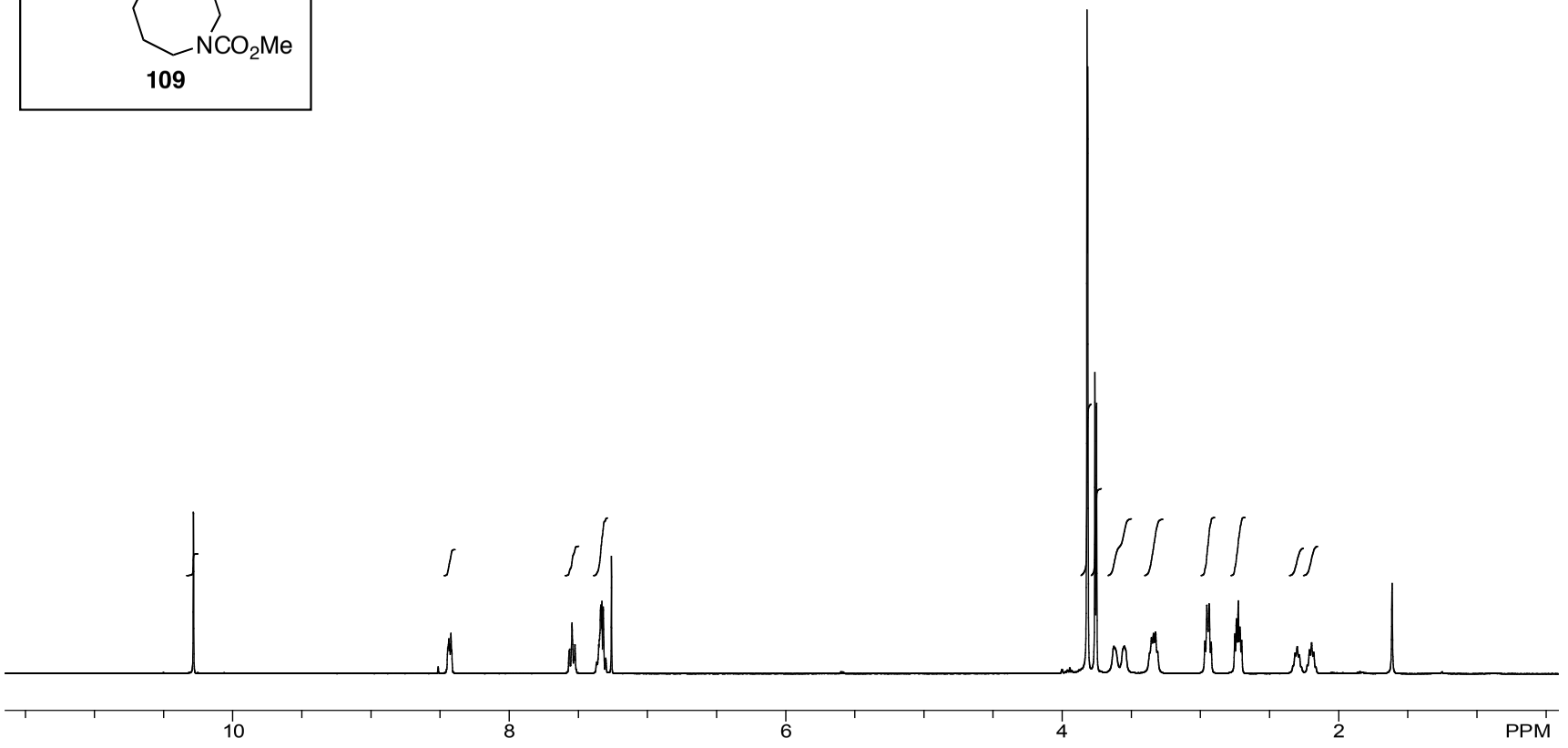

Figure A.4.22 ^{1}H NMR spectrum (400 MHz, $CDCl_3$) of compound **109**

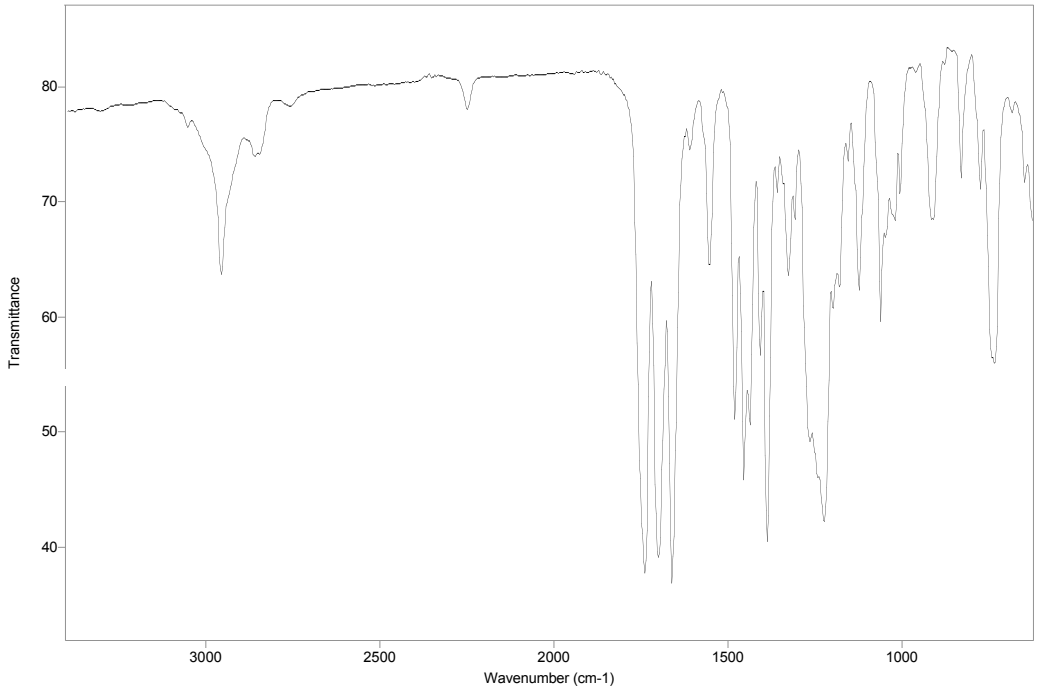

Figure A.4.23 FTIR spectrum (NaCl/thin film) of compound **109**

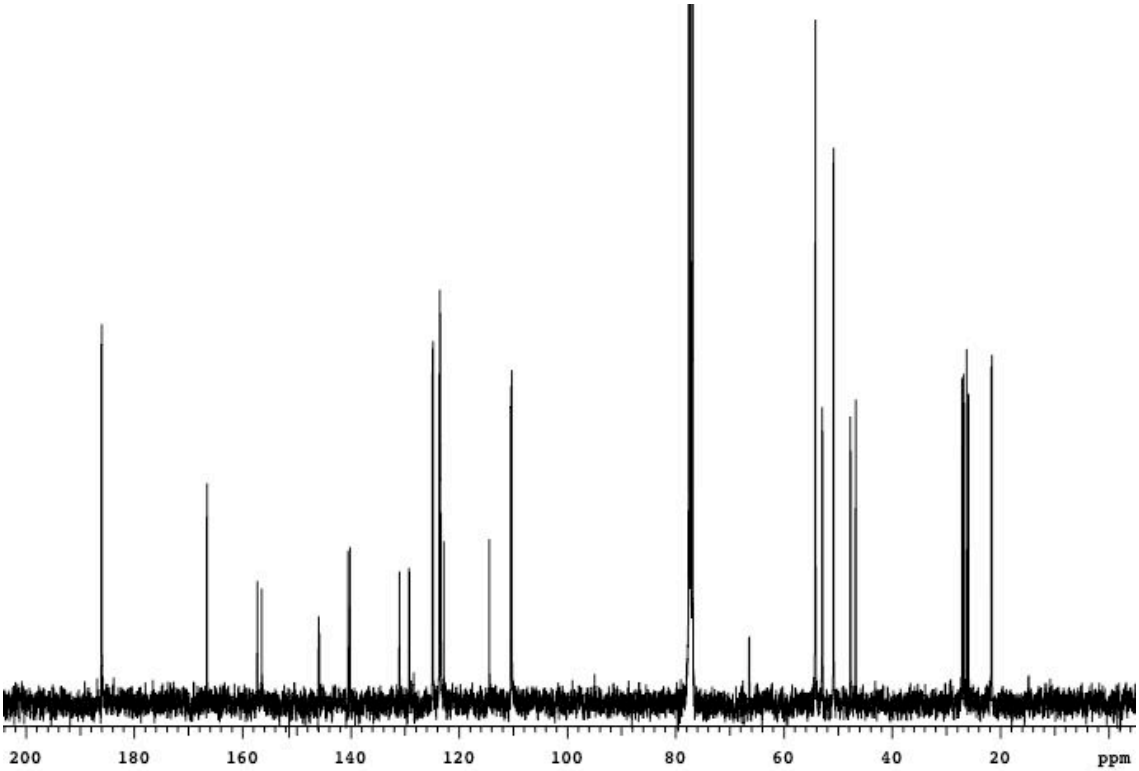

Figure A.4.24 ^{13}C spectrum (100 MHz, $CDCl_3$) of compound **109**

Appendix 5: X-Ray Crystallography Report Relevant to Chapter Four

A.5.1 X-Ray Crystallography Report for Pentacycle 106

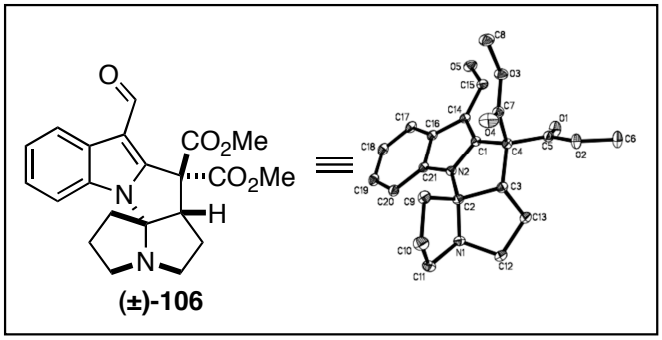

Table A.5.1.1 Crystal data and structure refinement for **106**

Identification code	wood03	
Empirical formula	C21 H23 N2 O5.50	
Formula weight	391.41	
Temperature	100(2) K	
Wavelength	0.71073 Å	
Crystal system	Orthorhombic	
Space group	Fdd2	
Unit cell dimensions	a = 21.7987(4) Å	α= 90°.
	b = 37.4386(6) Å	β= 90°.
	c = 9.13390(10) Å	γ = 90°.
Volume	7454.3(2) Å^3	
Z	16	
Density (calculated)	1.395 Mg/m^3	
Absorption coefficient	0.102 mm^{-1}	
F(000)	3312	
Crystal size	0.69 x 0.19 x 0.18 mm^3	
Theta range for data collection	2.16 to 33.19°.	
Index ranges	-33<=h<=33, -57<=k<=57, -14<=l<=12	
Reflections collected	26759	
Independent reflections	6759 [R(int) = 0.0283]	
Completeness to theta = 33.19°	99.9 %	
Absorption correction	None	
Max. and min. transmission	0.9818 and 0.9330	
Refinement method	Full-matrix least-squares on F^2	

Data / restraints / parameters	6759 / 1 / 262
Goodness-of-fit on F^2	1.033
Final R indices [I>2sigma(I)]	R1 = 0.0346, wR2 = 0.0898
R indices (all data)	R1 = 0.0388, wR2 = 0.0925
Largest diff. peak and hole	0.380 and -0.253 e.$Å^{-3}$

Table A.5.1.2 Atomic coordinates (x 10^4) and equivalent isotropic displacement parameters ($Å^2$ x 10^3) for **106**. U(eq) is defined as one third of the trace of the orthogonalized U^{ij} tensor.

	x	y	z	U(eq)
N(1)	1812(1)	561(1)	9172(1)	14(1)
N(2)	2102(1)	1088(1)	7729(1)	12(1)
O(1)	1069(1)	1072(1)	4115(1)	21(1)
O(2)	1471(1)	534(1)	3561(1)	18(1)
O(3)	2651(1)	1093(1)	3572(1)	17(1)
O(4)	2968(1)	595(1)	4713(1)	24(1)
O(5)	1862(1)	2084(1)	4852(1)	22(1)
C(1)	1992(1)	1184(1)	6324(1)	12(1)
C(2)	2193(1)	703(1)	7976(1)	12(1)
C(3)	1929(1)	552(1)	6527(1)	13(1)
C(4)	1983(1)	855(1)	5375(1)	12(1)
C(5)	1450(1)	845(1)	4281(1)	14(1)
C(6)	960(1)	464(1)	2581(1)	23(1)
C(7)	2594(1)	824(1)	4528(1)	14(1)
C(8)	3253(1)	1116(1)	2889(1)	21(1)
C(9)	2864(1)	615(1)	8362(1)	17(1)
C(10)	2807(1)	294(1)	9381(1)	22(1)
C(11)	2226(1)	386(1)	10241(1)	19(1)
C(12)	1355(1)	316(1)	8518(1)	18(1)
C(13)	1270(1)	457(1)	6966(1)	16(1)
C(14)	1947(1)	1553(1)	6212(1)	13(1)
C(15)	1856(1)	1756(1)	4896(1)	16(1)
C(16)	2039(1)	1688(1)	7682(1)	13(1)
C(17)	2032(1)	2031(1)	8306(1)	16(1)
C(18)	2128(1)	2063(1)	9798(1)	18(1)
C(19)	2237(1)	1763(1)	10685(1)	18(1)
C(20)	2241(1)	1420(1)	10101(1)	16(1)
C(21)	2139(1)	1390(1)	8603(1)	13(1)
O(6)	2500	2500	2785(2)	26(1)

Table A.5.1.3 Bond lengths [Å] and angles [°] for **106**

N(1)-C(2)	1.4713(13)
N(1)-C(12)	1.4800(14)
N(1)-C(11)	1.4832(14)
N(2)-C(1)	1.3538(12)
N(2)-C(21)	1.3859(12)
N(2)-C(2)	1.4736(12)
O(1)-C(5)	1.1999(13)
O(2)-C(5)	1.3369(12)
O(2)-C(6)	1.4528(13)
O(3)-C(7)	1.3394(12)
O(3)-C(8)	1.4547(13)
O(4)-C(7)	1.1952(13)
O(5)-C(15)	1.2291(13)
C(1)-C(14)	1.3898(13)
C(1)-C(4)	1.5065(13)
C(2)-C(9)	1.5399(14)
C(2)-C(3)	1.5499(14)
C(3)-C(13)	1.5335(14)
C(3)-C(4)	1.5512(14)
C(4)-C(5)	1.5328(14)
C(4)-C(7)	1.5447(13)
C(9)-C(10)	1.5252(16)
C(10)-C(11)	1.5289(16)
C(12)-C(13)	1.5233(16)
C(14)-C(15)	1.4359(14)
C(14)-C(16)	1.4483(14)
C(16)-C(17)	1.4055(13)
C(16)-C(21)	1.4141(14)
C(17)-C(18)	1.3833(16)
C(18)-C(19)	1.4052(16)
C(19)-C(20)	1.3907(15)
C(20)-C(21)	1.3913(14)

C(2)-N(1)-C(12)	107.76(8)
C(2)-N(1)-C(11)	107.73(8)
C(12)-N(1)-C(11)	113.66(8)
C(1)-N(2)-C(21)	109.84(8)
C(1)-N(2)-C(2)	115.42(8)
C(21)-N(2)-C(2)	134.60(8)
C(5)-O(2)-C(6)	115.75(8)
C(7)-O(3)-C(8)	114.04(8)
N(2)-C(1)-C(14)	110.27(8)
N(2)-C(1)-C(4)	109.32(8)
C(14)-C(1)-C(4)	140.36(9)
N(1)-C(2)-N(2)	113.00(8)
N(1)-C(2)-C(9)	106.86(8)
N(2)-C(2)-C(9)	111.83(8)
N(1)-C(2)-C(3)	107.03(8)
N(2)-C(2)-C(3)	100.06(7)
C(9)-C(2)-C(3)	118.09(8)
C(13)-C(3)-C(2)	102.08(8)
C(13)-C(3)-C(4)	114.75(8)
C(2)-C(3)-C(4)	106.60(7)
C(1)-C(4)-C(5)	113.95(8)
C(1)-C(4)-C(7)	109.78(8)
C(5)-C(4)-C(7)	108.98(8)
C(1)-C(4)-C(3)	102.02(8)
C(5)-C(4)-C(3)	111.50(8)
C(7)-C(4)-C(3)	110.45(8)
O(1)-C(5)-O(2)	125.40(10)
O(1)-C(5)-C(4)	126.11(9)
O(2)-C(5)-C(4)	108.47(8)
O(4)-C(7)-O(3)	124.65(10)
O(4)-C(7)-C(4)	124.86(9)
O(3)-C(7)-C(4)	110.49(8)
C(10)-C(9)-C(2)	103.27(8)
C(9)-C(10)-C(11)	101.83(8)
N(1)-C(11)-C(10)	105.35(9)
N(1)-C(12)-C(13)	104.04(8)

C(12)-C(13)-C(3)	102.21(8)
C(1)-C(14)-C(15)	126.69(9)
C(1)-C(14)-C(16)	105.57(8)
C(15)-C(14)-C(16)	127.68(9)
O(5)-C(15)-C(14)	123.70(10)
C(17)-C(16)-C(21)	118.81(9)
C(17)-C(16)-C(14)	133.86(10)
C(21)-C(16)-C(14)	107.31(8)
C(18)-C(17)-C(16)	118.47(10)
C(17)-C(18)-C(19)	121.63(10)
C(20)-C(19)-C(18)	121.19(10)
C(19)-C(20)-C(21)	116.83(10)
N(2)-C(21)-C(20)	129.94(9)
N(2)-C(21)-C(16)	107.01(9)
C(20)-C(21)-C(16)	123.05(9)

Symmetry transformations used to generate equivalent atoms:

Table A.5.1.4 Anisotropic displacement parameters ($Å^2$ x 10^3) for **106**. The anisotropic displacement factor exponent takes the form: $-2\pi^2[h^2a^{*2}U^{11} + ... + 2 h k a^* b^* U^{12}]$

	U^{11}	U^{22}	U^{33}	U^{23}	U^{13}	U^{12}
N(1)	16(1)	13(1)	15(1)	3(1)	1(1)	-2(1)
N(2)	14(1)	9(1)	13(1)	0(1)	0(1)	0(1)
O(1)	19(1)	18(1)	27(1)	-4(1)	-6(1)	4(1)
O(2)	18(1)	17(1)	18(1)	-6(1)	-4(1)	1(1)
O(3)	14(1)	21(1)	17(1)	3(1)	3(1)	1(1)
O(4)	21(1)	22(1)	30(1)	5(1)	9(1)	8(1)
O(5)	23(1)	15(1)	28(1)	6(1)	1(1)	-2(1)
C(1)	12(1)	11(1)	12(1)	0(1)	1(1)	0(1)
C(2)	13(1)	9(1)	14(1)	1(1)	1(1)	0(1)
C(3)	14(1)	10(1)	15(1)	-1(1)	1(1)	0(1)
C(4)	12(1)	12(1)	13(1)	-1(1)	1(1)	0(1)
C(5)	14(1)	14(1)	14(1)	-1(1)	0(1)	-1(1)
C(6)	24(1)	23(1)	23(1)	-7(1)	-8(1)	-2(1)
C(7)	14(1)	15(1)	14(1)	-2(1)	2(1)	-1(1)
C(8)	15(1)	26(1)	21(1)	3(1)	6(1)	0(1)
C(9)	13(1)	16(1)	22(1)	2(1)	-1(1)	2(1)
C(10)	19(1)	19(1)	28(1)	7(1)	-2(1)	4(1)
C(11)	21(1)	19(1)	19(1)	7(1)	-2(1)	-1(1)
C(12)	17(1)	17(1)	19(1)	2(1)	1(1)	-5(1)
C(13)	15(1)	17(1)	18(1)	0(1)	1(1)	-4(1)
C(14)	13(1)	10(1)	15(1)	0(1)	1(1)	0(1)
C(15)	14(1)	15(1)	17(1)	4(1)	1(1)	0(1)
C(16)	13(1)	10(1)	16(1)	-1(1)	1(1)	0(1)
C(17)	16(1)	11(1)	22(1)	-3(1)	1(1)	0(1)
C(18)	17(1)	15(1)	22(1)	-6(1)	2(1)	-2(1)
C(19)	17(1)	20(1)	17(1)	-6(1)	2(1)	-3(1)
C(20)	16(1)	16(1)	15(1)	-2(1)	0(1)	-2(1)
C(21)	12(1)	11(1)	15(1)	-1(1)	1(1)	-1(1)
O(6)	31(1)	29(1)	18(1)	0	0	-6(1)

Table A.5.1.5 Hydrogen coordinates (x 10^4) and isotropic displacement parameters ($Å^2$x 10^3) for **106**.

	x	y	z	U(eq)
H(3A)	2160	335	6207	15
H(6A)	1017	231	2111	35
H(6B)	941	650	1830	35
H(6C)	576	463	3141	35
H(8A)	3261	1318	2208	31
H(8B)	3337	894	2354	31
H(8C)	3566	1150	3646	31
H(9A)	3103	554	7474	20
H(9B)	3064	819	8864	20
H(10A)	3167	273	10035	26
H(10B)	2758	69	8823	26
H(11A)	2034	166	10641	23
H(11B)	2322	549	11062	23
H(12A)	963	324	9067	21
H(12B)	1509	67	8509	21
H(13A)	1001	669	6949	19
H(13B)	1097	271	6314	19
H(15A)	1788	1630	4009	19
H(17A)	1964	2236	7717	20
H(18A)	2119	2293	10233	22
H(19A)	2308	1795	11703	22
H(20A)	2311	1216	10696	19
H(6A)	2246(9)	2357(5)	3460(30)	45(5)

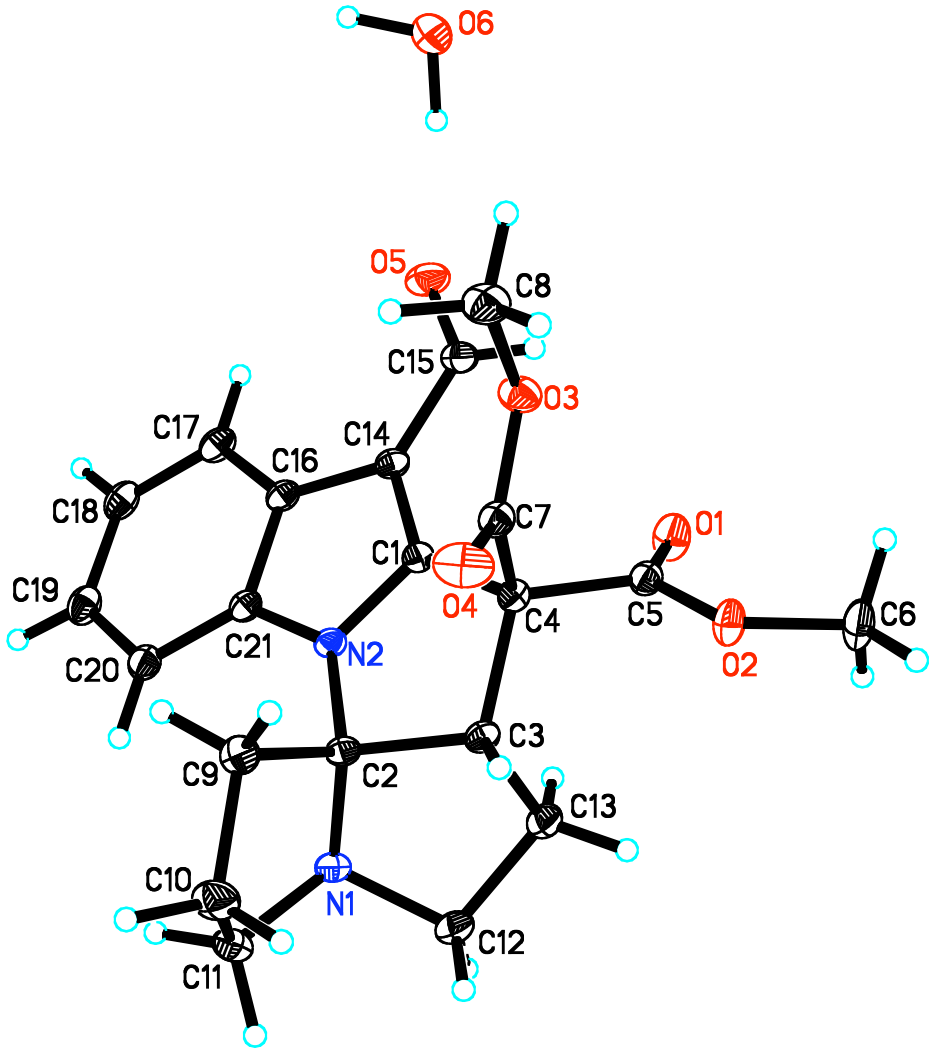
O6
O5
C8
C15
O3
C17
C14
C16
C18
C7
O1
C1
O4
C19
C4
C5
O2
C6
C21
N2
C20
C3
C9
C2
C13
C10
N1
C12
C11

Appendix 6: Notebook Cross-Reference

The following notebook cross-reference has been included to facilitate access to the original spectroscopic data obtained for the compounds present in this work. For each compound a name is given which corresponds to an original notebook reference.

Compounds Appearing in Chapter 2

Compound	Notebook
31	JJD_3_113, JJD_3_119, JJD_4_45, JJD_4_185, JJD_5_145
32	JJD_3_161, JJD_3_269, JJD_4_89, JJD_4_115, JJD_5_129, JJD_5_135, JJD_5_139, JJD_5_179, JJD_5_181
33	JJD_3_79, JJD_3_267, JJD_4_27, JJD_4_97, JJD_4_163, JJD_4_165
34	JJD_3_265, JJD_3_271, JJD_3_273, JJD_3_279, JJD_3_291, JJD_4_47, JJD_4_53, JJD_4_99, JJD_4_187
40	JJD_10_215
41	JJD_3_287, JJD_3_293, JJD_4_69, JJD_4_209, JJD_4_215
42	JJD_10_215
43	JJD_10_215
44	JJD_4_35, JJD_4_55, JJD_4_121, JJD_4_241, JJD_4_261
46	JJD_4_41
39	JJD_4_225, JJD_4_245, JJD_10_175
37	JJD_4_291, JJD_5_13, JJD_5_55, JJD_10_185
49	JJD_4_291, JJD_5_13, JJD_5_55, JJD_10_185
50	JJD_10_187
51	JJD_10_187

Compounds Appearing in Chapter 3

Compound	Notebook
52	JJD_5_29, JJD_5_97
53	JJD_5_35, JJD_5_45, JJD_5_103, JJD_5_169
54	JJD_5_57, JJD_10_177
55	JJD_5_71, JJD_5_89, JJD_10_183
58	JJD_5_79, JJD_10_191
57	JJD_5_79, JJD_10_191
56	JJD_5_79, JJD_10_191
59	JJD_5_109, JJD_5_131, JJD_5_137, JJD_5_141, JJD_5_175, JJD_5_177, JJD_5_183, JJD_5_185
60	JJD_5_115, JJD_5_133, JJD_5_151
61	JJD_5_123, JJD_5_147, JJD_5_153, JJD_5_169
63	JJD_10_145, JJD_10_149
64	JJD_10_173
62	JJD_5_125, JJD_5_143, JJD_5_149, JJD_5_159, JJD_5_171
65	JJD_5_127, JJD_5_155, JJD_5_173, JJD_5_189, JJD_5_195
66	JJD_5_127, JJD_5_155, JJD_5_173, JJD_5_189, JJD_5_195
70	JJD_10_193
69	JJD_10_193
71	JJD_6_251, JJD_6_263, JJD_10_165

Compounds Appearing in Chapter 4

Compound	Notebook
87	JJD_8_47, JJD_8_63
89	JJD_8_51, JJD_10_203
92	JJD_8_75, JJD_10_211
93	JJD_8_79, JJD_10_207
103	JJD_7_123, JJD_7_177
104	JJD_7_111, JJD_7_131, JJD_133
106	JJD_7_89, JJD_7_97, JJD_7_127, JJD_8_129
109	JJD_7_137

Bibliography

Andriantsiferana, M.; Besselievre, R.; Riche, C.; Husson, H. P. *"Structure of Ervitsine, A New Type of Alpha Acyl Indolic Alkaloid"*, *Tetrahedron Lett.* **1977**, *30*, 2587–2590.

Arata, Y.; Tanaka, K.; Yoshifuji, S.; Kanatomo, S. *"Studies on 1-Azabicyclo Compounds. XXVII. Synthesis of 1-Methyl-perhydroazocin-5-one from Pyrrolizidine"*, *Chem. Pharm. Bull.* **1979**, *27*, 981–983.

Baciocchi, E.; Giampiero, C.; Ruzziconi, R. *"Synthesis of 1,4-Dicarbonyl Compounds by the Ceric Ammonium Nitrate Promoted Reaction of Ketones with Vinyl and Isopropenyl Acetate"*, *Tetrahedron Lett.* **1987**, *28*, 5357–5360.

Balci, M. *"Cycloheptatriene-Norcaradiene Equilibrium"*, *Turk. J. Chem.* **1992**, *16*, 42–90.

Ban, Y.; Murakami, Y.; Iwasawa, Y.; Tsuchiya, M.; Takano, N. *"Indole Alkaloids in Medicine"*, *Med. Res. Rev.* **1988**, *8*, 231–308.

Beckman, J. A. *"Diseases of the Veins"*, *Circulation* **2002**, *106*, 2170–2172.

Berson, J. A.; Harter, D. R.; Klinger, H.; Grubb, P. W. *"7,7-Dicarbomethoxycycloheptatriene"*, *J. Org. Chem.* **1968**, *33*, 1669–1671.

Bhaskar, K. V.; Chu, W. L. A.; Gaskin, P. A.; Mander, L. N.; Murofushi, N.; Pearce, D. W.; Pharis, R. P.; Takahashi, N.; Yamaguchi, I. *"Structure Determination and Synthesis of a New Trihydroxy Gibberellin from Brassica campestris cotyledons and a Related Tetrahydroxy Derivative*

from Immature Seeds of Prunus persica", *Tetrahedron Lett.* **1991**, *32*, 6203–6206.

Buchi, G.; Warnhoff, E. W. *"The Structure Of Uleine"*, *J. Am. Chem. Soc.* **1959**, *81*, 4433–4434.

Carret, S.; Depres, J.-P. *"Access to Guaianolides: Highly Efficient Stereocontrolled Total Synthesis of (x)-Geigerin"*, *Angew. Chem. Int. Ed.* **2007**, *46*, 6870–6873.

Carroll, A. R.; Hyde, E.; Smith, J.; Quinn, R. J.; Guymer, G.; Forster, P. I. *"Actinophyllic Acid, a Potent Indole Alkaloid Inhibitor of the Coupled Enzyme Assay Carboxypeptidase U/Hippuricase from the Leaves of Alstonia actinophylla (Apocynaceae)"*, *J. Org. Chem.* **2005**, *70*, 1096–1099.

Cesarman-Maus, G.; Hajjar, K. A. *"Molecular Mechanisms of Fibrinolysis"*, *Br. J. Haematol.* **2005**, *129*, 307–321.

Chen, C.-L. *"Methodologies for the Synthesis of Functionalized Naphthols and Progress Toward the Total Synthesis of Vineomycinone B2 Methyl Ester and Actinophyllic Acid"*, **2007**, Ph.D. Dissertation, University of Texas at Austin, 2007.

Chou, S.-Y.; Chen, C.-H. *"Base-mediated Hydrolytic Cleavage with Chain Migration of 1-Chloromethyl-tetrahydropyranol[3,4-b]indoles: an Unusual Pathway to 2-Succinoyl Tryptophols"*, *Tetrahedron Lett.* **2006**, *47*, 6045–6048.

Chuang, C.-P.; Wang, S.-F. *"Manganese (III) Acetate Initiated Oxidative Free Radical Reaction of 3-Heteroaryl Substituted Malonates"*, *Synth. Commun.* **1994**, *24*, 1493–1505.

Clarke, C.; Fleming, I.; Fortunak, J. M. D.; Gallagher, P. T.; Honan, M. C.; Mann, A.; Nuebling, C. O.; Raithby, P. R.; Wolff, J. J. *"An Approach to the Synthesis of Gelsemine: The Intramolecular Reaction of an Allylsilane with an Acyliminium Ion for the Synthesis of One of the Quaternary Centers"*, *Tetrahedron Lett.* **1988**, *44*, 3931–3944.

Clarke, P. A.; Grist, M.; Ebden, M.; Wilson, C.; Blake, A. J. *"Synthetic Studies on the DEF-Rings of FR182877 and Hexacyclinic Acid"*, *Tetrahedron* **2005**, *61*, 353–363.

Corey, E. J.; Suggs, J. W. *"Pyridinium Chlorochromate-Efficient Reagent for Oxidation of Primary and Secondary Alcohols to Carbonyl Compounds"*, *Tetrahedron Lett.* **1975**, 2647–2650.

Curran, D. P.; Chang, C. T. *"Atom Transfer Cyclization Reactions of α-Iodo Esters, Ketones, and Malonates: Examples of Selective 5-exo, 6-endo, and 7-endo Ring Closures"*, *J. Org. Chem.* **1989**, *54*, 3140–3157.

Curtis, O. E., Jr.; Sandri, J. M.; Crocker, R. E.; Hart, H. *"Dicyclopropyl Ketone"*, *Org. Synth.* **1958**, *38*, 19–21.

Dolfini, J. E.; Dolfini, D. M. *"The Michael-Alkylation Ring Synthesis: Piperidine and Pyrrolidine Construction"*, *Tetrahedron Lett.* **1964**, *5*, 2103–2107.

Fujisawa, T.; Mobele, B. I.; Shimizu, M. *"A Short Synthesis of (–)-(4R,5S)-Sitophilure Using the Regio- and Stereoselective Reduction of 3-Acyltetrahydrothiopyran-4-ones with Baker's Yeast"*, *Tetrahedron Lett.* **1992**, *33*, 5567–5570.

Gaskell, A. J.; Joule, J. A. *"Structure Of Uleine-Relative Stereochemistry"*, *Chem. Ind. (London)* **1967**, 1089.

Goldhaber, S. Z.; Grasso-Correnti, N. *"Treatment of Blood Clots"*, *Circulation* **2002**, *106*, e138–e140.

Grubbs, R. H.; Miller, S. J.; Fu, G. C. *"Ring-Closing Metathesis and Related Processes in Organic Synthesis"*, *Acc. Chem. Res.* **1995**, *28*, 446–452.

Hart, H.; Curtis, O. E., Jr. *"A Simple Entry to Polycyclopropylated Molecules. Dicyclopropyl Ketone"*, *J. Am. Chem. Soc.* **1956**, *78*, 112–116.

Henderson, W. A., Jr.; Buckler, S. A. *"Nucleophilicity of Phosphines"*, *J. Am. Chem. Soc.* **1960**, *82*, 5794–5800.

Henderson, W. A., Jr.; Streuli, C. A. *"Basicity of Phosphines"*, *J. Am. Chem. Soc.* **1960**, *82*, 5791–5794.

Ishiyama, H.; Matsumoto, M.; Sekiguchi, M.; Shigemori, H.; Ohsaki, A.; Kobayashi, J. *"Two New Indole Alkaloids from Aspidosperma subincanum and Geissospermum vellosii"*, *Heterocycles* **2005**, *66*, 651–658.

Jackson, W. P.; Ley, S. V.; Morton, J. A. *"New Cyclization Procedure for Alkenyl-substituted β-Dicarbonyl Compounds using N-Phenylselenophthalimide"*, *J. Chem. Soc., Chem. Commun.* **1980**, 1028–1029.

Jackson, W. P.; Ley, S. V.; Whittle, A. J. *"Selenium-mediated Cyclization Reactions of Alkenyl-substituted β-Ketoesters"*, *J. Chem. Soc., Chem. Commun.* **1980**, 1173–1174.

Jones, D. W.; Thompson, A. M. *"Regioselective Suprafacial 1,5-Hydrogen Shifts in o-Quinodimethanes-A Route to 4-Deoxypodophyllotoxin"*, *J. Chem. Soc. Chem. Commun.* **1988**, 1095–1096.

Joshi, K. C.; Chand, P. *"Biologically-Active Indole-Derivatives"*, *Pharmazie* **1982**, *37*, 1–12.

Joule, J. A.; Ohashi, M.; Gilbert, B.; Djerassi, C. *"Alkaloid Studies-53 Structures Of Nine New Alkaloids From Aspidosperma Dasycarpon A DC"*, *Tetrahedron* **1965**, *21*, 1717–1734.

Kam, T. S.; Sim, K. M.; Lim, T. M. *"Tronoharine, a Novel Hexacyclic Indole Alkaloid from a Malayan Tabernaemontana"*, *Tetrahedron Lett.* **1999**, *40*, 5409–5412.

Konopelski, J. P.; Hottenroth, J. M.; Oltra, H. M.; Veliz, E. A.; Yang, Z. C. *"Synthetic Studies on Diazonamide A. Benzofuranone-Tyrosine and Indole-Oxazole Fragment Support Studies"*, *Synlett* **1996**, 609–611.

Koo, S. H.; Liebeskind, L. S. *"General Synthetic Entry to Highly-Oxygenated, Angularly-Fused Polycyclic Aromatic-Compounds"*, *J. Am. Chem. Soc.* **1995**, *117*, 3389–3404.

Koyama, K.; Hirasawa, Y.; Zaima, K.; Hoe, T. C.; Chan, K. L.; Morita, H. *"Alstilobanines A-E, New Indole Alkaloids from Alstonia angustiloba"*, *Biorg. Med. Chem.* **2008**, *16*, 6483–6488.

Kurono, M.; Kondo, Y.; Matsumoto, Y.; Oka, M.; Sawai, K. *"1-Azoniabicyclo[3.3.0]oct-1(5)-ene Salt Derivatives and Process for the Preparation of the Same"*, U.S. Patent 5,110,945, May 5, 1992.

Kurono, M.; Unno, R.; Inagaki, H.; Baba, Y.; Sawai, K. *"Preparation of 5-Cyanomethyl-1-azabicyclo[3.3.0]octane"*, JP 05286975, November 2, 1993.

Lee, P. H.; Cho, M.; Han, I.-S.; Kim, S. *"Facile Nucleophilic Substitution of 3-tert-butyl-Dimethylsilyloxyalk-2-enylphosphonium Salts"*, *Tetrahedron Lett.* **1999**, *40*, 6975–6978.

Leurs, J.; Nerme, V.; Sim, Y.; Hendriks, D. *"Carboxypeptidase U (TAFIa) Prevents Lysis from Proceeding into the Propagation Phase through a Threshold-Dependent Mechanism"*, *J. Thromb. Haemostasis* **2004**, *2*, 416–423.

Majetich, G.; Condon, S.; Hull, K.; Ahmad, S. *"1,3-Oxidative Rearrangements of Dienols"*, *Tetrahedron Lett.* **1989**, *30*, 1033–1036.

Marino, J. P.; Rubio, M. B.; Cao, G. F.; de Dios, A. *"Total Synthesis of (+)-Aspidospermidine: A New Strategy for the Enantiospecific Synthesis of Aspidosperma Alkaloids"*, *J. Am. Chem. Soc.* **2002**, *124*, 13398–13399.

Martin, C. L.; Overman, L. E.; Rohde, J. M. *"Total Synthesis of (+/-)-Actinophyllic Acid"*, *J. Am. Chem. Soc.* **2008**, *130*, 7568–7569.

Massiot, G.; Boumendjel, A.; Nuzillard, J. M.; Richard, B.; Lemenolivier, L.; David, B.; Hadi, H. A. *"Alkaloids from Alstonia-undulifolia"*, *Phytochemistry* **1992**, *31*, 1078–1079.

Meketa, M. L.; Mahajan, Y. R.; Weinreb, S. M. *"An Efficacious Method for the Halogenation of β-Dicarbonyl Compounds Under Mildly Acidic Conditions"*, *Tetrahedron Lett.* **2005**, *46*, 4749–4751.

Miranda, E. C.; Blechert, S. *"Gilbertin, A New Indole Alkaloid Type"*, *Tetrahedron Lett.* **1982**, *23*, 5395–5398.

Miyano, S.; Fujii, S.; Yamashita, O.; Toraishi, N.; Sumoto, K. *"Synthesis of $\Delta^{1[9]}$- and/or $\Delta^{8[9]}$-Dehydroindolizidines and Related Compounds"*, *J. Heterocyclic Chem.* **1982**, *19*, 1465–1468.

Miyano, S.; Somehara, T.; Nakao, M.; Sumoto, K. *"A Novel Synthesis of $\Delta^{4(8)}$-Dehydropyrrolizidinium Perchlorate"*, *Synthesis* **1978**, 701–702.

Ohashi, M.; Gilbert, B.; Joule, J. A.; Djerassi, C. *"Structures of Five New Aspidosperma Alkaloids Related to Uleine"*, *Experientia* **1964**, *20*, 363–364.

Piancatelli, G.; Scettri, A.; D'Auria, M. *"Pyridinium Chlorochromate: A Versatile Oxidant in Organic Synthesis"*, *Synthesis* **1982**, 245–258.

Rönn, M.; McCubbin, Q.; Winter, S.; Veigi, M. K.; Grimster, N.; Alorati, T.; Plamondon, L. *"Expedient Synthesis of MLN1251, A CCR5 Antagonist for Treatment of HIV"*, *Org. Process Res. Dev.* **2007**, *11*, 241–245.

Sakharov, D. V.; Plow, E. F.; Rijken, D. C. *"On the Mechanism of the Antifibrinolytic Activity of Plasma Carboxypeptidase B"*, *J. Biol. Chem.* **1997**, *272*, 14477–14482.

Shoda, H.; Nakamura, T.; Tanino, K.; Kuwajima, I. *"Lewis Acid Promoted Ene-like Reactions of Enol Ethers with Aldehydes"*, *Tetrahedron Lett.* **1993**, *34*, 6281–6284.

Showalter, H. D. H.; Sercel, A. D.; Leja, B. M.; Wolfangel, C. D.; Ambroso, L. A.; Elliott, W. L.; Fry, D. W.; Kraker, A. J.; Howard, C. T.; Lu, G. H.; Moore, C. W.; Nelson, J. M.; Roberts, B. J.; Vincent, P. W.; Denny, W. A.; Thompson, A. M. *"Tyrosine Kinase Inhibitors. 6. Structure-Activity Relationships Among N- and 3-Substituted 2,2'-Diselenobis(1H-indoles) for Inhibition of Protein Tyrosine Kinases and Comparative in vitro and in vivo Studies Against Selected Sulfur Congeners"*, *J. Med. Chem.* **1997**, *40*, 413–426.

Siegel, D. R.; Danishefsky, S. J. *"Total Synthesis of Garsubellin A"*, *J. Am. Chem. Soc.* **2006**, *128*, 1048–1049.

Snider, B. B.; Patricia, J. J.; Kates, S. A. *"Mechanism of Manganese(III)-Based Oxidation of β-Keto Esters"*, *J. Org. Chem.* **1988**, *53*, 2137–2143.

Spangler, L. A.; Swenton, J. S. *"Mechanistic Aspects of the Annelation Reactions of Benzocyclobutenedione Monoketals with Vinyllithium Reagents"*, *J. Org. Chem.* **1984**, *49*, 1800–1806.

Sumoto, K.; Mibu, N.; Irie, M.; Abe, N.; Miyano, S. *"Ring Transformation of 1,2,3,5,6,7-Hexahydropyrrolizinium Perchlorates into 1-Substituted 5-Oxo-perhydroazocines"*, *Chem. Pharm. Bull.* **1990**, *38*, 577–580.

Swaminathan, S.; Ranganathan, S.; Sulochana, S. *"N-Mannich Bases of 3-Substituted Indoles and Alkylations with Some N-Indolylmethyltrimethylammonium Iodides"*, *J. Org. Chem.* **1958**, *23*, 707–711.

Takeda, K.; Nakajima, A.; Yoshii, E. *"BF3 center dot Et(2)O-Mediated Intramolecular Allylstannane-Ketone Cyclizations: Formation of Bicyclo[4.1.0]hept-4-en-1-ols from 5-(Tributylstannyl)-3-cycloheptenones"*, *Synlett* **1996**, 753–754.

Taniguchi, T.; Martin, C. L.; Monde, K.; Nakanishi, K.; Berova, N.; Overman, L. E. *"Absolute Configuration of Actinophyllic Acid as Determined through Chiroptical Data"*, *J. Nat. Prod.* **2009**, *72*, 430–432.

Theis, C.; Bordeianu, R.; Latz, W. *"Process for Preparing 2-Aryl-2-chloromalonic Diesters"*, U.S. Patent 5,777,152, July 7, 1998.

Trnka, T. M.; Grubbs, R. H. *"The Development of L2X2Ru = CHR Olefin Metathesis Catalysts: An Organometallic Success Story"*, *Acc. Chem. Res.* **2001**, *34*, 18–29.

Trost, B. M. *"Organopalladium Intermediates in Organic Synthesis"*, *Tetrahedron* **1977**, *33*, 2615–2649.

Tsuji, J.; Minami, I. *"New Synthetic Reactions of Allyl Alkyl Carbonates, Allyl Beta-Keto Carboxylates, and Allyl Vinylic Carbonates Catalyzed by Palladium Complexes"*, *Acc. Chem. Res.* **1987**, *20*, 140–145.

Tsukano, C.; Siegel, D. R.; Danishefsky, S. J. *"Differentiation of Nonconventional "Carbanions"–The Total Synthesis of Nemorosone and Clusianone"*, *Angew. Chem. Int. Ed.* **2007**, *46*, 8840–8844.

Tuleen, D. L.; Stephens, T. B. *"Chlorination of Unsymmetrical Sulfides"*, *J. Org. Chem.* **1969**, *34*, 31–35.

Verin, S. V.; Tosunyan, D. E.; Kuznetsov, E. V. *"An Efficient Access to Alpha-Tetralones and their Derivatives via o-Quinodimethanes Generated by Isochromene Ring Cleavage"*, *Mendeleev Commun.* **1992**, 20–21.

Wang, W.; Boffa, M. B.; Bajzar, L.; Walker, J. B.; Nesheim, M. E. *"A Study of the Mechanism of Inhibition of Fibrinolysis by Activated Thrombin-Activable Fibrinolysis Inhibitor"*, *J. Biol. Chem.* **1998**, *273*, 27176–27181.

Wender, P. A.; Wolanin, D. J. *"Total Synthesis of Quadrone and Terrecyclic Acid A"*, *J. Org. Chem.* **1985**, *50*, 4418–4420.

Yang, D.; Gao, Q.; Lee, C.-S.; Cheung, K.-K. *"Novel Intramolecular Cyclopropanation Reaction of Unsaturated β-Keto Esters"*, *Org. Lett.* **2002**, *4*, 3271–3274.

Yang, D.; Gao, Q.; Lee, O.-Y. *"Lewis Acid Promoted Phenylseleno Group Transfer Tandem Radical Cyclization Reactions"*, *Org. Lett.* **2002**, *4*, 1239–1241.

Yee, N. K.; Farina, V.; Houpis, I. N.; Haddad, N.; Frutos, R. P.; Gallou, F.; Wang, X.; Wei, X.; Simpson, R. D.; Feng, X.; Fuchs, V.; Xu, Y.; Tan, J.; Zhang, L.; Xu, J.; Smith-Keenan, L. L.; Vitous, J.; Ridges, M. D.; Spinelli, E. M.; Johnson, M.; Donsbach, K.; Nicola, T.; Brener, M.; Winter, E.; Kreye, P.; Samstag, W. *"Efficient Large-Scale Synthesis of BILN 2061, a Potent HCV Protease Inhibitor, by a Convergent Approach Based on Ring-Closing Metathesis"*, *J. Org. Chem.* **2006**, *71*, 7133–7145.

Index

Actinophyllic Acid	1,3–5,7–12,15,88,90, 91,164,173,176,182
Aza-isobenzofulvene	176,178,182
Aza-Michael	15,16
Cyclization	6,20,23,165,169,170
Enamine	173,175,176,177,182
Iminium	5,175,178,179,182,192
Oxidative Transposition	24,26,28,82,83,85,90
Radical	165,169,171
Ring-Closing Metathesis	16,18,22,28,84,85
Thiomorpholine	87,88,89,91,110
Vinyl Grignard	28,81,83

About the Author

Joshua James Day was born February 17, 1982 in Bryn Mawr, Pennsylvania to Steven and Susan Day. Two months later the family moved to Colorado where Josh grew up in Littleton. During his younger years Josh enjoyed playing sports with his brothers Ryan and Camden.

All three boys attended Dakota Ridge High School after graduating from Summit Ridge Middle School. During high school Josh enjoyed outdoor activities including hiking, fishing, snowboarding, and golf. He played varsity baseball at Dakota Ridge and helped his team reach the State playoffs his senior year.

After graduation Josh attended the Colorado School of Mines in Golden, Colorado. At the end of his first year he decided that he wanted a larger University experience and transferred to Colorado State in Fort Collins, Colorado as a biochemistry student. During the summer of his junior and senior years Josh worked in the laboratory of Professor Olve Peersen with a telomere end binding protein. A second chemistry major was added after he took a yearlong organic chemistry class with Professor DeBruin and discovered a fascination with organic molecules. Josh graduated from Colorado State University *magna cum laude* and later that summer married his longtime girlfriend Melissa. Together they packed up a 15-foot moving truck and drove halfway across the country to New Haven, Connecticut.

In the fall of 2004 Josh began graduate studies in organic chemistry at Yale University. Following his first semester at Yale Josh joined the laboratory of Professor John L. Wood to pursue a total synthesis of the indole alkaloid actinophyllic acid. After his second year of graduate studies Josh, along with three other graduate students, helped to move the Wood laboratory to Colorado State University. As luck would have it, he ended up exactly where he started.

After five exciting and wonderful years in the Wood group Josh has accepted a postdoctoral position in the laboratory of Professor Brian M. Stoltz at the California Institute of Technology, to begin September 2009.